ABSTRACT

| | |
|---|---|
| Title of Dissertation: | MULTIFACETED APPROACHES TO CONTROL FUSARIUM HEAD BLIGHT IN WHEAT: GENETIC MAPPING, MECHANISTIC STUDIES, AND FUNGICIDE EFFICACY ANALYSES |
| | Lovepreet Singh, Doctor of Philosophy, 2022 |
| Dissertation directed by: | Associate Professor, Dr. Nidhi Rawat, Department of Plant Science and Landscape Architecture |

Fusarium Head Blight (FHB), caused by the fungal pathogen *Fusarium graminearum*, is the second most important disease of wheat globally. This doctoral research contributes toward improving the two most widely used FHB management strategies: development of resistant cultivars and the use of fungicides. Given the quantitative nature of FHB resistance, pyramiding of multiple quantitative trait loci (QTLs) is required to develop resistant cultivars. Marker-

assisted selection using diagnostic Kompetitive Allele-Specific PCR (KASP) assays is a cost and time-efficient approach. Toward this end, a previously identified resistance QTL from a moderately resistant soft red winter wheat cultivar Jamestown located on chromosome 1B was genetically mapped and diagnostic KASP assay was developed for it. Furthermore, a robust gene specific KASP marker was developed and validated for *Fhb1*, the most widely used QTL for resistance against FHB. Previously, a *Pore-forming toxin-Like* (*PFT*) gene was identified as the major underlying gene for *Fhb1*-mediated resistance in wheat. In the present research, functional characterization of *PFT* was done toward improving the understanding of the molecular mechanisms of FHB resistance. Ectopic expression of *PFT* in Arabidopsis conferred a broad-spectrum resistance against multiple fungal pathogens. PFT protein was purified from heterologous expression in *Nicotiana benthamiana* and used for various bioassays to elucidate the biological function of its individual domains. The experimental evidence supported our working hypothesis of PFT's atypical mechanism of resistance. Working on the chemical control options for FHB, the efficacy and appropriate timing of application was investigated of a newly recommended fungicide for FHB-'Miravis Ace.' Overall, the knowledge and resources developed in this research would contribute towards improved integrated disease management of FHB in wheat.

# MULTIFACETED APPROACHES TO CONTROL FUSARIUM HEAD BLIGHT IN WHEAT: GENETIC MAPPING, MECHANISTIC STUDIES, AND FUNGICIDE EFFICACY ANALYSES

by

Lovepreet Singh

Dissertation submitted to the Faculty of the Graduate School of the
University of Maryland, College Park, in partial fulfillment
of the requirements for the degree of
Doctor of Philosophy
2022

Advisory Committee:
Dr. Nidhi Rawat, Chair
Dr. James Culver
Dr. Shunyuan Xiao
Dr. Vijay Tiwari
Dr. H. Corby Kistler
Dr. Abani Pradhan

# Dedication

I dedicate this dissertation to the children in war-stricken parts of the world and all the volunteers who contribute toward improving their lives.

# Acknowledgements

Foremost, I would like to express my gratitude to Dr. Nidhi Rawat for providing me this opportunity to work on a multi-disciplinary and impactful research project. Thank you for your guidance and continuous support throughout this five-year journey.

Many thanks to my graduate committee: Dr. James Culver, Dr. Shunyuan Xiao, Dr. Vijay Tiwari, Dr. H. Corby Kistler, and Dr. Abani Pradhan. I highly appreciate your time, input, and consideration during this process. Thank you, Dr. Culver, for always being available to offer troubleshooting solutions. Thank you, Dr. Xiao, for sharing your ideas and several plasmids. Special thanks to Dr. Tiwari for guidance on the 1B project and for late evening phone calls to cheer me up during the downtime. Many thanks to Dr. Kistler for mentoring and helping me establish networks in the FHB research community.

Many thanks to present and past members of Rawat and Tiwari Lab (Bhavit, Alex, Janelle, Adam, and James) for constant companionship and collaboration. Thanks for making the lab environment a welcoming and encouraging workplace. Thanks to Taylor for being my go-to lab mate for helping hand in experiments and reviewing my writing. I thank Arunima for screening PFT transgenic plants with multiple fungal pathogens. My sincere appreciation to Inderjit for his help with the bioinformatics analyses. Special thanks to Gautam and Anmol for help with the 1B project. I am thankful to undergraduate interns in the lab for help with harvesting, threshing, and inoculations. Notably, help from Reilly, Caleb, Victoria, Sai, and Khanoot has been very valuable.

I am very grateful to Dr. Rose Hammond for collaborating on the heterologous protein expression project and training me with all the protein biology work. Many thanks to Dr. Jason Wight, Louis Thorne, and Joe Crank for all the help with planting and fungicide application in the field studies.

A special thanks to greenhouse staff: Sydney Wallace and Meghan Holbert. Thank you for your extraordinary efforts to make sure that the plant grows happily in the greenhouse and for always being available to fix things at short notice. A special appreciation for Qi, Culver, and Hu labs for being my go-to places for borrowing chemicals, equipment, or troubleshooting suggestions. Thank you to UMD PSLA chair Dr. Erwin and staff members for sustaining a welcoming and respectful professional space. Special thanks to Habtamu, Shaun, Anita, Govind, and Chiti for being great colleagues.

Thank you to my graduate peer mentors: Aimee, Yvette, and Scott. For always being there to listen, support, help, and inspire.

Finally, I would like to extend my gratitude to my family. To my parents, Uncle ji, Auntie ji, my beautiful wife (Harpreet Kaur), and loving baby boy (Karmann Singh) for your unconditional love and support. Lastly, many thanks to the Sikh congregation in Maryland for all the spiritual and emotional support.

# Table of Contents

# List of Tables

## Chapter 2



## Chapter 3



## Chapter 4



## Chapter 5



## Chapter 6

## Chapter 7

# List of Figures

## Chapter 1



## Chapter 2

## Chapter 3



## Chapter 4

## Chapter 5

## Chapter 7

# List of Abbreviations

| | |
|---|---|
| FHB | fusarium head blight |
| DON | deoxynivalenol |
| SNP | single nucleotide polymorphism |
| QTL | quantitative trait loci |
| PFT | pore-forming toxin-like |
| MAS | DNA marker assisted selection |
| RIL | recombinant inbred line |
| PCR | polymerase chain reaction |
| KASP | kompetitive allele specific PCR |
| PDA | potato dextrose agar |
| MBB | mung bean broth |
| PSS | percentage of symptomatic spikelets |
| BSR | broad spectrum resistance |
| GFP | green fluorescent protein |
| RPM | revolution per minute |
| DMI | demethylation inhibitor |
| SDHI | succinate dehydrogenase inhibitor |
| FDK | fusarium damaged kernels |

# Chapter 1: Literature Review

## 1.Wheat

### *1.1. Economic Importance*

Wheat is the second most important and most widely cultivated food crop across the globe. It is cultivated in more than 219 million ha area and yields more than 760 million tons annually (FAOSTAT, 2020). It meets around 20% of the total daily caloric need and protein intake of the global human population (FAOSTAT, 2019). Wheat is the first domesticated crop plant. Contemporary wheat cultivars include hexaploid (2n=6x=46, AABBDD) bread wheat (*Triticum aestivum* ) and tetraploid (2n=4x=28, AABB) pasta/durum wheat (*Triticum durum*). Around 95% of wheat grown worldwide is bread wheat and the remaining 5% is durum (Peng et al., 2011).

The United States of America (USA) is the fourth-largest wheat producer and second-largest wheat exporter in the world (FAOSTAT, 2022). In the USA, cultivated wheat is divided into six market classes based on the end use and growing conditions: hard red winter (HRW), hard red spring (HRS), soft red winter (SRW), hard white (HW), soft white (SW), and durum wheat. (https://www.uswheat.org/). HRW is valued for general-purpose flour, pan and flat breads, and croissants. It is grown in the Great Plains (North Dakota, South Dakota, Nebraska, Kansas, Oklahoma, and Texas) Pacific Northwest (Washington, Idaho, and Montana), and California. HRS is ideal for artisan breads, pizza crust and bagels. It is mainly grown in the North Central region (Montana, North Dakota, South Dakota, and Minnesota). SRW is used for making specialty

products such as cookies, crackers, pretzels, etc. It is cultivated in the mid-Atlantic, Southeastern and Great Lakes regions (Maryland, Virginia, Ohio, North Carolina, South Carolina, Georgia, Kentucky, Illinois, Tennessee, Arkansas, Mississippi, Michigan, and Wisconsin). HW is primarily valued for Asian noodles and grown in Nebraska, Kansas, and California. SW is blended as an additive to other wheat type for softer texture to be utilized in specialty products like sponge cakes. SW is mainly grown in the Pacific Northwest (Washington, Oregon, and Idaho). Finally, durum wheat is ideal for pasta food products and is mainly grown in North Dakota and Montana.

### *1.2. Wheat improvement: challenges and opportunities*

Hexaploid bread wheat has three ancestral genomes: A, B and D genome. Each of the three genomes consists of seven homoeologous groups encompassing the forty-two total wheat chromosomes. Within the individual genomes, 14 chromosomal pairs are homologous in evolutionary nature. The three homoeologous chromosomal groups however are not identical with homologs of another group but share high similarity among each other. The complex polyploid genome of wheat has its own advantages and disadvantages.

One of the major advantages of polyploid is genome buffering. Due to this wheat can tolerate deletion of large chromosomal segments or even a whole chromosome substitution. Therefore, polyploidy enabled development to deletion, substitutions and nullisomic lines which were a great resource for classical genetics studies in wheat (Sears, 1953; Endo and Gill, 1996). On the contrary, performing genomics and transcriptomics studies is very challenging due to the complications of homeolog gene copies. For instance, gene function analysis by targeted

local lesions in genome (TILLING), virus-induced gene silencing (VIGS) or CRISPR gene editing require silencing of all three homeolog copies.

In addition, wheat's polyploidy complexity made complete genome sequencing a timely challenge. Despite being one of the most important crop, a complete reference genome assembly was only just completed 2018 (Consortium (IWGSC) et al., 2018). The size of wheat genome is 17 Gb making it ~8-times bigger than maize and ~40 times bigger than rice genome (Arumuganathan and Earle, 1991; Consortium (IWGSC) et al., 2018) ). Additionally, the wheat genome consists very high number of repetitive DNA sequences (85% ) with only 2% of coding regions (Consortium (IWGSC), 2014; Consortium (IWGSC) et al., 2018). With a coverage of 94% of the genome, 107,891 high confidence genes have been identified in the whole wheat genome. Regardless of genome complexity challenges, wheat reference genome availability has spurred a new era for genomics-based wheat improvement. Furthermore, the availability of exome capture data, extensive transcriptional atlas of homoeologous genes, and genome assemblies of ten diverse wheat cultivars opens new avenues in wheat gene discovery (Consortium (IWGSC) et al., 2018b; Ramírez-González et al., 2018; He et al., 2019a; Walkowiak et al., 2020).

Global wheat production is impaired by various biotic and abiotic stresses (Velásquez et al., 2018; Gupta et al., 2020). Around 21.5% of wheat production is lost to fungal pathogens and insect pests globally every year (Savary et al., 2019). Therefore, enhancing genetic resistance in wheat against fungal pathogens is critical to achieving global food security (Bailey-Serres et al., 2019; Gerten et al., 2020).

## 2. Fusarium Head Blight of Wheat

### *2.1. Economic Importance*

Fusarium Head Blight (FHB) is one of the most important diseases of wheat worldwide. Globally, FHB causes the second-highest yield losses in wheat (Savary et al., 2019). In addition to serious yield losses, *F. graminearum* contaminates food and feed with mycotoxins (primarily deoxynivalenol, DON), rendering adverse short- and long-term effects on human and animal health (McMullen et al., 2012). First reported in England in 1884, FHB remerged as a global threat to wheat production after a century (McMullen et al., 1997, 2012; Ma et al., 2020) Globally, FHB epidemics have been reported at almost annual intervals since the 1970s in major wheat growing countries across North America, South America, Asia, and Europe (Ma et al., 2020). In the USA, total annual losses associated with FHB have been reported as high as $1.4 billion (Wilson et al., 2017).

### *2.2. Pathogen profile*

FHB is caused by multiple species of filamentous ascomycetes fungus, *Fusarium* (Parry et al., 1995). FHB is primarily caused by the members of Fusarium graminearum species complex (FGSC). FGSC comprises 16 phylogenetically distinct species distributed worldwide (Sarver et al., 2011; Aoki et al., 2012). Among these, *F. asiaticum* is the major pathogen of FHB in Asia while *F. graminearum* is predominantly responsible for FHB in North and South America (Sarver et al., 2011). However, *F. graminearum* is distributed worldwide (O'Donnell et al., 2004); consequently, it is arguably the most important causal agent for FHB.

The sexual form of *F. graminearum* is a homothallic ascomycete, therefore, undergoes limited outcrossing. The fungus produces two types of asexual spores. First, macroconidia are septate, sickle-shaped and produced on the compact masses of hyphae known as sporodochium. Second, are less common chlamydospores that are globose shape and thick walled. The sexual spores called ascospores are produced in a sac like structures called asci. Asci are organized inside the flask-shaped fruiting body called a perithecium (Goswami and Kistler, 2004; Guenther and Trail, 2005). Together, the ability to reproduce sexually and asexually contributes positively toward evolution and adaptation.

*F. graminearum* has a wide host range including wheat, barley, maize, rice, oats and other grasses including *Agropyron, Agrostis, Bromus, Setaria, Secale, Lolium, Echinochloa, Sorghum and Poa* and economically important dicot genera including *Cucumis, Glycine, Medicago, Trifolium, and Lycopersicon* (Goswami and Kistler, 2004). In addition to being a pathogen, *F. graminearum* thrives as a symptomless endophyte on North American wild grasses (Lofgren et al., 2018). Hence, it is adapted to versatile lifestyles by surviving as a saprophyte, endophyte or a hemi-biotrophic pathogen. In the future, *F. graminearum* could pose greater threat to crop productivity since climate change is more likely to favor adaptability of *F. graminearum* as a pathogen over its saprophytic mode of survival (Vaughan et al., 2016).

*F. graminearum* has four chromosomes. The first whole genome sequence of *F graminearum* was released by Broad institute, Center for Genome Research in May 2003. A highly virulent strain NRRL 31084 (PH-1) was sequenced with 10 X genome coverage resulting in 36 Mb genome size (Goswami and Kistler, 2004). *F. graminearum* genome has very few

repetitive DNA sequences and transposable elements. *F graminearum* has more pathogenesis related protein compared to non-pathogenic filamentous fungi, including hydrolytic enzymes, predicted transcription factors and transmembrane transporters (Cuomo et al., 2007). Comparison of the PH-1 genome with another highly pathogenic strain GZ3639 revealed high single nucleotide polymorphism (SNP) density regions mainly located near telomere, a region with high recombination rates. Furthermore, comparison with related species revealed that these SNP hotspots also exhibit high interspecific variability. High SNP density regions overwhelmingly contain genes involved in plant-fungal interaction, ultimately, suggesting these localized polymorphism hotspots could be the results of host-pathogen coevolution (Cuomo et al., 2007).

*F graminearum* genome contains 18 secondary metabolite biosynthesis gene clusters (Ma et al., 2010). One of the important secondary metabolites produced by *F. graminearum i*s trichothecene. Trichothecenes are a class of mycotoxins that are harmful to human and animal health. Primarily, *F. graminearum* produces type B trichothecene, which have a keto group at C-8 position, including deoxynivalenol (DON), nivalenol (NIV) and their acetylated derivatives, during the wheat infection. Based on the type of trichothecene produced, *F. graminearum* isolates can be classified into four major chemotypes: 3-acetyl DON (3-ADON), 15-acetyl DON (15-ADON), NIV (Goswami and Kistler, 2004; Alexander et al., 2011), and the novel type A trichothecene NX-2 (Varga et al., 2015)Predominantly, ADON and NX-2 isolates are found in North America and NIV isolates in Asia. However, shifts in chemotypes diversity are being observed globally. For instance, 3- ADON and 15-ADON chemotypes have been reported thus

favoring DON isolates over NIV in Japan and China (Suga et al., 2008; Yang et al., 2008; Zhang et al., 2010). Additionally, the replacement of largely distributed 15-ADON populations by more aggressive 3-ADON populations has been reported in North America (Ward et al., 2008). ADON gets converted into DON in wheat grains, during the bread making process (Wu and Wang, 2015) and in the intestine before absorption (Chain (CONTAM) et al., 2017). Therefore, making DON a major mycotoxin of concern in FHB.

Indeed, DON is the most prevalent mycotoxin in cereal grains worldwide with the second highest incidence rate (58 %) in raw cereals and the highest incidence rate (56%) in processed cereal products (Lee and Ryu, 2017). High DON contamination renders food and feed products unfit for human and animal consumption. DON is a protein synthesis inhibitor and leads to aberrant intracellular signaling. In animals, acute exposure to DON causes vomiting and feed refusal whereas chronic exposure leads to growth retardation and immunotoxicity (Pestka, 2010). Additionally, DON is phytotoxic and acts as a virulence factor for FHB in wheat (Bai et al., 2002; Jansen et al., 2005). It induces Reactive Oxygen Species (ROS) production and stimulates programmed cell death thus assisting virulence of necrotrophic *F. graminearum* in wheat (Desmond et al., 2008) .

### *2.3. Disease Epidemiology*

FHB is a monocyclic disease with little or no secondary spread (Figure 1.1). In the field conditions, the life cycle of *F. graminearum* starts with the landing of airborne ascospores on the flowering wheat spikes. Warm and moist weather conditions which coincide with wheat

flowering, favor the maturation of perithecia borne on overwintering saprophytic mycelia on infected crop debris (Markell and Francl, 2003). Successful infection of wheat heads by *F. graminearum* requires at least 24 hours of a warm (25 °C) and humid (100 % RH) environment (Parry et al 2005). With the favorable conditions, the ascospores are forcibly released from perithecia (Trail et al., 2002) and are dispersed to host plant via wind, rain, or insects (Parry et al., 1995). Anthesis is the most susceptible growth stage to FHB infection in wheat (Schroeder and Christensen, 1963).

After spore germination, hyphae grow exteriorly on florets and glumes eventually entering by direct penetration or through natural openings like stomata, and openings between lemma and palea containing thin-walled epidermal cells (Bushnell et al., 2003; Boenisch and Schäfer, 2011).The fungus grows intercellularly and asymptomatically during a brief apparent biotrophic phase (Goswami and Kistler, 2004; Trail, 2009). Upon switching to the necrotrophic phase, it grows intracellularly and radially causing necrosis of host tissue. After the infection, the fungus spreads to other spikelets through vascular bundles of rachilla and rachis (Ribichich et al., 2000; Bushnell et al., 2003). Ultimately, leading to premature bleaching of spikelets and shriveled kernels with DON accumulation. In the colonized plant tissue, stems particularly, haploid mycelium prepares for sexual reproduction by forming hyphae with binucleate cells. The dikaryotic hyphae fuse to form perithecium which serves as overwintering structures on crop debris (Guenther and Trail, 2005).

Macroconidia are another important source of inoculum (Goswami and Kistler, 2004). During wet conditions, salmon pink colored sporodochia can be seen on infected plant surface.

Conidia are dispersed to short distances through rain splashes as compared to long distance dispersal by airborne ascospores (Manstretta et al., 2015).

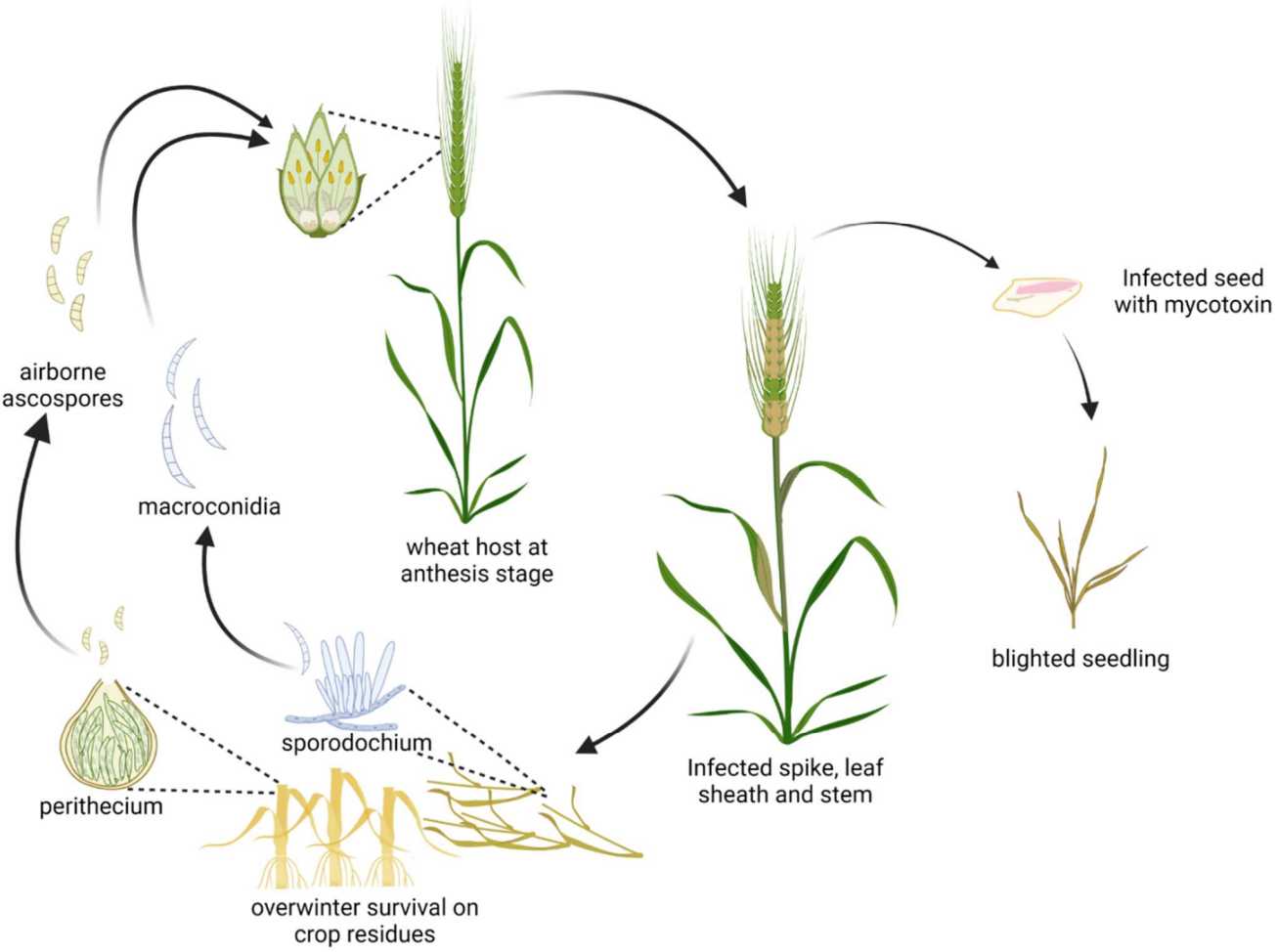


**Figure 1. 1. Disease cycle of Fusarium Head Blight in wheat.** Illustration created with BioRender.com

### *2.4. FHB management in wheat*

To control FHB, measures are required to reduce inoculum quantity, prevent inoculum dispersal and, prevent infection of spikelets (Parry et al., 1995). Towards this end, multipronged disease management approach is necessary. The prevalent FHB management approaches include: cultural practices, fungicide application, and resistant cultivars (Salgado et al., 2011; McMullen et al., 2012).

#### *2.4.1. Cultural practices*

The wide host range of FHB pathogens provides more opportunities for overwintering and inoculum reservoirs. Importantly, a major source of inoculum is ascospores produced on debris of major hosts, small grain cereals and maize. Evidently, continuous wheat cultivation or wheat-corn rotation system significantly increases FHB (Sutton, 1982; Dill-Macky and Jones, 2000). Therefore, cultural practices like crop rotation and soil tillage have been recommended to reduce the initial FHB inoculum. Dill- Mackey and Jones (2000) studied the effect of crop rotation and tillage practices on FHB management in wheat. FHB incidence and severity were significantly lower in wheat followed by soybean as compared to corn. Wheat -soybean rotation had 15 % lower FHB incidence and 31 % lower severity compared to wheat-corn rotation. Wheat followed by soybean had 50 % lower DON than wheat followed by corn. With regards to tillage, Moldboard plow treatment had significantly lower disease incidence, severity and DON content compared to no-tillage treatment. Hence, suggesting that field level residue borne- inoculum play

important role and strategies to reduce infected crop residue can assist in controlling FHB. However, practices like tillage might not be feasible given the soil conservation legislation in several states across the USA.

*2.4.2. Fungicide based Management*

In the USA, fungicides are applied to around 70 % of wheat acreage to manage FHB (Wilson et., 2017). The most widely evaluated and used fungicides against FHB are based on triazole chemistry (Paul et al., 2018b). Triazole group belongs to Demethylation Inhibitor (DMI) or Sterol Biosynthesis Inhibitors (SBI) fungicide class with FRAC code 3. DMIs inhibits C14-demethylation step during sterol biosynthesis in fungi. Sterols are important component of fungal cell membrane ensuring its stability and permeability. Thus, Triazoles are site specific fungicides which inhibit fungal growth by compromising fungal cell membrane integrity (Ziogas and Malandrakis, 2015).

In a multivariate meta-analysis study by Paul et al. (2008), efficacies for different triazole based fungicides were compared in controlling FHB and DON. The study included data from 100 uniform fungicide trials (UFTs) organized by US Wheat and Barley scab initiative (USWBSI) across 14 states and 11 years. The goal of UFTs is to identify fungicides with highest and consistent control efficacies across locations, wheat types, years and cropping systems. The fungicides included: propiconazole, prothioconazole, tebuconazole, metconazole, and a tank mix of prothioconazole+ tebuconazole. Overall, the control efficacies ranged from 32 to 52 % for the FHB index and 12 to 45 % for DON. For the FHB index, tebuconazole + prothioconazole mix had highest control efficacy (52 %) followed by metconazole (50%), prothioconazole (48%),

tebuconazole (40 %), and propioconazole (32 %). For DON, metconazole had highest control efficacy (45 %) followed by prothioconazole (43 %), prothioconazole + tebuconazole (42 %), tebuconazole (23 %) and propioconazole (12 %). In all cases, fungicide efficacies were higher in spring wheat than in soft winter wheat.

Strobilurins (FRAC 11) class of fungicides are effective against foliar diseases of wheat and are known to have a positive physiological effect on crop yield. However, it is strongly recommended to avoid strobilurins to control FHB, because in addition to being relatively ineffective, this fungicide class increases the mycotoxin level compared to non- treated check especially when applied at the anthesis stage (Ellner, 2005; Paul et al., 2018b).

One of the most important factors affecting fungicide efficacy for FHB control is application timing. The efficacy of fungicides varies with different plant stages (Audenaert et al., 2011; Paul et al., 2018). As mentioned before, wheat is most susceptible to FHB at anthesis because initial *Fusarium* sp. infection commonly starts on the extruded anthers (Parry et al, 1995; Pugh et al. 1933). In wheat, anthesis has been found to be the most effective timing of fungicide application to control FHB (Audenaert et al., 2011b; Paul et al., 2018a). Anthesis, described as extrusion of anthers from the florets, is divided in to three stages. The early stage (Feekes 10.5.1) is characterized by anther extrusion in the middle third of spike. The mid stage (Feekes 10.5.2) include anther extrusion from the upper third of spikes. The late stage (Feekes 10.5.3) is indicated by anther extrusion from the bottom third of the spike. For the fungicide application recommendation, anthesis is defined as a stage when 50 % of the primary tillers reach Feekes 10.5.1 stage in the field. In US wheat production systems, usually only a single

fungicide spray is economically viable, restricting the effective window of fungicide application to anthesis stages which lasts 3-4 days (McMullen et al. 1997; D'Angelo et al. 2014). This small opportune timing of application, especially when coinciding with wet weather, makes fungicide application for FHB management tricky and sometimes not feasible at all. Therefore, possibility to widen the spray window by testing fungicide efficacy at pre-anthesis or post-anthesis stage has been explored previously (Edwards and Godley, 2010; Yoshida et al., 2012; D'Angelo et al., 2014; Paul et al., 2018a). In the multi-state trials with triazole fungicides, post-anthesis application performed better than pre-anthesis application for controlling the FHB and DON (Paul et al., 2018a). However, control efficacy is achieved best at anthesis and remains the recommended stage of fungicide application for FHB (D'Angelo et al., 2014; Paul et al., 2018a).

*2.4.3. Growing resistant cultivars*

Deploying genetic resistance is the most effective and economical strategy for FHB management (McMullen et al., 2012). However, only moderately resistant cultivars are available to growers. Therefore, breeding for FHB resistance remains one of the major goals of wheat breeding programs across the globe (Ma et al., 2020; Fernando et al., 2021). Genetic resistance has been reported to complement fungicide application (Salgado et al., 2011; Willyerd et al., 2012). For instance, combining genetic resistance and prothioconazole + tebuconazole application resulted in more than 70 % reduction in FHB index and DON (Willyerd et al., 2012).

### *2.5. Genetics of FHB resistance*

FHB resistance is quantitative in nature, therefore, controlled by multiple loci and exhibits high Genotype × Environment interaction (Mesterházy, 1995). Furthermore, FHB resistance is horizontal in nature, thus, do not exhibit pathogen isolate specific response (Snijders and Van Eeuwijk, 1991; van Eeuwijk et al., 1995). Given the biology of FHB, the complex genetic nature of FHB resistance is further complicated by passive resistance factors including morphological and development traits such as plant height, date of flowering and anther extrusion. These passive resistance traits should be taken into consideration while characterizing FHB resistance in field conditions (Buerstmayr et al., 2020). Originally, Schroeder and Christensen (1963) described two types of resistance against FHB: Type I resistance: resistance against initial infection and Type II resistance: resistance to the spread of infection within the spike (Schroeder and Christensen, 1963). This classification is based on the symptom development only and does not suggest underlying resistance physiology. Later Mesterhazy (1995) included three additional types of FHB resistance, Type III: resistance to DON accumulation, , Type IV: resistance to Kernel damage, and Type V: tolerance to yield loss (Mesterházy, 1995). In wheat, Type II resistance has been widely investigated and characterized (Rudd et al., 2001; Buerstmayr et al., 2009a) because there is a well-developed protocol to screen Type II resistance. On the other hand, Type I resistance is difficult to assess and therefore less reports are found. FHB resistance has been identified in all the three primary, secondary, and tertiary gene pools of wheat. Asian spring wheat landraces or cultivars are the sources of most

effective and widely used FHB resistance which include Sumai3, Wangshuibai, and Nyu Bai (Buerstmayr et al., 2020)

Quantitative Trait Loci (QTLs) for FHB resistance have been reported in almost all the chromosomes of wheat genome (Buerstmayr et al., 2009b, 2020). Most of the QTLs are minor effect with low stability and only few major effect QTLs have been identified in wheat. Only seven QTLs have been mendelized and assigned gene names including: *Fhb1, Fhb2, Fhb3, Fhb4, Fhb5, Fhb6, and Fhb7* (Cuthbert et al., 2006a, 2007a; Qi et al., 2008a; Xue et al., 2010a, 2011a; Cainong et al., 2015a; Guo et al., 2015a). *Fhb1, Fhb2, Fhb3, Fhb6 and Fhb7* confers Type II resistance whereas *Fhb4 and Fhb5* contributes Type I resistance. *Fhb1* is derived from Chinese cultivar 'Sumai 3' and it is located on the distal segment of chromosome 3BS (Cuthbert et al., 2006b). Sumai 3 also contains *Fhb2* on the short arm of chromosome 6BS (Cuthbert et al., 2007b). *Fhb3* is derived from a tetraploid wheat relative *Leymus racemosus* and was transferred to wheat via Robertsonian Wheat-*Leymus racemosus* translocation line which contained translocation between short arm of chromosome of *Leymus* (7LrS) and long arm of chromosome 7A (7AL) (Qi et al., 2008a). *Fhb4* is derived from the distal region of chromosome 4BL of Chinese cultivar 'Wangshubai' (Xue et al., 2010). *Fhb5* was fine mapped to pericentromeric region of the short arm 5A chromosome of the same cultivar (Xue et al., 2011). *Fhb6* was isolated from perennial grass *Elymus tsukushiensis* and mapped to the subterminal region of the short arm of chromosome 1E. This QTL was transferred to wheat by developing disomic chromosome addition and translocation lines with *Elymus* (Cainong et al., 2015b). *Fhb7,* derived from *Thinopyrum* spp., is the latest addition to the list of major effect QTLs for FHB. It is

located on chromosome 7El and was transferred to the distal region of chromosome 7DL by Robertsonian translocation (Guo et al., 2015). Finally, it should be noted that most of the major effect resistance sources are derived from non-adapted backgrounds. Therefore, their introgression into contemporary US cultivars can be challenging due to associated linkage drag or QTL x background interactions. Thus, it is highly desirable to characterize and utilize native sources of genetic resistance derived from adapted germplasm (Liu et al., 2013; Carpenter et al., 2020).

### *2.6. Molecular Wheat – Fusarium graminearum interactions*

#### *2.6.1. Arsenals of F. graminearum*

The pathogenicity factors of *Fusarium* species can be classified into basic and specific virulence genes. The basic virulence genes are general factors that are commonly present in phytopathogenic fungi. The general pathogenicity factors of *F. graminearum* include: mitogen-activated protein kinase (MAPK) signaling pathway genes, Ras proteins (small GTPases), components of G signaling pathways, and velvet complex components and cAMP pathways (Ma et al., 2013).

The specific virulence factors are key signatures of specialized host-pathogen interactions. One of the major players in the specific host-pathogen interaction are effectors. Effectors are molecules of diverse nature (RNA, protein, or secondary metabolites) secreted by pathogens that target host proteins or processes during infection (Kamoun, 2007). Among *Fusarium* pathogens, effectors are well studied in tomato pathogen, *F. oxysporum f. sp.*

*lycopersici. SIX* (secreted in xylem) genes encodes for the extracellular effectors which interact with tomato resistance genes in gene-for-gene fashion (Houterman et al., 2008). Although there are no reports for gene-for-gene interactions in *F. graminearum*, in silico secretome analyses revealed presence of possible effectors such as small, cysteine-rich, amino acids repeat-containing proteins (Brown et al., 2012). Recently, Menteges et al (2020) identified 88 up-regulated putative effectors from the transcriptomics analysis of infection cushions of *F. graminearum* on wheat. They characterized a highly induced putative effector, FgPE1 which was predicted to encode 151 amino acid long protein with an Aa1 -like domain present in other fungal effectors. FgPE1 was localized at the fungal-plant cell wall interface but did not play role in modulating the virulence. Hence, further studies are required to identify and characterize *F. graminearum*-specific fungal effectors.

Considering the broad definition of effectors, two well-known secreted effectors of *F. graminearum* are the secreted lipase FGL1 and mycotoxin DON (Ilgen et al., 2008). Voigt et al (2005) isolated and functionally characterized FGL1. They demonstrated that knock-out mutant *Δfgl1* exhibited reduced virulence compared to wild type in both wheat and maize. Similar results were later reported in barley (Ilgen et al., 2008). Furthermore, FGL1 partially restored the pathogenicity in non-virulent mitogen-activated kinase mutant (*Δgpmk1)* on wheat host (Salomon et al., 2012).

Unlike FGL1, DON is a virulence factor for only wheat host, not barley or maize (Jansen et al., 2005; Ilgen et al., 2008). Although DON deficient mutant, *Δtri5*, establishes initial infection, it cannot penetrate through the rachis node which is the major passage for pathogen

spread in wheat spike. Furthermore, *Δtri5* infected rachis node exhibited a high level of cell wall thickening suggesting that DON subverts defense responses leading to cell wall thickening (Jansen et al., 2005; Ilgen et al., 2008). To investigate the underlying molecular events of DON-dependent susceptibility, Bonnighausen et al (2018) performed metabolic profiling of rachis node infection by wild type (WT) and Δ*tri5*. The major noticeable differences were the accumulation of polyamines including putrescine and γ-aminobutyric acid (GABA), and reactive oxygen species (ROS) metabolites in the WT. Polyamines are known to induce DON biosynthesis and ROS leads to programmed cell death which facilitate the proliferation of necrotrophic pathogens. On the other hand, accumulation of metabolites associated to Jasmonic Acid (JA) related defense were noticeable in the mutant. Interestingly, both the genotypes accumulated similar levels of cell wall metabolites. Thus, the previously supported notion on the role of cell wall thickening (Jansen et al., 2005) might not be a major factor in DON-mediated susceptibility. The authors conclude that DON-mediated ROS activation and subversion of JA-related defense responses might be more important in manifesting the disease reaction.

*2.6.2. Defense Tactics of Wheat*

Defense responses in wheat can be classified as basal and specific defense responses. Walter et al (2009) reviewed the series of basal defense response in the host plants in response *to F. graminearum* infection. Which includes:

1. Upregulation of basal defense genes encoding for pathogenesis related (PR) proteins: PR-1, PR-2 (β1-3, glucanase, PR-3 (chitinase) , PR-4 (wheatwin), PR-5 (thaumatin-like

protein) . Chitinases and glucanases degrade fungal cell walls and help to sense fungal intrusions

2. Release of cutin-derived elicitors to initiate signaling for cuticle repair
3. Activation of phenylpropanoid pathway to synthesize antimicrobial phenolics
4. Cell wall thickening
5. ROS and mycotoxin detoxification

2.6.2.1 Role of Phytohormones

Phytohormones are critical regulators of plant defense response against pathogens. Among various phytohormones, Salicylic acid (SA), Jasmonic Acid (JA), and Ethylene (ET) are the major player in defense signaling (Bari and Jones, 2009). In general, SA-related defense response protects against biotrophs whereas JA and ET related responses curb necrotrophic pathogens (Glazebrook 2005). However, several studies report more complex crosstalk between these pathways which might depend upon a particular pathosystem (Bari and Jones, 2009). Wheat –*F. graminearum* pathosystem is no exception in this regard. Both SA and JT have been reported to positively modulate resistance against FHB (Makandar et al., 2010; Ding et al., 2011; Wang et al., 2018). Given the antagonistic relationship between SA and JA, temporal aspect of this crosstalk is very crucial. SA play role in the early phase of infection whereas JA related response is crucial in the later stage. This temporal response corelates well with the short biotrophic phase followed by the necrotrophic lifestyle of *F. graminearum*. Notably, resistance genotypes seems to have better temporal coordination of SA -JA crosstalk compared to

susceptible genotypes (Ding et al., 2011; Wang et al., 2018). The role of ET is ambiguous in this host-pathogen interaction (Wang et al., 2018). Some reports suggest that ET positively regulate resistance (Li and Yen, 2008; Ding et al., 2011) while other studies conclude ET mediated susceptibility (Chen X. et al., 2009; Xiao et al., 2013).

2.6.2.2. Molecular Mechanism of FHB resistance genes

To date, only *Fhb1* and *Fhb7* (Wang et al., 2020) QTLs have been cloned to identify underlying gene products. Three independent studies have reported map-based cloning of *Fhb1* (Rawat et al., 2016; Li et al., 2019; Su et al., 2019, 1). In the first study, Rawat et al (2016) identified a pore-forming toxin-like gene (PFT) as a major contributor to Fhb1 resistance. PFT is predicted to be a chimeric plant lectin with two amaranthin domains (agglutinin domains of *Amaranthus caudatus)* and one bacterial epsilon toxin (ETX) / mosquitocidal toxin (MTX) domain of aerolysin pore-forming toxin family (Rawat et al., 2016). Both second and third studies identified another gene, histidine-rich calcium-binding protein (*His*), as a major contributor to *Fhb1* mediated resistance. However, they reported conflicting gene functional analysis results. In the second study, Su et al. (2019) concluded that *His* is a susceptibility factor since its silencing in the susceptible Bobwhite cultivar enhanced resistance whereas overexpression did not. On the contrary, a third study claimed that same *His copy is* a resistance gene because its transformation in a susceptible cultivar enhanced FHB resistance (Li et al., 2019). In an effort to reconcile these conflicting findings on *His,* it was proposed that the gene might have a dominant-negative effect (Lagudah and Krattinger, 2019). However, such speculation awaits experimental evidence. Given

the conflicting results on *His* functional analysis and absence of an obvious defense related domain, plausible hypothesis on its molecular mode of action remains elusive.

On the other hand, the possible mode of action can be inferred from the predicted protein structure of PFT. PFT is atypical resistance protein with a combination of two types of domains, both of which are known to have defense roles. So far proteins with domain architecture of two amaranthin domains and an aerolysin pore-forming toxin domain have been partially characterized in wheat (Puthoff et al., 2005), flax (Faruque et al., 2015), cucumber (Dang et al., 2017) and *Rumex acetosa* plants (Manzano et al., 2017). Out of these, only wheat HFR-2 is involved in plant defense against insects (Puthoff et al., 2005). Therefore, PFT is the only protein with its kind of domain architecture known to be involved in defense against phytopathogenic fungi.

Plant lectins contain one or more agglutinin domains that reversibly bind to carbohydrates; they are known to play a role in defense against insects, nematodes, bacteria, fungi, and viruses (Lannoo and Van Damme, 2014). Plant lectins have been classified into twelve different families and specificity for binding to carbohydrates varies among these families (Van Damme et al ., 2008). To date, the biological activity of amaranthin domains has only been characterized for lectins extracted from *Amaranthus* species. These amaranthins specifically bind to *N*-acetylgalactosamine and T-antigens (Transue et al., 1997; Hernández et al., 2001). However, given the sequence variation between the amaranthin domains, differences in their carbohydrate binding specificity are expected which could define their specific biological role (Dang et al., 2017). It is speculated that PFT has binding specificity towards one of the components of fungal cell wall

including chitin monomer *N*- acetylglucosamine and β- 1,3 glucan. Whether PFT binds specifically to *F. graminearum,* or other fungi could determine broad-spectrum potential of PFT.

Aerolysin like pore-forming proteins (PFPs) are present in all kingdoms of life including bacteria, archaea, fungi, plants, and animals (Szczesny et al., 2011). The presence of PFPs in eukaryotes could be due to recurrent horizontal gene transfers (Moran et al., 2012). Bacterial PFPs compromise host membrane permeabilization by making pore structures. The mechanism of pore formation by bacterial PFPs has been well studied. PFPs are present in the form of a single soluble peptide in the cytosol. Upon getting in contact with protein receptors or lipid or carbohydrate molecules of host cell membranes, PFPs get activated by proteolytic cleavage and oligomerize. The oligomer complex get inserted into the host membrane leading to the formation of a transmembrane pore-forming complex (Peraro and van der Goot, 2016).

The presence of aerolysin pore-forming domain in PFT suggests that PFT could compromise the fungal cell membrane by making pores, which is partially supported by the fact that expression of the ETX/MTX domain of PFT in yeast resulted in toxicity at low OD levels (He et al., 2019b). As mentioned before, the specificity towards the fungal membrane could be contributed by amaranthin domains. Therefore, it can be hypothesized that PFT interacts with fungal cell wall via amaranthin domain and kill fungal cells by making pores in the fungal membrane through ETX/MTX pore-forming domain.

Recently, Wang et al (2020) developed a high-quality genome assembly of *Thinopyrum elongatum* to clone *Fhb7*. Cloning of *Fhb7* revealed that it encodes a glutathione-S- transferase (GST) that irreversibly detoxifies trichothecene mycotoxins and provides resistance against FHB

in wheat. Sequence homology analysis revealed no obvious paralogs in other plant species whereas high sequence similarity was found in the GST of an endophytic fungus *Epichloe* sp. Therefore, unraveling a unique evolutionary path for a plant disease resistance gene undergoing horizontal gene transfer from a fungus.

Taken together, atypical resistance genes with a potential broad spectrum resistance mechanism have been identified against FHB in wheat.

**Dissertation overview**

This dissertation research contributes towards the overall goal of effective integrated disease management of FHB in wheat. Growing resistant cultivars and applying fungicides are two primary options for controlling FHB. However, moderately resistant cultivars and partially effective fungicides sometimes fail to ensure proper control during heavy disease epidemics. Hence, there is a need of enhancing genetic resistance against FHB and developing fungicides with high efficacy.

Genetic resistance against FHB can be improved by discovering and characterizing novel genetic resistance and pyramiding it with existence resistance. Towards this end, In **chapter 2**, I characterized native genetic resistance in widely grown high yielding SRW wheat cultivar, "Jamestown". The target QTL region was refined and KASP marker assay was developed for precise MAS. KASP assay is being validated in large population set by Dr Gina Brown-Guedira, USDA, Raleigh, NC. The manuscript is in preparation to be published in "Theoretical and

Applied Genetics" journal. In **chapter 3**, I developed KASP assay from the underlying gene of *Fhb1* QTL for precise MAS. The Chapter 3 was published in "The Plant Pathology Journal"(Singh et al., 2019).

Understanding of molecular mechanism of quantitative resistance is very limited in crop plants. In **chapter 4 and 5**, the studies were performed towards understanding the molecular mechanism of FHB resistance mediated by *PFT.* In **chapter 4**, broad-spectrum resistance potential of *PFT* was characterized against multiple economically important fungal pathogens. Dr. Arunima Sinha contributed significantly to this study by screening *PFT* transgenics against three fungal pathogens: *Colletotrichum higginsianum*, *Sclerotinia sclerotiorum* and *Botrytis cinerea*. This chapter is in preparation to be published in "The Plant Journal". In **chapter 5**, PFT and its domains were functionally characterized. Dr Rose Hammond, USDA, Beltsville, MD contributed significantly to this chapter by cloning PFT and its domains in Potato Virus X vectors and performing agroinfiltration for these constructs. Inderjit Singh Yadav performed protein ligand docking analysis.

Widely used triazole fungicides provide only up to 50% protection against FHB (Paul et al., 2008; Willyerd et al., 2012) and fungicide resistance against triazoles are being reported in FHB pathogens (Yin et al., 2009; Spolti et al., 2014; Hellin et al., 2018) . Hence there is need of more effective fungicides with diverse mode of action. Towards this end, In **chapter 6**, I evaluated a new fungicide, Miravis Ace (a proprietary mix of Pydiflumetofen and Propiconazole active ingredients produced by Syngenta Inc.). Miravis Ace is based on succinate dehydrogenase inhibitor (SDHI) and demethylation inhibitor (DMI) mode of actions. This chapter was published

in “Plant Health Progress Journal”(Singh et al., 2020). Fungicide application timing is a critical factor for controlling FHB. In **chapter 7**, fungicide application timing of Miravis Ace was evaluated and this chapter was published in “Plant Health Progress” journal (Singh et al., 2021).

# Chapter 2: High resolution mapping and development of diagnostic KASP marker for FHB QTL in 'Jamestown' cultivar

## 2.1. Introduction

Wheat (*Triticum aestivum* L.) is the second most important food crop and contributes to one fifth of the calories and protein consumed by human population (FAOSTAT, 2019). Hence, sustainable wheat production is very critical for global food security. Fusarium Head Blight (FHB), caused by *Fusarium graminearum*, is one of the most devastating diseases of wheat worldwide leading to significant yield losses (Savary et al., 2019). FHB epidemics have been increasingly reported throughout the major wheat-producing countries in the last two decades (Ma et al., 2020). For instance, total annual losses associated with FHB have been reported as high as $ 1.4 billion in the US (Wilson et al., 2017). In addition to posing a major threat to food security, FHB-associated mycotoxin (primarily deoxynivalenol, DON) contamination inflicts a serious risk to humans and livestock health. Crop management practices and fungicide applications are partially effective in controlling FHB in wheat. The cultivation of FHB resistant varieties is the most effective, economically, and environmentally friendly strategy to manage FHB in wheat (McMullen et al., 2012). Therefore, breeding for FHB resistance remains one of the major goals of wheat breeding programs across the globe (Li et al., 2022).

FHB resistance is quantitative in nature and therefore, controlled by multiple loci and exhibit high Genotype × Environment (G× E) interaction (Mesterházy, 1995). In wheat, quantitative trait loci (QTLs) for FHB resistance have been reported in almost all the

chromosomes (Buerstmayr et al., 2009b, 2020). However, most of the QTLs exhibit minor effect with low stability and only few major effect QTLs have been identified in wheat. Till date only seven QTLs have been mendelized and assigned with gene names including: *Fhb1* on 3BS derived from *T. aestivum* variety Sumai 3 (Cuthbert et al., 2006), *Fhb2* on 6BS also from Sumai3 (Cuthbert et al., 2007), *Fhb3* on 7A derived from *Leymus racemosus* (Qi et al., 2008a), *Fhb4* on 4B derived from *T. aestivum* cv. Wangshuibai (Xue et al., 2010a), *Fhb5* on 5A derived from Wangshuibai (Xue et al., 2011a), *Fhb6* on 1A derived from *Elymus tsukushiensis* (Cainong et al., 2015a), and *Fhb7* on 7D derived from *Thinopyrum ponticum* (Guo et al., 2015a). Since most of these major effect resistance sources are derived from non-adapted backgrounds (Asian landraces or wild relatives), their introgression into locally adapted cultivars can be challenging due to associated linkage drag or background interactions. Thus, it is highly desirable to characterize and utilize native sources of genetic resistance derived from adapted germplasm (Liu et al., 2013; Carpenter et al., 2020).

Recently, two novel FHB resistance QTLs, *QFHB.vt-1B.1* and *QFHB.vt-1B.2*, were identified and characterized on the long arm of 1B chromosome of a soft red winter (SRW) wheat cultivar 'Jamestown'(Carpenter et al., 2020). The QTL effects were validated in three different populations. The *QFHB.vt-1B.1* explained up to 19.4% phenotypic variation for FHB severity and up to 9.2% variation for DON. The phenotypic variation explained by *QFHB.vt-1B.2* was up to 15.9% and 10.7% for FHB severity and DON, respectively.

DNA marker-assisted selection (MAS) is highly desirable for FHB resistance given challenges associated with phenotyping: high G×E interactions and requirement of adult plant

screening (Buerstmayr et al., 2009b). Single Nucleotide Polymorphism (SNP) markers are the markers of choice among contemporary breeding programs due to high throughput, gel-free detection, and low cost (Gupta et al., 2001; Singh and Singh, 2015). Kompetitive allele specific PCR (KASP) is a high-throughput and breeder friendly fluorescence-based genotyping platform for SNP markers (Semagn et al., 2014). KASP marker assays are being used for successful pyramiding of various QTLs for diverse traits in wheat (Kaur et al., 2020). Increasingly available genomics resources are providing new tools for marker development which were not available before in wheat (Consortium (IWGSC) et al., 2018b; Ramírez-González et al., 2018; He et al., 2019a; Walkowiak et al., 2020).

Although KASP assays for MAS were developed for Jamestown FHB QTLs, the QTLs were mapped across significantly large intervals (Carpenter et al., 2020). Therefore, the objectives of this study were to perform high-resolution mapping of the Jamestown FHB 1B QTL and develop diagnostic KASP assays for precise MAS for pyramiding of FHB resistance genes and alleles into elite wheat germplasm.

## 2.2. Materials and Methods

### *Plant material*

A previously reported recombinant inbred line (RIL) population at F5:8 generation developed from parents Pioneer Brand '25R47' (PR) and Jamestown (JT) cultivar was used in this study (Carpenter et al , 2020). Out of the two parents, PR is susceptible to FHB whereas JT is a widely adapted, high yielding and moderately FHB resistant soft red winter wheat cultivar.

The JT (PI 653671) cultivar resulted from a cross between the 'Roane' (PI 612958) and Pioneer Brand '2691' (PI 590941) developed by Virginia Tech wheat breeding group (Griffey et al., 2010). This has also been used in various Southern and Mid-Atlantic wheat breeding programs as a donor for FHB resistance (Griffey et al 2010).

A high-resolution mapping population was developed by crossing one highly susceptible RIL (PJT_62) and one highly resistant RIL (PJT_72). The four hundred seventy-five F2 individuals were genotyped and phenotyped for FHB. Subsequently, F2:3 families of selected F2 plants were used for genotypic and phenotypic analyses. Plants were maintained in greenhouse conditions with a day temperature of 25 ± 2 °C and night temperature at 22 ± 2 °C. Timely irrigation, fertilizer and insecticide treatments were applied.

***Fungal inoculum preparation and inoculations***

A highly aggressive strain of *Fusarium graminearum*, GZ3639, was used for all the greenhouse experiments in the study. The inoculum was prepared in Mung Bean Broth (MBB). MBB was prepared by steeping 20 g of mung bean seeds in 500 ml of hot water for 40 minutes. The collected filtrate was autoclaved and cooled. For macroconidia production, two mycelial plugs from one week old culture on Potato Dextrose Agar (PDA) were added per 50 ml of MBB and incubated at 28 °C and 250 rpm for 7-10 days. The spore culture was filtered through cheese cloth and macroconidia concentration was measured using hemocytometer. The macroconidia concentration was adjusted to $1 \times 10^5$ spores/ ml by diluting with sterile water. The spores were harvested freshly before each inoculation.

Inoculations were performed at pre-anthesis to anthesis stage. Tenth and eleventh spikelets from the base of the spikes were marked with a black permanent marker, and 10 µl of inoculum was injected between the lemma and palea of the florets (one floret/spikelet) using pipette. Inoculated spikes were covered with moisture saturated clear plastic bags for 72 h to provide high humidity for disease development.

***Disease assessment***

Two disease assessment parameters including FHB severity and DON content were measured. FHB severity was measured as percentage of symptomatic spikelets (PSS). PSS was measured by recording number of infected spikelets below the inoculation point including the tenth spikelet. Measurements were taken at 28 days post inoculation (dpi).

Inoculated spikes from each plant were harvested at maturity and manually threshed. Seeds from all inoculated spikes of each genotype per plant were pooled and ground to fine powder. The ground powder was redistributed to three replicates and used for the estimation of DON content. The DON content measurements were performed at USWBSI DON-testing laboratory at the University of Minnesota using gas chromatography-mass spectrometry (GC-MS) as previously described (Singh et al 2021).

***Marker development and genotyping***

For marker development, the previously reported flanking markers of 1B FHB QTL (Carpenter et al., 2020), IWB43992 and IWB7443, were localized on the reference genome RefSeq v 1.1 (International Wheat Genome Sequence Consortium) at the long arm of 1B

chromosome (Consortium (IWGSC) et al., 2018b). The 1B FHB QTL region spanned from 330.214153 Mb to 476. 880056 Mb with total length of 147 Mb. Total 150 primer pairs were designed at the regular intervals in the target 147 Mb region. The 1B genome specific PCR primers were designed using GSP software with default settings (Wang et al., 2016) or manual alignments with software SnapGene and screened for the polymorphism. 1B genome specificity was confirmed using the DNA of Nulli-tetrasomic line for 1B chromosome as a control. Out of 150, total 12 1B specific sequence-based markers with one or more than one SNP were identified and used for genotyping (Table 2.1).

For DNA extraction, leaf tissue was collected at the three-leaf stage in the 1.2 ml 96-deep well plates. After a snap freezing in the liquid nitrogen, tissue was ground into fine powder with metal beads using TissueLyser II (Qiagen, Germantown, MD). DNA was extracted using BioSprint 96 DNA Plant Kit (Qiagen, Germantown, MD) and KingFisher Flex system (Thermo Scientific, Waltham, MA) following manufacturer's protocol. The Polymerase Chain reactions (PCR) were performed in 25 µl reaction volume including 5 µl of 5X MyTaq buffer (Meridian Bioscience, Cincinnati, OH), 2 µl of each forward and reverse primers (4 µM/ µl), 0.1 µl of My Taq DNA Polymerase (Meridian Bioscience, Cincinnati, OH) and 50 ng of DNA template. A touch down PCR profile from 64 °C to 58 °C (95 °C for 5 min, 7 cycles of 95 °C for 45 sec, 64-58 °C for 45 sec with a decrease of 1 °C per cycle, 72 °C for 1 min, followed by 27 cycles of 95 °C for 45 sec, 58 °C for 45 sec, 72 °C for 1 min, and a final extension of 72 °C for 7 min) was ran on T100 thermal cycler (Bio-rad Laboratories Inc., CA). PCR products were resolved with agarose gel electrophoresis to check amplification and specificity. PCR products were cleaned up with

ExoSAP-IT reagent and then sequenced in-house using BigDye Terminator v3.1 cycle sequencing Kit and 3730xl DNA Analyzer (Thermo Scientific, Waltham, MA).

***KASP marker assay development***

Three 1B genome specific SNP markers at the target interval were used to develop KASP assays. The guidelines by Makhoul et al., ( 2020) were followed to design primers maintaining both genome and allele specificity. The allele specific SNP and genome specific SNP were kept at the 3' end of reverse and common forward primer, respectively. The FAM and HEX tags were appended the 5' end of the allele specific reverse primers. Ten microliters of KASP assay reaction included 5 µl of LGC KASP master mix, 0.14 µl of primer assay mix, and 5 µl of DNA template (10 ng/ µl). The assay mix included 12 µM of each reverse allele specific primer and 30 µM of common forward primer. The reactions were run on the BIO-RAD CFX96 Real Time System-C1000 touch thermal cycler using all channels option. The running profile was as follows: 94 °C for 15 min, 10 cycles of 94 °C for 20 s, 65-57 °C for 60 s with a decrease of 0.8 °C per cycle, followed by 39 cycles of 94 °C for 20 s and 57 °C for 60 s, with a subsequent plate reading step at 35 °C for 60 s. The allele calling was performed using allele discrimination mode of BIO-RAD CFX manager 3.1 version software.

***Statistical analyses***

Data were analyzed using GraphPad Prism version 9.3.1 and R statistical analysis software. In most cases, PSS and DON data were Log transformed to stabilize variances. One-Way Analysis of Variance (ANOVA) was performed followed by Fisher's LSD to detect

**Table 2. 1.** Genome specific sequence based polymorphic markers developed in this study.

| Marker name | Forward sequence 5'-3' | Reverse sequence 5'-3' | Physical coordinates on 1B | Gene ID |
|---|---|---|---|---|
| 330_1B_FHB | CAGGGTGTAAATGCACTGTGT | GAAGAAATTATCCGTGCTTGTTG | 330503665..330509502 | *TraesCS1B02G183800* |
| 336_1B_FHB | TCTGTCAAACCGCAATGAAG | AGATGAAAAGCCTGGGGG | 336202986..336205768 | *TraesCS1B02G187900* |
| 340_1B_FHB | CCTGGATCTAGTCATGAAACTTG | CACCAAATGCTAATGGCTCA | 340463564..340465967 | *TraesCS1B02G189800* |
| 349_1B_FHB | TGCTCTGATCCACCAAATACCAA | GCGACAGAGATGGCCTGCA | 349569330..349570806 | *TraesCS1B02G194500* |
| 355_1B_FHB | TTTCCATGTAACCTCGCAAAGA | ACCAGAACAAAACCACTGAGCAC | 355155044..355157167 | *TraesCS1B02G197600* |
| 357_1B_FHB | AGGTGCCACTTCAAACCTCG | CGAAAGTTCATTGAGCCGA | 357205847..357209219 | *TraesCS1B02G199000* |
| 364_1B_FHB | TTAAGCTGGCCAAATACTGTTTA | CTCATGGCCTATGTACGTCCG | 364289869..364294526 | *TraesCS1B02G202700* |
| 375_1B_FHB | ATAGCTACTTTTGCGATTCCAGG | GACCTGGGTAACCATTCCA | 375812152..375817099 | *TraesCS1B02G207800* |
| 380_1B_FHB | CGCTGCCACTCCTCCTTC | AACAAATTCATCCGTTTAGCTCC | 380435896..380440076 | *TraesCS1B02G209500* |
| 395_1B_FHB | AGTCAAAATCTGGATCGCCTCTA | GCTTCGACCATGATCACATT | 395258203..395260226 | *TraesCS1B02G218100* |
| 450_1B_FHB | CGCTGCGCTCTGTCACAT | GATTGACAGCACATACATGAGG | 450608891..450612736 | *TraesCS1B02G255800* |
| 491_1B_FHB | TGCTTCACCGATTCTCCGA | GAACATGCAAGAAAAGATACCAC | 491081622..491087500 | *TraesCS1B02G282200* |

**Table 2. 2**. Sequences of KASP primers developed in this study.

| Primer | Sequence 5'-3'[a] |
|---|---|
| KASP330-R | **GAAGGTGACCAAGTTCATGCT**TGCTTAATGCTGACATGGGTAAAAA*A* |
| KASP330-S | **GAAGGTCGGAGTCAACGGATT**TGCTTAATGCTGACATGGGTAAAAA*G* |
| KASP330-common | GTC*A*CTTAACAGGAGAGATAGAAGAA*C*A*A* |
| KASP340-R | **GAAGGTGACCAAGTTCATGCT**AGTGTTCCCTATTTTGAGCAAAAG*C* |
| KASP340-S | **GAAGGTCGGAGTCAACGGATT**AGTGTTCCCTATTTTGAGCAAAAG*A* |
| KASP340-common | ACATTA*T*GAATTTT*C*ACGTAA*A*CAAC*GC* |
| KASP355-R | **GAAGGTGACCAAGTTCATGCT**ATCAACGTGCAACTAATACATCTTAC*T* |
| KASP355-S | **GAAGGTCGGAGTCAACGGATT**ATCAACGTGCAACTAATACATCTTAC*C* |
| KASP355-common | *T*CACTAGTAATCGTGTA*T*GTGC*A* |

[a]Allele and genome specific SNPs are underlines and italicized. FAM and HEX sequences are highlighted in bold font.

statistically significant differences between genotypes. Single marker regression analyses in F2 population were performed using R package ggpubr.

## 2.3. Results

### *Identification of critical RILs*

Jamestown FHB QTL region was previously mapped to a 18.8 cM region on the peri-centromeric region of the long arm of chromosome 1B flanked by marker IWB43992 (74.4 cM) and IWB7443_1B (55.6 cM) in Pioneer25R47/ JT population (Carpenter et al. 2020). Physical location of these flanking markers on the long arm of 1B chromosome revealed 147 Mb region from 330 to 477 Mb coordinates. Total of twelve 1B genome specific sequence-base SNP markers were developed spanning the 160 Mb region downstream of IWB7443_1B (Table 2.1). After genotyping the RILs population, we identified five critical RILs with break points in the 147 Mb region: PJT_39, PJT_73, PJT_61, PJT_62, and PJT_7.

### *Phenotyping of critical RILs*

The set of critical RILs was robustly phenotyped for FHB response in the greenhouse conditions for three seasons. In addition to assessing disease severity by measuring PSS, DON content was measured for two seasons. In all three seasons, genotypes varied significantly (p

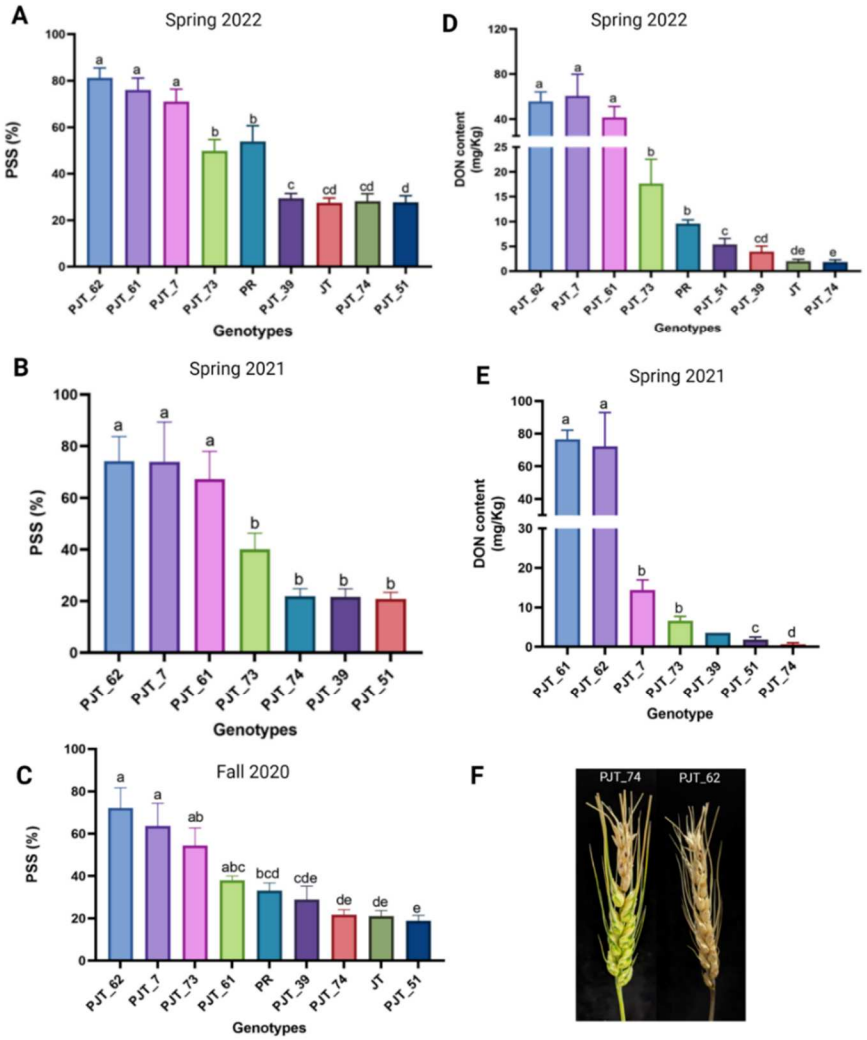


**Figure 2. 1. Phenotyping of critical RILs.** Mean PSS ±SE during spring 2022 (A), spring 2021 (B), and fall 2020 (C). Mean DON content ±SE during spring 2022 (D) and Spring 2021 (E). ( F) FHB symptoms in two contrasting RILs: PJT_74 and PJT_62 which used as parents of high ±SE resolution mapping population. Data for A, C, D, and E were log transformed before statistical analysis. Bars with different letter in each panel are statistically significantly different from each other at p value <0.05.

value < 0.001) for PSS. In spring 2022, the mean PSS ranged from 27 to 81 % (Figure 2.1 A). In 2021, mean PSS ranged from 21 to 74% (Figure 2.1 B).

A similar range of 18 to 72 % was observed for mean PSS in Fall 2020 (Figure 2.1 C). Statistical analysis for the mean differences enabled classification of the critical RILs into two phenotypic classes. PJT_62, PJT_61, PJT_7, and PJT_73 were identified as susceptible RILs with statistically significantly (p value <0.05) higher PSS than the resistant parent JT. On the other hand, PJT_39, PJT_51 and PJT_74 had significantly (p value <0.05) lower PSS value than these susceptible RILs and were identified as resistant RILs.

Similar trends were observed for the DON content. Genotypes varied significantly (p value < 0.001) for DON content in Spring 2021 and 2022. In 2022, mean DON content ranged from 1.8 to 60 mg/kg (Figure 2.1 D). In 2021, mean DON content varied from 0.7 to 77 mg/Kg (Figure 2.1 E). In agreement with the PSS, PJT_62, PJT_61, PJT_7, and PJT_73 RILS had significantly higher DON content than resistant RILS, PJT_39, PJT_51 and PJT_74.

The resistance response of original parents (PR and JT) of the RILs population was less contrasting than some of the susceptible and resistant RILS (Figure 2.1). For instance, mean PSS in JT compared to PR was lower by 26% and mean DON content was lower by 7.5 mg/Kg in Spring 2022 (Figure 2.1 A, D). Whereas mean PSS in PJT_74 compared to PJT_62 was 53% lower and mean DON content was lower by 54 mg/Kg (Figure 2.1 A, D). Therefore, some of these RILs were transgressive segregants.

***Refining mapping interval using critical RILs***

Comparative phenotypic and genotypic analyses of critical RILs helped in further narrowing the 147 Mb target region (Figure 2.2). Analysis of susceptible PJT_7 and PJT_39 ruled out the region downstream of 395 Mb. Analyses of susceptible PJT_61, PJT_62 and PJT_73 RILs narrowed down the target region between 330 to 355 Mb. Hence, 147 Mb mapping interval was further refined to 25 Mb.

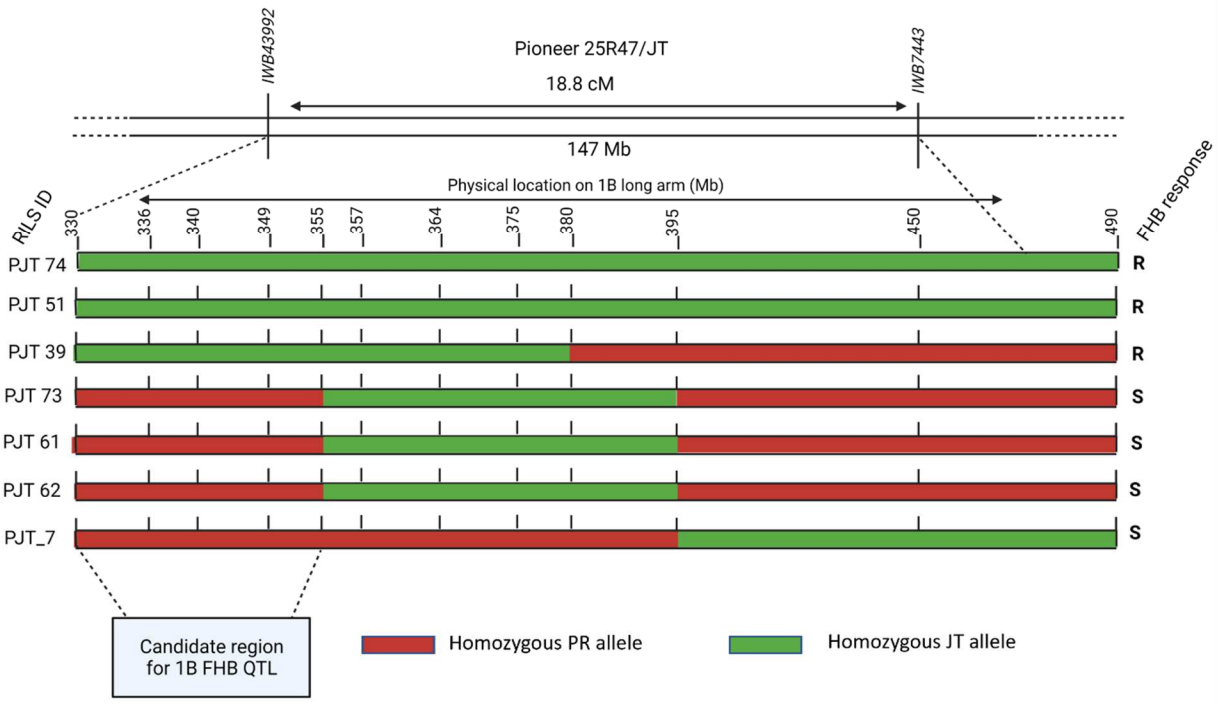


**Figure 2. 2. Mapping of 1B FHB QTL using critical RILs.** Genotyping scores were assigned based on the sequencing based GSP SNP markers. R: resistant to FHB and DON; S: susceptible to FHB and DON.

***Phenotypic and genotypic analyses of F2 mapping population***

PJT_62 and PJT_74 had consistently highly contrasting response to FHB (Figure 2.1) and were used to develop high resolution mapping population. Four hundred seventy-five F2 individuals of PJT_62/PJT_74 population were phenotyped for PSS. The mean PSS of the F2 population was 43.3% with a range of 18 to 100%. The frequency distribution of mean PSS of F2 individuals was continuous, therefore, indicating that PSS is controlled by multiple QTLs in this population (Figure 2.3.). Three KASP marker assays were developed at 330, 340 and 355 Mb region to genotype the F2 population (Table 2.2). All three KASP assays clearly differentiated for homozygous resistant, homozygous susceptible and heterozygous genotypes (Figure 2.4). F2 genotyping, and phenotyping data was used to perform single marker regression analysis. All three markers 330 ($r = 0.11$, *p value* = 0.016), 340 ($r = 0.15$, *p value* = 0.0011), and 355 ($r = 0.15$, *p value* = 0.0011) showed weak but positive and highly significant association with the PSS phenotype.

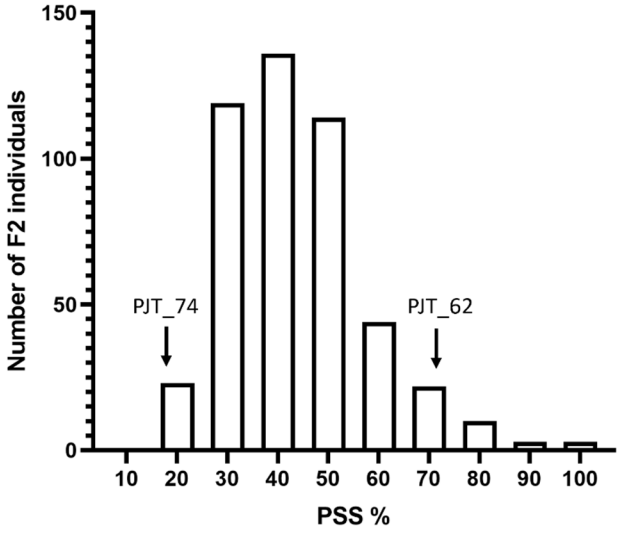


**Figure 2. 3. Frequency distribution for PSS (%) in the PJT_62/PJT_74 F2 population.**

***Mapping of 1B FHB QTL to a 6 Mb physical region***

To further narrow down the 25 Mb QTL region, recombinants were identified in this target region. Out of the 475 F2 individuals, only two plants had recombination in the target region. The 211_F2 plant was heterozygous for 330 and 340 markers and homozygous resistant for 355 marker (Figure 2.6). The 442_F2 had homozygous susceptible genotype for 330 and 340 markers whereas heterozygous for the 355 marker. After genotyping with additional sequencing-based markers, we identified break point for 211_F2 at 340 region and for the 442_F2 individual at the 349 region (Figure 2.6).

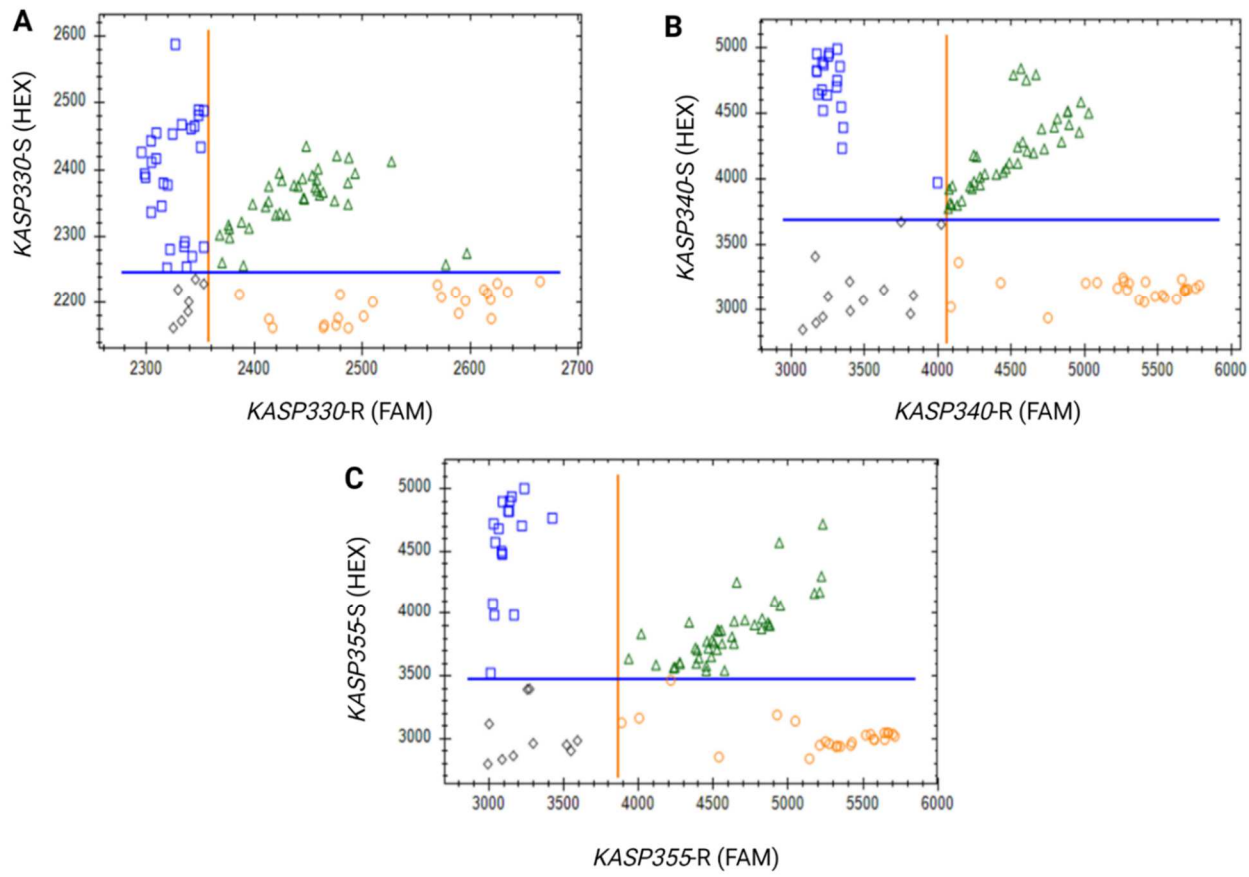


**Figure 2. 4. KASP assays developed in the study to genotype high resolution mapping population**. KASP assay developed for 330_ 1B _FHB (A), 340_1B_FHB (B), and 355 _1B_FHB (C) markers. Orange circles: homozygous for JT allele; Blue squares: homozygous for PR allele; Green triangle: heterozygous with JT/PR alleles; Black diamonds: no template controls (NTC) and nulli 1B DNA.

Subsequently, F2:3 families of 211 and 442 individual were screened for homozygous recombinants. Eight and eleven homozygous recombinants in the target 25 Mb region for F2:3 families of 211_F2 and 442_F2 plants, respectively. The selected F2 individuals and F2:3 families were tested for FHB response and DON content (Figure 2.5). The recombinant F2 plants and their F2:3 families had statistically significantly ($p < 0.05$) lower mean PSS and mean DON content compared to the susceptible parent PJT_62. Therefore, genotypic, and phenotypic analysis of recombinant F2 individuals narrowed the target region to 6 Mb between 349 and 355 Mb region (Figure 2.6).

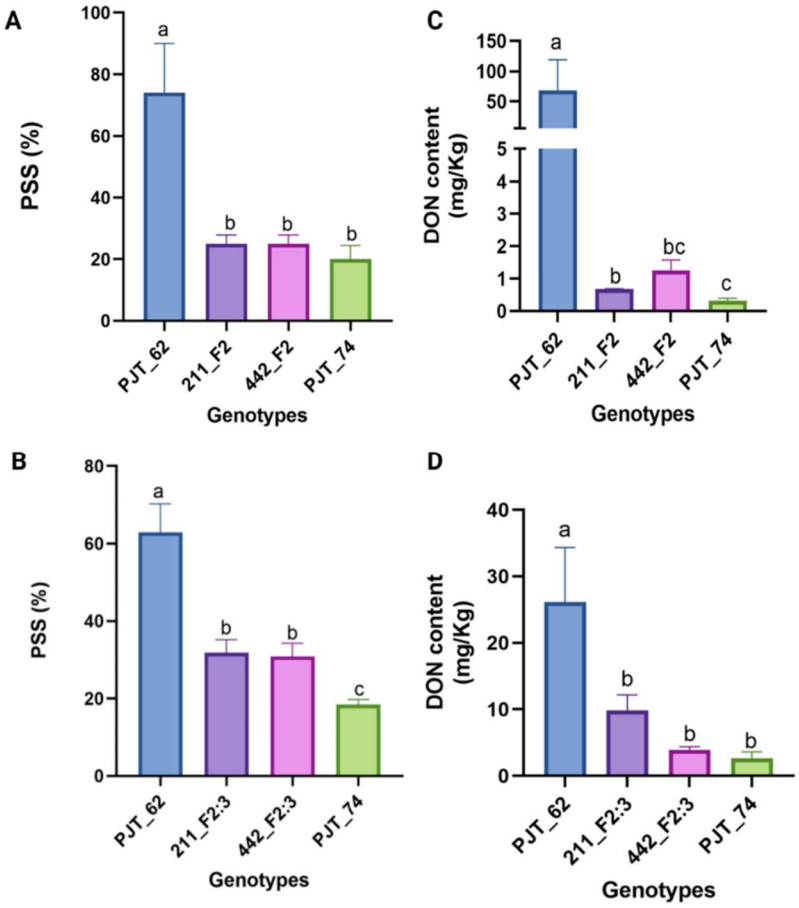


**Figure 2. 5. Phenotyping of recombinant F2 individuals and their homozygous recombinant F3 progenies.** A) Mean PSS ±SE of F2 plants and the parents (PJT_62 and PJT_74). B) Mean PSS ±SE of homozygous recombinant F2:3 progenies and the parents. C) DON content ±SE of F2 plants and the parents (PJT_62 and PJT_74). D) DON content ±SE of homozygous recombinant F2:3 progenies and the parents. Data were log transformed before the statistical analysis. Bars with different letters in each panel are statistically significantly different from each other at p value <0.05.

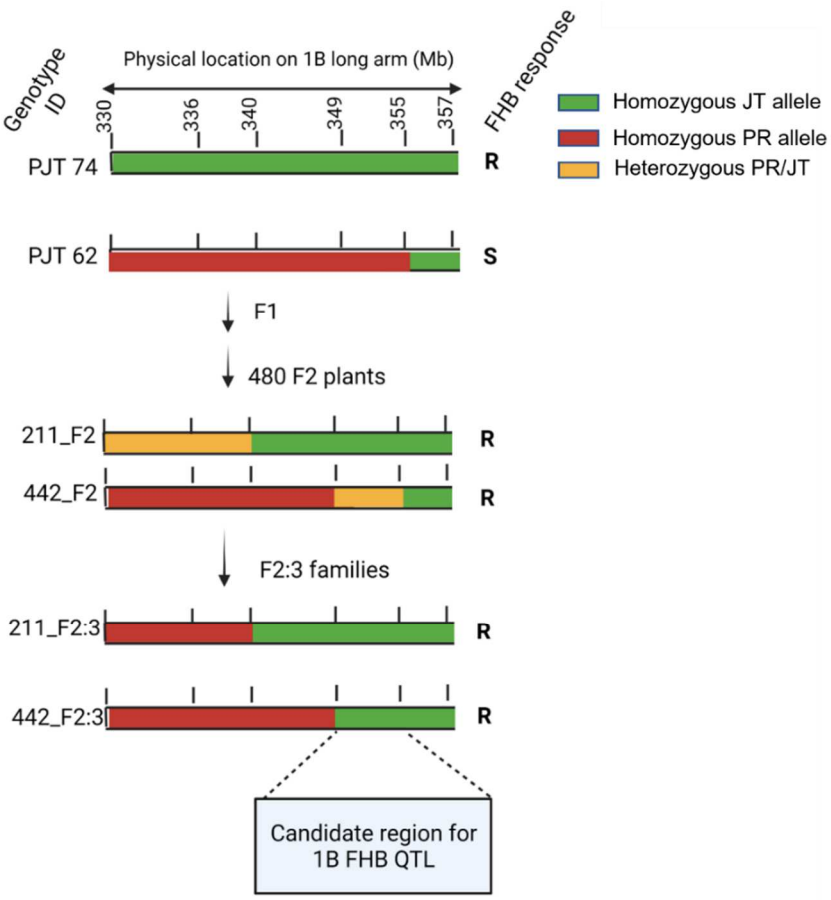


**Figure 2. 6. Mapping of 1B FHB QTL to 6 Mb interval.** High resolution mapping population was developed by crossing highly susceptible RIL PJT_62 and highly resistant RIL PJT_74. F2 population and F2:3 progenies were genotyped using KASP assays in the 25 Mb target region and genotypes were confirmed using sequencing based GSP SNP markers. R: resistant to FHB and DON; S: susceptible to FHB and DON.

***Candidate genes in the 6 Mb target region***

Total of 32 putative high confidence genes were retrieved form the IWGSC ref v 1.1 database in the 6 Mb target region (Table 2.3). The gene expression of these genes was analyzed in response to general disease stress and specific *F. graminearum* inoculations using publicly available transcriptomics data (Borrill et al., 2016; Ramírez-González et al., 2018). Out of 32 genes, 10 genes showed differential expression in response to disease stress (Figure 2.6 A). Subsequently, response of these 10 genes against *F. graminearum* at different time points was analyzed (Figure 2.6B). Three out of 10 disease responsive genes showed enhanced expression in response to *F. graminearum* specially at 48 and 96 hpi. These three *F. graminearum* responsive genes are putative Glutathione-S-transferase (GST) genes which are part of the GST cluster at 349 Mb region (Table 2.3).

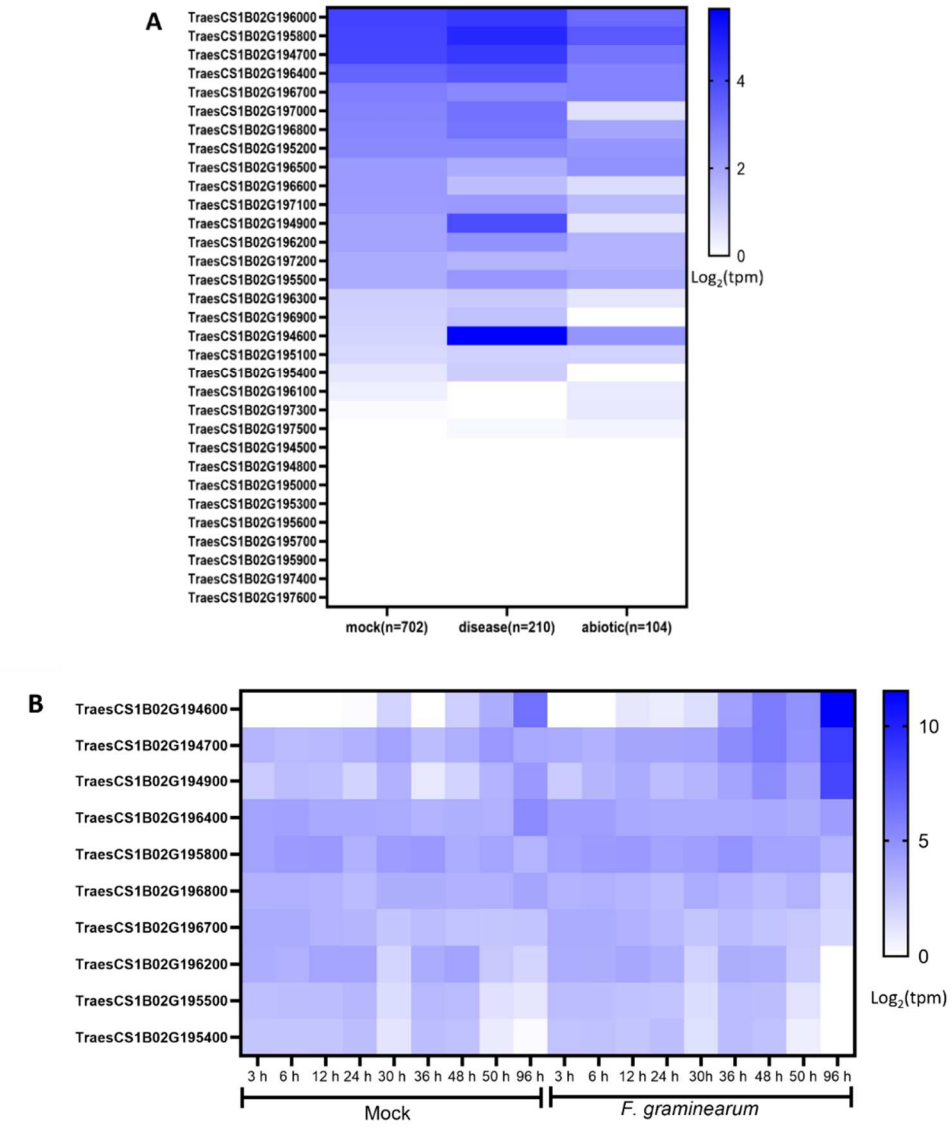


**Figure 2. 7.** Gene expression analysis of the putative high confidence genes in the target 6 Mb region. A) Gene expression pattern of all the 32 genes in responses to disease and abiotic stress. B) Gene expression pattern of 10 genes with differential gene expression to disease stress in response to *F. graminearum* inoculations at different time points. Data were obtained from the wheat expression browser (expVIP).

## 2.4. Discussion

Deploying genetic resistance is the most economical and sustainable strategy to control FHB in wheat. Given the genetics of FHB resistance with high GXE interaction, phenotypic evaluation of FHB resistance needs to be repeated over multiple environments. Therefore, phenotypic selection to improve FHB resistance is very time consuming and resource intensive (Bai and Shaner, 2004). Employing MAS using diagnostic markers can significantly improve the selection efficiency for improving FHB resistance. For developing a diagnostic marker, high resolution mapping of target region is prerequisite. Previously, two novel FHB resistance QTLs were identified in the high yielding and moderately FHB resistant cultivar "Jamestown"(Carpenter et al., 2020). This study reports the high-resolution mapping of one of the QTL, *QFHB.vt-1B.2.* Using the genotype and phenotype data of recombinants in the target interval, *QFHB.vt-1B.2* was placed in the in 6 Mb region between 349 and 355 Mb interval and a diagnostic KASP marker was developed from the flanking marker at 355 Mb.

Using recently completed wheat reference genome specific polymorphic markers were developed with in the 147 Mb physical region spanned by Jamestown FHB QTLs. These markers enabled the identification of critical set of RILs with recombination in the 147 Mb region. Comparative analysis of genotype and robust FHB and DON phenotype data narrowed down the target region to 25 Mb between 330 to 355 Mb region. The target 25 Mb region is located very close to the centromere and low recombination rates are reported in the

pericentromeric region of wheat (Saintenac et al., 2009; Jordan et al., 2018). Despite expected low recombination rate, recombinants were identified in the 25 Mb region by developing high-resolution mapping population between two contrasting RILs. Using the genotype and phenotype data of recombinants, Jamestown FHB QTL interval was further refined to 6 Mb region between 349 and 355 Mb.

KASP marker assays are breeder friendly, cost-effective marker platform for high throughput SNP genotyping of breeding materials (Semagn et al., 2014). For FHB resistance, diagnostic markers for *Fhb1* have been developed and have been widely used for MAS in breeding programs (Su et al., 2018; Singh et al., 2019). Development of co-dominant KASP markers is challenging in polyploids like wheat compared to diploid crops since genome specificity needs to be taken in consideration while developing KASP assays (Allen et al., 2013; Makhoul et al., 2020). In this study, three 1B genome specific KASP marker assays were developed. All three KASP assays clearly differentiated between homozygous and heterozygous individuals and followed expected genotyping ratio (1:2:1) in the F2 population. The KASP assay developed from a flanking marker, *KASP355,* would enable precise MAS for Jamestown FHB QTL.

The 6 Mb target region includes 32 high confidence genes. Using the publicly available transcriptomics data, differential expression in 10 of the 32 gene in response to disease stress was observed. Among them, only three genes responded with enhanced expression to *F. graminearum* infection which includes *TraesCS1B02G194600*, *TraesCS1B02G194700*, and *TraesCS1B02G194900*. These three genes encode putative Glutathione-S-transferase (GST).

GSTs are primarily known to be involved in cellular detoxification by conjugating the reduced glutathione to various hydrophobic and electrophilic compounds (Armstrong, 1997). GSTs are diverse class of enzymes widely distribute in prokaryotes and eukaryotes including plants. In plants, GSTs are involved in oxidative stress metabolism and also contributes to biosynthesis and transport of secondary metabolites (Loyall et al., 2000; Roxas et al., 2000; Dixon et al., 2010; Zhuge et al., 2020). Recently, one of the major effect FHB QTL, *Fhb7,* was cloned and reported to encode a GST (Wang et al., 2020). GST encoded by *Fhb7* had no similarity with plant GSTs but was homologous to a GST of an endophytic fungi suggesting horizontal gene transfer of *Fhb7*. Using biochemical studies, it was demonstrated that Fhb7 detoxified DON and other FHB trichothecenes by conjugating reduced glutathione to their epoxy group (Wang et al., 2020). While further studies are required to confirm causal gene in the target region, presence of GST cluster is very intriguing given their role in FHB specific detoxification has been demonstrated previously.

In conclusion, the native resistance to FHB severity and DON in SRW Jamestown cultivar we refined to a 6 Mb region. The breeder friendly diagnostic KASP marker developed in the study would be very useful resource for pyramiding FHB QTLs. Three potential candidate genes encoding putative GST with differential expression in response to disease stress and FHB infection were located in the target region. Hence, the resources developed in this study would enable efficient deployment of Jamestown FHB QTL and facilitate the efforts to identify underlying causal gene.

**Table 2. 1.** Putative high confidence genes in the 6 Mb 1B FHB target region.

| Gene ID | Physical location | Predicted Function | Key Domain |
|---|---|---|---|
| TraesCS1B02G194500 | 349569330..349570806 | Glutathione S-transferase | PF02798: Glutathione S-transferase, N-terminal domain; PF00043: Glutathione S-transferase, C-terminal domain |
| TraesCS1B02G194600 | 349571820..349572250 | Glutathione S-transferase | PF02798: Glutathione S-transferase, N-terminal domain |
| TraesCS1B02G194700 | 349595182..349596291 | Glutathione S-transferase | PF02798: Glutathione S-transferase, N-terminal domain; PF13410: Glutathione S-transferase, C-terminal domain |
| TraesCS1B02G194800 | 349725883..349740971 | Glutathione S-transferase | PF13417: Glutathione S-transferase, N-terminal domain |
| TraesCS1B02G194900 | 349830457..349831844 | Glutathione s-transferase, putative | PF13417: Glutathione S-transferase, N-terminal domain; PF13410: Glutathione S-transferase, C-terminal domain |
| TraesCS1B02G195000 | 349837971..349841397 | Cytochrome P450 family protein, expressed | PF00067: Cytochrome P450 |
| TraesCS1B02G195100 | 350025824..350028386 | Subtilisin-like protease | PF05922: Peptidase inhibitor I9; PF00082: Subtilase family; PF02225: PA domain |
| TraesCS1B02G195200 | 350391339..350397150 | Phospholipase D | PF00168: C2 domain; PF00614: Phospholipase D Active site motif; PF12357: Phospholipase D C terminal |
| TraesCS1B02G195300 | 350396376..350399362 | Oxygen-dependent choline dehydrogenase | PF00732: GMC oxidoreductase; PF05199: GMC oxidoreductase |
| TraesCS1B02G195400 | 350441372..350444210 | Ubiquitin carboxyl-terminal hydrolase-like protein | PF00917: MATH domain |

| | | | |
|---|---|---|---|
| TraesCS1B02G195500 | 350630695..350631492 | Peptidoglycan-binding LysM domain-containing protein | PF01476: LysM domain |
| TraesCS1B02G195600 | 350791880..350795469 | Na(+)/H(+) antiporter NhaB | |
| TraesCS1B02G195700 | 350875711..350876696 | Dehydration-responsive element binding factor protein | PF00847: AP2 domain |
| TraesCS1B02G195800 | 351439663..351441438 | Arogenate dehydratase | PF00800: Prephenate dehydratase |
| TraesCS1B02G195900 | 352333774..352335843 | Protein DETOXIFICATION | PF01554: MatE |
| TraesCS1B02G196000 | 352389744..352393541 | 2-oxoglutarate (2OG) and Fe(II)-dependent oxygenase superfamily protein | PF14226: non-haem dioxygenase in morphine synthesis N-terminal; PF03171: 2OG-Fe(II) oxygenase superfamily |
| TraesCS1B02G196100 | 352530115..352530312 | F-box and associated interaction domains-containing protein | |
| TraesCS1B02G196200 | 352878734..352883055 | U-box domain-containing protein 4 | PF00514: Armadillo/beta-catenin-like repeat |
| TraesCS1B02G196300 | 352888930..352891812 | Protein COFACTOR ASSEMBLY OF COMPLEX C SUBUNIT B CCB2, chloroplastic | PF11152: Cofactor assembly of complex C subunit B, CCB2/CCB4 |
| TraesCS1B02G196400 | 353274992..353277504 | F-box protein PP2-A13 | PF14299: Phloem protein 2 |
| TraesCS1B02G196500 | 353941810..353946564 | COP9 signalosome complex subunit 1 | PF10602: 26S proteasome subunit RPN7; PF01399: PCI domain |
| TraesCS1B02G196600 | 353945896..353947782 | Rhomboid-like protein | PF01694: Rhomboid family |
| TraesCS1B02G196700 | 354221647..354226486 | Protein kinase | PF00069: Protein kinase domain |
| TraesCS1B02G196800 | 354228370..354233215 | Ankyrin repeat-containing protein, putative | PF13637: Ankyrin repeats (many copies); PF00023: Ankyrin repeat |
| TraesCS1B02G196900 | 354233182..354235219 | Alpha/beta-Hydrolases superfamily protein | PF12146: Serine aminopeptidase, S33 |
| TraesCS1B02G197000 | 354239074..354240785 | Alpha/beta-Hydrolases superfamily protein | PF00561: alpha/beta hydrolase fold |
| TraesCS1B02G197100 | 354541706..354545485 | Membrane protein insertase YidC | PF02096: 60Kd inner membrane protein |

| | | | |
|---|---|---|---|
| TraesCS1B02G197200 | 354655124..354660718 | Membrane protein insertase YidC | PF02096: 60Kd inner membrane protein |
| TraesCS1B02G197300 | 354921905..354930229 | Membrane protein insertase YidC | PF02096: 60Kd inner membrane protein |
| TraesCS1B02G197400 | 354983169..354989241 | Membrane protein insertase YidC | |
| TraesCS1B02G197500 | 355103257..355107535 | Membrane protein insertase YidC | |
| TraesCS1B02G197600 | 355155044..355157167 | Actin-depolymerizing factor | PF00241: Cofilin/tropomyosin-type actin-binding protein |

# Chapter 3: Development and Validation of a perfect KASP Marker for Fusarium Head Blight Resistance Gene *Fhb1* in Wheat

Lovepreet Singh[1], James A Anderson[2], Jianli Chen[3], Bikram S Gill[4], Vijay K Tiwari[1], and Nidhi Rawat[1*]

[1]Department of Plant Science and Landscape Architecture, University of Maryland, College Park, MD 20742, USA

[2]Department of Agronomy and Plant Genetics, University of Minnesota, St. Paul, MN 55108, USA

[3]Department of Plant, Soil, and Entomological Sciences, University of Idaho, Aberdeen, ID 83210, USA

[4]Wheat Genetics Resource Center, Department of Plant Pathology, Kansas State University, Manhattan, Kansas, KS 66506, USA

***Corresponding author:** nidhirwt@umd.edu

This work was published in Singh et al., (2019). Headings and figure numbers were modified for consistency within this dissertation. Supplementary information is included in Appendix.

## 3.1. Abstract

Fusarium head blight (FHB) is a devastating wheat disease with a significant economic impact. *Fhb1* is the most important large effect and stable QTL for FHB resistance. A pore-forming toxin-like (*PFT*) gene was recently identified as an underlying gene for *Fhb1* resistance. In this study, I developed and validated a *PFT*- based Kompetitive allele specific PCR (KASP) marker for *Fhb1*. The KASP marker, PFT_KASP, was used to screen 298 diverse wheat breeding lines and cultivars. The KASP clustering results were compared with gel-based gene specific markers and the widely used linked STS marker, UMN10. Eight disagreements were found between KASP_PFT and UMN10 assays among the tested lines. Based on the genotyping and sequencing of genes in the *Fhb1* region, these genotypes were found to be common with a previously characterized susceptible haplotype. Therefore, our results indicate that PFT_KASP is a perfect diagnostic marker for *Fhb1* and would be a valuable tool for introgression and pyramiding of FHB resistance in wheat cultivars.

## 3.2. Introduction

Fusarium head blight (FHB), also known as head scab, is a devastating wheat disease with a significant economic impact. FHB incidences have been reported at epidemic levels across the USA, several parts of Canada, Europe, China and Korea since the 1990s {Citation}The total direct and indirect losses due to FHB in wheat and barley were estimated to be $ 7.67 billion from 1993 to 2001 across nine states in the northern Great Plains and the Central USA (Nganje et al., 2004).

In addition to lower yields, FHB infected grains accumulate trichothecenes and estrogenic mycotoxins that make grain unfit for animal and human consumption (Goswami and Kistler, 2004). Deoxynivalenol (DON) is the major toxin associated with FHB (McMullen et al., 1997) and its consumption causes vomiting, feed refusal, and diarrhea in animals (Bennett and Klich, 2003)In North America, *Fusarium graminearum* Schwabe is reported as a major causal agent of FHB. Besides wheat, the pathogen also infects other important cereal crops including barley, corn, oat, and rye (Goswami and Kistler, 2004).

Among various management practices, growing disease resistant cultivars is the most effective and economical disease management strategy against FHB (McMullen et al., 1997). Although quantitative trait loci (QTLs) associated with FHB have been found on all the wheat chromosomes, *Fhb1* is the most important large effect and stable QTL for FHB resistance (Buerstmayr et al., 2009b). *Fhb1* confers resistance against spread of the pathogen on the spike after initial infection, also known as type II resistance (Schroeder and Christensen, 1963). *Fhb1* is located on the short arm of chromosome 3B (Anderson et al., 2001; Xiao et al., 2011)A pore-forming toxin-like (*PFT*) gene was identified as an underlying gene for *Fhb1* resistance. *PFT* is a 3,472 bp gene with two exons which is predicted to encode two agglutinin domains and one pore forming ETX/MTX2 domain (Rawat et al., 2016).

DNA marker-assisted selection (MAS) is highly desirable for selecting FHB resistance because of its quantitative nature, high Genotype X Environment interaction (GXE), and requirement of adult plant screening (Buerstmayr et al., 2009b). Traditionally, MAS for *Fhb1* has been reported using linked simple sequence repeat (SSR) markers (Zhou et al., 2003; Miedaner et

al., 2006; Anderson et al., 2007; Wilde et al., 2007; Xie et al., 2007).However, linked SSR markers have limitations in their utility. First, recombination between the marker and underlying gene might occur after multiple selection cycles. Second, lack of polymorphism might become an issue with introgression into diverse genetic backgrounds. Third, haplotype variation of markers not associated with the causal gene can result in false positives or false negatives. Finally, SSR markers are gel-based markers and require a fragment analysis step in addition to polymerase chain reaction (PCR). Single Nucleotide Polymorphism (SNP) markers are the markers of choice among contemporary breeding programs due to high throughput, gel-free detection, and low cost (Gupta et al., 2001; Singh and Singh, 2015). Kompetitive allele specific PCR (KASP) is a high-throughput and breeder friendly fluorescence-based genotyping platform for SNP markers (Semagn et al., 2014). In wheat, KASP markers have been developed and validated for leaf rust resistance (Neelam et al., 2013), stem rust resistance (Babiker et al., 2015), wheat streak mosaic virus resistance (Tan et al., 2017)and pre-harvest sprouting resistance(Cabral et al., 2014). Although SNP markers (Bernardo et al., 2012)and a linked functional KASP markers (Rasheed et al., 2016; Su et al., 2018) have been reported for *Fhb1*, a gene specific perfect KASP marker has not been reported. Therefore, gene specific perfect KASP marker derived from *PFT* might enhance breeding efficiency for FHB resistance. The objectives of this study were to develop and validate a robust gene specific KASP marker for *Fhb1*.

## 3.3. Materials and Methods

### *Plant materials*

Previously, five different haplotypes for the *Fhb1* region, including one resistant (R) and four susceptible (S1, S2, S3, and S4) haplotypes were reported by Rawat et al (2016) in a panel of 40 land races and cultivars with well characterized FHB phenotype. *PFT* was present only in R and S3 haplotypes, and both haplotypes differ by two SNPs (Rawat et al. 2016). The panel of 40 landraces was used to test diagnostic ability of the KASP marker. For marker validation, 75 breeding lines from University of Idaho's spring wheat breeding program were used. Additionally, 223 diverse wheat entries including cultivars and breeding lines maintained at the University of Minnesota wheat breeding program was used for genotyping.


**Figure 3.1. Multiple sequence alignment of wheat accessions representing R and S3 haplotypes for PFT.** Shanasui, Wannin2, Sumai-3, Huoshawmai, Shuilizhan, and 701 Chokwang contain R haplotype, whereas Jingzhou1, Nanda2419, and Emai6 possess S3 haplotype. Asterisks designate the consensus sequence among all the genotypes. The position of allele specific and common primer is highlighted as bold underlined. The SNP targeted for developing PFT_KASP is highlighted as bold italics.

***Primer design***

For developing a *PFT* specific KASP marker, the G/A polymorphism between R and S3 haplotype at 2181 nucleotide position was targeted where G nucleotide was specific to R haplotype (Figure 3.1). The KASP marker, PFT_KASP, was designed at the target SNP from LGC genomics

(LGC Ltd, Teddington, UK). The sequences of two allele specific reverse primers and one common forward primer for PFT_KASP are given in Table 3.1. For validating the PFT_KASP marker, the 298 wheat breeding lines and cultivars were also screened for the STS marker UMN10 (Liu et al. 2008), gel-based gene specific markers for *PFT* (PFT_GSP), and a neighboring gene *SGNH* (SGNH_GSP) belonging to GDSL lipase superfamily in the *Fhb1* region (Table 3.1). The PFT_GSP was designed to target the G/A polymorphism between R and S3 haplotypes. The SGNH_GSP was also designed specifically amplify R haplotype. Additionally, neighboring genes Histidine-rich Ca-binding (His) and Terpene Synthase (TS) were sequenced in the eight lines showing disagreements between PFT_KASP and UMN10 using the markers provided in Table 3.1.

***Genotyping assays***

The KASP assay was performed in 10 µl reaction volume which included 5 µl KASP master mix, 0.14 µl KASP primer assay mix and 5 µl of 10 ng/ µl DNA template. The amplification and Fluorescent end-point reading were performed on a BIO-RAD CFX 96 (Bio-Rad Laboratories Inc., Hercules, CA, USA). The following cycling conditions were used: 94 ºC for 15 min, ten touchdown cycles of 94 ºC for 20 s and 61-55 ºC (dropping 0.6 ºC per cycle) for 1 min; followed by 26 cycles of 94 ºC for 20s and 55 ºC for 1 min. The Fluorescent end-point reading was done at 30 ºC for 1 min. The allele discrimination mode of BIO-RAD CFX manager 3.1 software was used for genotype calling.

**Table 3. 1.** List of primers used in the study

| Marker | Primer | Sequence (5'-3') |
|---|---|---|
| PFT_KASP | Reverse_G | AGCTGGGAATGAAGGAACCTGC |
| | Reverse_A | AGCTGGGAATGAAGGAACCTGT |
| | Common Forward | GTGATTATCTCTCCCATCTTATGTTTGCAA |
| PFT_GSP | Forward | ATAATCTCCTTGATGCTTTTACT |
| | Reverse | ACTATCAAGGCCCTCAATACCA |
| SGNH_GSP | Forward | CAATTCCAGCAGTTCATCAAC |
| | Reverse | CATACCCGCAACACACAT |
| His | Forward | AAGGAGAAGAAGCTCAAGTCG |
| | Reverse | CTGGGTTCAGCAGAGTTCGCAC |
| TS | Forward | GTACACTCGGGACCGTATGGTC |
| | Reverse | GGAGATGTCGTTGAGGAAGCGG |
| UMN10 (Liu et al. 2008) | Forward | CGTGGTTCCACGTCTTCTTA |
| | Reverse | TGAAGTTCATGCCACGCATA |

It is important to note that the distinction of S3 haplotype from R haplotype in this KASP assay is based on just one SNP, the strict use of the above thermocycler profile is recommended. The PCR for PFT_GSP and SGNH_GSP was performed in 25µl reaction volume including 5µl of 5x MyTaq$^{TM}$ Buffer (Bioline), 2 µl of each forward and reverse primer (4µM/µl), 0.1 µl of 5 U/ µl MyTaq$^{TM}$ DNA Polymerase (Bioline) and 75 ng of DNA template. The PCR amplifications were run on T100$^{TM}$ thermal cycler (Bio-Rad Laboratories Inc., Hercules, CA, USA) by using cycling profile as follows: 95 ºC for 5 min, five touchdown cycles of 95 ºC for 45 s, 65-60 ºC (dropping 1 ºC per cycle) for 45 s and 72 ºC for 1 min; followed by 27 cycles of 95 ºC for 45 s, 60 ºC for 45 s and 72 ºC for 1 min; with final extension for 7 min at 72 ºC.

The PCR products were visualized with ethidium bromide after running on 1.8 % agarose gels. The methods for UMN10 genotyping were as described previously (Liu et al. 2008).

**Table 3. 2.** Genotyping results of PFT_KASP, UMN10, SGNH_GSP, and PFT_GSP markers on the set of University of Idaho wheat breeding lines used for validation of PFT_KASP marker.

| Breeding line ID | Pedigree | PFT_KASP | UMN10 | SGNH_GSP | PFT_GSP |
|---|---|---|---|---|---|
| A12023S-1 | IDO850/W14//IDO852 | S | S | S | S |
| A12023S-4 | IDO850/W14//IDO852 | S | S | S | S |
| A12023S-5 | IDO850/W14//IDO852 | S | S | S | S |
| A12025S-1 | IDO850/W14//IDO854 | S | S | S | S |
| A12025S-2 | IDO850/W14//IDO854 | R | R | R | R |
| A12025S-4 | IDO850/W14//IDO854 | S | S | S | S |
| A12035S-1 | IDO851/W14//IDO851 | S | S | S | S |
| A12037S-3 | IDO851/W14//IDO854 | S | S | S | S |
| A12037S-5 | IDO851/W14//IDO854 | S | S | S | S |
| A12037S-7 | IDO851/W14//IDO854 | S | S | S | S |
| A12056S-10 | IDO852//IDO852/W14 | S | S | S | S |
| A12056S-11 | IDO852//IDO852/W14 | S | S | S | S |
| A12056S-12 | IDO852//IDO852/W14 | S | S | S | S |
| A12056S-13 | IDO852//IDO852/W14 | S | S | S | S |
| A12062S-6 | IDO854/W14//IDO851 | R | R | R | R |
| A12062S-8 | IDO854/W14//IDO851 | R | H | R | R |
| A12062S-9 | IDO854/W14//IDO851 | R | H | R | R |
| IDO1405S | 2016 F311 E border | S | S | S | S |
| A12063S-9 | IDO854/W14//IDO854 | S | S | S | S |

| | | | | | |
|---|---|---|---|---|---|
| A12063S-10 | IDO854/W14//IDO854 | S | S | S | S |
| A12063S-12 | IDO854/W14//IDO854 | S | S | S | S |
| A12064S-1 | IDO854/W14//IDO854 | S | S | S | S |
| A12064S-2 | IDO854/W14//IDO854 | S | S | S | S |
| A12064S-8 | IDO854/W14//IDO854 | S | S | S | S |
| A12064S-9 | IDO854/W14//IDO854 | S | S | S | S |
| A12064S-11 | IDO854/W14//IDO854 | S | S | S | S |
| A12077S-2 | IDO696//IDO696/W14 | S | S | S | S |
| A12084S-3 | IDO687//IDO687/W14 | R | H | R | R |
| A12084S-5 | IDO687//IDO687/W14 | R | H | R | R |
| A12084S-6 | IDO687//IDO687/W14 | R | H | R | R |
| A12084S-7 | IDO687//IDO687/W14 | S | S | S | S |
| A12086S-3 | IDO687/W14//IDO687 | R | R | R | R |
| A12086S-10 | IDO687/W14//IDO687 | R | R | R | R |
| A12086S-12 | IDO687/W14//IDO687 | R | R | R | R |
| A12086S-13 | IDO687/W14//IDO687 | S | S | S | S |
| A12004S-1 | IDO694/N9016/3/JFSN*4/IDO584 (70-5)//Lassik | S | S | S | S |
| A12004S-3 | IDO694/N9016/3/JFSN*4/IDO584 (70-5)//Lassik | S | S | S | S |
| A12004S-10 | IDO694/N9016/3/JFSN*4/IDO584 (70-5)//Lassik | S | S | S | S |
| A12004S-14 | IDO694/N9016/3/JFSN*4/IDO584 (70-5)//Lassik | S | S | S | S |
| **IDO1603S** | 2016 Gp 100 | **S3** | **R** | **S** | **S** |
| UI Stone | 2016 Gp 100 | S | S | S | S |
| A12004S-15 | IDO694/N9016/3/JFSN*4/IDO584 (70-5)//Lassik | S | S | S | S |
| A12004S-16 | IDO694/N9016/3/JFSN*4/IDO584 (70-5)//Lassik | S | S | S | S |

| | | | | | |
|---|---|---|---|---|---|
| A12004S-17 | IDO694/N9016/3/JFSN*4/IDO584 (70-5)//Lassik | S | S | S | S |
| A12004S-18 | IDO694/N9016/3/JFSN*4/IDO584 (70-5)//Lassik | S | S | S | S |
| **A12004S-19** | IDO694/N9016/3/JFSN*4/IDO584 (70-5)//Lassik | **S3** | **R** | **S** | **S** |
| A12004S-20 | IDO694/N9016/3/JFSN*4/IDO584 (70-5)//Lassik | S | S | S | S |
| A12004S-21 | IDO694/N9016/3/JFSN*4/IDO584 (70-5)//Lassik | S | S | S | S |
| **A12004S-24** | IDO694/N9016/3/JFSN*4/IDO584 (70-5)//Lassik | **S3** | **R** | **S** | **S** |
| A12004S-27 | IDO694/N9016/3/JFSN*4/IDO584 (70-5)//Lassik | S | S | S | S |
| A12004S-28 | IDO694/N9016/3/JFSN*4/IDO584 (70-5)//Lassik | S | S | S | S |
| A12004S-29 | IDO694/N9016/3/JFSN*4/IDO584 (70-5)//Lassik | S | S | S | S |
| A12004S-30 | IDO694/N9016/3/JFSN*4/IDO584 (70-5)//Lassik | S | S | S | S |
| A12041S-1 | IDO851/N9016//IDO851 | S | S | S | S |
| A12041S-3 | IDO851/N9016//IDO851 | S | S | S | S |
| A12041S-4 | IDO851/N9016//IDO851 | S | S | S | S |
| A12041S-5 | IDO851/N9016//IDO851 | S | S | S | S |
| A12079S-1 | IDO686/N9016//IDO686 | S | S | S | S |
| A12089S-3 | IDO687/N9016//IDO687 | S | S | S | S |
| A12089S-6 | IDO687/N9016//IDO687 | R | H | R | R |
| A12089S-7 | IDO687/N9016//IDO687 | S | S | S | S |
| A12089S-8 | IDO687/N9016//IDO687 | S | S | S | S |
| A12089S-9 | IDO687/N9016//IDO687 | S | S | S | S |
| A12089S-10 | IDO687/N9016//IDO687 | S | S | S | S |
| A12089S-11 | IDO687/N9016//IDO687 | S | S | S | S |
| A12089S-12 | IDO687/N9016//IDO687 | R | R | R | R |
| A12089S-13 | IDO687/N9016//IDO687 | S | S | S | S |
| A12089S-14 | IDO687/N9016//IDO687 | S | S | S | S |

| | | | | | |
|---|---|---|---|---|---|
| A12089S-16 | IDO687/N9016//IDO687 | S | S | S | S |
| A12089S-18 | IDO687/N9016//IDO687 | S | S | S | S |
| A12089S-19 | IDO687/N9016//IDO687 | S | S | S | S |
| A12089S-20 | IDO687/N9016//IDO687 | S | S | S | S |
| A12089S-21 | IDO687/N9016//IDO687 | S | S | S | S |
| A12039S-2 | IDO851/Futai 8944//IDO854 | R | H | R | R |
| A12039S-3 | IDO851/Futai 8944//IDO854 | S | S | S | S |

*Disagreements between PFT_KASP and UMN10 are highlighted in red font.

**R- presence of resistant allele; S- presence of susceptible allele in case of UMN10 and absence of allele for PFT_KASP, PFT_GSP and SGNH_GSP; H-presence of both resistant and susceptible alleles; S3- presence of non-functional *PFT* allele (S3 haplotype)

### 3.4. Results and discussion

The KASP assay developed for *PFT* targeted the SNP between R and S3 haplotype (Figure 3.1), and all the other susceptible haplotypes do not have *PFT* therefore, PFT_KASP behaves as a dominant marker. The PFT_KASP assay accurately clustered genotypes into three clusters of R haplotype, S3 haplotype and other susceptible haplotypes in a diverse set of wheat germplasm (Figure 3.2). Since the rate of recombination is very low in the *Fhb1* region (Rawat et al., 2016; Schweiger et al., 2016), other co-dominant markers known from the *Fhb1* region such as widely used UMN10 (Liu et al., 2008) or recently reported HRC-GSM (Su et al. 2018) may be used to discern heterozygosity or homozygosity in breeding programs.

To validate the specificity of PFT_KASP, it was used in conjunction with SGNH_GSP, PFT_GSP and UMN10 marker to genotype a set of 75 spring wheat breeding lines from Idaho's wheat breeding program (Table 3.2). Thirteen lines were found to be resistant with PFT_KASP, SGNH_GSP and PFT_GSP, whereas three additional lines gave 'R' genotype with UMN10. The lines that showed resistant haplotype with PFT_KASP had Sumai 3- derived or related *Fhb1* gene in their pedigree. Similarly, in the panel of 223 cultivar and breeding lines from Minnesota, 24 were found to be resistant using PFT_KASP, SGNH_GSP and PFT_GSP markers, whereas five additional lines were scored as 'R' using UMN10 marker (Appendix I). Genotyping data

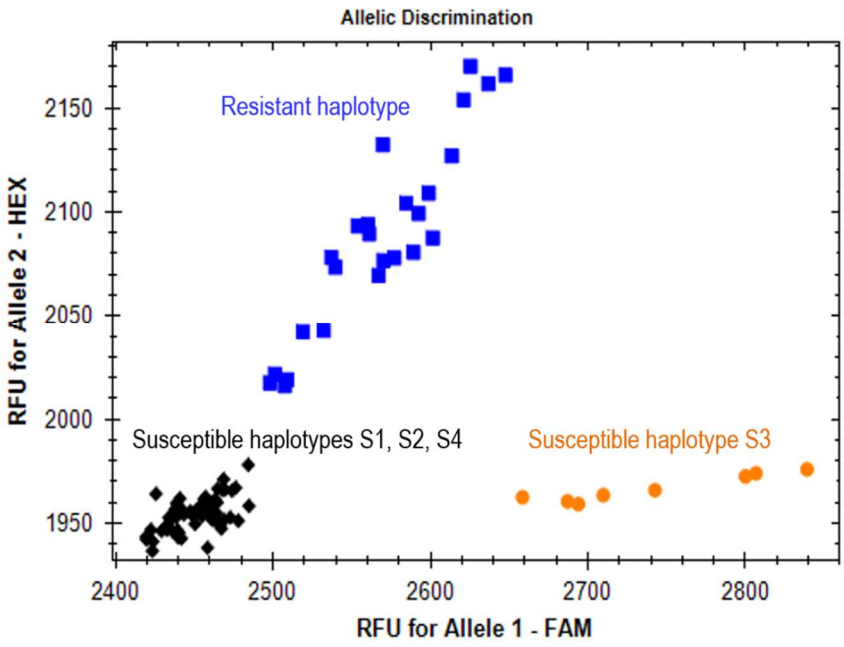


**Figure 3. 2. Genotyping results of PFT_KASP marker on panel of different genotypes and controls**. Genotypes clustered as blue squares in the upper left corner are homozygous for resistant (R) haplotype. Genotypes clustered in the lower right corner as orange circles are homozygous for susceptible (S3) haplotype. Genotypes which do not possess either allele are clustered with NTCs (No template control) as black diamonds in the lower left corner.

for all 298 lines was in complete agreement with each other for PFT_KASP, SGNH_GSP and PFT_GSP markers, whereas 8 disagreements were observed between them and UMN10 marker.

**Table 3. 3.** Haplotypes of genes spanning Fhb1 region in the eight lines showing disagreements between PFT_KASP and UMN10 genotyping

| Entry | Gene/marker[a] Haplotypes | | | | |
|---|---|---|---|---|---|
| | *TS*[b] (107455-110336) | *His*[b] (111389-112213) | UMN10[c] (128656-128857) | *PFT*[c] (163305-166507) | *SGNH*[c] (195191-196533) |
| IDO1603S | R | R | R | S3 | S |
| A12004S-19 | R | R | R | S3 | S |
| A12004S-24 | R | R | R | S3 | S |
| H0900081 | R | R | R | S3 | S |
| Lassik | R | R | R | S3 | S |
| UC1603 | R | R | R | S3 | S |
| UC1618 | R | R | R | S3 | S |
| 9263 | R | R | R | S3 | S |

[a]Genes/markers and their respective physical coordinates in Sumai 3 *Fhb1* region sequence (KX907434.1) where TS: Terpene Synthase, His: Histidine rich calcium-binding protein, PFT: Pore-forming toxin-like gene, and SGNH: SGNH Plant lipase

[b]Haplotypes identified based on sequencing

[c]Haplotypes identified based on genotyping with markers

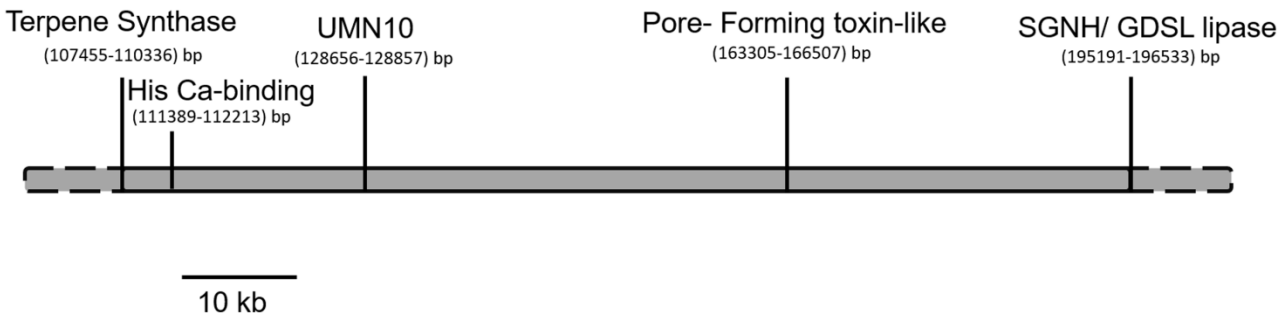


**Figure 3.3.** Order and location of genes and markers on Fhb1 genomic assembly (Rawat et al., 2016) used to resolve the haplotypes of the eight breeding lines/cultivars with disagreement between UMN10 and PFT.

The disagreement in genotypes of the eight lines for PFT_KASP and UMN10 among the total 298 lines screened could be due to any genetic recombination that may be present between *PFT* and UMN10 or a possibility of a different haplotype in these lines as compared to other susceptible haplotypes. It should be noted that rate of recombination is known to be very low for this region (Schweiger et al. 2016). To discern the origin of the disagreement in these lines, two genes located upstream of UMN10 in the *Fhb1* region were sequenced: Histidine rich calcium-binding protein (*His*) and Terpene Synthase (*TS*). Figure 3.3 shows the location and order of all the markers used for resolving the disagreements. The sequences of *His* and *TS* matched to the 'R' haplotype in all the eight entries with disagreements, whereas PFT and SGNH genotyping showed them to be susceptible haplotypes (Table 3.3), this was similar to a previously characterized susceptible 'S3' haplotype reported in Rawat et al. (2016). The 'R' score for these eight lines identified with UMN10 was not accurate and further validated the sensitivity of

PFT_KASP assay and lack of polymorphism in UMN10 between R and S3 haplotypes. Previously, UMN10 has been used for conducting MAS for *Fhb1* with an assumption of tight marker and trait linkage (Zhang et al. 2016). However, the UMN10 based KASP marker developed in a previous study detected some false positives (Rasheed et al. 2016). Thus, our results underscore the limitation of linked markers over perfect markers.

PFT_KASP is a perfect diagnostic marker for *Fhb1* and will be a valuable resource for wheat breeders to develop FHB resistant cultivars. It will enhance the efficiency of introgression and pyramiding of FHB resistance genes in wheat varieties.

### 3.5. Acknowledgements

This work was supported by the USDA National Institute of Food and Agriculture, Hatch project 1016879 and Maryland Agricultural Experiment Station via MAES Grant No. 2956952.

# Chapter 4: Wheat Pore-Forming toxin-like (*PFT*) gene confers broad-spectrum resistance against fungal pathogens in transgenic Arabidopsis.

## 4.1. Introduction

Plants encounter various life-threatening microbial pathogens in the environment including fungi, bacteria, viruses, and nematodes. Fungal pathogens cause the greatest damage to global food crop production than any other pathogenic microbes (Savary et al., 2019). Growing disease resistance cultivars is the most cost-effective and environmentally friendly approach to manage fungal diseases. Most of the characterized plant disease resistance (R) genes confer resistance against specific strains of pathogens in gene-for-gene interaction fashion (Jones and Dangl, 2006; Dodds and Rathjen, 2010). R gene mediated resistance has often limited durability in the field conditions (Ning and Wang, 2018; Stam and McDonald, 2018). Furthermore, host resistance might not be available in some pathosystems. Another class of less studied disease resistance is broad spectrum resistance (BSR). BSR genes confers resistance to two or more pathogen species or against the majority of races of same species (Kou and Wang, 2010; Li et al., 2020). Given their wider applicability and long durability, BSR genes are ideal targets for engineering disease resistance in crop plants (Ning and Wang, 2018; Li et al., 2020; Tian et al., 2020). Therefore, the identification and characterization of BSR is a major goal in crop improvement.

Wheat Pore-forming toxin-like (*PFT*) gene confers durable resistance against various *Fusarium sp.*, which cause Fusarium Head Blight in wheat. *PFT* encodes an atypical resistance protein with a combination of two types of domains, both of which are known to have defense roles. PFT is predicted to be a chimeric plant lectin with two amaranthin domains (agglutinin domains of *Amaranthus caudatus)* and one bacterial epsilon toxin (ETX) / mosquitocidal toxin (MTX2) domain of aerolysin pore-forming toxin family (Rawat et al., 2016). So far proteins with domain architecture of two amaranthin domains and an aerolysin pore-forming toxin domain have been partially characterized in wheat (Puthoff et al., 2005), flax (Faruque et al., 2015), cucumber (Dang et al., 2017) and *Rumex acetosa* plants (Manzano et al., 2017). Out of these, only wheat HFR-2 is involved in plant defense against insects (Puthoff et al., 2005). Therefore, PFT is the only protein with its kind of domain architecture known to be involved in defense against phytopathogenic fungus. It is proposed that the agglutinin domains could recognize fungal-specific carbohydrates and ETX/ MTX2 domain might induce pores in fungal cell membrane ultimately arresting fungal growth (Rawat et al., 2016). Its predicted mechanism of action makes PFT a suitable candidate for characterizing its broad-spectrum action against diverse fungal pathogens.

Subcellular localization can provide valuable insight into protein function (Shaw 2006; Tanz et al., 2013). Fluorescent protein (FP) tagging is one of the major tools for predicting protein localization in the plant cell (Tanz et al., 2013). Furthermore, FP tagging based protein localization using Confocal Laser Scan Microscopy (CLSM) could provide valuable insight into

the molecular mechanism of resistance genes by examining live subcellular interactions between FP tagged resistance protein and FP tagged pathogen. For example, Wang et. al (2009) revealed the molecular mode of action of broad-spectrum resistance protein RPW8.2 using FP tagging. They demonstrated the localization of yellow fluorescence protein (YFP) tagged RPW8.2 to extra-haustorial membrane of powdery mildew fungus. Thus, encasing of fungal haustorium by RPW8.2 protein leads to disease resistance (Wang et al., 2009).

Given the domain architecture of PFT, it is hypothesized that PFT confers broad spectrum resistance against fungal pathogens. To test this hypothesis, Arabidopsis transgenic plants expressing wheat *PFT* were generated and tested for their resistance response to four economically important fungal pathogens. Additionally, subcellular localization patterns of GFP tagged PFT were studied.

## 4.2. Materials and Methods

### *Cloning of PFT into a plant expression vector and plant transformation*

To derive *PFT* cDNA sequence, RNA extracted from the wheat cultivar 'Sumai 3' was reverse transcribed using Superscript III reverse transcription kit (ThermoFisher Scientific, Waltham, MA). The full length *PFT* with attB flanking sites was amplified using *PFT* primers (Table 4.1). The attB *PFT* PCR product was cloned into entry vector pDONR221 using gateway BP clonase reaction (ThermoFisher Scientific, Waltham, MA). LR clonase reaction was

performed to clone *PFT* into plant expression destination vector pK7WGF2 (Karimi et al., 2002) with an enhanced green fluorescent protein (EGFP) tag at N terminus and driven by 35S CaMV promoter. Thus, the resulting GFP: PFT fusion construct had both kanamycin resistance gene (*nptII*) and GFP fluorescence which served as selectable markers. The construct was confirmed for accuracy by Sanger sequencing and was transformed into *Agrobacterium tumefaciens* strain GV3101 via electroporation. Previously, Arabidopsis (*Arabidopsis thaliana)* ecotype Landsberg erecta (Ler) has been reported to be susceptible to *F. graminearum* infection (Urban et al., 2002; Chen et al., 2006). Therefore, Ler ecotype was used for transformation. Ler plants were transformed using floral dip method (Clough and Bent, 1998). $T_0$ seeds were plated on MS media with Kanamycin (50 mg/liter). Kanamycin-resistant $T_1$ plants were further screened for GFP signal using Nikon Eclipse epifluorescence microscope. $T_1$ plants were grown for $T_2$ seeds, which were further selected for homozygous individuals. Two to three independent $T_2$ families were used for disease assays.

**Table 4. 1.** Primers used in this study.

| Primer name | Forward sequence (5'-3') | Reverse sequence (5'-3') | Reference |
|---|---|---|---|
| PFT_BP | GGGGACAAGTTTGTACAAAAAAGCAGGCTTCATGTTTCCGCTGTCAGCTTTG | GGGGACCACTTTGTACAAGAAAGCTGGGTCCTATCACAGGTGTTCTTCTTTGG | this study |
| TRI6 | TCTTTGTGAGCGGACGGGACTTTA | ATCTCGCATGTTATCCACCCTGCT | Horevaj et al., ( 2011) |
| ChITS2 | AAAGGTAGTGGCGGACCCTC | GGCAAGAGTCCCTCCGGAT | Salvador-Guirao et al., (2018) |
| SsTub | ACCTCCATCCAAGAACTC | GAACTCCATCTCGTCCAT | Wei et al., (2022) |
| Bc-CutA | AGCCTTATGTCCCTTCCCTTG | GAAGAGAAATGGAAAATGGTGAG | Ono et al., (2020) |
| UBC | TGTAACCATGGGCGTTCGGGTA | ACCCGAACCTGAACCGAACTGA | Czechowski et al., (2005) |

***Plant growth conditions***

Arabidopsis plants were grown in a growth chamber at 22-23 °C temperature with 50-70 % relative humidity (RH). For plants to be tested for leaf assays, the light intensity was maintained in the range of 80 -110 µmol $m^{-2}$ $s^{-1}$ with 10/14 h light/dark cycle. For the plants to be tested for floret assay, the light / dark cycle was adjusted to 16/ 8 h with same light intensity. The plants were irrigated and fertilized as needed.

***Fungal pathogens and inoculum preparation***

For *Fusarium graminearum* inoculations, a highly virulent strain of, GZ3639, was used in this study. The conidial inoculum was produced in mung bean broth (MBB). MBB was

prepared by steeping 20 g of mung bean seeds in 500 ml of hot water for 40 minutes. The collected filtrate was autoclaved and cooled. For macroconidia production, two 1cm mycelial plugs taken from one week old fungal culture on Potato Dextrose Agar (PDA) plate were added to 50 ml MBB and shaken at 200 rpm at 28 °C for 7-10 days. To collect conidia, the spore culture was filtered through sterile cheesecloth and centrifuged at 4,000 g for 8 min. The spore pellet was resuspended in sterile water and quantified using a hemocytometer. The spores were freshly harvested before each disease assay and adjusted to the desirable concentration using sterile water.

*Colletotrichum higginsianum* was provided by Dr. Melvin Bolton, USDA-ARS Fargo, North Dakota. Conidia production was induced on Oatmeal Agar (30 g ground oats, 15 g Agar per 1 L water). The spores were harvested from a one-week-old culture with the help of 100 µl pipette and suspended in sterile water. The spore suspension was filtered through two layers of cheese cloth and quantified using a hemocytometer. Finally, the spore concentration was adjusted to $5 \times 10^5$ spores/ ml.

*Sclerotinia sclerotiorum* was provided by Dr. Kate Everts, University of Maryland. The fungal mycelia were grown on PDA plate at room temperature. Mycelial plugs 5-mm in diameter taken from a five-day old culture were used as inoculum.

*Botrytis cinerea* strain B05-10 was used for inoculations. The fungus was cultured on PDA plates at 22 °C. Fungal spores were harvested from 9-days-old cultures and suspended in sterile water with 0.02% Tween-20. The suspension was filtered through two layers of cheesecloth, and the concentration of spores was adjusted to $5x10^5$ spores/ml.

***Leaf inoculation assays***

For leaf *F. graminearum* inoculations, detached leaf assays were performed as described by Chen et al (2006) with some modifications. Rosette leaves were collected from 4–5-week-old plants. The leaves were wounded at the adaxial surface on the mid rib by making point injury with 10 µl pipette tip and transferred to a clear petri plate lined with 2-3 layers of sterile wet Kimwipes. Five microliters of inoculum with the concentration of $5 \times 10^5$ spores/ ml amended with 75 µM of deoxynivalenol (DON) (Sigma Aldrich) was applied to wounded site. The petri plate was sealed using parafilm and placed in a dew chamber maintaining 100% RH at 25 °C and light intensity of 60 µmol $m^{-2}$ $s^{-1}$ with 12/12 h light/dark cycle.

Similar step up and incubation conditions were used for *C. higginsianum, B. cinerea and S. sclerotiorum* disease assays with the following exceptions. No DON was used in the inoculations for these pathogens. No mid-rib injury was made for the *S. sclerotiorum* infection assay.

***F. graminearum floral inoculations***

Since *F. graminearum* uses inflorescences to gain entry in the wheat plants, assays in Arabidopsis inflorescences should be phenologically similar to wheat. Therefore, floral inoculations of the transgenic Arabidopsis plants were performed following Urban et al. (2002) with some modifications. Six-week-old plants with open flowers and developing siliques were selected for inoculations. Inoculum was adjusted to $1 \times 10^5$ spores/ml in sterile water with 0.001% Silwet L-77. The inoculum was applied using a fine mist spray bottle. Seven to ten spray puffs

were applied per inflorescence while keeping spray bottle at a distance of 5 cm. The inoculated plants were kept in large clear plastic box and maintained in a growth chamber at 23 °C for 7-8 days. The base of the box was filled with water to a depth of 5 cm and its lid and walls were sprayed with water to maintain 100% RH. For the first 2 days, plants were maintained in the dark by covering the box with black cover. At fourth day, the lid was slightly opened to maintain approximately 80% RH.

***Disease assessment***

Disease severity of leaf assays of all the fungal pathogens was assessed using two methods: Disease Severity (DS) Index and Fungal biomass. For the DS index measurement, images were collected at 5 days post-inoculation (dpi), 6 dpi, 54 hours post inoculation (hpi), aor 5 dpi for *F. graminearum*, *C. higginsianum, S. sclerotiorum,* and *B. cinerea,* respectively. Each leaf was scored using the categorical disease scale used by Chen et al (2006). The disease scores were based on the symptom severity and ranged from 0-5. The scores were assigned as follows:

0- No symptoms

1- Chlorosis / discoloration restricted to site of inoculation

2- Less than 25 % area with Chlorosis/ discoloration

3- 25-50% area with Chlorosis/ discoloration

4- 50-70 % area with Chlorosis/ discoloration

5- 100% area with Chlorosis/ discoloration

The DS index was calculated based on the following equation:

$$\text{DS Index (\%)} = \frac{\sum nS_i}{NS_m} \times 100$$

Where n is the number of leaves with each disease score ($S_i$), N is the total number of leaves, and $S_m$ is the maximum disease score possible (i.e., 5).

For fungal biomass assessment, infected leaf samples were collected at 36 hpi, 6 dpi, 48 hpi, or5 dpi for *F. graminearum*, *C. higginsianum, S. sclerotiorum,* and *B. cinerea,* respectively. DNA was extracted using the BioSprint 96 DNA Plant Kit (Qiagen) and normalized to 20 ng/ µl. The real-time qPCR was performed in a 10 µl reaction volume containing 3 µl of DNA template, 5 µl of 2X AzuraView GreenFast qPCR Blue Mix LR (Azura genomics) and 400 nM of each forward and reverse primers. Thermal cycler profile included initial denaturation of 95 °C for 5 min, followed by 39 cycles of 95 °C for 30 s, 62 °C for 20 s and 72 °C for 20 s. *Tri6 , ITS2, tubulin,* and *Cutinase A* were used as target genes for estimating the DNA content of *F. graminearum* (Horevaj et al., 2011), *C. higginsianum* (Salvador-Guirao et al., 2018)*, S. sclerotiorum* (Wei et al., 2022)*,* and *B. cinerea* (Ono et al., 2020)*,* respectively. The gene for *Arabidopsis ubiquitin-conjugating enzyme* (*UBC*) was used as a reference (Czechowski et al., 2005) (Table 4.1). Primer efficiencies for the target and reference genes were in the range of 100-110%, therefore, gene expression data was analyzed using the $2^{-\Delta\Delta CT}$ method (Livak and Schmittgen, 2001; Schmittgen and Livak, 2008).

For the floral assays, disease severity was measured by estimating fungal biomass. The infected inflorescence tissue was collected 8 dpi by flash freezing in liquid nitrogen and stored at

-80 °C. The protocol of quantifying *F graminearum* biomass using qPCR was same as described above.

***Protein extraction, gel electrophoresis and Western blot analysis***

To characterize the transgenic plants that were expressing intact PFT protein correctly, Western blotting of plants from homozygous families was performed. Four leaf discs (~ 80 mg tissue) were collected and grounded into fine powder in liquid nitrogen. Ground tissue was mixed in 400 µl of protein extraction buffer (50 mM $NaH_2PO_4$, pH 8.0; 300 mM NaCl; 10 mM imidazole; 10 % glycerol, 0.1% Triton X, 1 µM PMSF). Cell debris was removed by centrifugation at 20, 000 g for 20 min at 4 °C. The supernatant containing the soluble fraction was quantified using a Pierce Detergent Compatible Bradford Assay Kit (ThermoFisher Scientific, Waltham, MA). Around 20 µg of total soluble protein fraction was mixed with Laemmli sample loading buffer. After incubating at 95 °C for 10 min, samples were loaded on a Novex 10-20% Tris-glycine mini gel (Invitrogen, Waltham, MA) under denaturing conditions. The proteins were blotted to a nitrocellulose membrane. The membrane was probed with a 1: 5000 dilutions of polyclonal anti-GFP antibody solution (Invitrogen, Waltham, MA) followed by a 1:5000 dilution of goat anti-rabbit alkaline phosphatase- labeled antibodies (LGC SeraCare, Inc.). The membrane was developed using the BCIP/NBT alkaline phosphatase substrate system (LGC SeraCare, Inc.).

### *Live cell imaging using Laser Scanning Microscopy (LSM)*

GFP:PFT subcellular localization patterns were observed using airyscan mode of Zeiss LSM 980 Airyscan 2 Laser Scanning Confocal microscope at the imaging core facility of the University of Maryland, College Park, MD. Four- to 6-day-old seedlings were mounted in MS medium. For plasmolysis, seedlings were treated with 1 M NaCl in MS for 10 minutes before imaging. GFP was excited using 488 nm laser line and captured using BP420-480 and BP496-550 emission filters. Zen Blue software, Image J and Power Point were used for figure preparation.

### *Statistical analysis*

Data were analyzed using GraphPad Prism version 9.3.1 (GraphPad Software, San Diego, CA). Data sets were checked for the normality assumption using Shapiro-Wilk test and Q-Q plots. One Way Analysis of Variance (ANOVA) followed by Dunnett's multi comparisons test or Student's t-tests were performed for declaring statistical significance.

## 4.3. Results

### *Generation of GFP: PFT transgenics in Arabidopsis*

PFT was cloned in a gateway cloning vector pK7WGF2 (Karimi et al., 2002) with an enhanced green fluorescent protein (EGFP) tag at the N terminus and driven by a 35S CaMV promoter and Kanamycin resistance gene (Figure 4.1.A). The selection efficiency with

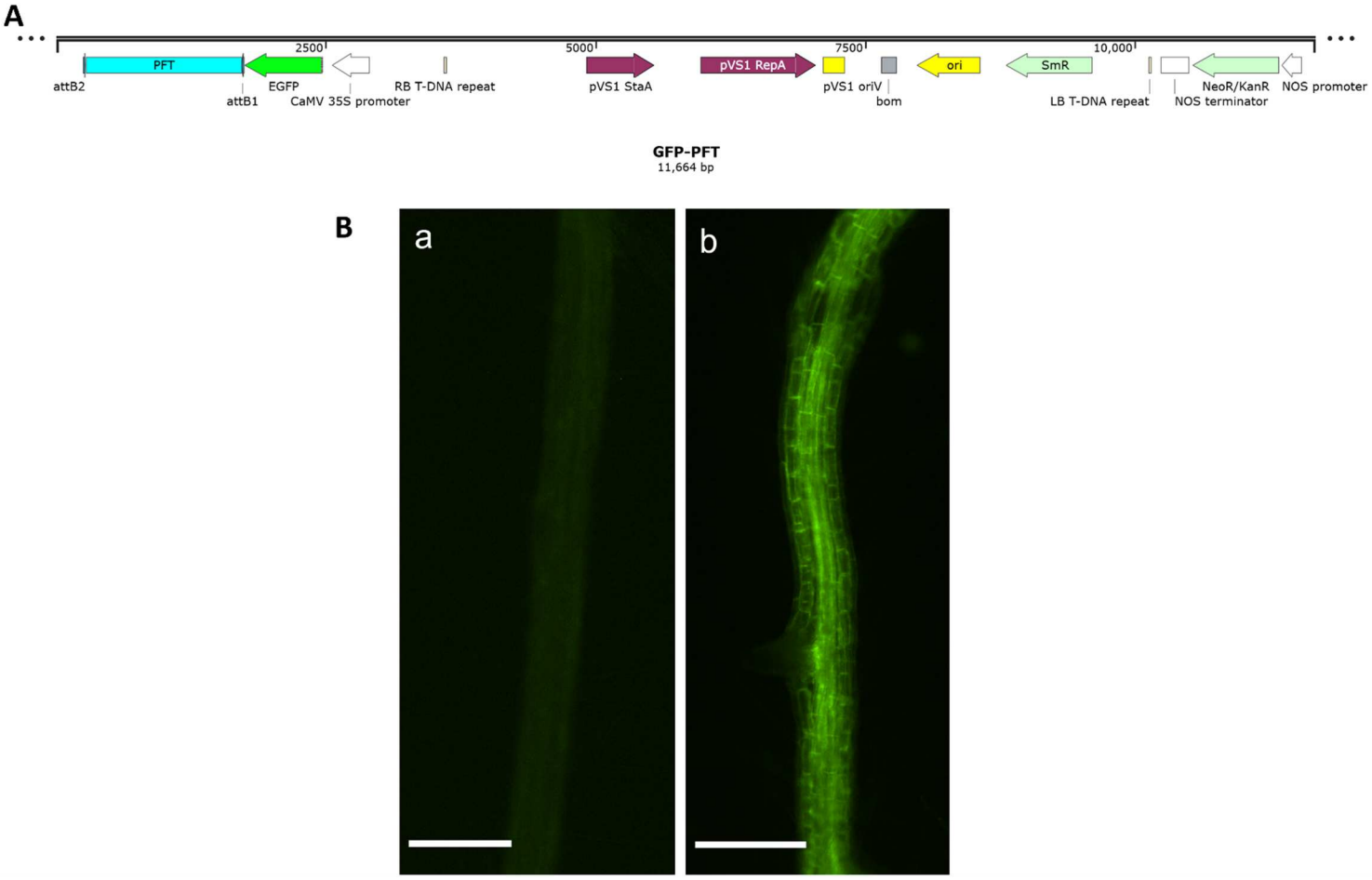


**Figure 4. 1.** Generating and selecting GFP: PFT transgenics in Arabidopsis. A) Map of PFT cloned in pK7WGF2. Scale units in base pairs (bp). B) Screening of GFP: PFT transgenics using epi-fluorescence microscope. a) Wild type Arabidopsis root; b) root of a kanamycin resistant, GFP expressing T2 plant seedling; scale bar = 50 µm.

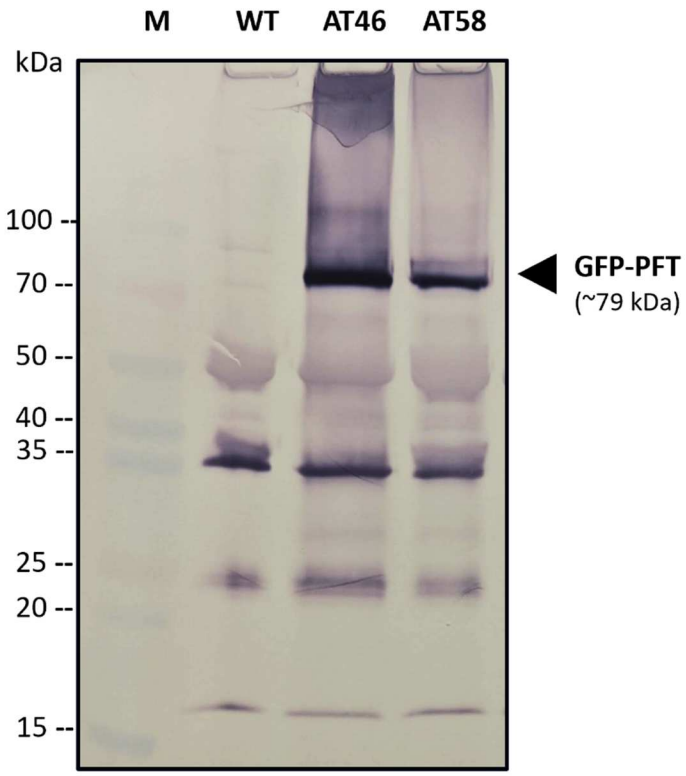


**Figure 4. 2. Western blot analysis of GFP: PFT expressed in Arabidopsis transgenic plants.** The membrane was probed with anti-GFP antibody followed by anti-goat anti-rabbit IgG and detected using alkaline phosphate-based detection. Equal amount of soluble protein was loaded in each lane. kDa: Kilo Dalton; M: protein marker; WT: Wild type Arabidopsis Ler ; Arabidopsis Ler expressing GFP:PFT: AT46 and AT58. Arrowhead indicates GFP:PFT fusion protein.

kanamycin resistance ranged from 2-4 %. Kanamycin resistant T1 plants were then screened for GFP signal using an epifluorescence microscope (Figure 4.1.B). Fifty percent of the Kanamycin resistant T1 plants had GFP signal. The remaining 50% with no GFP signal were discarded. T1 plants with GFP signal were grown for seed increase and their T2 families were tested for segregation. Ultimately, three independent non-segregating T2 families were used for disease bioassays in this study. The GFP:PFT fusion protein was confirmed in selected T2 plants via western blot analysis (Figure 4.2). A specific band of ~ 79 kDa was detected in the GFP-PFT fusion protein transgenic plants by anti-GFP antibody. The size of PFT on SDS PAGE is ~ 52 kDa and size of GFP is ~27 kDa. Therefore, presence of unique ~79 kDa band only in transgenics and not in WT confirms the production of complete fusion protein in GFP: PFT transgenics.

***Enhanced resistance to F. graminearum in Arabidopsis leaves by PFT***

Response to *F. graminearum* in GFP:PFT expressing Arabidopsis leaves was assessed based on visual symptoms and fungal biomass. While WT plants had larger chlorotic lesions with white mycelial growth, GFP:PFT transgenics had smaller lesion size with no visible mycelial growth ( Figure 4.3. A). Mean disease severity (DS) index score for WT was 75 %. Mean DS index for GFP: PFT transgenics was significantly lower and ranged from 58-63% (Figure 4.3.B). Using a more sensitive assay, biomass of the *F. graminearum* on the infected leaves was measured based on the relative copy number of the *TRI6* gene. GFP:PFT transgenics

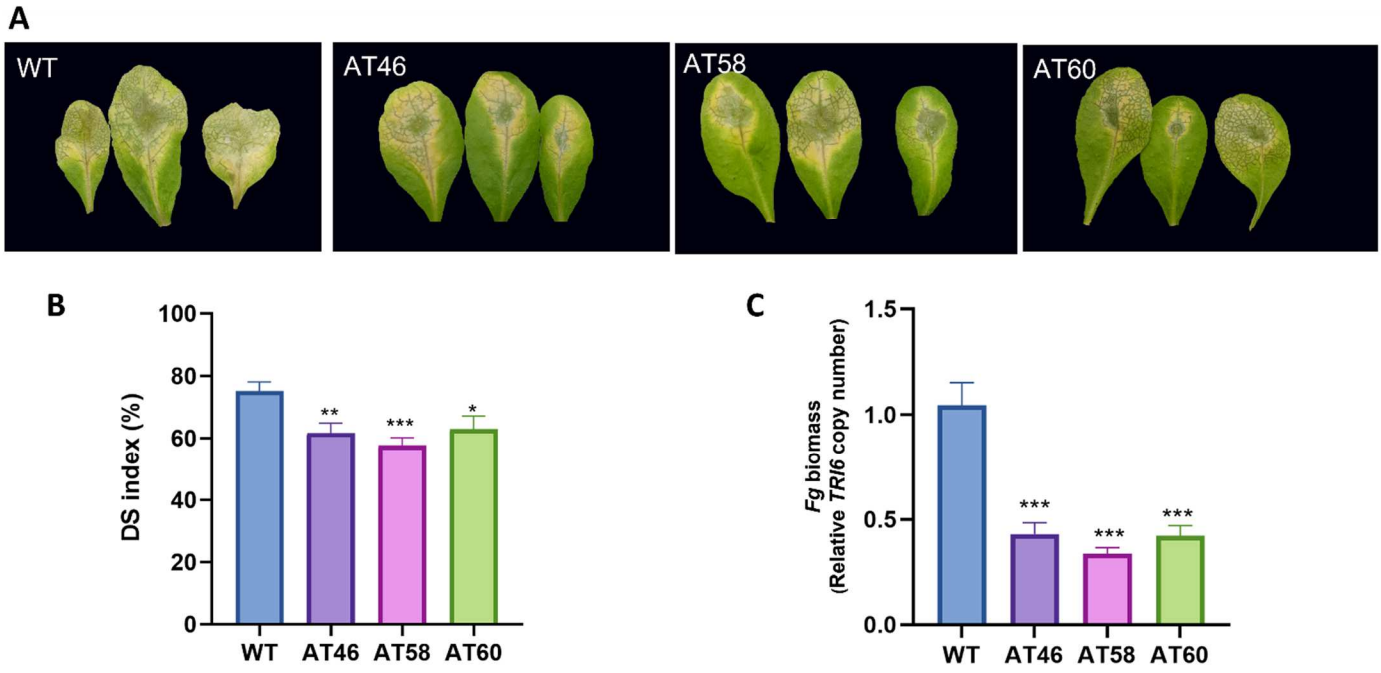


**Figure 4. 3. Transgenic Arabidopsis plants expressing GFP:PFT with reduced disease severity on leaves infected with *F. graminearum.*** A) Disease symptoms observed 5 days post inoculation (dpi). WT: Wild type Arabidopsis Ler; T2 Arabidopsis Ler families expressing GFP:PFT: AT46, AT58 and AT60. B) Disease Severity (DS) Index of WT and transgenic lines measured 5 dpi. Data represents means with standard error from ten biological replicates. C) Fungal biomass of F. graminearum detected by qPCR on inoculated leaves 3 dpi. Relative fold change of *TRI6* gene was measured by $2^{-\Delta\Delta CT}$ method by normalizing data with Arabidopsis *UBC* gene and using WT as reference. Data represents means with standard error from ten biological replicates. Bars with *, ** and *** indicates that corresponding data is statistically different from WT at $p < 0.05$, $p < 0.01$, and $p < 0.001$, respectively.

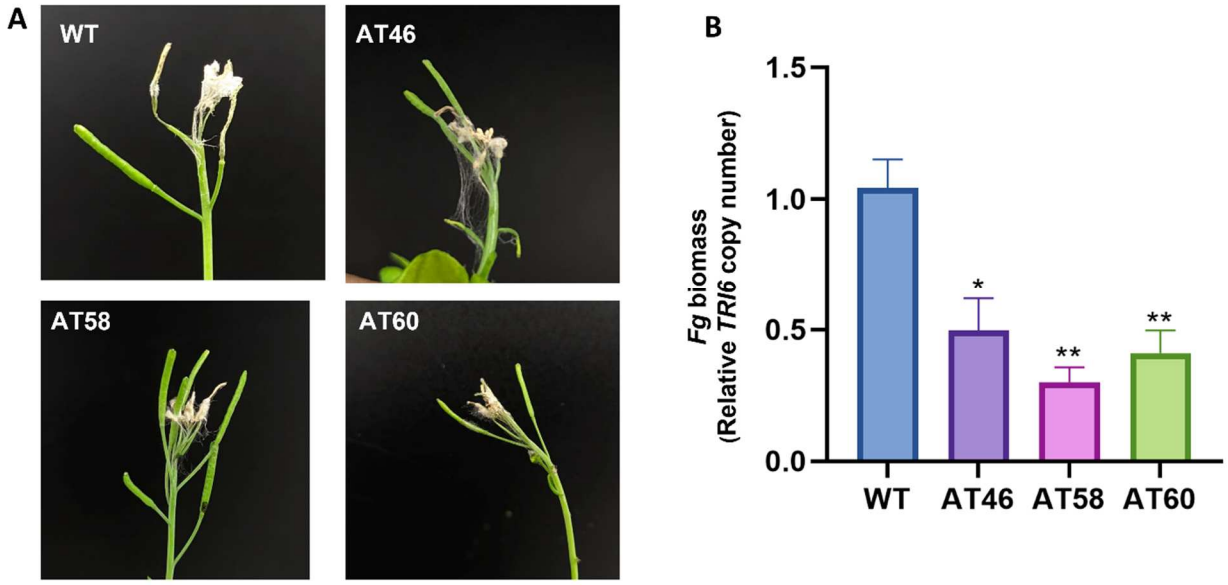


**Figure 4. 4. Transgenic Arabidopsis plants expressing GFP:PFT with reduced disease severity on florets infected with *F. graminearum*.** A) Disease symptoms observed 8 days post inoculation (dpi). WT: Wild type Arabidopsis Ler; T2 Arabidopsis Ler families expressing GFP:PFT: AT46, AT58 and AT60. B) Fungal biomass of F. graminearum detected by qPCR on inoculated florets 8 dpi. Relative fold change of *TRI6* gene was measured by $2^{-\Delta\Delta CT}$ method by normalizing data with Arabidopsis *UBC* gene and using WT as reference. Data represents means with standard error from four biological replicates. Bars with * and ** indicates that corresponding data is statistically different from WT at $p < 0.05$ and $p < 0.01$, respectively.

had significantly lower (P <0.001) fungal biomass compared to WT (Figure 4.3.C). Compared to WT, fungal biomass in AT46, AT58, and AT60 was 58%, 67 % and 59% lower, respectively. Taken together, GFP:PFT expression significantly reduced *F. graminearum* infection in inoculated Arabidopsis leaves.

***Enhanced floral resistance to F. graminearum in PFT transgenics***

Floral tissues are the major site of infection of *F. graminearum* in wheat. Therefore, GFP:PFT transgenics were tested for floral infection. In the WT, flowers completely collapsed with necrotic peduncle and extensive necrosis of young siliques occurred (Figure 4.4.A). On the other hand, GFP:PFT transgenics had intact peduncle and silique necrosis was not observed. To quantify the disease response, *F. graminearum* fungal biomass was measured by performing relative quantification of *TRI6* gene copy number (Figure 4.4.B). *TRIi6*-based quantification of *F. graminearum* showed 51%, 70%, and 59% lower fungal biomass in AT46, AT58, and AT60 families, respectively compared to the WT. *F. graminearum* biomass was significantly (p value < 0.05) lower in all three families compared to WT.

***PFT confers resistance to C. higginsianum***

Response of GFP: PFT against *C. higginsianum* was assessed based on visual symptoms and fungal biomass. WT plants had larger chlorotic lesions and GFP: PFT transgenics had very small lesion at the point of inoculation. (Figure 4.5.A). Mean DS index score for WT ler was 35%. Mean DS index for GFP: PFT transgenics was significantly lower (p< 0.001) and ranged

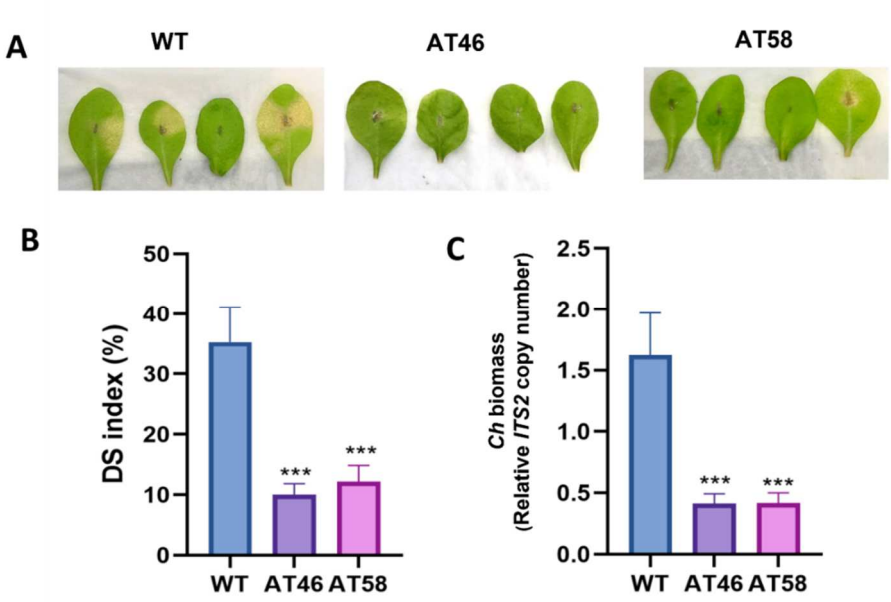


**Figure 4. 5. Transgenic Arabidopsis plants expressing GFP:PFT with reduced disease severity on leaves infected with *C. higginsianum.*** A) Disease symptoms observed 6 days post inoculation (dpi). WT: Wild type Arabidopsis Ler; T2 Arabidopsis Ler families expressing GFP:PFT: AT46 and AT58 B) Disease Severity (DS) Index of WT and transgenic lines measured 6 dpi. Data represents means with standard error from ten biological replicates. C) Fungal biomass of *C. higginsianum* detected by qPCR on inoculated leaves 6 dpi. Relative fold change of *ITS2* gene was measured by $2^{-\Delta\Delta CT}$ method by normalizing data with Arabidopsis *UBC* gene and using WT as reference. Data represents means with standard error from ten biological replicates. Bars with *, ** and *** indicates that corresponding data is statistically different from WT at $p < 0.05$, $p < 0.01$, and $p < 0.001$, respectively

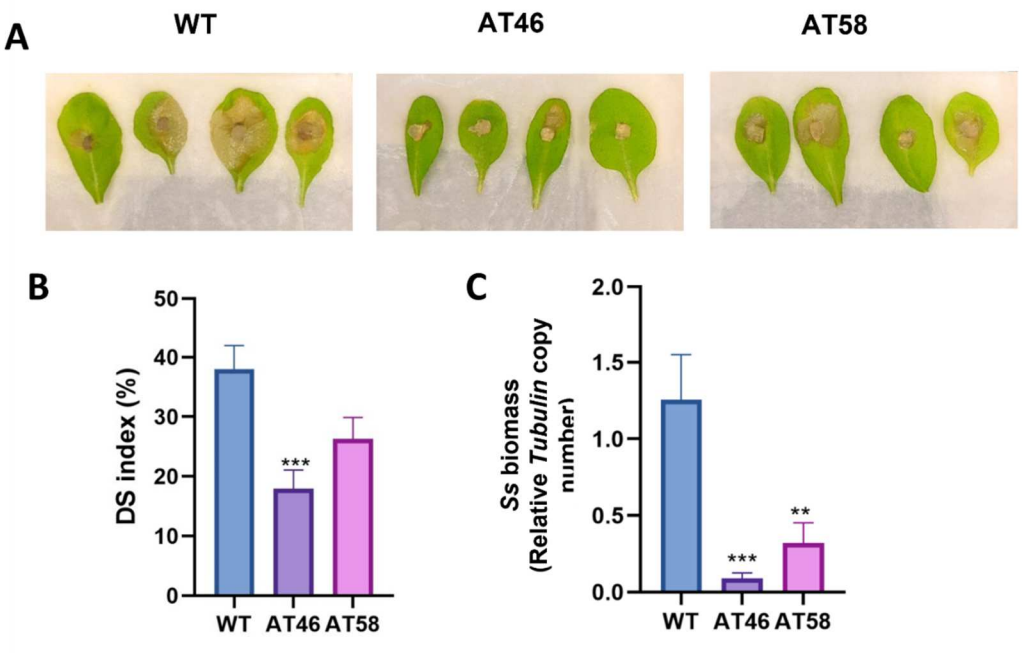


**Figure 4. 6. Transgenic Arabidopsis plants expressing GFP:PFT with reduced disease severity on leaves infected with *S. sclerotiorum.*** A) Disease symptoms observed 54 hours post inoculation (hpi). WT: Wild type Arabidopsis Ler; T2 Arabidopsis Ler families : AT46 and AT58 B) Disease Severity (DS) Index of WT and transgenic lines measured 54 hpi. Data represents means with standard error from ten biological replicates. C) Fungal biomass of *S. sclerotiorum* detected by qPCR on inoculated leaves 48 hpi. Relative fold change of *Tubulin* gene was measured by $2^{-\Delta\Delta CT}$ method by normalizing data with Arabidopsis *UBC* gene and using WT as reference. Data represents means with standard error from ten biological replicates. Bars with *, ** and *** indicates that corresponding data is statistically different from WT at $p < 0.05$, $p < 0.01$, and $p < 0.001$, respectively.

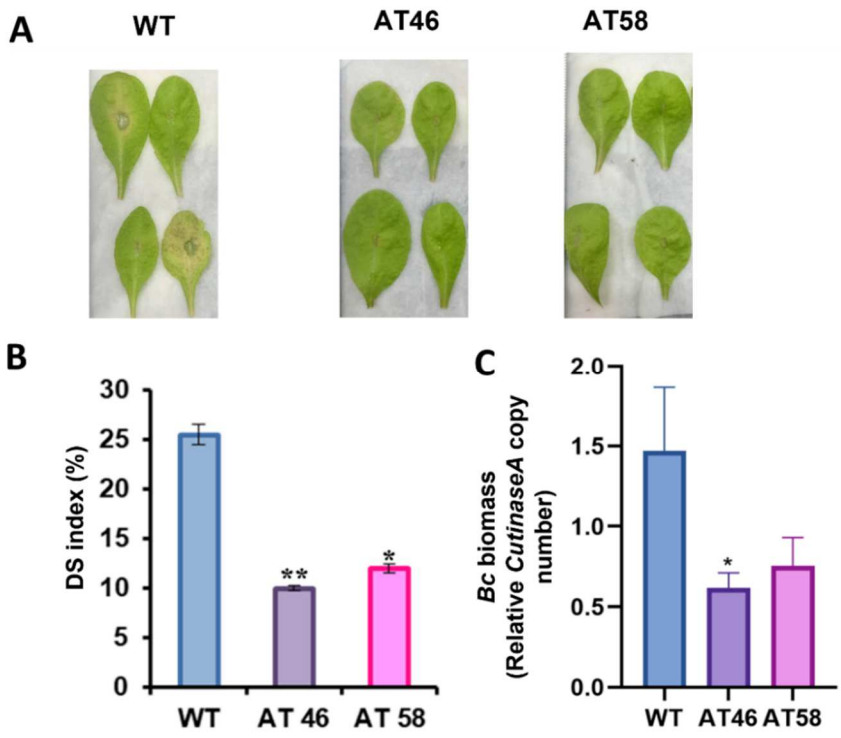


**Figure 4. 7. Transgenic Arabidopsis plants expressing GFP:PFT with reduced disease severity on leaves infected with *B. cinerea.*** A) Disease symptoms observed 5 days post inoculation (dpi). WT: Wild type Arabidopsis Ler; T2 Arabidopsis Ler families : AT46 and AT58. B) Disease Severity (DS) Index of WT and transgenic lines measured 5 dpi. Data represents means with standard error from ten biological replicates. C) Fungal biomass of *B. cinerea* detected by qPCR on inoculated leaves 5 dpi. Relative fold change of *CutinaseA* gene was measured by $2^{-\Delta\Delta CT}$ method by normalizing data with Arabidopsis *UBC* gene and using WT as reference. Data represents means with standard error from ten biological replicates. Bars with *, ** and *** indicates that corresponding data is statistically different from WT at $p < 0.05$, $p < 0.01$, and $p < 0.001$, respectively.

from 10-12% (Figure 4.5.B). *C. higginsianum* biomass was quantified by monitoring relative gene copy number of *ITS2 (internal transcribed spacer)* gene. The *C. higginsianum* biomass was four fold less in GFP:PFT transgenics compared to WT (Figure 4.5.C). Therefore, statistically significantly ($p<0.001$) lower disease severity and pathogen growth indicate that PFT enhances resistance against *C. higginsianum.*

***PFT enhances resistance to S. sclerotiorum***

GFP:PFT transgenics had smaller necrotic lesions compared to WT during *S. sclerotiorum* infection (Figure 4.6.A) Mean DS Index for WT (38% ) was statistically significantly lower than one AT46 transgenic family (18%). Although not statistically significant, mean DS Index of AT58 family was numerically lower than WT. For more accurate disease assessment, the fungal biomass was measured by monitoring the relative gene copy number of *Tubulin* gene. Both the transgenic families had significantly ($p<0.01$) lower biomass than WT (Figure 4.6.B). Compared to WT, *S. sclerotiorum* biomass was lower by factor of 14 and 4 in AT46 and AT 58, respectively. Thus, PFT enhances resistance against *S. sclerotiorum* infection.

***PFT confers resistance to B. cinerea***

The disease severity of WT with *B. cinerea* infection was lowest among all the fungi tested (Figure 4.7.A). However, mean DS Index of WT was still significantly ($p <0.05$) higher than the GFP:PFT transgenic families (Figure 4.7.B). The relative copy number of gene *Cutinase*

*A* was estimated to measure biomass of *B. cinerea*. While both the transgenic families had reduced fungal biomass, the difference was only statistically significant ($p < 0.05$) in case of AT46 family. Overall, ectopic expression of PFT reduced disease severity and growth of *B. cinerea* in Arabidopsis.

***Subcellular localization patterns of GFP:PFT***

The subcellular localization pattern of GFP:PFT were observed using high resolution Airysan CLSM. Since no GFP only band was detected in western blot analysis of GFP: PFT transgenics (Figure 4.2). The subcellular patterns should be solely due to the GFP:PFT fusion protein. The epidermal cells of hypocotyl, leaves, and roots of 4- to 6-day-old Arabidopsis seedlings were imaged (Figure 4.8). In the hypocotyl epidermal cells, GFP: PFT was localized in the cortical cytoplasm, cytoplasmic strands, and potentially in ER bodies (Figure 4.8.A). In the medial plane, nucleus localization was observed in addition to the cytoplasmic localization near plasma membrane (Figure 4.8.B). Similar localization patterns were observed in the leaves and root cells (Figure 4.8.C/D). Interestingly after plasmolysis of epidermal cells of hypocotyl and roots, the GFP:PFT exhibited localization at the plasma membrane- cell wall connections called Hechtian strands (HS) (Figure 4.9). In addition to plasma membrane, HS also contains components of cytoplasm, ER and cytoskeleton elements (Lang-Pauluzzi and Gunning, 2000).

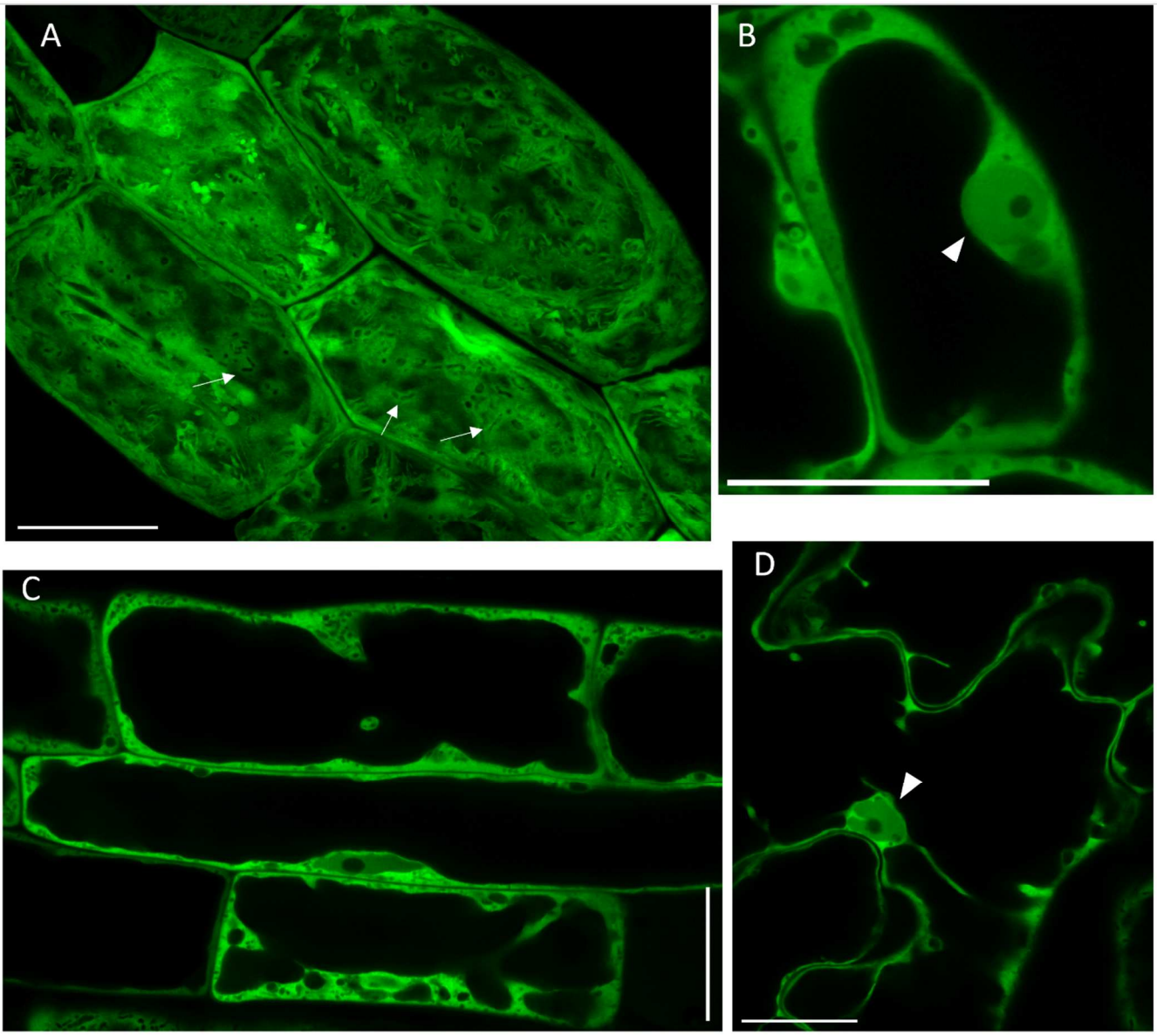


**Figure 4. 8.** Subcellular localization pattern of GFP:PFT. A) Maximum intensity projection of epidermal cells of hypocotyl; B) Medial plane of an epidermal hypocotyl cell; C) medial plane of root epidermal cell in elongation zone; D) Medial plane of leaf pavement cells. Arrowheads indicate nucleus; Arrows indicate potential ER bodies. Scale bar = 20 μm.

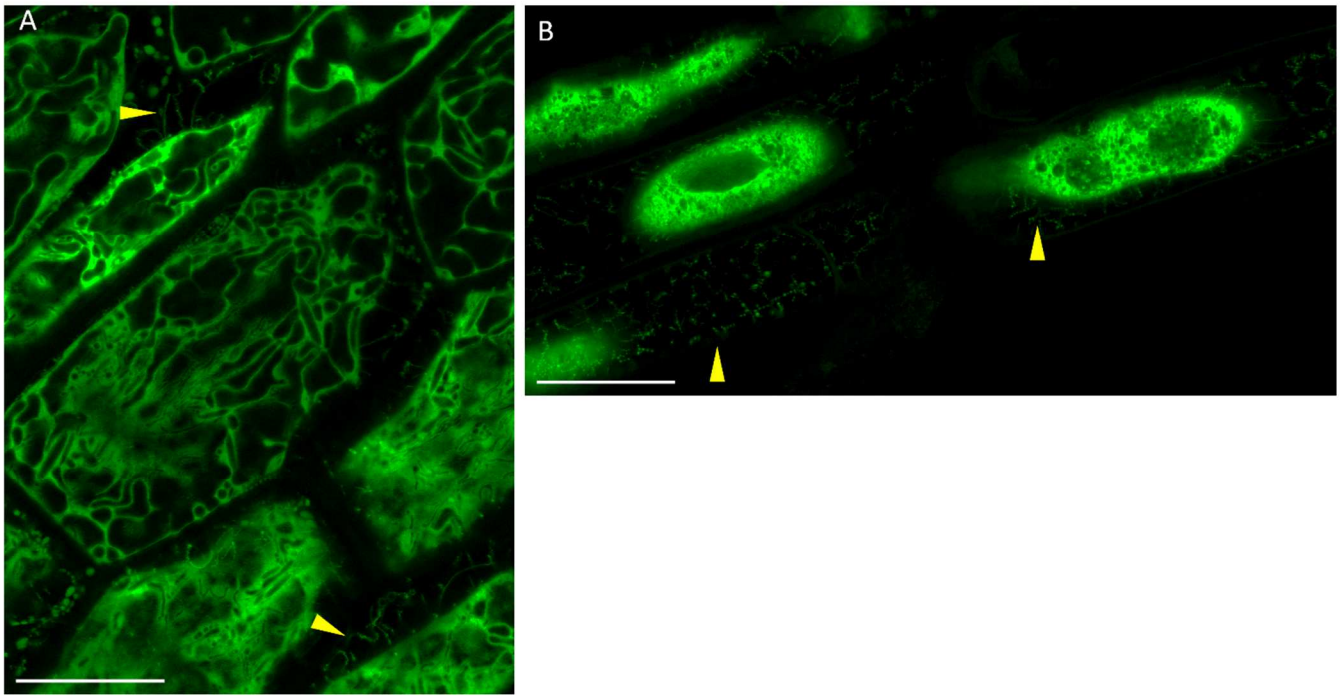


**Figure 4. 9. Subcellular localization pattern of GFP:PFT in the cortical plane of plasmolyzed hypocotyl (A) and root (B) epidermal cells.** Arrowheads indicate Hechtian Strands (HS). Scale bar = 20 µm.

### 4.4. Discussion

Enhancing resistance against fungal pathogens is one of the major goals of crop improvement to ensure global food security (Bailey-Serres et al., 2019; Gerten et al., 2020). Therefore, characterization of broad-spectrum resistance genes is very critical which are effective against multiple species or genera of pathogens. *PFT* is an atypical resistance gene

which confers durable resistance against Fusarium Head Blight in wheat (Rawat et al., 2016). In this study, the ability of *PFT* to confer broad-spectrum resistance against fungal pathogens was characterized. *PFT* was ectopically expressed in the model plant Arabidopsis and assessed its response against four economically important fungal pathogens.

Arabidopsis is a model plant to study the plant-pathogen interactions because of ease of performing functional studies and being susceptible to several economically important fungal, oomycetes, bacterial and viral pathogens (Mauch-Mani and Slusarenko, 1993; Andargie and Li, 2016). Findings from Arabidopsis- *F. graminearum* interactions can be translated to wheat- *F. graminearum* interactions. Therefore, PFT transgenics were generated in Arabidopsis. To determine if PFT maintains its function irrespective of plant background, the response of PFT Arabidopsis transgenics was assessed against *F. graminearum*. PFT transgenics enhanced resistance compared to WT in both leaf and floral assays.

The predicted mechanism of PFT-mediated resistance suggests broad-spectrum resistance against fungal pathogens. To test this hypothesis, PFT transgenics were screened against pathogens belonging to economically important fungal genera including *Colletotrichum*, *Sclerotinia*, and *Botrytis*. For all three pathogens, PFT transgenics had significantly reduced disease severity and fungal biomass accumulation, therefore, suggesting that PFT provides broad-spectrum resistance against fungal pathogens. Previously characterized, BSR genes conferring resistance against multiple pathogens belong to various classes including membrane-associated pattern recognition receptors, nucleotide-binding leucine-rich repeat ( NLR) proteins, defense signaling proteins, pathogenesis-related proteins, and non-host resistance proteins (Li et

al., 2020). In wheat, *Lr34* (=*Yr18/Sr57/Pm38*) encoding ABC transporter (Krattinger et al., 2009) and *Yr46*/*Lr67* encoding hexose transporter (Moore et al., 2015) are two well characterized BSR genes which provide resistance against multiple fungal pathogens. (Krattinger et al., 2019; Bräunlich et al., 2021). Transgenic expression of *Lr34res* in barley, rice, maize, and sorghum has been shown to enhance their resistance against various biotrophic or hemi-biotrophic fungal pathogens (Krattinger et al., 2016; Schnippenkoetter et al., 2017; Sucher et al., 2017; Boni et al., 2018). Recently, it was shown in wheat and barley that abscisic acid (ABA) is the substrate for the LR34 ABC transporter and *LR34res*-mediated ABA redistribution contributes to the resistance against multiple fungal pathogens. A nonfunctional hexose transporter, resulting from mutation in two critical amino acids of *Yr46*/*Lr67,* confers resistance against multiple fungal pathogens including leaf rust (*Puccinia triticina*), stripe rust (*Puccinia striiformis* f. sp. *tritici*; ), stem rust (*Puccinia graminis* f. sp. *tritici*) and powdery mildew (*Blumeria graminis*) in wheat (Moore et al., 2015; Julius et al., 2017). Recently, a wall associated Kinase (WAK), *TaWAK-6D* was reported to confer resistance against two fungal pathogens: *Fusarium pseudograminearum* and *Rhizoctonia cerealis*, causing Fusarium crown rot and sharp eyespot diseases, respectively (Qi et al., 2021). Hence, PFT is a new addition to the list of BSR genes in wheat against hemibiotrophic and necrotrophic fungal pathogens.

Fluorescence protein (FP) tagging is a useful tool to investigate subcellular level host pathogen interactions using advanced fluorescence microscopy. In this study, GFP:PFT fusion construct was developed to determine subcellular localization patterns of PFT. Additionally, GFP: PFT fusion construct also helped with the screening of transgenic plants at the protein

expression level. However, GFP is substantially large protein tag with size of 27 KDa. Furthermore, GFP fusion protein could undergo cleavage separating GFP signal from tagged protein. In our case, GFP:PFT protein stayed intact. Given the resistance response, GFP tag did not seem to interfere with function of PFT protein. Live cell imaging revealed nucleocytoplasmic localization of PFT in Arabidopsis leaves and root cells. Although the majority of membrane-bound receptor lectins are known to modulate plant defense, a new class of nucleocytoplasmic lectins has been increasingly reported to be involved in plant defense (Van Damme et al., 2004; Lannoo and Van Damme, 2014). For instance, wheat hessian fly resistance ( *Hfr2*) gene which has a similar domain architecture to PFT is also a nucleocytoplasmic lectin (Puthoff et al., 2005; Lannoo and Van Damme, 2014). Localization of PFT in the hechtian strands (HS) is also notable. Previously, role of HS in plant defense against fungi has been suggested (Mellersh and Heath, 2001). Taken together, GFP:PFT transgenics characterized in this study have specific subcellular localization patterns and would be very useful resource to further investigate subcellular level interactions between PFT and FP tagged fungal pathogens.

In conclusion, this study provided evidence of broad-spectrum resistance against fungal pathogens mediated by the wheat *PFT* gene. *PFT* is a valuable addition to the limited pool of plant BSR genes. The FP tagged PFT transgenics developed in this study would be great resource to study *PFT* mediated host-pathogen interactions at the subcellular level.

# Chapter 5: Functional analysis of wheat Pore-Forming toxin-like (PFT) protein provides insight into its molecular mechanism of plant disease resistance

## 5.1. Introduction

Fungal pathogens cause the most significant damage to global food crop production than any other pathogenic microbes (Savary et al., 2019). The plant immune system is composed of two layers: pathogen-associated molecular pattern (PAMP)- triggered immunity (PTI) and effector-triggered immunity (ETI). PTI is a broad-spectrum basal defense response that protects plants from non-host pathogens. ETI is a specific defense response against virulent pathogens that are capable of subverting PTI. ETI is the basis for classical R gene-mediated resistance (Jones and Dangl, 2006; Dodds and Rathjen, 2010) . ETI is effective against biotrophs and hemibiotrophs but does not work against necrotrophs (Glazebrook, 2005; Mengiste, 2012). The molecular basis of ETI has been well studied and has enabled engineering for disease resistance against biotrophs and hemibiotrophs without fitness cost (Xu et al., 2017). On the other hand, the molecular basis of defense against necrotrophs is poorly understood, especially in crop plants (Mengiste, 2012). The quantitative nature of resistance against necrotrophs is the major challenge in studying the molecular and biochemical mechanisms underlying such resistance. Since resistance against necrotrophic pathogens is conferred mainly by multiple small effect

genes, it is difficult to perform functional studies for factors individually (Poland et al., 2009; Corwin and Kliebenstein, 2017).

*Fusarium graminearum* is a necrotrophic/hemibiotrophic pathogen that causes the devastating disease, Fusarium Head Blight (FHB), in wheat and barley (Goswami and Kistler, 2004). FHB epidemics have been reported in wheat-growing regions worldwide since 1990 (Windels, 2000). FHB ranks second on the list of pests and pathogens causing economic damage to global wheat production (Savary et al., 2019). In addition to reducing grain yield, *F. graminearum* impairs grain quality by producing trichothecene mycotoxins. Deoxynivalenol (DON), one of the major mycotoxins produced by *F. graminearum*, is a potent eukaryotic protein synthesis inhibitor known to cause vomiting, convulsions, and toxic aliment aleukia (Bennett and Klich, 2003; McMullen et al., 2012). Therefore, FHB is a threat to food security and safety.

Deploying host resistance is the most economical and environmentally friendly management strategy for FHB. Although various quantitative trait loci (QTLs) have been reported throughout the wheat genome for FHB resistance, *Fhb1* is the most stable and large effect QTL, which has been used in global wheat breeding programs for decades (Anderson et al., 2001 ). Pore-forming toxin-like (*PFT*) gene has been identified as the major factor of *Fhb1*-mediated resistance (Rawat et al., 2016). The molecular basis of PFT's resistance mechanism has not been studied, but the possible mode of action can be inferred from its predicted structure. PFT is an atypical resistance protein with two types of domains, both of which are known to have defense roles. PFT is predicted to be a chimeric plant lectin with two amaranthin domains

(agglutinin domains of *Amaranthus caudatus)* and one bacterial epsilon toxin (ETX) / mosquitocidal toxin (MTX) domain of aerolysin pore-forming toxin family (Rawat et al., 2016). So far, proteins with domain architecture of two amaranthin and pore-forming toxin have been partially characterized in wheat (Puthoff et al., 2005), flax (Faruque et al., 2015), cucumber (Dang et al., 2017), and *Rumex acetosa* plants (Manzano et al., 2017). Out of these, only wheat HFR-2 is involved in plant defense against insects (Puthoff et al., 2005). Therefore, PFT is the only protein with its kind of domain architecture known to be involved in defense against phytopathogenic fungi.

Plant lectins contain one or more agglutinin domains that reversibly bind to carbohydrates; they play a role in defense against insects, nematodes, bacteria, fungi, and viruses (Lannoo and Van Damme, 2014). Lectins with amaranthin domain family specifically bind to *N*-acetylgalactosamine and T-antigens (Transue et al., 1997; Hernández et al., 2001). However, given the sequence variation between the amaranthin domains, differences in their carbohydrate-binding specificity are expected, which could define their specific biological role (Dang et al., 2017). We speculate that PFT has binding specificity towards one of the fungal cell wall components, including chitin monomer *N*- acetylglucosamine and β- 1,3 glucan. Whether PFT binds specifically to *F. graminearum* or other fungi could determine the broad-spectrum resistance potential of PFT. Aerolysin-like pore-forming proteins (PFPs) are present in all kingdoms of life, including bacteria, archaea, fungi, plants, and animals (Szczesny et al., 2011). Bacterial PFPs compromise host membrane permeabilization by making pore structures (Peraro and van der Goot, 2016). The presence of the aerolysin pore-forming domain in PFT suggests

that PFT could compromise the fungal cell membrane by making pores. As mentioned before, the specificity towards the fungal membrane could be contributed by the amaranthin domains. Therefore, I hypothesize that PFT interacts with the fungal cell wall via the amaranthin domains and compromises the fungal cells' integrity by making pores in the fungal membrane through ETX/MTX pore-forming domain.

The objective of this study was to characterize PFT and its individual domains functionally. In this regard, I purified functionally active PFT protein through heterologous expression in the model plant *Nicotiana benthamiana* and tested its agglutination and *in vitro* antifungal activity. Additionally, the role of individual domains of PFT was investigated.

## 5.2. Materials and methods

### *In silico analysis of PFT*

The tertiary structure of PFT was built using homology-based and *de novo* modeling. For homology-based modeling, crystal structures matching agglutinins (Agg) and pore-forming (ETX) domains were identified as a template from the Protein Data Bank (PDB), and modeling was performed using the Modeller software (Eswar et al., 2006). *De novo* modeling was performed using the AlphaFold software (Jumper et al., 2021). The boundaries of domains on the three-dimensional models of PFT were marked based on the Conserved Domain Database (CDD) of NCBI (Lu et al., 2020). To compare the accuracy of homology-based and *de novo*

models of PFT, Ramachandran plots were generated using PDBsum software (Laskowski et al., 2018).

Additionally, using Chimera X (Pettersen et al., 2021), both the models were superimposed on the Agg reference template to select the best model for protein-ligand docking analysis. Docking analysis was done to identify the most favored monosaccharide ligand for the Agg domain of PFT. The ligands were: one plant cell wall related carbohydrate, Glucose (Glc) and two fungal cell wall related carbohydrates, N-acetylglucosamine (GlcNAc) and chitosan. Homology-based PFT model was used as protein. The docking analysis was performed using AutoDock Vina (Eberhardt et al., 2021). All the protein structure visualizations were performed using Chimera X.

***Plasmid constructions***

For expression in bacteria, PFT was synthesized as a codon-optimized gene for expression in *E. coli* and cloned into pET19b by GenScript (Piscataway, NJ) (Figure 5.1.A). The plasmid construct contained a 6xHis tag at amino-terminal (N-terminal) to enable protein purification by affinity purification using Ni-NTA resins. pET19b: PFT was transformed into electrocompetent *E. coli* DH10B cells for maintenance and long-term storage. For heterologous protein expression, the plasmid was transformed into chemically competent *E. coli* strain BL21 (DE3).

For heterologous protein expression in *N. benthamiana* plants, two different systems were used: 1-*Agrobacterium*-mediated gateway binary plant expression vector and 2- Potato

Virus-X mediated expression. Full-length PFT cDNA and its Agg and ETX domains were amplified from the reverse transcribed RNA of the wheat cultivar 'Sumai 3'. The full-length PFT cDNA and its domains (Agg and ETX) were amplified by appending 6xHis- tag at the 5' end using primers listed in Table 5.1 and separately cloned into the pENTR/D-TOPO vector (Invitrogen, Waltham, MA) via directional TOPO cloning following manufacturer's recommendations. The resulting $His_6$-PFT, $His_6$-Agg, and $His_6$-ETX amplicons (Figure 5.1 B) were cloned in a plant expression vector pGWB402 (Nakagawa et al., 2007) with a CaMV 35S promoter (Figure 5.1 A) by performing LR cloning reaction following manufacturer's recommendations (Invitrogen, Waltham, MA). pGWB402:$His_6$-PFT, pGWB402:$His_6$-Agg, and pGWB402:$His_6$-ETX vectors were maintained in TOP 10 *E. coli* cells.

The second system employed Potato Virus X (PVX) based expression vectors (Chapman et al., 1992). pGDPVXMCS (Figure 5.1.A) vector with full-length PVX genome in pGD plasmid backbone (Lim et al., 2010) was used to express full-length PFT and its domains using restriction enzyme cloning. Given the large size of pGDPVXMCS, PFT and its domains were first cloned into an intermediate pSKAS vector. pSKAS is a pBluescript Sk+ based vector that contains 4945 to 6541 base pairs of PVX- based vector pP2C2S and an extended multiple cloning site. The cloning of inserts from pSKAS into pGDPVXMCS vector must require use of *Apa*I restriction site. Since PFT cDNA has an *Apa*I site, a silent mutation was introduced at 786 bp position (C to T) to eliminate *Apa*I site by performing site-directed mutagenesis using Q5 Site -Directed Mutagenesis Kit (New England Biolabs, MA). The full length PFT cDNA and its domains (Agg and ETX) were amplified by appending 6xHis- tag and *Bam*HI restriction site at 5' end and

*Hind*III restriction site at 3'end using primers listed in Table 5.1. The resulting amplicons were digested using *BamH*I and *Hind*III and inserted into similarly digested pSKAS vector. Subsequently, pSKAS: $His_6$-PFT , pSKAS: $His_6$-Agg, and pSKAS: $His_6$-ETX plasmids were digested with *Apa*I and *Spe*I and inserts were cloned into similarly digested pGDPVXMCS plasmid. The resulting pGDPVXMCS: $His_6$-PFT, pGDPVXMCS: $His_6$-Agg, and pGDPVXMCS: $His_6$-ETX were maintained in *E. coli* Top 10 cells (Life Technologies, Waltham, MA).

***Bacterial recombinant expression and purification***

The pET19b: PFT plasmid was transformed into chemically competent *E. coli* strain BL21 (DE3) for heterologous protein expression. Five milliliters of LB broth containing ampicillin (50 µg/ml) were inoculated with a bacterial colony and incubated overnight at 37 °C and 225 rpm. One ml of overnight culture was added to 100 ml of LB plus ampicillin in a 500 ml Erlenmeyer flask. The culture was grown at 37 °C and 225 rpm until an OD600 of 0.5-0.6. For inducing the protein production, isopropyl-b-D-1-thiogalactopyranoside (IPTG) was added to the culture at 1mM final concentration with subsequent shaking at 225 rpm for 8 h at 37 °C. The bacterial cells were harvested by centrifuging the cultures at 4,000 rpm and 4 °C for 20 min. The bacterial pellet was stored at – 80 °C until use. Protein purification was performed using BugBuster Master Mix Protein Extraction Reagent (EMD Millipore, Burlington, MA) using the manufacturer's instructions.

***Agroinfiltration of N. benthamiana leaves***

The pGWB402:$His_6$-PFT, pGWB402:$His_6$-Agg, and pGWB402:$His_6$-ETX plasmids were transformed into the GV3101 strain of *Agrobacterium tumefaciens* using electroporation. Similarly, through electroporation, pGDPVXMCS: $His_6$-PFT, pGDPVXMCS: $His_6$-Agg, and pGDPVXMCS: $His_6$-ETX plasmids were transformed into *A. tumefaciens* strain EHA105. Agrobacterium colonies were grown on LB agar containing appropriate antibiotics. LB agar was amended with rifampicin (25 µg/ml) and spectinomycin (50 µg/ ml) for pGWB402 constructs and for pGDPVXMCS constructs, rifampicin (25 µg/ml) and kanamycin were used (50 µg/ ml). Ten milliliters of LB broth with antibiotics were inoculated with agrobacterium colonies. The culture was grown overnight at 28 °C and 250 rpm in an incubator shaker. The cultures were centrifuged for 8 min at 6000 g at room temperature. The bacterial pellets were resuspended in an infiltration medium (10 mM MgCl2, 10 mM MES pH 5.7, 150 µM acetosyringone). The volume of bacterial culture was adjusted so that $OD_{600}$ of 0.7 could be achieved in a fixed volume of infiltration buffer. After the resuspension, cultures were incubated at room temperature with gentle shaking for 4 h. Subsequently, cultures were mixed individually with a similarly prepared culture of pGDp19 (expressing viral encoded silencing suppressor protein) plasmid at the ratio of 1:10 (pGDp19: pGWB402/pGDPVXMCS constructs).

**Table 5. 1.** Primers used in this study.

| Primer name | Sequence 5'-3' | Vector system | Remarks |
|---|---|---|---|
| DTOPO_PFT_N_F | CACCATGCATCACCATCACCATCACATGTTTCCGCTGTCAGCT | pGWB402 | Forward primer for PFT and Agg |
| DTOPO_PFT_N_R | TCACAGGTGTTCTTCTTTGGTATGGAA | pGWB402 | Reverse primer for PFT and ETX |
| DTOPO_Agg_N_R | TCATTCAATGCACCGCATTTTTACTTC | pGWB402 | Reverse primer for Agg |
| DTOPO_ETX_N_F | CACCATGCATCACCATCACCATCACATGGTTTCTCGAGACATCTAT | pGWB402 | Forward primer for ETX |
| HindIII_N_PFT_F | TAAGCAAAGCTTATGCATCACCATCACCATCACATGTTTCCGCTGTCAGCT | pSKAS/pGDPVX | Forward primer for PFT and Agg |
| BamH1_N_PFT_R | TGCTTAGGATCCTCACAGGTGTTCTTCTTT | pSKAS/pGDPVX | Reverse primer for PFT and ETX |
| BamH1_N_Agg_R | TGCTTAGGATCCTCATTCAATGCACCGCATTTTTA | pSKAS/pGDPVX | Reverse primer for Agg |
| HindIII_N_ETX_F | TAAGCAAAGCTTATGCATCACCATCACCATCACATGGTTTCTCGAGACATCTATG | pSKAS/pGDPVX | Forward primer for ETX |

Five- to six-week-old *N. benthamiana* plants grown in a growth chamber at 22°C temperature, 50 % relative humidity and under 12 h light conditions were used for infiltration. Three to four fully expanded leaves were infiltrated at the abaxial surface with a 1 ml needless syringe. For pGWB constructs, leaves were harvested four days post infiltration. For pGDPVXMCS constructs, infiltrated leaves

were harvested 6 days post infiltration (dpi) and systemically infected leaves were harvested 12-14 dpi. All the leaves were snap frozen in liquid nitrogen and stored at -80 °C until use.

***Protein extraction from N. benthamiana leaves***

The leaf tissue was ground in liquid nitrogen. Ice cold protein extraction buffer (50 mM $NaH_2PO_4$, pH 8.0; 300 mM NaCl, 10 mM imidazole, 10 % glycerol) amended with 1µM PMSF and 0.5 X Halt protease inhibitor cocktail was added to the ground leaf tissue at the 5:1 (buffer: tissue) ratio. The homogenate was centrifuged at 40,000 g and 4 °C for 30 min, and soluble protein fraction was collected as supernatant.

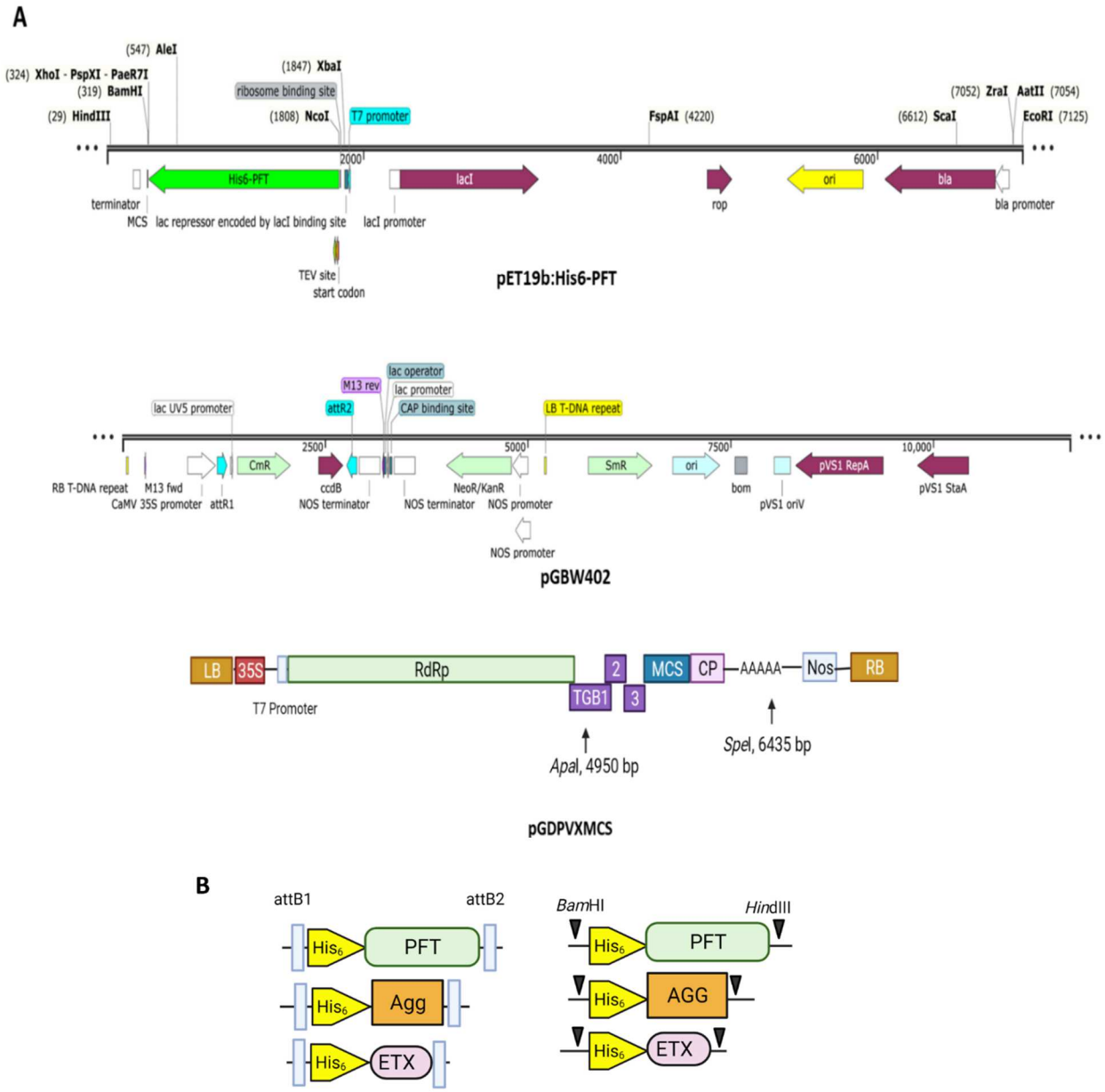


**Figure 5. 1. Schematic of plasmid construction in the study**. **A)** Expression vectors used in the study. **B)** Gene constructs used for heterologous expression in plants. Maps were constructed using SnapGene and BioRender software.

***Protein purification using nickel resins (IMAC) under native conditions and quantification***

To purify $His_6$ tagged proteins, affinity purification was performed using Ni-NTA His-Bind resin and Ni-NTA Buffer Kit, following the manufacturer's instructions (Millipore Sigma, Burlington, MA). Briefly, fifty milliliters of the soluble protein fraction were mixed with 5 ml of equilibrated His-Bind resins and incubated overnight with gentle shaking at 4 °C. Protein lysate and resin slurry mix was loaded onto 20 ml gravity columns to let the flow through pass. Protein-bound resins were washed with 4 column volumes of wash buffer (50 mM $NaH_2PO_4$, pH 8.0; 300 mM NaCl, 20 mM imidazole). Subsequently, His-bound proteins were eluted in ten fractions of 1 ml each using elution buffer (50 mM $NaH_2PO_4$, pH 8.0; 300 mM NaCl, 250 mM imidazole). Fractions containing the proteins of interest were pooled and concentrated using Amicon Ultra-4 centrifugal filters with 10 kDa molecular weight cutoff (Millipore Sigma, Burlington, MA). The concentrated protein fraction was dialyzed against protein storage buffer (50 mM Tris-HCl, 1mM $CaCl_2$, pH 8.0) overnight at 4 ºC using a Slide-A-Lyzer Mini Dialysis device with a 10 kDa molecular weight cutoff (ThermoFisher Scientific, Waltham, MA). All the purification steps were performed under refrigerated conditions or on ice. Protein was quantified using Pierce Detergent Compatible Bradford Assay Kit following the manufacturer's protocol (ThermoFisher Scientific, Waltham, MA). The known concentrations of Bovine Serum Albumin (BSA) were used to create a standard curve. Protein purifications were verified by running 10 % SDS-PAGE followed by Simply Blue Coomassie staining or western blotting as described below.

***Protein gel electrophoresis and Western blot analysis***

Protein fractions were analyzed by SDS-PAGE using Novex Wedge Well 10% Tris-Glycine Gels (Invitrogen, Waltham, MA). Protein samples were mixed with Laemmli sample loading buffer and incubated at 95 °C for 10 min. Samples were resolved on SDS-PAGE at 225 V for 45 min using 1X SDS running buffer in the XCell Surelock Mini-Cell (Invitrogen, Waltham, MA). The gel was stained using Coomassie-based Simply Blue stain (Invitrogen, Waltham, MA) following the manufacturer's recommendations to visualize the total protein profile after electrophoresis. For Immunodetection by Western Blot, the proteins were blotted to a nitrocellulose membrane with a pore size of 45 µm (Invitrogen, Waltham, MA) using the XCell II Blot module (Invitrogen, Waltham, MA). For blocking, the membrane was treated with 5 % BSA in TBS (20 mM Tris-HCl, 150 mM, pH 7.6) solution at room temperature for 2 h. The membrane was then probed with 1: 1000 dilution of monoclonal anti-His antibody (Sigma Aldrich, Burlington, MA) in an antibody diluting solution (TBS containing 0.1% Tween 20 and 2.5% BSA) for overnight at 4 °C. Subsequently, the membrane was washed three times with wash buffer (TBS containing 0.05% Tween 20) for 10 minutes each and then treated with a 1:5000 dilution of goat anti-mouse alkaline phosphatase-labeled IgG in an antibody diluting solution for 2 h at room temperature (LGC SeraCare, Inc.). After three washes of 10 min each with wash buffer, the membrane was developed using the BCIP/NBT alkaline phosphatase substrate system (LGC SeraCare, Inc.).

***Peptide Sequencing and Analysis***

The homogenate containing recombinant $His_6$-PFT expressed in *E. coli* was resolved on a 10% SDS-PAGE gel and stained with Simply blue (as described above). A discrete band corresponding to 54 kDa was excised and shipped to the Proteomics/ Mass Spectrometry Research Facility of Mitchell Cancer Institute, University of South Alabama. The samples were analyzed using MALDI MS/ MS-MS. Peptide sequence analysis was performed using Matrix science Mascot software using the following settings: 10 ppm window for the precursor mass; a 0.6 Da fragment matching allowing two missed cuts; carbamidomethyl fixed modification; unrestricted taxonomy search.

***RNA extraction and Reverse Transcription -PCR (RT-PCR)***

Tissue was collected from systemically infected leaves of pGDPVXMCS: $His_6$-PFT, pGDPVXMCS: $His_6$-Agg, and pGDPVXMCS: $His_6$-ETX expressing plants 10 days post infiltration. Total RNA was extracted using the Direct-Zol kit per the manufacturer's recommendation (Zymo Research, Irvine, CA). After DNase treatment with NEB DNaseI (Ipswich, MA, USA), cDNA synthesis was performed using the AzuraQuant cDNA synthesis kit (Azura genomics, Raynham, MA, USA). PCR was performed using the primers used for cloning the inserts in pSKAS vectors (Table 5.1). PCR was performed in 25 µl reaction volume containing 2 µl of cDNA, 5 µl of MyTaq DNA Polymerase Buffer (Meridian Bioscience, Cincinnati, OH), and 400 nM of each forward and reverse primer. A touchdown Polymerase Chain reaction (PCR) profile was used as follows: 95 °C for 5 min, seven cycles of 95 °C for 45

s, 64-58 °C for 45 s with a decrease of 1 °C per cycle, 72 °C for 1 min, followed by 27 cycles of 95 °C for 45 s, 58 °C for 45 s, 72 °C for 1 min, and a final extension of 72 °C for 5 min was used. PCR products were resolved on Ethidium Bromide stained 2% Agarose gel for 1 h and visualized under UV.

***Hemagglutination assay***

To test the ability of $His_6$-PFT to bind with cell surface glycoproteins, a hemagglutination assay was performed. Five percent rabbit erythrocytes (Lampire Biological Labs, Pipersville, PA) were washed three times in protein storage buffer (50 mM Tris-HCl, 1mM $CaCl_2$, pH 8.0). For washing, red blood cell solution was pelleted by centrifuging at 500 g and 4 °C for 10 min; the supernatant was removed, and cells were resuspended in the buffer. After the third centrifugation, the cell pellet was resuspended at 2% concentration. For hemagglutination assay, 20 µl of 2% erythrocyte suspension and 20 µl of affinity-purified $His_6$-PFT (1.5 mg/ml) were mixed on a glass slide and incubated for 10 min at room temperature. For negative control, erythrocytes were separately incubated with buffer and $His_6$-ETX (1.5 mg/ml). The hemagglutination patterns were observed using a 20X objective lens under a compound light microscope.

***Glycan Microarray analysis***

To determine the binding specificity of agglutinin domains of PFT, affinity-purified $His_6$-PFT and $His_6$-ETX fractions were screened against an array of 300 Glycans. The glycan array screening was performed by RayBiotech (Peachtree Corners, GA). A RayBio® Glycan Array

300 Kit was used, which contains blocks of 300 synthetic glycan spots where each spot is replicated three times along with positive and negative control spots for normalization. Samples were biotinylated, and label- based approach was used. Each sample was incubated with the array at 2 μg/ml concentration. Data were normalized and analyzed using RayBio Analysis software.

***In vitro antifungal assay***

To test *in vitro* antifungal activity of PFT, purified $His_6$-PFT was treated macroconidia of *F. graminearum*. As described previously, *F. graminearum* macroconidia were produced in Mung Bean Broth (MBB). Briefly, MBB was prepared by steeping 20 g of mung bean seeds in 500 ml of hot water, and the collected filtrate was autoclaved and cooled. For macroconidia production, two 1cm mycelial plugs taken from one week old fungal culture on a Potato Dextrose Agar (PDA) plate were added to 50 ml MBB and shaken at 200 rpm at 28 ºC for 7-10 days. The spore culture was filtered through a sterile cheesecloth and centrifuged at 4,000 g for 8 min. The spore pellet was resuspended in Potato Dextrose Broth (PDB) and quantified using a hemocytometer. The spore concentration was adjusted to 80,000 spores $ml^{-1}$ in PDB. Fifty microliters of spore suspension were mixed with 50 μl of purified $His_6$-PFT (10 mg/ ml) or protein storage buffer in a flat bottom 96-well microtiter plate and incubated at 25 ºC in the dark. Spore germination and hyphal growth were observed under bright-field settings using a Nikon Eclipse microscope after 12-14 h of incubation. The hyphal lengths of treated spores were measured using Image J software.

## 5.3. Results

### *In silico analysis of PFT*

Based on the CDD search, the coordinates of three domains of 478 amino acids (aa) long PFT protein were identified: Agglutinin domain 1 (7- 166 aa), Agglutinin domain 2 (171-305 aa), and ETX/MTX2 aerolysin pore-forming domain (351-475 aa). The three-dimensional structure of PFT was predicted using homology-based and *de novo* modeling. No single crystal structure with both Agg and ETX domains was available for homology-based modeling. Therefore, two crystal structures belonging to one of the domain types were used. For the Agg domain, chain A structure from *Amaranthus caudatus* (PDB ID: IJXL) was used as a reference template (Transue et al., 1997). IJXL had 33% sequence similarity with the Agg domain of PFT. For the ETX domain, Natterin-like protein from zebra fish (PDB ID: 5DI0) was used as a reference template (Jia et al., 2016). 5DI0 had 31.4% sequence similarity with the ETX domain of PFT. The PFT structure models predicted by homology-based and *de novo* modeling are shown in Figure 5.2. Since two different references were used to build a homology-based model, the connection between Agg and ETX domain was not predicted well, which is evident from the large linker between Agg and ETX domain in the homology-based model. On the other hand, *de novo* modeling predicted better structure in the region between Agg and ETX domain. The prediction accuracy between the two models were compared by evaluating their Ramachandran plots. The percentage of residues in the most favored region was 90.6 % for the *de novo* model while only 84 % for the homology-based model. The percentage of residues in the disallowed

region was 0.2% for the de novo model whereas it was 2.6% for the homology-based model. Therefore, higher prediction accuracy of PFT model was achieved through *de novo* modelling.

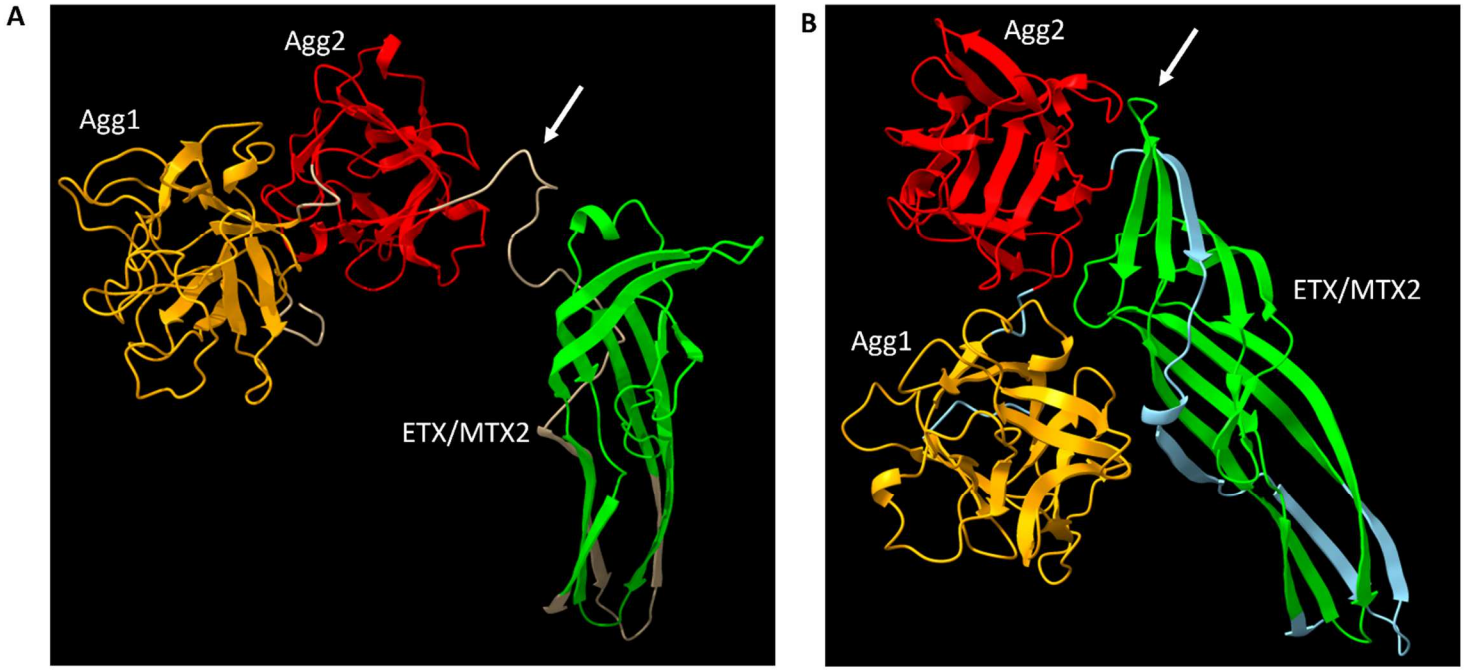


**Figure 5. 2. The predicted three-dimensional protein structures of PFT**. A) Homology-based model predicted uisng MODELLER. B) De novo model buid using AlphaFold. Domain labelling is based on the coordinates identified using NCBI CDD. Arrow indicate the connector loop between two domain types.

The protein-ligand docking was performed to check the binding affinity of the Agg domain of PFT against different monosaccharide ligands. Although the homology-based PFT model had overall lower prediction accuracy, it maintained the ligand-binding site (Figure 5.3).

On the other hand, the ligand binding site was lost in the *de novo* model. Therefore, the homology-based model was used for docking analyses. The diagrammatic representation of PFT and ligand interactions and their binding energy values are shown in Figure 5.4. The binding energies were -4.7, -4.0, and -6.4 for Glc, GlcNAc, and chitosan, respectively. Glc is a monomer of cellulose, a major component of the plant cell wall. GlcNAc is a monomer of chitin, a major fungal cell wall component. Chitosan is another important component of fungal cell wall. Higher binding energy in negative suggests a higher affinity of ligand towards the protein's binding site. Although, binding energies for Glc and GlcNAc were comparable, higher negative binding energy for chitosan suggests preferential affinity of PFT towards specific components of fungal cell wall.

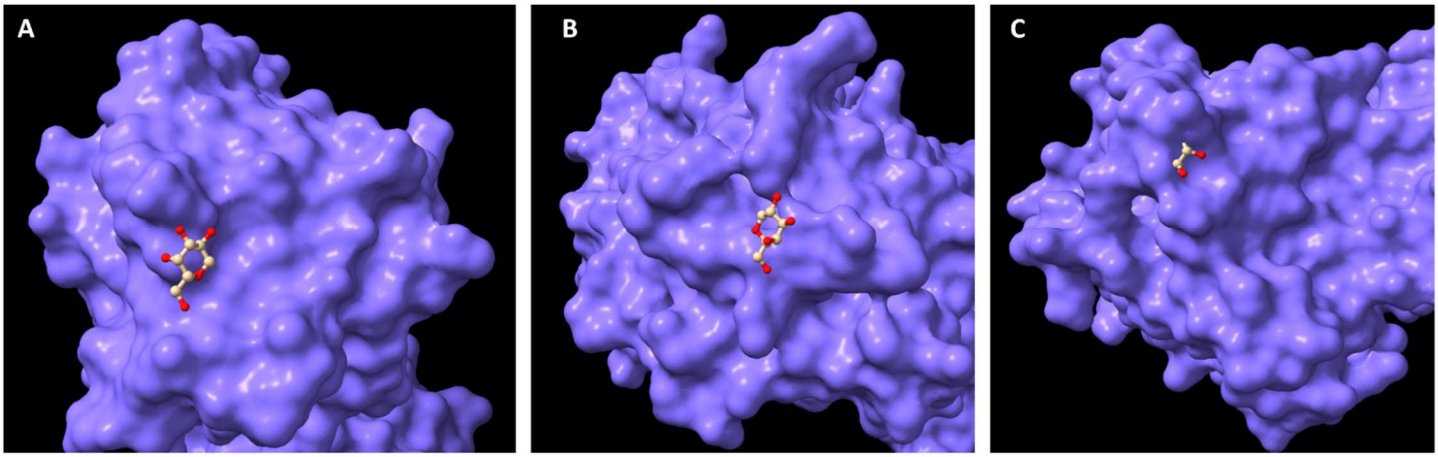


**Figure 5. 3. Binding pockets of the Agg domain of reference template IJXL** (A), homology-based PFT model **(B),** and de novo PFT model **(C)** with respect to the ligand beta-D-galactose (Gal2)

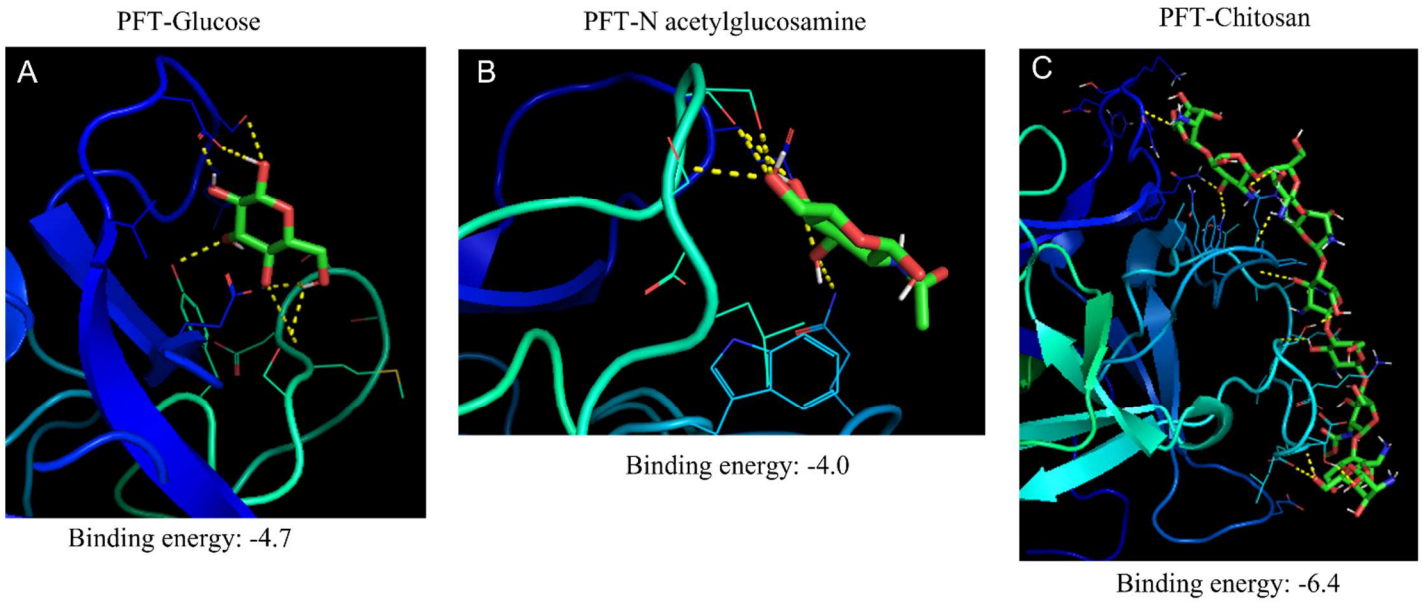


**Figure 5. 4. Docking analysis of PFT and ligands. A)** Glc: Glucose, **B)** GlcNAc: N-acetyl glucosamine and **C)** Chitosan.

***Expression of PFT in bacteria***

For functional characterization of wheat PFT, codon optimized PFT with N terminal 6X His tag was expressed in pET19b expression vector in *E. coli* BL21 (DE3) cells. SDS PAGE analysis of total fractions at 0, 2, 4, 6, and 8 h after the IPTG induction showed an inducible protein band of 54 kDa size (Figure 5.5.A). The theoretical molecular weight of $His_6$-PFT is estimated to be 54.69 kDa, indicating the expression of full $His_6$-PFT in bacteria. However, SDS

PAGE analysis of soluble and insoluble fractions revealed that $His_6$-PFT was exclusively present in the insoluble fraction (Figure 5.5.B). Therefore, suggesting the accumulation of PFT as inclusion bodies (IBs).

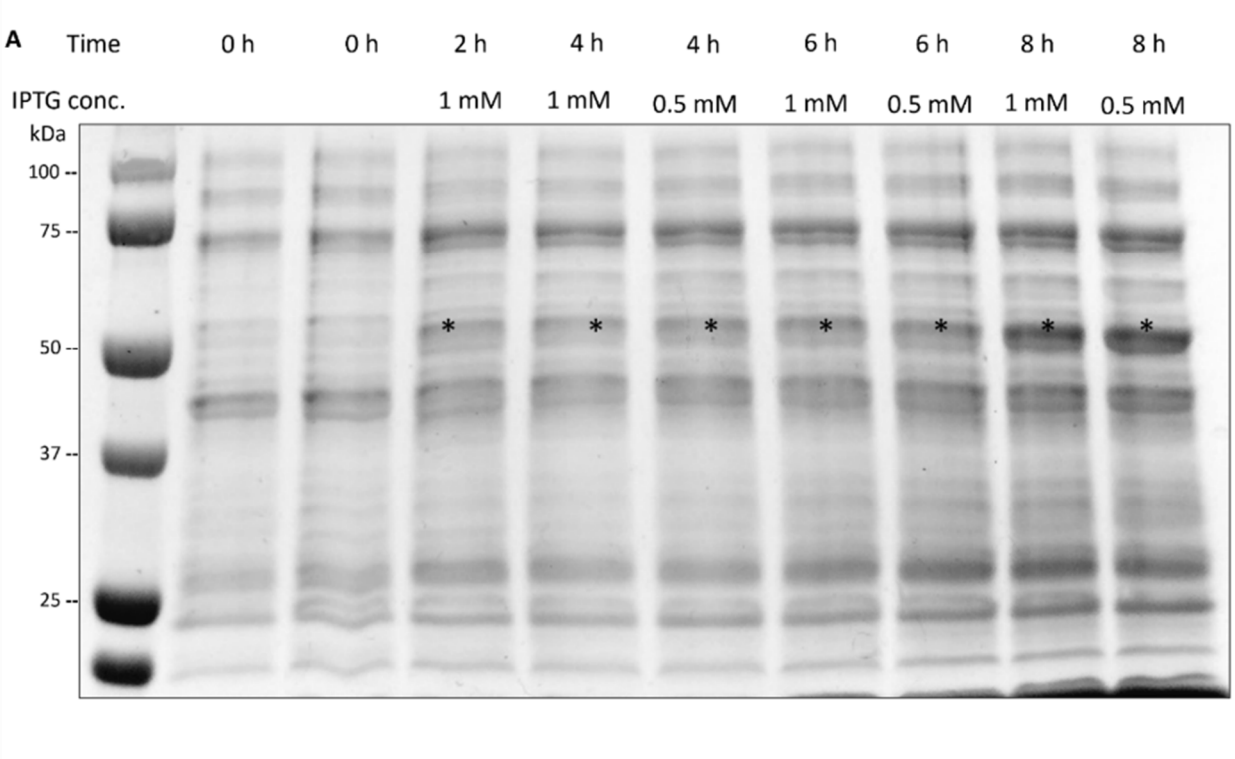

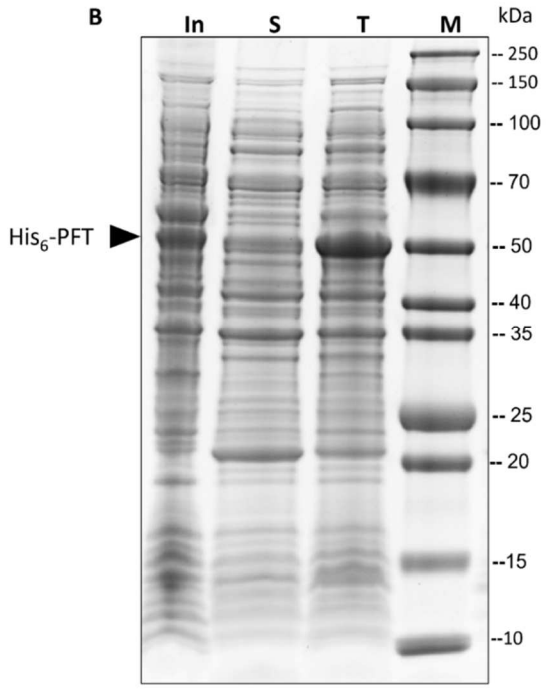


**Figure 5. 5. Recombinant protein production of $His_6$-PFT in *E. coli.* A)** SDS-PAGE analysis of $His_6$-PFT expression at different time points and concentrations of IPTG. **B)** SDS-PAGE analysis of Total (T), soluble (S), and insoluble (In) fractions collected after IPTG induction. Gel was stained with SimplyBlue Stain. M = ProSignal Full-Range Prestained Protein Ladder; kDa= kilo Dalton. Arrowhead indicates $His_6$-PFT specific band.

PFT specific protein band was isolated and sequenced. Peptide sequencing confirmed the expression of PFT in *E. coli* (Figure 5.6). PFT was the second-best match and only plant protein in a peptide BLAST against the NCBI nr protein database (Figure 5.6.A). A total of seven peptide sequences were obtained with the size range of 9 to 21 amino acids (Figure 5.6.B). These peptide sequences covered 20% of the PFT sequence and were located throughout the protein sequence.

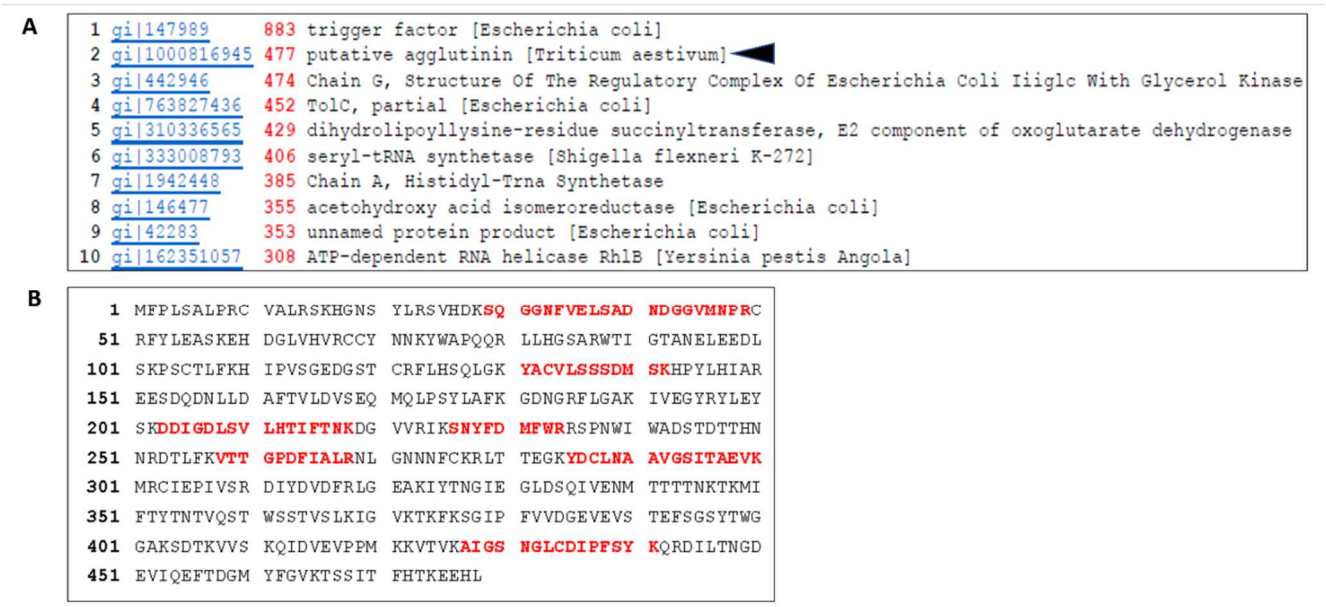


**Figure 5. 6. Peptide sequencing of His$_6$-PFT expressed in *E. coli.*** **A)** BLAST results of peptides against NCBI nr protein database. **B)** Alignment of seven peptides recovered from sequencing of His$_6$-PFT gel band on the protein sequence of PFT. Arrowhead indicates PFT sequence as a BLAST hit. Bold red represents the recovered seven peptide sequences covering 20% of the PFT sequence.

To extract PFT from *E. coli*, expression at low temperatures was tried to minimize IB formation. However, in that case, the protein could not be produced in detectable amounts in the soluble fraction (data not shown). Given the challenges of protein extraction and correct refolding from IBs, we switched to plant-based heterologous expression system.

***Expression of recombinant PFT and its domains using PVX based expression system in N. benthamiana***

A PVX-based expression vector with CaMV 35 S promoter for was used for heterologous expression of PFT and its domains. The Agrobacterium-mediated infection with the pGDPVXMCS: His6-PFT, pGDPVXMCS: His6-Agg, and pGDPVXMCS: His6-ETX was done on the 3-4 fully expanded leaves of *N. benthamiana* plants. After 10 days of inoculation, RNA from young foliar tissue was extracted, and RT-PCR was done to confirm the systemic expression of PFT and the individual domains (Figure 5.7. A). However, the three constructs produced different effects on the infiltrated plants. The infiltrated and systemically infected leaves of pGDPVXMCS: $His_6$-ETX vector expressing plants showed extensive cell death leading to necrosis, whereas no necrosis was observed in the case of pGDPVXMCS: $His_6$-PFT and pGDPVXMCS: $His_6$-Agg constructs. (Figure 5.7. A). Thus, suggesting that either the whole PFT or the Agg domain was not toxic to the plant cells; however, the ETX domain was toxic. Furthermore, indicating that the Agg domain provides specificity of recognition to PFT, and in its absence, ETX is detrimental even to the plants. Although strong phenotypic effects using the PVX expression system were observed, protein purifications of PFT and its domains were not

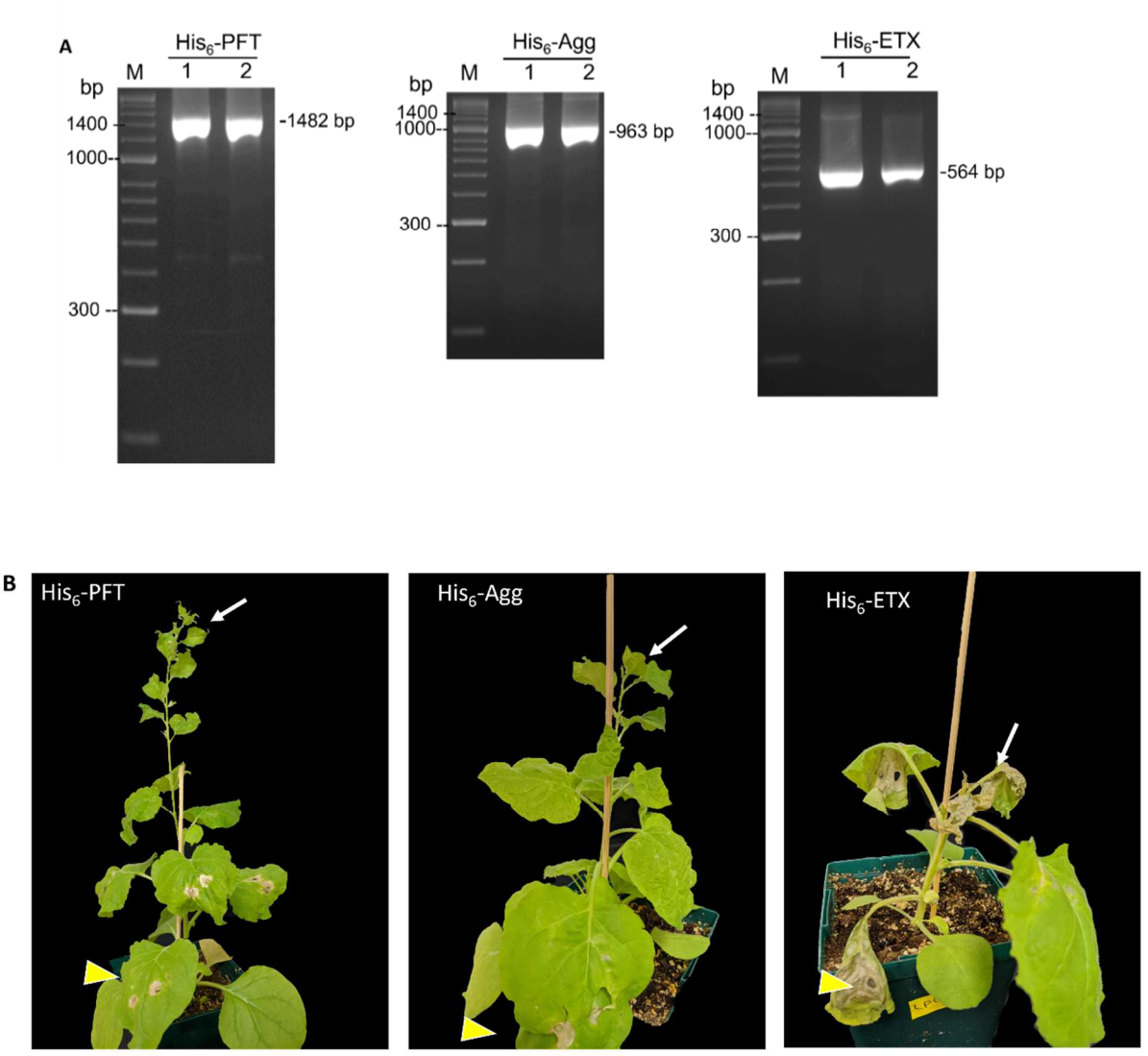


**Figure 5. 7. Expression of PFT and its domains using PVX based expression system. A)** Reverse Transcription - PCR (RT-PCR ) of systemically infected *N. benthamiana* leaves expressing PFT and its domains in PVX based vectors 10 days post infiltration. **B)** *N. benthamiana* plants expressing PFT and its domains in PVX based vectors two weeks post infiltration. Arrowheads indicate infiltrated leaves and arrow indicate systemically infected leaves; M = 50 base pair (bp) DNA ladder.

successful using this system. Therefore, another plant expression system was used to isolate and characterize PFT and its domains.

***Expression of recombinant PFT and its domains using transient expression system in N. benthamiana***

PFT and the Agg and ETX domains were transiently expressed in *N. benthamiana* using gateway binary vector, pGBW402, with CaMV 35 S promoter. Like expression in *E coli*, similar size band of $His_6$-PFT was detected from expression in *N. benthamiana.* $His_6$-PFT was recovered in the soluble fraction and could purify it further using Ni-NTA His resins under native conditions (Figure 5.8, Figure 5.9). SDS PAGE analysis followed by Coomassie staining revealed a similar size band in the control pGDp19 construct as well (Figure 5.8). However, no such band was detected during the western blot analysis of soluble lysate and elute fraction of pGDp19 (Figure 5.9). One of the subunits of Rubisco, the most abundant plant protein, has a similar size. Therefore, western blot analysis was required after every purification to confirm the presence of $His_6$-PFT, which was obscured in the Coomassie-stained SDS PAGE due to the Rubisco subunit. Like $His_6$-PFT, $His_6$-ETX was also soluble and could be purified using affinity chromatography under native conditions (Figure 5.9). The molecular weight of $His_6$-ETX perfectly matched its theoretical weight of 20.06 kDa. $His_6$-Agg was not recovered in the soluble fraction (data not shown); therefore, it could not be purified further. We did not observe any necrosis or cell death in leaves transiently expressing pGBW402:$His_6$-PFT, pGBW402:$His_6$-Agg, and pGBW402:$His_6$-ETX vectors. We could produce substantial amounts for His6-PFT and

His6-ETX for downstream assays using the transient expression system. For example, 260 µg of $His_6$-PFT affinity-purified protein was obtained from 30 g (Fresh weight) of leaf tissue.

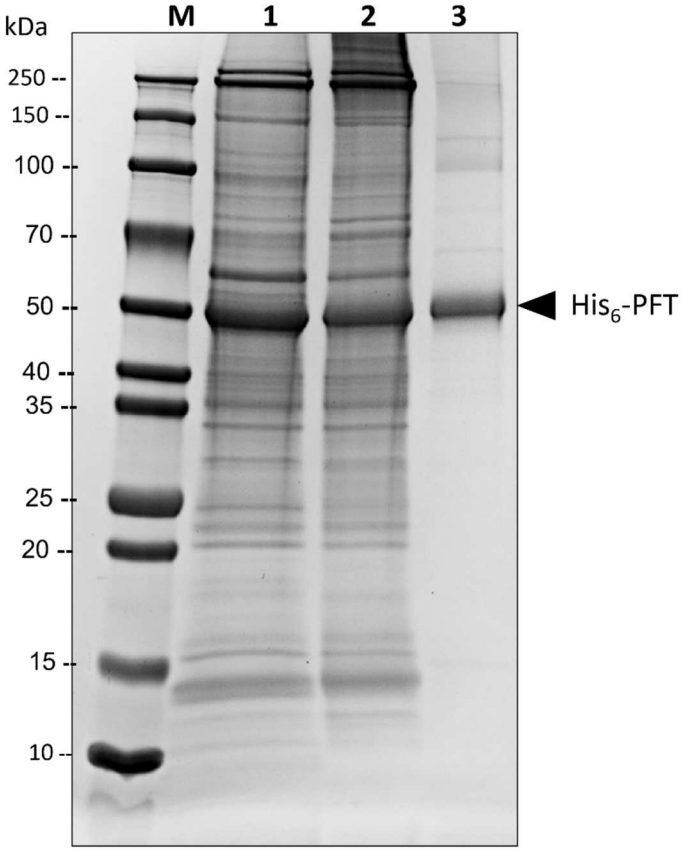


**Figure 5. 8. Recombinant protein production of $His_6$-PFT in *N. benthamiana*.** SDS-PAGE analysis of p19 (1), $His_6$-PFT lysate (2), and $His_6$-PFT elute (3) fractions. 20 µg of 1 and 2 and 2 µg of 3 were resolved on gel followed by staining with SimplyBlue Stain. M = ProSignal Full-Range Prestained Protein Ladder; kDa= kilo Dalton. Arrowhead indicates $His_6$-PFT band which coincides with Rubisco band in 1 and 2.

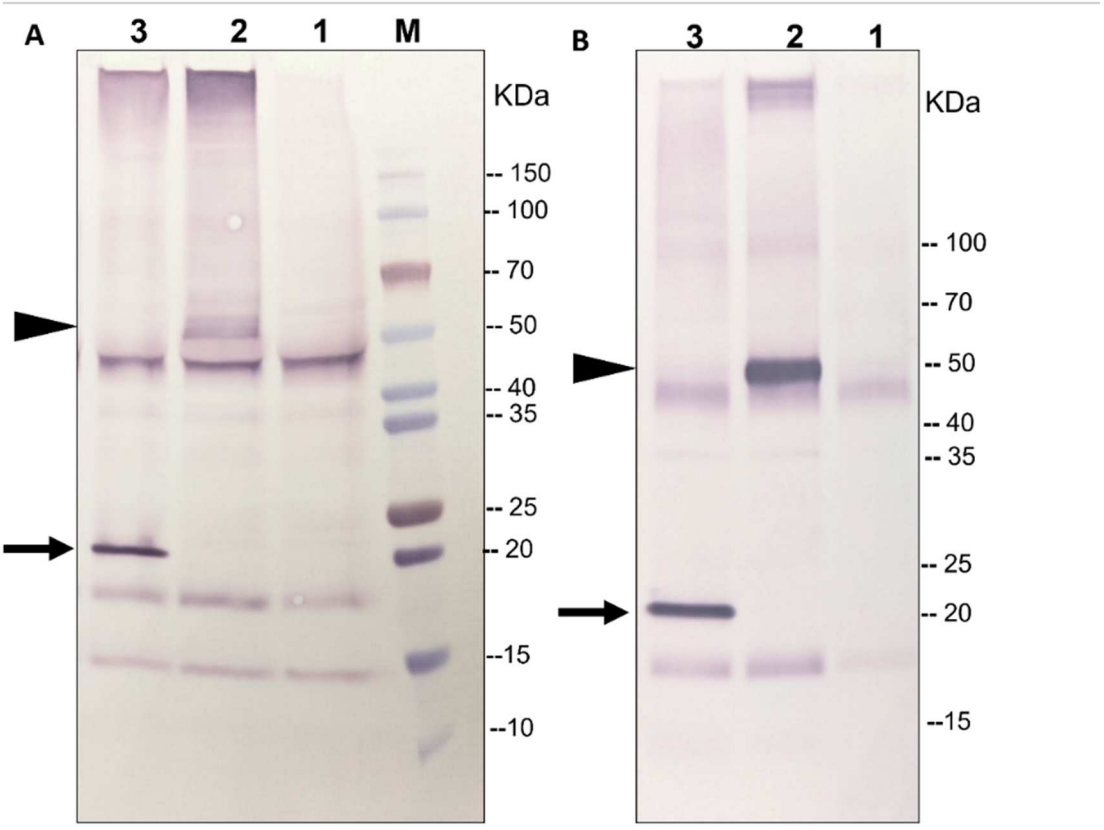


**Figure 5. 9. Western Blot analysis of $His_6$-PFT and $His_6$-ETX expressed in *N. benthamiana.* A)** Immunoblot of soluble fractions of p19 (1), $His_6$-PFT (2), and $His_6$-ETX after protein extraction. **B)** Immunoblot of elution fractions of p19 (1), $His_6$-PFT (2), and $His_6$-ETX (3) after affinity chromatography with Ni-NTA resins. Membranes were incubated with a monoclonal anti-His antibody followed by AP conjugated goat anti-mouse IgG.M = ProSignal Full-Range Prestained Protein Ladder; kDa= kilo Dalton. Arrowhead indicates $His_6$-PFT band and arrow indicates $His_6$-ETX band.

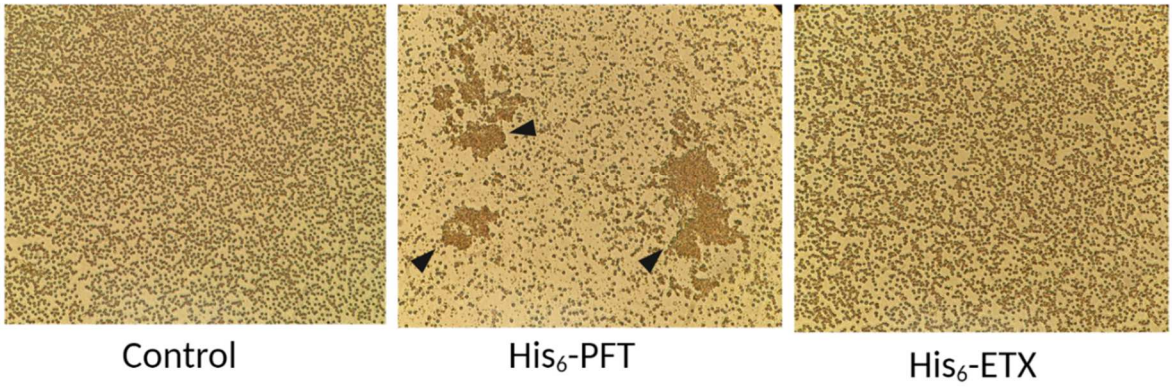


**Figure 5. 10. Hemagglutination assay of $His_6$-PFT and $His_6$-ETX expressed in *N. benthamiana***. Rabbit erythrocytes were treated with control (protein storage buffer), and affinity purified $His_6$-PFT and $His_6$-ETX. Images were taken under 20X objective lens. Arrowhead indicates agglutination of erythrocytes

***Hemagglutination activity of purified PFT and its domains***

PFT is predicted to be a chimeric lectin protein. Lectins are known to reversibly bind to carbohydrates on the cell surface and lead to agglutination of cells. This hemagglutination property of lectins is tested by treating lectins with different kinds of erythrocytes, and most commonly, rabbit red blood cells are used. This property of PFT was tested by incubating $His_6$-PFT with 2% rabbit erythrocytes. During initial attempts, the assay was perfomed in a standard PBS buffer. Even using the 2 mg/ml protein concentration, no agglutination pattern was observed (data not shown). One class of lectins called c-type lectins is known to require Ca 2+

ions for their activity. To test if Ca 2+ ions are required for the hemagglutination activity of PFT, we exchanged the buffer with 50 mM Tris-HCl, 1mM $CaCl_2$, pH 8.0. In the presence of Ca 2+ ions, $His_6$-PFT agglutinized 2 % rabbit erythrocytes at 1.5 mg/ml concentration (Figure 5.10). On the other hand, no agglutination was observed due to $His_6$-ETX and buffer. The absence of hemagglutination in $His_6$-ETX indicate that this property is specific to the Agg domain of PFT. Furthermore, hemagglutination activity of $His_6$-PFT suggested that functionally active PFT protein could be purified from heterologous expression in *N. benthamiana*.

***PFT specifically binds to glycans with chitin monomer***

To determine the specific binding affinity of PFT, $His_6$-PFT and $His_6$-ETX protein fractions were screened against an array of 300 types of glycans. RayBio® Glycan Array 300 was used, containing three replicate spots of each of 300 glycans and twelve spots of positive control, and six negative control spots. $His_6$-ETX was used as a negative control since it possesses the same background proteins, which are also present in affinity-purified $His_6$-PFT. Therefore, the binding affinity of specifically the Agg domain of PFT could be tested. The experiment was performed in two replicates, and the results were in complete agreement between replicates. The two µg/ ml sample concentration gave good signal intensity to compare relative differences in binding patterns of $His_6$-PFT and $His_6$-ETX (Figure 5.11.A). Out of the 300 glycans, eleven glycans showed strong and specific signals for $His_6$-PFT. These glycans had relative fluorescent units (RFU) values of more than 4,000 (Figure 5.11.B).

Interestingly, all the eleven glycans had one or multiple units of monosaccharide, GlcNAc (Figure 5.11.C). Furthermore, although in a comparatively lower RFU range (962 – 2164), the binding affinity of $His_6$-PFT was 26, 24, and 85 % higher than $His_6$-ETX for ß-GlcNAc-Sp, GlcNAc-ß-1,6-GlcNAc-ß-Sp, and Chitin-trisaccharide-Sp1glycans, respectively (Appendix 5.1). Hence, glycan screening validated the in-silico analysis of PFT's binding affinity towards the fungal cell wall specific carbohydrate monomers.

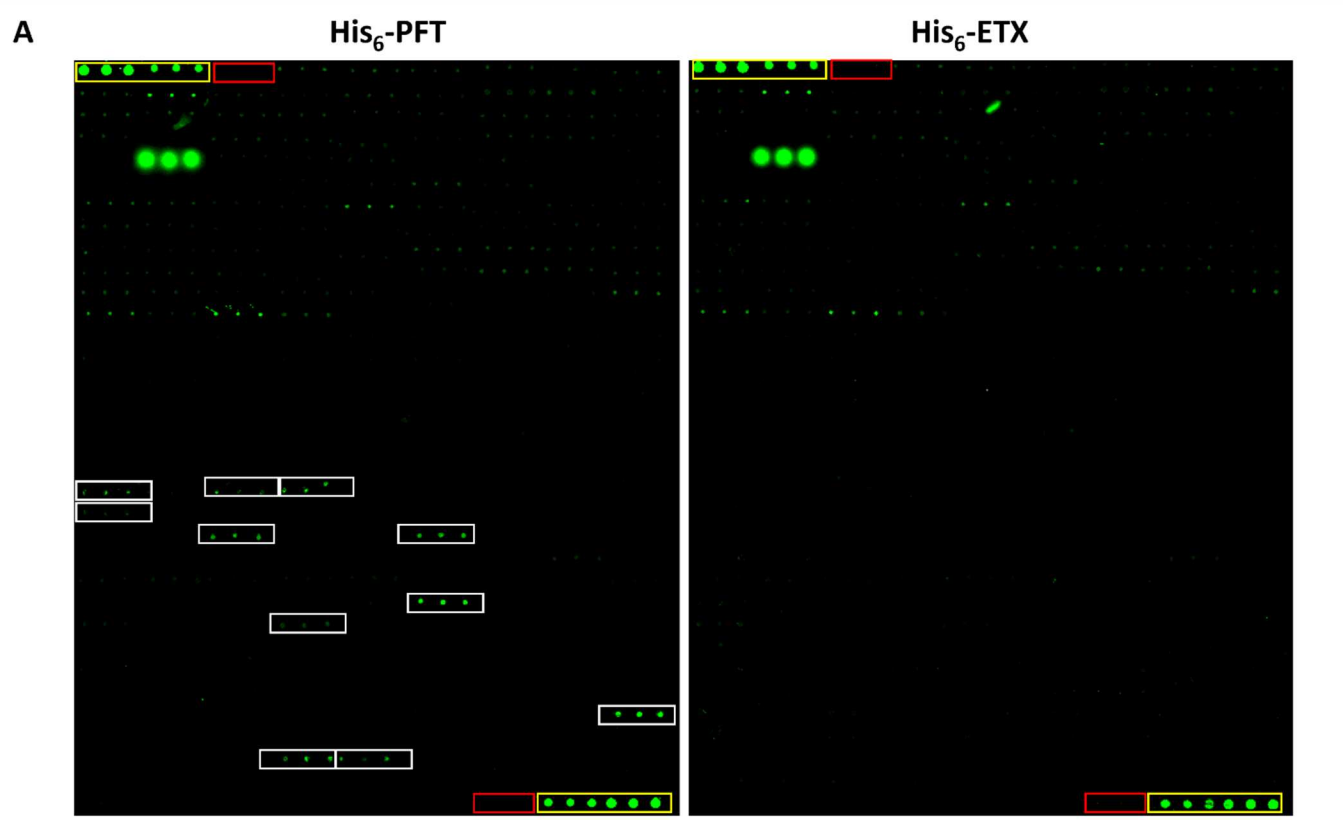

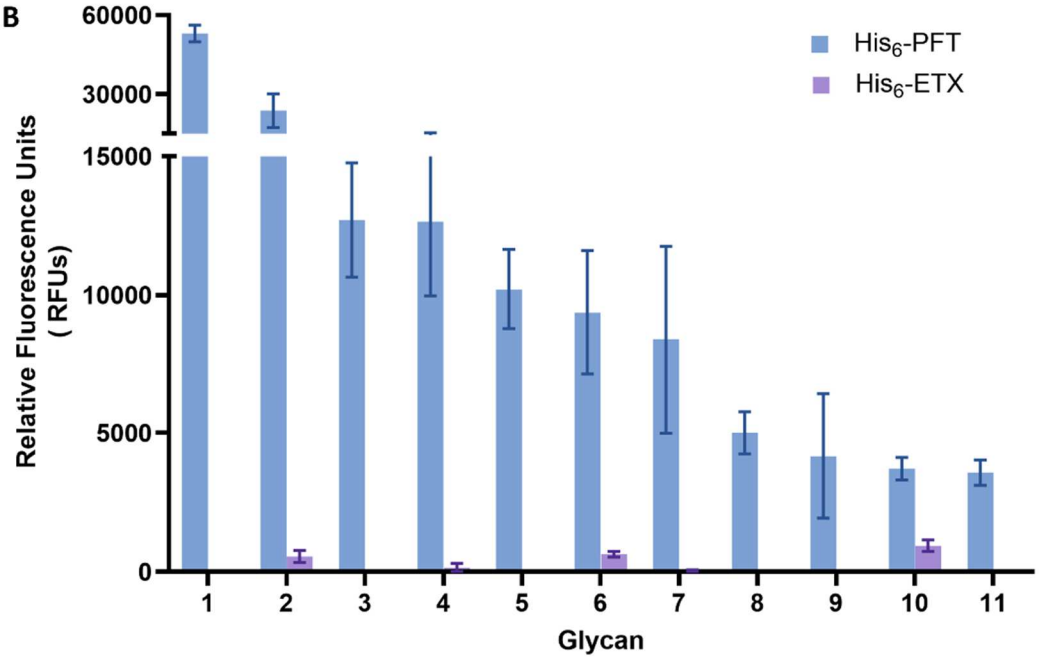
B
60000
30000
15000
10000
5000
0
Relative Fluorescence Units
( RFUs)
His6-PFT
His6-ETX
1
2
3
4
5
6
7
8
9
10
11
Glycan

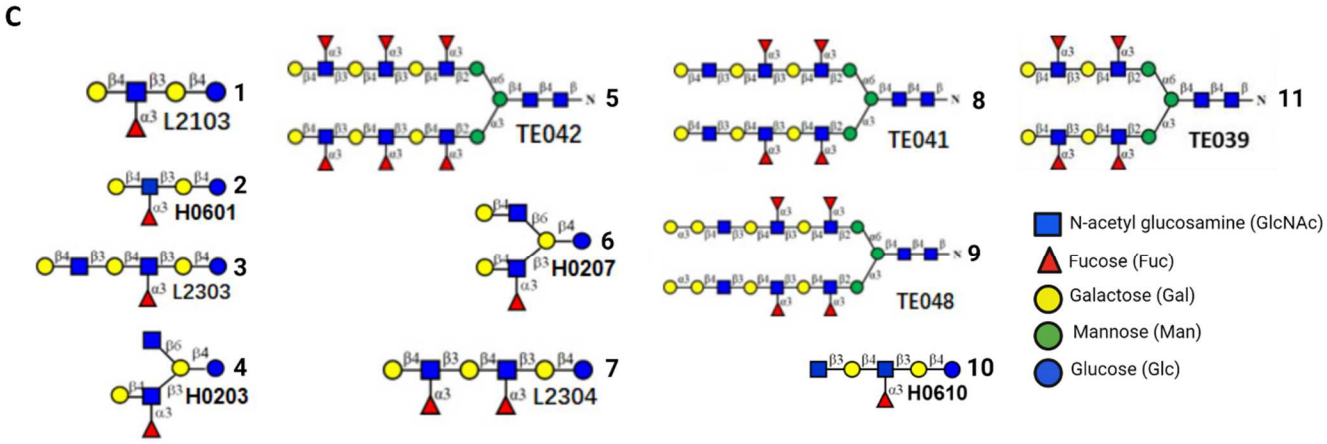
C
1
L2103
2
H0601
3
L2303
4
H0203
5
TE042
6
H0207
7
L2304
8
TE041
9
TE048
10
H0610
11
TE039
N-acetyl glucosamine (GlcNAc)
Fucose (Fuc)
Galactose (Gal)
Mannose (Man)
Glucose (Glc)

**Figure 5. 11.** Binding of $His_6$-PFT and $His_6$-ETX to Glycan array 300. **A)** Binding patterns of $His_6$-PFT and $His_6$-ETX on the Glycan array 300. Yellow box and red boxes highlight positive and negative controls, respectively. White boxes highlight specific binding of $His_6$-PFT. **B)** Mean RFU (±SEM) of eleven out of the 300 glycans specifically binding to $His_6$-PFT. **C)** Structure of glycans specifically binding to $His_6$-PFT with highest affinity. The names of the glycans in A and B are: **(1)** Gal-ß-1,4-(Fuc-a-1,3-)GlcNAc-ß-1,3-Gal-ß-1,4-Glc-Sp5, **(2)** Gal-ß-1,4-(Fuc-a-1,3-)GlcNAc-ß-1,3-Gal-ß-1,4-Glc-Sp5 , **(3)** Gal-ß-1,4-GlcNAc-ß-1,3-Gal-ß-1,4-(Fuc-a-1,3-)GlcNAc-ß-1,3-Gal-ß-1,4-Glc-Sp5 , **(4)** Gal-ß-1,4-(Fuc-a-1,3-)GlcNAc-ß-1,3-(GlcNAc-ß-1,6-)Gal-ß-1,4-Glc-Sp5, **(5)** Gal-ß-1,4-(Fuca-1,3-)GlcNAc-ß-1,3-Gal-ß-1,4-(Fuc-a-1,3-)GlcNAc-ß-1,3-Gal-ß-1,4-(Fuc-a-1,3-)GlcNAc-ß-1,2-Man-a-1,3-[Gal-ß-1,4-(Fuca-1,3-)GlcNAc-ß-1,3-Gal- ß-1,4-(Fuc-a-1,3-)GlcNAc-ß-1,3-Gal-ß-1,4-(Fuca-1,3-)GlcNAc-ß-1,2-Man-a-1,6-]Man-ß-1,4-GlcNAc-ß-1,4-GlcNAc-ß-Asn , **(6)** Gal-ß-1,4-(Fuc-a-1,3-)GlcNAc-ß-1,3-(Gal-ß-1,4-GlcNAc-ß-1,6-)Gal-ß-1,4-Glc-Sp5 , **(7)** Gal-ß-1,4-(Fuc-a-1,3-)GlcNAc-ß-1,3-Gal-ß-1,4-(Fuc-a-1,3-)GlcNAc-ß-1,3-Gal-ß-1,4-Glc-Sp5 , **(8)** Gal-ß-1,4-GlcNAc-ß-1,3-Gal-ß-1,4-(Fuc-a-1,3-)GlcNAc-ß-1,3-Gal-ß-1,4-(Fuc-a-1,3-)GlcNAc-ß-1,2-Man-a-1,3-[Gal-ß-1,4-GlcNAc-ß-1,3-Gal-ß-1,4-(Fuc-a-1,3-)GlcNAc-ß-1,3-Gal-ß-1,4-(Fuc-a-1,3-)GlcNAc-ß-1,2-Man-a-1,6-]Man-ß-1,4-GlcNAc-ß-1,4-GlcNAc-ß-Asn , **(9)** Gal-a-1,3-Gal-ß-1,4-GlcNAc-ß-1,3-Gal-ß-1,4-(Fuc-a-1,3-)GlcNAc-ß-1,3-Gal-ß-1,4-(Fuca-1,3-)GlcNAc-ß-1,2-Man-a-1,3-[Gal-a-1,3-Gal-ß-1,4-GlcNAc-ß-1,3-Gal-ß- 1,4-(Fuca-1,3-)GlcNAc-ß-1,3-Gal-ß-1,4-(Fuc-a-1,3-)GlcNAc-ß-1,2-Man-a-1,6-]Man-ß-1,4-GlcNAc-ß-1,4-GlcNAc-ß-Asn , **(10)** GlcNAc-ß-1,3-Gal-ß-1,4-(Fuc-a-1,3-)GlcNAc-ß-1,3-Gal-ß-1,4-Glc-Sp5 , **(11)** Gal-ß-1,4-(Fuca-1,3-)GlcNAc-ß-1,3-Gal-ß-1,4-(Fuca-1,3-)GlcNAc-ß-1,2-Man-a-1,3-[Gal-ß-1,4-(Fuc-a-1,3-)GlcNAc-ß-1,3-Gal-ß-1,4-(Fuc-a-1,3-)GlcNAc-ß-1,2-Man-a-1,6-]Man-ß-1,4-GlcNAc-ß-1,4-GlcNAc-ß-Asn.

### *Antifungal activity of purified PFT*

To test the antifungal property of PFT, 10 mg/ml of affinity-purified $His_6$-PFT was incubated macroconidia of *F. graminearum*. We observed spore germination patterns under a microscope after 12-14 hours of incubation. The protein storage buffer was used as a control. Any pronounced spore germination inhibition due to PFT was not observed when compared with buffer, and neither any abnormal hyphal growth was apparent. However, looking at the frequency distribution of hyphal length of germinated spores, 72% of the PFT-treated spores had a hyphal length of less than 1300 µm, whereas only 46 % of the buffer-treated spores fell in this category (Figure 5.12).

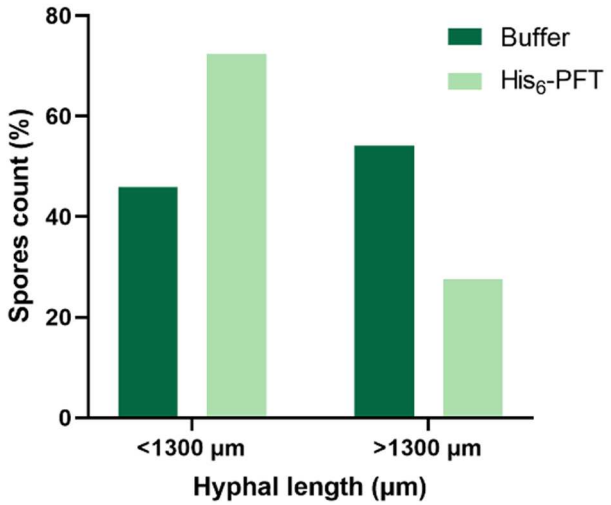


**Figure 5. 12. Effect of $His_6$-PFT treatment on the hyphal length of *F. graminearum* germinating spores**. Percentage frequency distribution of hyphal length of buffer (N=24) and $His_6$-PFT(N=29) treated germinating spores.

## 5.4. Discussion

The understanding of quantitative disease resistance lags in crop plants. In this study, I functionally characterized one of the most important disease resistance genes, PFT, that provides quantitative resistance against Fusarium Head Blight in wheat. The predicted domain architecture of PFT makes it a unique atypical disease resistance gene. I investigated the molecular mechanism of PFT-mediated resistance by functionally characterizing its agglutinin (Agg) and pore-forming domains (ETX). To do so, I performed heterologous expression of PFT in bacterial and plant systems. I was able to purify functionally active PFT protein and obtain experimental evidence that supports the predicted functions of its domains.

Purifying the functionally active PFT was a major prerequisite to testing the hypothesis. Two heterologous expression systems were employed: bacterial and plant based. Due to its simplicity and scalability, first bacterial expression system was used. PFT was successfully in *E. coli*, and peptide sequencing confirmed the identity of both its domain types. However, PFT was exclusively present in insoluble fractions indicating its accumulation in inclusion bodies (IBs), which was not surprising since most of the overexpressed toxic proteins accumulate in IBs. Hence, this suggests the potential toxicity of PFT due to the presence of the ETX domain. Due to challenges associated with purifying the correctly folded active protein from IBs (Bhatwa et al., 2021), I switched to a heterologous plant expression system. The plant-based heterologous expression system is now even used at commercial scales to synthesize antibodies and vaccines. First, Potato Virus X-based expression system was used, which has been previously used to purify functionally various active (Nemchinov et al., 2006; Kovalskaya et al., 2011, 2016;

Hammond et al., 2019). Although systemic expression at the transcript level was monitored and observed the differential phenotypic effect of PFT and its individual domains using this system, the overexpressed PFT protein and its domains could not be purified. Therefore, PFT and its individual domains were transiently expressed using a gateway binary plant expression vector. PFT and its ETX domain were recovered in the soluble fraction and were successfully purified under native conditions using Ni NTA His binding resins. Agg domain was obtained in insoluble fraction and could not be purified. In contrast to PVX-based expression, any differential phenotypic effects during transient overexpression of PFT and its domains were not observed. Such disagreement could be attributed to a difference in viral-based expression versus transient expression using binary vectors. I can speculate two possibilities: either the dosage effect where virus-based expression could have higher protein accumulation or the location effect where virus-based expression could accumulate protein in both intercellular and intracellular places compared to only intracellular accumulation in transient expression. Both of these possibilities require further experimentation for validation. Nevertheless, substantial amount of purified protein could be obtained for further functional analyses using the transient expression system.

PFT has a unique domain architecture that has not been previously reported in plant disease resistance genes. However, its individual domains are known to contribute towards defense responses. Its two amaranthin-type agglutinin (Agg) domains could impart property that reversibly binds to glycans on the biological surfaces. This property of the Agg domain of PFT was tested by performing a hemagglutination assay. PFT agglutinized 2% rabbit erythrocytes, indicating the active Agg domain of purified protein isolated in this study. Although previously

characterized amaranthin domains are known to bind to *N*-acetylgalactosamine and T-antigens (Transue et al., 1997; Hernández et al., 2001), the binding pattern of uncharacterized proteins may vary and needs to be identified (Dang et al., 2017). First, its affinity was examined towards the towards major carbohydrates of plant and fungal cell walls through *in silico* docking analyses. The docking analyses revealed a higher affinity towards chitosan. To experimentally verify the specific binding affinity of the Agg domain of PFT, affinity-purified $His_6$-PFT and $His_6$-ETX fractions were screened against an array of 300 glycans. Compared to ETX, PFT was specifically bound to eleven glycans with strong affinity, and all of these had one or more monomers of monosaccharide, N-acetylglucosamine (GlcNAc). GlcNAc is a major monosaccharide of the fungal cell wall and is not commonly found in plants. Therefore, indicating the ability of the Agg domain of PFT to bind to the fungal cell wall specifically. The pore-forming domain (ETX) of PFT could impart the function of making pores in cell membranes suggesting its toxicity potential. In this regard, first line of evidence was the accumulation of PFT in inclusion bodies during overexpression in bacterial cells. Furthermore, necrosis was observed in the leaf tissue of *N. benthamiana* plants transiently or systematically expressing only the ETX domain using a PVX-based expression system. The fact that no necrosis was observed in similarly expressed complete PFT protein and Agg domain suggests that ETX imparts toxicity to PFT, and Agg domain guides its action by providing specificity to its mode of action.

To put all the pieces together and test our hypothesis, the antifungal activity of purified PFT protein was tested by performing an *in vitro* assay. The asexual spores of *F. graminearum*

were incubated with purified PFT and buffer control, and PFT did not have a dramatic effect on spore germination or hyphal shape. However, a numerical reduction in mean hyphal length and a higher frequency of PFT incubated spores with shorter hyphal lengths was observed. One of the possibilities for subtle effects of PFT could be a requirement of particular buffer environment mimicking the plant environment for its activity. Hence, it could be challenging to demonstrate the drastic effect of PFT on fungal hyphae. Furthermore, more sensitive assays could be used to test its effect. For instance, propidium iodide uptake assays can be performed to test if PFT compromises fungal cell membrane permeability.

While further experimentation is needed to completely unravel the molecular mechanism of PFT-mediated resistance, this study provides critical experimental evidence indicating its mode of action against fungal pathogens. Towards this end, individual domains of PFT were functionally characterized. This study demonstrated the hemagglutination activity and specific binding of the Agg domain towards a major exclusive monosaccharide of the fungal cell walls. Although characterization of the ETX domain requires further studies, outcomes of heterologous expression in bacteria and plants partly support its toxicity. Taken together, functional characterization of PFT and its domains provide new insights into the mechanism of atypical major effect quantitative disease resistance genes in crop plants.

## 5.5. Acknowledgments

The authors acknowledge the University of Maryland supercomputing resources (http://hpcc.umd.edu) made available for conducting the research reported in this chapter. Purchase of the Zeiss LSM 980 Airyscan 2 was supported by Award Number 1S10OD025223-01A1 from the National Institute of Health.

# Chapter 6: Efficacy assessment of a new fungicide Miravis Ace for control of Fusarium Head Blight in wheat

Lovepreet Singh[1], Jason P. Wight[1], Joseph Crank[1], Louis Thorne[1], Yanhong Dong[2], Nidhi Rawat[1*]

[1]Department of Plant Sciences and Landscape Architecture, University of Maryland, College Park, MD 20742

[2]Department of Plant Pathology, University of Minnesota, St. Paul, MN 55108

***Corresponding author:** nidhirwt@umd.edu

This work was published in Singh et al., (2020). Headings and figure numbers were modified for consistency within this dissertation.

## 6.1. Abstract

Fusarium Head blight (FHB) is a serious disease of wheat and barley that leads to significant economic losses and deteriorated grain quality because of the associated mycotoxins. Genetic resistance and use of fungicides are the methods used to control FHB. However, in weather conditions conducive for FHB epidemics, higher levels of genetic resistance as well as greater efficacy of fungicides are required to adequately control this disease. Due to the extensive use of a single mode of action for management of FHB, there is a need to diversify fungicides used to lower the risk of resistance development in pathogen populations. In this two year study, we evaluated the performance of a new fungicide, Miravis-Ace (a proprietary mix of Pydiflumetofen and Propiconazole active ingredients produced by Syngenta Inc.) for controlling FHB. It is a mix of succinate dehydrogenase inhibitor (SDHI) and DeMethylation Inhibitor (DMI) fungicides and can add diversity to the fungicide toolkit for FHB management. The level of control of FHB and deoxynivalenol (DON) achieved by spraying Miravis-Ace at anthesis (Feeke's growth stage 10.5.1) was found to be equivalent to that provided by the currently recommended products for managing FHB and reducing DON in wheat and barley.

## 6.2. Introduction

Fusarium Head Blight (FHB) is a devastating disease of wheat and barley worldwide. The causal pathogen of FHB in the United States (US) is *Fusarium graminearum* Schwabe (teleomorph *Gibberella zeae* (Schwein.) Petch) (McMullen et al., 1997; Goswami and Kistler, 2004). The pathogen infects plants at flowering and leads to not only direct yield losses due to poor-seed development, but also contamination of grain with associated mycotoxins such as deoxynivalenol (DON) and nivalenol (NIV) (McMullen et al., 1997; Jones and Mirocha, 1999). High humidity and warm temperatures at flowering and post-anthesis favor disease development (Cowger et al., 2009). Disease risk modelling has been used to provide spray recommendations to wheat growers based on weather conditions favorable for disease development via the risk-map tool (http://www.wheatscab.psu.edu/). Efforts to manage FHB using strictly cultural methods such as crop rotation and tillage are not entirely feasible and/or effective (Dill-Macky and Jones 2000).

Popular control measures currently used by farmers include use of resistant varieties and fungicide application (Mesterházy et al., 2011). However, the level of control achieved by even a combination of both of these approaches is not satisfactory under weather conditions favorable for disease progress and thus the search for new products with higher efficacy continues. Active ingredients, prothioconazole, tebuconazole, metcaonazole and prothioconazole, currently used to control FHB are all Triazol fungicides (FRAC code 3) (Mesterházy et al. 2011). Recently there have been reports of *F. graminearum* isolates from Brazil, China, Germany, and the US that have cross-resistance to some of the currently used fungicides (Klix et al., 2007; Yin et al., 2009; Spolti

et al., 2012, 2014). Spolti et al. (2014) reported a population of *F. graminearum* showing resistance against tebuconazole as well as metconazole fungicides. Similar reports from Brazil confirmed that the populations of *F. graminearum* are evolving resistance to multiple triazole based fungicides (Sploti et al. 2012). Although, reports of resistant *F. graminearum* isolates are not very frequent so far, but these examples clearly indicate the need to diversify fungicide chemistry options for managing FHB.

Recently, a new product was launched by Syngenta for controlling FHB in wheat and barley by the name of Miravis-Ace. It is a combination of pydiflumetofen (FRAC code 7, succinate dehydrogenase inhibitor (SDHI)) and Propiconazole (FRAC code 3, DeMethylation Inhibitors DMI)) fungicides. This paper reports the results of a two-year study conducted to test the efficacy of Miravis-Ace in controlling FHB and DON content in wheat and compare its performance to currently used products.

## 6.3. Materials and Methods

### *Field design*

A Soft red winter wheat cultivar, Shirley, known to be susceptible to FHB (https://officialvarietytesting.ces.ncsu.edu/wheat-variety-characteristics-2017/), was used to compare the efficacies of fungicides for control of FHB and DON content in 2017 and 2019. The experiments were conducted at the Wye Research and Education Center of the University of Maryland (-76.150108 longitude, 38.913689 latitude) during the planting seasons of 2016-2017, and 2018-2019. The experimental design consisted of six treatments and a non-treated control in

four replications in Randomized Complete Block Design with plot size of 1.5 m x 3.9 m. All experiments were conducted on no-till plots with corn-stubble from previous growing cycles to ensure high inoculum load for infection of the plants, as crop residues are known to enhance FHB in wheat (Dill-Macky and Jones, 2000).

***Fungal inoculation***

Three *F. graminearum* isolates were collected, one each from Clarksville, Beltsville, and Wye farm locations in Maryland, and were tested for their aggressiveness and DON production-efficiency in greenhouse tests on susceptible plants. An equal mixture of these three isolates was used to generate macro-conidia for inoculations. Macroconidia were generated in mung bean broth two weeks prior to the field inoculations following Dill-Macky (2003). Briefly, 40 g mung beans were steeped in 1 liter distilled water for 40 minutes, followed by filtering and autoclaving. Spore counts were measured on a hemocytometer, and final volumes were adjusted to a spore concentration of 1 x $10^5$ macroconidia/ ml. The normalized spore suspensions were filtered through cheesecloth prior to use. Wheat spikes were spray inoculated with 400 ml of normalized spore suspension per plot (approximating 4 x $10^7$ macroconidia per plot) one day prior to fungicide application using a CO2–powered backpack sprayer equipped with a single TeeJet Flat fan nozzle.

***Fungicide application***

Fungicides (Table 6.1) were sprayed at anthesis (Feeke's growth stage 10.5.1) with a $CO_2$ backpack sprayer equipped with twinjet nozzles at a $30^o$ angle from the horizontal at a height of 25 cm above the canopy. Two different concentrations of Miravis-Ace fungicide were used (0.8

l/ha and 1.0 l/ha) because during the test years the product was not commercially available and the two rates were suggested to be tested by the company representative providing the product. All fungicides were applied as premixed products, except A19649 +Tilt 3.6 EC which were tank-mixed. Each fungicide treatment included Induce, a non-ionic surfactant, at 0.25% (v/v) concentration. Inoculated plots without any fungicide treatments were used as untreated control for the study.

**Table 6. 1.** Fungicide treatments used in the study.

| Product Name | Active ingredient, Manufacturer | Application rate |
|---|---|---|
| Caramba 0.75 SL | Metconazole, BASF Corp. | 1.1 l/ha |
| Prosaro 421 SC | Prothioconazole + Tebuconazole, Bayer Crop Science | 0.5 l/ha |
| Folicur 3.6 F | Tebuconazole, Bayer Crop Science | 0.3 l/ha |
| A19649 +Tilt 3.6 EC | Pydiflumetofen solo + Propiconazole, Syngenta | 0.6 l/ha + 0.3 l/ha |
| Miravis ACE | Pydiflumetofen + Propiconazole, Syngenta | 0.8 l/ha |
| Miravis ACE | Pydiflumetofen + Propiconazole, Syngenta | 1.0 l/ha |
| Non-treated Control | - | - |

***Disease assessments***

The disease incidence and severity were measured three weeks after fungicide spray treatments following Paul et al (2005). Fifty spikes from each plot were randomly selected for disease evaluation. Disease Incidence (I) was calculated by counting the number of symptomatic spikes among the total number of spikes observed in that plot. Disease severity (S) was calculated

as the average total number of diseased spikelets per spike. Disease Index (Index) was calculated as a product of S and I divided by 100. Disease ratings were taken at Feeke's growth stage 11.2 (soft dough) in all plots, so that the healthy spikes were still green and not senescent.

Grain samples were harvested after maturity from each plot using a combine harvester. To avoid any loss of seed during threshing, the air flow over the kernel sieves was reduced so that essentially very few light/ scabby kernels were blown away while harvesting the grains. Post-harvest examination of fusarium damaged kernels (FDK) was done by randomly collecting scoops of 100 seeds and counting the scabby kernels in each set. Readings were averaged across three subsamples of each sample.

***DON content***

DON content was measured at USWBSI DON-testing laboratory at University of Minnesota by GC/MS following Mirocha et al. (1998). Briefly, 4 g of ground samples were extracted with 16 mL of acetonitrile/water (84/16, v/v) in 50 mL centrifuge tubes. Each sample was placed on a shaker for 1 h, and then 4 ml of the extract was passed through a column packed with 18C and aluminum oxide (1/3, w/w). One milliliter of the filtrate was evaporated to dryness under nitrogen at room temperature, and 100 µl of Trimethylsilyl (TMS) reagent (TMSI/TMCS, 100/1) was added to the vial, rotating the vial so that the reagent makes contact with residue on the sides of the vial. The vial was placed on a shaker for 10 min, and then 1 mL of isooctane containing 4 µg/mL Mirex was added and shaken gently. HPLC water (1ml) was added to quench the reaction and the vial was vortexed so that the milky isooctane layer becomes

transparent. The upper layer was transferred into a GC vial for GC/MS analysis (Shimadzu GCMS-QP2010, Shimadzu Corporation, Kyoto, Japan) and readings were recorded.

***Statistical analyses***

Disease incidence, severity, index, FDK, and DON content data were analyzed using PROC GLIMMIX of SAS University version 9.4 (SAS institute Inc., Cary NC) separately for each year. FDK data for year 2017 were transformed using arcsine-square-root transformation and DON data for 2019 were log transformed before analysis to stabilize variances. Mean separations were performed using Fisher's Least Significant Difference (LSD) test at a 5% level of significance. In case of overall non-significant treatment effect, individual fungicide means were compared with non-treated control using Dunnett adjustment in GLIMMIX.

***Weather conditions***

Since weather plays a very important role in determining abundance of inoculum, development of disease occurrence and disease progression, temperature and precipitation data was recorded for the months of April, May, June and July months of 2017, and 2019. Weather data was recorded by the weather station at the Wye Research and Education Center. Precipitation was measured by NOAH IV electronic weighing bucket precipitation gauge, whereas air temperature was measured by HMP45C-L, Vaisala Temperature and RH Probe at a height of 6 feet from the ground level.

## 6.4. Results

### *FHB incidence, severity, and index*

Both years had warm and humid spring and summer seasons, conducive for the incidence and development of FHB (Table 6.2). Fungicide treatment significantly affected FHB incidence during 2017 (P value = 0.0001), and 2019 (P value= 0.0003) (Table 6.3). In 2017, mean FHB incidence ranged from 37.4 to 60.2 % (Table 6.3). Caramba, Prosaro, and Miravis Ace 0.8 l/ha and 1.0 l/ha treatments at significantly reduced FHB incidence. Folicur and A19649+Tilt tank mix were not significantly different from the non-treated control for FHB incidence in 2017. Disease incidence was higher in 2019, ranging from 65 to 87.5 %. All fungicide treatments, except Folicur, significantly reduced FHB incidence.

Caramba, Prosaro, Miravis Ace 0.8 l/ha and Miravis Ace 1.0 l/ha significantly reduced disease severity in both the years. FHB severity was not significantly reduced following application of Folicur. Mean FHB severity ranged from 28.6 to 42.6 %, and 17.8 to 40.4 % in 2017, and 2019, respectively (Table 6.3). In 2017 Prosaro and Caramba had lowest FHB severity followed by Miravis Ace 1.0 l/ha, whereas in 2019, Miravis-Ace 1.0 l/ha had lowest FHB severity among all the treatments. Disease severity was not reduced following application of Folicur in any of the years.

Caramba, Prosaro, and both Miravis Ace applications reduced FHB index in both the trial years. Application with Folicur did not significantly reduce FHB index in any of the years. The mean FHB index ranged from 10.9 to 25.9 in 2017 (Table 6.3). In 2017, Caramba, Prosaro,

Miravis Ace 0.8 l/ha and Miravis Ace 1.0 l/ha significantly lower FHB index as compared to non-treated control. FHB indices for Folicur and A19649+Tilt tank mix treatment were not significantly different from non-treated control. In 2019, mean FHB index varied from 11.8 to 33.5 in Miravis-Ace1.0 l/ha and Folicur, respectively. All the fungicide treatments except Folicur had significantly lower index as compared to non-treated control. A19649+Tilt tank mix was equally effective as Miravis Ace 0.8 l/ha and had statistically similar index to Miravis Ace 1.0 l/ha, Caramba and Prosaro.

**Table 6. 2.** Mean temperatures and total precipitation during 2017 and 2019 field seasons at the Wye Research and Education Center, University of Maryland.

| Year | Month | Temperature (°C) | Total precipitation (mm) |
|---|---|---|---|
| 2017 | April | 15.6 | 54.1 |
| | May | 17.2 | 151.1 |
| | June | 23.2 | 43.2 |
| | July | 25.9 | 224.5 |
| 2019 | April | 14.9 | 94.5 |
| | May | 19.3 | 107.2 |
| | June | 23.08 | 94.5 |
| | July | 26.2 | 160.0 |

***Fusarium damaged kernels (FDK)***

The fungicide treatments had significant effect on mean FDK in 2017 (P value = 0.0223) and 2019 (P value = 0.0013) (Table 6.3). In 2017, mean FDK varied from 6.5 to 9.8 %. Caramba, Prosaro

and A19649+Tilt tank mix had significantly lower FDK value as compared to non-treated control. In contrast to trends observed for incidence, severity, and index, mean FDK percentages for both Miravis Ace treatments were significantly similar to the non-treated control. In 2019, mean FDK ranged from 9.2 to 18.1 %. All the fungicides had significantly lower FDK as compared to non-treated control.

***DON content***

The fungicide treatment had significant effect on mean DON content in 2019 (P value <0.0001) but nonsignificant effect in 2017 (P value = 0.109) (Table 6.3). Although overall treatment effect was nonsignificant in 2017, Caramba, Prosaro, A19649+Tilt tank mix and both Miravis treatments had significantly lower mean DON content as compared to the non-treated control. In 2019, mean DON content ranged from 1.5 to 4.2 ppm. All the fungicide treatments except Folicur significantly reduced mean DON content as compared to non-treated control.

**Table 6. 3.** FHB Incidence, FHB severity, FHB Index, Fusarium damaged kernels and DON content with the treatments in the study.

| **Treatment** | **2017** | | | | | **2019** | | | | |
|---|---|---|---|---|---|---|---|---|---|---|
| | **Incidence**[§] **%** | **Severity** **%** | **Index** | **FDK** **%** | **DON** **ppm** | **Incidence** **%** | **Severity** **%** | **Index** | **FDK** **%** | **DON** **ppm** |
| Caramba | [€]41.4±3.7[b] | 28.6±2.5[c] | 11.9±1.7[b] | 6.5±0.6[c] | 2.1±0.5* | 65±3.5[**b**] | 30.1±3.9[bc] | 19.7±3.1[c] | 9.2±1.2[c] | 2.0±0.2[bc] |
| Prosaro | 37.4±2.2[b] | 28.6±3.7[c] | 10.9±1.8[b] | 7.8±0.2[bc] | 1.7±0.2* | 67.5±5.2[**b**] | 32.6±3.1[b] | 22.2±3.3[b] | 10.6±2.1[bc] | 1.7±0.2[bc] |
| Folicur | 58.9±4.0[a] | 35.0±2.8[abc] | 20.9±3.0[a] | 8.8±0.5[ab] | 2.4±0.3 | 82.5±3.2[a] | 40.4±2.9[a] | 33.5±3.4[a] | 13.7±1.7[b] | 3.4±0.5[a] |
| A19649+Tilt | 59.2±4.0[a] | 38.6±2.0[ab] | 22.9±2.2[a] | 8.0±0.4[bc] | 2.3±0.1* | 67.5±3.2[**b**] | 24.3±1.4[cd] | 16.3±1.1[bc] | 9.2±1.0[c] | 1.7±0.1[l] |
| Miravis-Ace 0.8 l/ha | 42.6±4.0[b] | 31.4±2.7[bc] | 13.6±2.2[b] | 8.8±0.5[ab] | 2.2±0.6* | 71.2±2.4[**b**] | 22.7±2.3[d] | 16.3±2.1[bc] | 9.4±2.0[c] | 1.5±0.2[c] |
| Miravis-Ace 1.0 l/ha | 40.8±1.7[b] | 30.3±1.7[bc] | 12.3±0.8[b] | 8.2±0.6[ab] | 2.0±0.3* | 66.2±1.2[**b**] | 17.8±1.1[d] | 11.8±0.6[c] | 9.8±0.7[bc] | 2.2±0.1[b] |
| Control | 60.2±3.0[a] | 42.6±3.9[a] | 25.9±3.5[a] | 9.8±0.6[a] | 3.6±0.4 | 87.5±1.4[a] | 34.8±3.6[ab] | 30.4±3.0[a] | 18.1±1.7[a] | 4.2±0.6[a] |
| ***F Value* | 9.07 | 3.06 | 6.38 | 3.32 | 2.02 | 7.64 | 10.54 | 12 | 6.05 | 12.46 |
| *P Value* | 0.0001 | 0.0303 | 0.001 | 0.0223 | 0.109 | 0.0003 | <0.0001 | <0.0001 | 0.0013 | <0.0001 |

[§]Incidence = mean proportion of diseased spikes; Severity = mean proportion of diseased spikelets per spike; Index = mean proportion of diseased spikelets in infected spikes; FDK= Fusarium damaged kernels percentage of shriveled and discolored kernels; DON = deoxynivalenol content in harvested grains.

[€]Means (± SE) with the same letters in each column are not statistically significantly different ($\alpha$ = 0.05) according to Fisher's protected LSD test.

[*]Fungicide means with * in each column are statistically significantly different ($\alpha = 0.05$) from control according to Dunnett-Hsu test.

[**]*F* value = *F* statistics and *P* value = probability value based on the linear mixed model analyses; FDK 2017 data were arcsine transformed and DON 2019 data was log transformed.

### 6.5. Discussion

Weather conditions were conducive for disease development in both the years (Table 6.2). Fungicide treatments with Prosaro and Caramba resulted in lower mean disease indices and DON content across both years. These results agree with the previous knowledge of triazol fungicides effectively controlling FHB in field conditions as well as greenhouse settings (Homdork et al., 2000; Maria Menniti et al., 2003; Paul et al., 2008). New test product-Miravis Ace performed as well as the more commonly known triazol fungicides for reducing FHB and DON content in both trial years.

In both years Miravis-Ace provided statistically significant ($P < 0.05$) control on FHB index, FDKs and DON content over the non-treated control. The level of control provided on FHB index, FDKs and DON by Miravis-Ace was statistically similar ($P > 0.05$) to that by Prosaro and Caramba in both years. All three fungicides provided superior control over Folicur (Tebuconazole) and a tank mix of A9469 and Tilt (Pydiflumetofen solo + Propiconazole). Overall, Miravis-Ace treatment at 1.0

l/ha concentration provided superior control over the lower concentration of 0.8 l/ha treatment in both the years in terms of reducing FHB incidence, severity, and consequently FHB index. This is the full-strength concentration recommended by the manufacturer for commercial application in wheat and barley for FHB.

The results of this study suggest that the new fungicide Miravis-Ace can provide similar control on FHB and DON content in wheat, as the presently used triazol fungicides. It should be noted that the results are based on fungicide application at flowering (Feeke's stage 10.5.1), which is the recommended stage for fungicide application with the current products.

### 6.6. Acknowledgements

Funding from US Wheat and Barley Scab Initiative (Grants # 59-0206-6-018 and 59-0206-4-023), Maryland Agricultural Experiment Station, Maryland Crop Improvement Association and Maryland Grain Producers Utilization Board (Grant # 2018397, 2019332) is gratefully acknowledged. Technical support of Yields Trials Center of the University of Maryland is thankfully acknowledged. The authors are thankful to Dr. Arv Grybauskus for critical reading of the manuscript.

# Chapter 7: Evaluation of application timing of Miravis-Ace for control of Fusarium head blight in wheat

Lovepreet Singh[1], Taylor Schulden[1], Jason P. Wight[1], Joseph Crank[1], Louis Thorne[1], John E. Erwin[1], Yanhong Dong[2], Nidhi Rawat[1*]

[1]Department of Plant Sciences and Landscape Architecture, University of Maryland, College Park, MD 20742

[2]Department of Plant Pathology, University of Minnesota, St. Paul, MN 55108

*Corresponding Author: nidhirwt@umd.edu

This work was published in Singh et al., (2021). Headings and figure numbers were modified for consistency within this dissertation.

**7.1. Abstract**

Fusarium Head Blight (FHB) is a serious disease of wheat and barley that not only lowers yield, but also contaminates the grain with associated mycotoxins such as deoxynivalenol (DON). Chemical control options for FHB and DON include application of triazole fungicides at the anthesis or flowering stage. This presents practical challenges for growers in managing FHB, as the appropriate timing window typically lasts only 3-4 days. If this small window is missed, due to weather conditions or technical problems, fungicide application is less effective in controlling FHB and DON. The present work was conducted over two years (2019 and 2020) to test the efficacy of a new fungicide (pydiflumetofen + propiconazole) from Syngenta labelled as Miravis-Ace in controlling FHB and DON content at 50% head emergence (Feeke's 10.3), anthesis (Feeke's 10.5.1) and end of flowering (Feeke's 10.5.3) stages. Prosaro 421 SC, a standard FHB control triazol fungicide, was used at all three stages for comparison with the test fungicide. Miravis-Ace application at 50% head emergence provided significant control over the non-treated check for FHB incidence (2020), FHB severity (2019) and DON content (2019) with control efficacies as high as 51%, 69% and 52%, respectively. However, mean control percentages relative to the check were highest with Miravis-Ace at anthesis in both 2019 and 2020 for all the FHB parameters. In conclusion, 50% head emergence provides statistically significant control on FHB and DON, but anthesis was the most effective application stage for Miravis-Ace.

## 7.2. Introduction

Fusarium Head Blight (FHB) is one of the most important diseases of wheat, barley and other small grain cereals worldwide (Parry et al., 1995; McMullen et al., 1997; Mesterházy et al., 2011). The major causal organism of FHB in the United States is *Fusarium graminearum.* FHB not only causes significant yield losses, but also the associated mycotoxins such as deoxynivalenol (DON) are hazardous for human or animal consumption(McMullen et al., 2012; Miedaner et al., 2016). The annual cost of disease management and direct impact of FHB outbreaks exceeds $1.4 billion in the US alone(Wilson et al., 2018). The US Food and Drug Administration regulates DON levels, and grain exceeding 1 ppm DON is considered unfit for human consumption (Nutrition, 2020). Farmers have to bear the additional burden of testing their grains for DON and alleviating DON levels by grain sorting or mixing with uncontaminated grains to bring the DON levels down to a permissible range (Gilbert and Woods, 2006). Integrated approaches including use of appropriate fungicides, planting resistant varieties, and cultural practices such as avoiding corn-wheat rotation or managing crop residues are recommended for managing FHB in wheat(Dill-Macky and Jones, 2000; Goswami and Kistler, 2004; Cowger et al., 2016). Fungicide application is one of the most effective ways of controlling FHB in wheat (Mesterházy et al., 2011). Triazole fungicides (FRAC code 3) with active ingredients such as prothioconazole, tebuconazole, and metconazole are used to control FHB (Paul et al., 2008; Mesterházy et al., 2011).

Due to the unique epidemiology of FHB, the efficacy of fungicides varies with different plant stages (Audenaert et al., 2011a; Paul et al., 2018a). Wheat is most susceptible to FHB at

anthesis because initial *Fusarium* sp. infection commonly starts on the extruded anthers (Parry et al, 1995; Pugh et al. 1933). Anthesis (Feeke's stage 10.5.1) has been found to be the most effective timing of fungicide application for FHB (Audenaert et al., 2011b; Paul et al., 2018a). In US wheat production systems, usually only a single fungicide spray is economically viable, restricting the effective window of fungicide application to only 3-4 days (McMullen et al., 1997; D'Angelo et al., 2014). This small opportune timing of application, especially when coinciding with wet weather, makes fungicide application for FHB management tricky and sometimes not feasible at all. Therefore, possibility to widen the spray window by testing fungicide efficacy at pre-anthesis or post-anthesis stage has been explored previously(Edwards and Godley, 2010; Yoshida et al., 2012; D'Angelo et al., 2014; Paul et al., 2018a). In multi-state trials with triazole fungicides, post-anthesis application performed better than pre-anthesis application for controlling the FHB and DON(Paul et al., 2018a). The chemical control of FHB and DON vary among active ingredients, wheat types, and locations(Paul et al., 2008). Therefore, fungicide application timing needs to be tested for new fungicide products for specific growing regions and wheat classes.

Recently, a new fungicide chemistry combination of pydiflumetofen (FRAC code 7, succinate dehydrogenase inhibitor (SDHI)) and propiconazole (FRAC code 3, Demethylation Inhibitor (DMI)), labelled as Miravis-Ace was launched by Syngenta. In our previous study, Miravis-Ace application at anthesis was found to be equally effective as standard triazole fungicides in controlling FHB and DON (Singh et al., 2020). Miravis-Ace is claimed to provide a significant control of FHB even if sprayed before anthesis at 50%-head-emergence

stage(https://www.syngenta-us.com/fungicides/miravis-ace). Additionally, its effectiveness at post-anthesis stage application needs to be evaluated. The ultimate goal of this study is to determine if the Miravis-Ace application window can be broadened for effective control of FHB and DON. The study was conducted to test and compare the effect of Miravis-Ace application at 50 % Head emergence (Feeke's stage 10.3), anthesis (Feeke's 10.5.1), and post-anthesis (Feeke's 10.5.3) stages in controlling FHB and DON. Prosaro 421 SC, a standard FHB control triazol fungicide, was used for comparison. To determine the most appropriate stage, both the fungicides were evaluated under high disease pressure conditions at 50% head emergence, anthesis, and 4-6 days after anthesis in this 2-year study.

## 7.3. Materials and methods

### *Experimental design*

The experiments were conducted at the Beltsville Agriculture Research Center of the University of Maryland (39.012591 latitude, -76.825845 longitude) during the planting seasons of 2018-2019, and 2019-2020. A soft red winter wheat cultivar, Shirley, known to be highly susceptible to FHB was used for all experiments(Singh et al., 2020). Shirley was planted in 1.7 m × 4.6 m plots in both years. The experimental design was randomized complete block consisting of four replicate blocks in 2019 and three replicate blocks in 2020 with a factorial arrangement. The factorial combination included fungicide and fungicide application timing. All the experiments were conducted on artificially inoculated no-till plots with corn-stubble from

previous growing cycles to ensure high inoculum load for infection of the plants, as crop residues are known to enhance FHB in wheat (Dill-Macky and Jones, 2000).

***Fungal inoculum preparation and inoculation***

Infected corn kernel inoculum was used for field inoculations which produces ascospores over a long period in the field, similar to natural inoculum (Gilbert and Woods, 2006; Yoshida et al., 2012). Three aggressive *F. graminearum* isolates were collected from three different farm locations across the state of Maryland including Clarksville, Beltsville, and Wye Mills. An equal mixture of these three isolates was used to prepare the infected corn kernel inoculum using the method of Gilbert and Woods (2006). Briefly, corn kernels were soaked in water for 16 hours, autoclaved and then allowed to cool overnight. One-week old PDA cultures of the three *F. graminearum* isolates were then blended in 150 ml sterile water with 0.2 g of streptomycin sulfate per 7.5 kg corn kernels and thoroughly mixed into the corn kernels. The mixture was incubated for two weeks at room temperature and was turned once a week. After incubation, the colonized kernels were dried for 2-3 weeks in a drying air oven at 32 °C and stored in dry and cool conditions until their field use in gunny bags. When wheat plants were at the tillering stage, the infected corn kernels were spread manually in experimental plots at a density of $40g/m^2$. Misting was applied to the field daily from 9 pm to 7 am on a 10 min cycle every 80-min to maintain high humidity conditions for optimal fungal growth. Misting was stopped three weeks post-flowering.

***Fungicide application***

Table 7.1 lists the active ingredients, rate of application, growth stages and dates of fungicide applications tested in the study. The two fungicides included: DMI fungicide Prosaro 421 SC (prothioconazole + tebuconazole) and SDHI and DMI fungicide Miravis-Ace SE (pydiflumetofen + propiconazole). Each fungicide mixture included a non-ionic surfactant, Induce (Helena Chemical Co., Collierville, TN), at concentration of 0.25% (v/v). The fungicide applications were made at three different growth stages: 50 % head emergence or pre-anthesis (Feeke's 10.3), anthesis (Feeke's 10.5.1), and post-anthesis (Feeke's 10.5.3). Hereafter 50 % head emergence applications of Miravis-Ace and Prosaro are abbreviated as ME and PE, respectively; anthesis applications of Miravis-Ace and Prosaro are abbreviated as MA an PA, respectively; and post-anthesis applications of Miravis-Ace and Prosaro are abbreviated as ML and PL, respectively. Fungicides were applied with a $CO_2$ backpack sprayer equipped with forward and backward spraying twinjet nozzles at a $30^o$ angle from the horizontal at the height of 25 cm above the canopy. The spray pressure was maintained at 40 psi, and the rate of spray was 20 gallons per acre. Inoculated plots without any fungicide or surfactant treatments were used as untreated control for the study.

***Disease and post-harvest assessments***

Disease incidence and severity were measured three weeks after flowering (Paul et al. 2005). Fifty spikes from each plot were randomly selected for disease evaluation. FHB incidence was calculated by counting the number of symptomatic spikes among the total number of spikes observed in that plot. FHB severity was calculated as the average total number of diseased spikelets per spike. Disease ratings were taken at Feeke's growth stage 11.2 (soft dough) in all plots, so that the healthy spikes were still green and not senescent.

**Table 7. 1.** Fungicides, Plant growth stages and dates of fungicide application selected in the study.

| Product | Active Ingredient | Rate of application | Name of Treatment: Flowering stage | Feeke's Growth Stage | Dates of Fungicide Application | |
|---|---|---|---|---|---|---|
| | | | | | 2019 | 2020 |
| Prosaro 421 SC | Prothioconazole+Tebuconazole | 0.5 l/ha | PE: Heads 50% emerged | Feeke's 10.3 | May 8 | May 18 |
| | | | PA: Anthesis | Feeke's 10.5.1 | May 14 | May 22 |
| | | | PL: Post-anthesis | Feeke's 10.5.3 | May 18 | May 26 |
| Miravis-Ace SE | Pydiflumetofen+ Propiconazole | 1.0 l/ha | ME: Heads 50% emerged | Feeke's 10.3 | May 8 | May 18 |
| | | | MA: Anthesis | Feeke's 10.5.1 | May 14 | May 22 |
| | | | ML: Post-anthesis | Feeke's 10.5.3 | May 18 | May 26 |
| Non-treated control | | - | - | - | - | - |

Grain samples were harvested after maturity from each plot using a combine harvester. To avoid any loss of seed during threshing, the air flow over the kernel sieves was reduced so that essentially very few light/ scabby kernels were blown away while harvesting the grains. Random samples of 100 g each per replicate were taken for DON content analysis. DON content was measured at USWBSI DON-testing laboratory at University of Minnesota by GC/MS following Mirocha et al. (1998). Briefly, DON in each ground wheat sample was extracted with acetonitrile/water (84/16, v/v) solvent, and the extract was cleaned by passing through a column packed with C18 packing material and aluminum oxide (1/3, w/w). DON was derivatized using a trimethylsilylating reagent (N-trimethylsilylimidazole/trimethylchlorosilane, 100/1, v/v), and analyzed by GC/MS (Singh et al., 2020).

***Statistical analyses***

To test the effects of fungicide, application timing, and their interaction on FHB severity, incidence, and DON, all the data was analyzed using PROC GLIMMIX in SAS (SAS 9.4, Cary, NC). Data were analyzed separately for each year where fungicide, application timing, and their interaction were treated as fixed effects and block treated as random effect. Before analyses, FHB severity and incidence data was arcsine-square-root-transformed and DON data was log-transformed as needed to stabilize variances. To determine statistically significant effects, the *estimate* statement in PROC GLIMMIX was used to establish specific contrast with the untreated check and among other treatment combinations.

The efficacy of each specific treatment for FHB severity, incidence and DON was estimated as a mean percent control value (C) using the formula below:

$$C = [ (X – Y)/ X] \times 100$$

where X is the mean of the parameter of interest in non-treated control plots and Y is the mean of each parameter in treated plots. While comparing two different treatments, X was replaced with the mean of the reference treatment.

***Weather conditions***

Weather plays a very important role in determining the abundance of inoculum, disease occurrence, and disease progression. Therefore, weather data including temperature and precipitation were recorded for the month of April, May, June, and July in 2019 and 2020. Weather data were recorded by the weather station at the Beltsville Research and Education Center. Precipitation was measured by NOAH IV electronic weighing bucket precipitation gauge, whereas air temperature was measured by HMP45C-L, Vaisala Temperature and RH Probe at a height of 6 feet from the ground level.

## 7.4. Results and discussion

***Different weather conditions in 2019 and 2020***

The mean temperatures and precipitation recorded from April 15 to June 21, which is the period for disease initiation and development in the region, are shown in Figure 7.1. Although both

seasons had same number of rain events (30), cumulative rainfall was higher in 2019 (245 mm) as compared to 2020 (195 mm). The spring 2020 season had overall lower temperatures than those in 2019. For example, on May 8, 2019, the average temperature was 27 ºC, whereas on May 8, 2020 it was 17 ºC. This led to slower development of wheat as well as *Fusarium* in 2020. Similarly, anthesis stage was recorded as May 14 in 2019, but it was May 22 in 2020 (Table 7.1). Consequently, 2020 had moderate disease pressure in non-treated control plots (incidence = 64.4 % and severity = 26.71 %) as compared to severe disease pressure (incidence = 95.31 % and severity = 35.57 %) in 2019 (Figure 7.2). Nevertheless, due to the heavy inoculum density maintained in the experimental plots with corn kernels and artificial misting setup, acceptable levels of FHB were maintained both in 2019 and 2020.

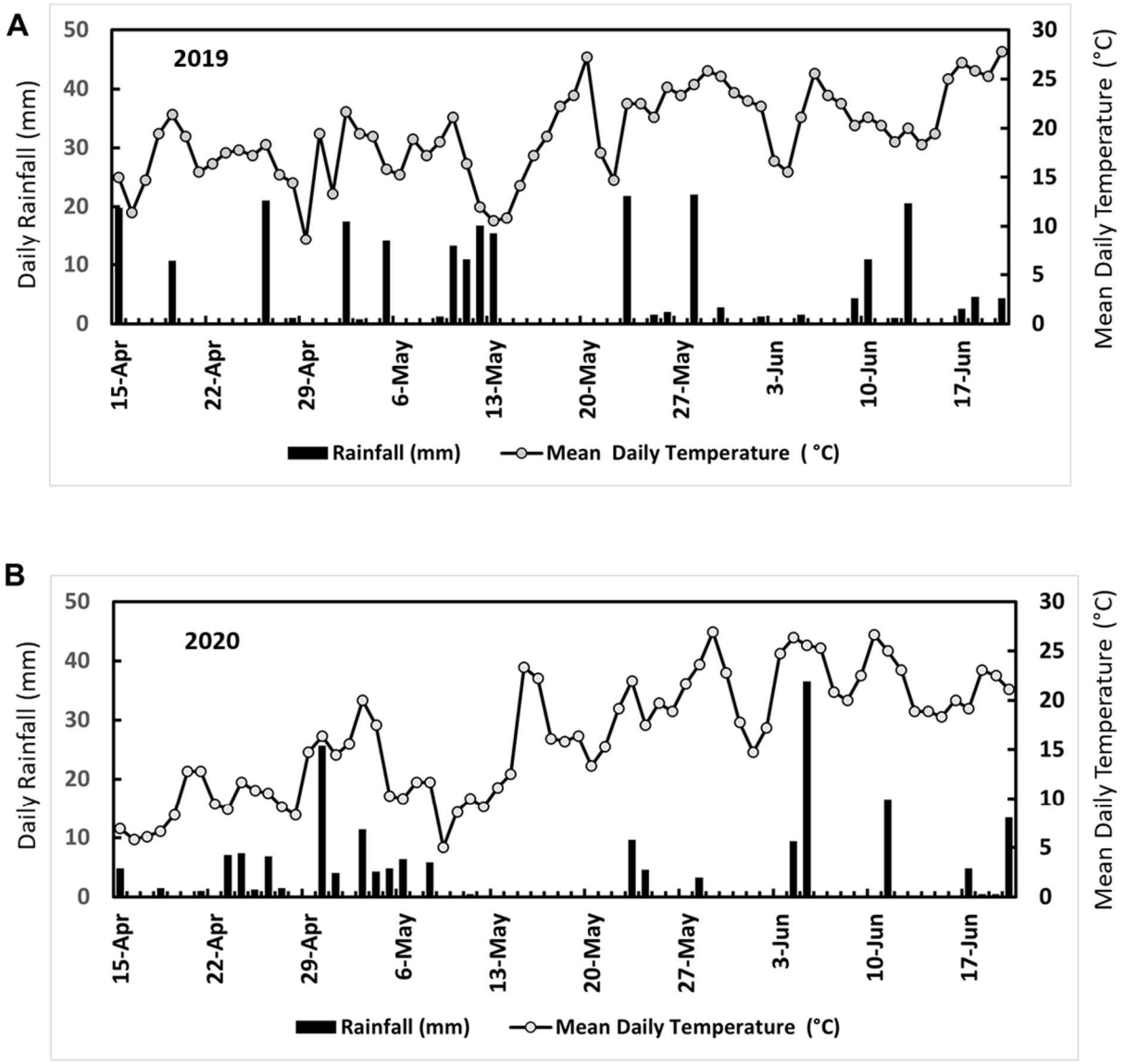


**Figure 7. 1. Daily mean temperature and daily rainfall during the Fusarium Head Blight screening period in 2019 (A) and 2020 (B).**

***Analysis of effect of fungicide and application timing on FHB and DON content***

The results of linear mixed model analyses of the effects of fungicide, application timing, and fungicide*timing interaction on FHB incidence (Incidence 2019, arcIncidence 2020), severity (Severity 2019 and arcSeverity 2020), and DON (logDON) are summarized for both years in Table 7.2. In both years, the fungicide*timing interaction was non-significant for all the parameters except for logDON in 2019. There was a significant effect of fungicide on incidence, severity, and DON in both years, but no significant effects were observed due to fungicide application timing.

To determine the statistical significance of the treatment effects, pairwise contrasts of least significant means were made for various treatments with reference to the non-treated check as well as among treatments for each year (Table 7.3).

**Table 7. 2.** Summary statistics of data collected to evaluate the effects of fungicide and fungicide application timing on FHB Incidence, Severity, and DON content in soft red winter wheat 'Shirley' in each study year.

| | | FHB Incidence[a] | | FHB Severity[a] | | DON[a] | |
|---|---|---|---|---|---|---|---|
| **Year** | **Factors[b]** | ***F* value[c]** | ***P* value[c]** | ***F* value** | ***P* value** | ***F* value** | ***P* value** |
| 2019 | FUNGICIDE | 18.38 | <.0001 | 69.52 | <.0001 | 64.58 | <.0001 |
| | TIMING | 0.48 | 0.6246 | 0.52 | 0.6022 | 2.78 | 0.0824 |
| | FUNGICIDE*TIMING | 2.64 | 0.0587 | 1.09 | 0.3849 | 3.36 | 0.0255 |
| 2020 | FUNGICIDE | 15.82 | 0.0002 | 10.73 | 0.0011 | 24.56 | <.0001 |
| | TIMING | 0.78 | 0.4743 | 0.94 | 0.4128 | 0.15 | 0.8591 |
| | FUNGICIDE*TIMING | 0.54 | 0.7059 | 0.26 | 0.9013 | 1.21 | 0.3435 |

[a] Incidence = Fusarium Head Blight incidence (mean proportion of infected spikes); Severity = Fusarium Head blight severity (mean proportion of bleached spikelets per spike); DON = deoxynivalenol content of harvested kernels (ppm).

[b] FUNGICIDE= Fungicides include Prosaro and Miravis-Ace; TIMING= Fungicide application timing incudes application at 50 % Head emergence, anthesis, and post-anthesis stage.

[c] *F* = F statistic and P= probability based on the mixed model analyses of severity, incidence and log transformed DON data in 2019; arcsine-transformed incidence, arcsine-transformed severity and log transformed DON data in 2020.

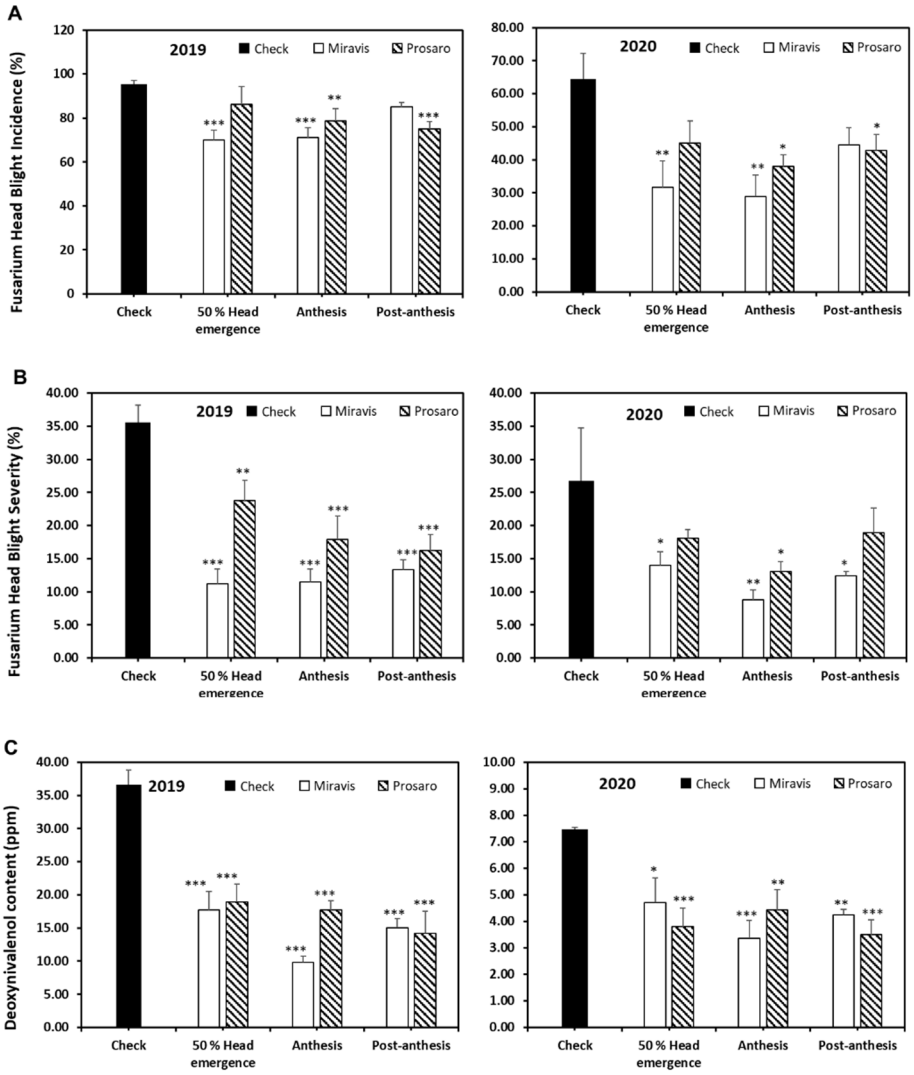


**Figure 7. 2. Raw mean values (±SE) of FHB incidence (A), severity (B), and deoxynivalenol content (C) for the untreated check, fungicides and fungicide application timings applied to soft red winter wheat cultivar ('Shirley') during 2019 and 2020.** The treatments with *, **, and *** are statistically significantly different from the untreated check at alpha 0.05, 0.01, and 0.001, respectively.

***FHB and DON content levels in different treatments***

Mean disease and DON levels varied between 2019 and 2020 (Figure 7.2). Having a warmer testing season, 2019 had severe disease pressure with FHB incidence ranging from 70 to 95.31 % (Figure 7.2.A), FHB severity from 11.18 to 35.57 % (Figure 7.2.B), and DON content ranging from 9.80 to 36.57 ppm (Figure 7.2.C). On the other hand, with comparatively low temperatures during the testing season, 2020 had moderate disease pressure. In 2020, mean incidence ranged from 28.89 to 64.44 % (Figure 7.2.A), mean severity varied from 8.82 to 26.71 % (Figure 7.2.B), and mean DON content ranged from 3.37 to 7.47 ppm (Figure 7.2.C). In both years, fungicide treated plots had lower mean values for incidence, severity and DON as compared to non-treated plots. In general, Miravis application at anthesis stage (MA) resulted in the lowest mean values for incidence, severity, and DON in both years (Figure7.2).

***Pair-wise comparison of test fungicides on FHB and DON content***

In 2019, all the treatments had significantly lower incidence as compared to the untreated check except ML and PE. At the pre-anthesis application, Miravis-Ace had significantly lower incidence compared to Prosaro. Differences were not significant between the two fungicides at anthesis and post-anthesis application. For Miravis-Ace, anthesis (MA) and pre-anthesis (ME) application significantly reduced incidence compared to post-anthesis application (ML). Notably, ME was effective in significantly reducing incidence compared to ML. All the treatments were effective in significantly reducing severity as compared to the untreated check. Between

fungicides, the only significant difference was observed for pre-anthesis application, where Miravis-Ace outperformed Prosaro to reduce severity. For Miravis-Ace, differences between anthesis and other application timings were not statistically significant. For DON, all treatments had significantly lower mean values as compared to the untreated check. Unlike incidence and severity, Miravis-Ace significantly lowered mean DON content only at anthesis application when compared to Prosaro. For Miravis-Ace, anthesis application was most effective in reducing DON content and the difference was statistically significant compared to pre-anthesis and post-anthesis applications.

In 2020, trends were very similar for incidence as all treatments had significantly lower mean values compared to check except ML and PE. Although differences between Miravis-Ace and Prosaro were not statistically significant at different application timings, ME and MA mean incidence values were lower than PE and PA, respectively. For Miravis-Ace, anthesis application had lower mean incidence than 50%-head-emergence and post-anthesis applications but differences were not statistically significant. ME exhibited numerically lower mean incidence compared to ML, but the difference was not statistically significant. With the two exceptions: PE and PL, all the treatments were effective in significantly reducing severity compared to the untreated check. No statistically significant differences were observed between the two fungicides at any application timing. Although not statistically significant, MA had lower severity means as compared to ME and ML. For DON content, all the treatments led to a significant reduction as compared to the untreated check. In 2020, differences between anthesis application versus other application timings were not statistically significant for Miravis-Ace.

**Table 7. 3**. Summary statistics and percent control for the planned comparisons to test the effects of fungicide and fungicide application timing on FHB incidence, severity, and deoxynivalenol (DON) content in soft red winter wheat variety 'Shirley' during 2019 and 2020.

| | | FHB Incidence[a] | | | FHB Severity[a] | | | DON[a] | | |
|---|---|---|---|---|---|---|---|---|---|---|
| **Year** | **Contrast[b]** | **Diff[c]** | ***P* value[d]** | **C[e]** | **Diff** | ***P* value** | **C** | **Diff** | ***P* value** | **C** |
| 2019 | ME vs. Check | -25.31 | 0.0003 | 26.56 | -24.4 | <0.0001 | 68.60 | -18.85 | <0.0001 | 51.54 |
| | MA vs. Check | -24.06 | 0.0005 | 25.24 | -24.1 | <.0001 | 67.75 | -26.77 | <0.0001 | 73.20 |
| | ML vs. Check | -10.31 | 0.0961 | 10.82 | -22.19 | <0.0001 | 62.38 | -21.52 | <0.0001 | 58.85 |
| | PE vs. Check | -9.06 | 0.1410 | 9.51 | -11.82 | 0.0028 | 33.23 | -17.62 | 0.0003 | 48.18 |
| | PA vs. Check | -16.56 | 0.0104 | 17.37 | -17.63 | <.0001 | 49.56 | -18.87 | 0.0001 | 51.60 |
| | PL vs. Check | -20.31 | 0.0023 | 21.31 | -19.32 | <.0001 | 54.32 | -22.40 | <0.0001 | 61.25 |
| | ME vs. PE | -16.25 | 0.0117 | 18.84 | -12.57 | 0.0016 | 52.93 | -1.23 | 0.6507 | 6.49 |
| | MA vs. PA | -7.50 | 0.2199 | 9.52 | -6.47 | 0.0802 | 36.06 | -7.9 | 0.0011 | 44.63 |
| | ML vs. PL | 10.00 | 0.1060 | -13.33 | -2.87 | 0.4259 | 17.66 | 0.88 | 0.4636 | -6.21 |
| | MA vs. ME | 1.25 | 0.8355 | -1.75 | 0.29 | 0.9349 | -2.53 | -7.92 | 0.0015 | 80.82 |
| | MA vs. ML | -13.75 | 0.0298 | 19.30 | -1.91 | 0.5948 | 16.65 | -5.25 | 0.0126 | 53.57 |
| | ME vs. ML | -15.00 | 0.0188 | 17.65 | -2.20 | 0.5401 | 16.46 | 2.68 | 0.3838 | -17.77 |
| 2020 | ME vs. Check | -32.78 | 0.0031 | 50.87 | -12.72 | 0.0462 | 47.62 | -2.77 | 0.0160 | 37.08 |
| | MA vs. Check | -35.55 | 0.0017 | 55.17 | -17.88 | 0.0043 | 66.94 | -4.10 | 0.0004 | 54.89 |
| | ML vs. Check | -20.00 | 0.0524 | 31.04 | -14.30 | 0.0253 | 53.54 | -3.23 | 0.0082 | 43.24 |
| | PE vs. Check | -19.45 | 0.0585 | 30.18 | -8.65 | 0.1953 | 32.38 | -3.67 | 0.0017 | 49.13 |

| | | | | | | | | | |
|---|---|---|---|---|---|---|---|---|---|
| PA vs. Check | -26.44 | 0.0140 | 41.03 | -13.61 | 0.0331 | 50.95 | -3.03 | 0.0103 | 40.56 |
| PL vs. Check | -21.67 | 0.0376 | 33.63 | -7.74 | 0.2351 | 28.98 | -3.97 | 0.0007 | 53.15 |
| ME vs. PE | -13.33 | 0.1692 | 29.62 | -4.08 | 0.4304 | 22.59 | 0.90 | 0.3014 | -23.68 |
| MA vs. PA | -9.11 | 0.3258 | 23.97 | -4.28 | 0.3381 | 32.67 | -1.07 | 0.1416 | 24.14 |
| ML vs. PL | 1.67 | 0.8659 | -3.90 | -6.55 | 0.2350 | 34.54 | 0.73 | 0.2671 | -20.86 |
| MA vs. ME | -2.78 | 0.7732 | 9.61 | -5.16 | 0.2634 | 58.48 | -1.33 | 0.0979 | 39.60 |
| MA vs. ML | -15.55 | 0.1134 | 35.00 | -3.59 | 0.4068 | 40.65 | -0.87 | 0.1712 | 25.74 |
| ME vs. ML | -12.78 | 0.1860 | 28.75 | 1.57 | 0.7625 | -12.68 | 0.47 | 0.7490 | -11.02 |

[a]Incidence = Fusarium Head Blight incidence (mean proportion of infected spikes); Severity = Fusarium Head blight severity (mean proportion of bleached spikelets per spike); DON = deoxynivalenol content of harvested kernels (ppm).

[b]Check = untreated check; ME, MA and ML refer to Miravis-Ace application at 50% head emergence, anthesis and post-anthesis, respectively; PE, PA and PL refer to Prosaro application at 50% head emergence, anthesis and post-anthesis, respectively.

[c] Diff= differences between raw mean values are shown here; transformed Least Significant means were used to construct contrasts for DON 2019, Incidence 2020, Severity 2020, and DON 2020 data.

[d] *P*= probability based on the mixed model analyses of Incidence, Severity, and log transformed DON data in 2019; arcsine-transformed Incidence, arcsine-transformed Severity, and log transformed DON data in 2020.

[e] C = mean percent control value.

***Control efficacies of fungicide treatment combinations for FHB and DON content***

Although the disease pressure was variable (Figure 7.2), the control efficacies for FHB and DON content were similar between both years (Table 7.3). In 2019, the highest control efficacies relative to the check were, 26.56% (ME), 68.60% (ME), and 73.20% (MA) for incidence, severity, and DON, respectively. Out of all treatment combinations, Miravis-Ace applied at pre-anthesis had the highest control efficacy relative to the check for incidence and severity while Miravis-Ace applied at anthesis was most effective for DON. During 2020, Miravis-Ace applied at anthesis had the highest control efficacies for incidence (55.17%), severity (66.94%) and DON (54.89%) relative to the check. In general, for visual FHB symptoms (incidence and severity), Miravis-Ace seems to outperform Prosaro at pre-anthesis application, with significant effects in some cases. However, no such consistent trends were observed for DON.

## 7.5. Conclusion

In spite of the lower mean temperatures in 2020, the misted nursery supplemented with *Fusarium*-inoculated corn kernels provided conducive conditions for development of FHB in both years. Miravis-Ace application at anthesis provided the lowest ratings of FHB incidence, severity, and DON content in both test years. This result is supported by previous work establishing anthesis as the most appropriate timing for fungicide application due to the unique epidemiology of FHB(Paul et al., 2008, 2018a; Audenaert et al., 2011a). As expected, Prosaro application at

anthesis was also found to be similarly effective in significantly reducing all three parameters (Paul et al., 2018; Singh et al., 2020). Application of Miravis-Ace at 50% head emergence provided significant control for FHB compared to the untreated check with control efficacies as high as 50.87 %, 68.60 %, and 51.54 % for incidence (2020), severity (2019), and DON (2019), respectively. Post-anthesis application of Miravis-Ace did not perform as well to reduce incidence and severity but numerically outperformed pre-anthesis application in reducing DON levels. In conclusion, Miravis-Ace may provide a wider window for controlling various FHB parameters, however anthesis application remains the optimal timing for consistently reducing DON levels.

### 7.6. Acknowledgements

Funding support from US Wheat and Barley Scab Initiative to NR (59-0206-0-179) and YD (59-0206-0-177) is thankfully acknowledged. Authors also thank Maryland Grain Producers Utilization Board and Maryland Crop Improvement Association for financial support.

## Conclusions and future directions

Fusarium Head Blight (FHB), caused by the fungal pathogen *Fusarium graminearum*, is the second most important disease of wheat globally. This doctoral research contributes toward improving the two most widely used FHB management strategies: development of resistant cultivars and the use of fungicides.

Towards the goal of improving FHB genetic resistance in wheat cultivars, breeder friendly and high- throughput KASP marker assays were developed for pyramiding FHB QTLs. A robust gene specific KASP marker was developed for most widely used FHB QTL, *Fhb1*. A large FHB QTL interval from Jamestown cultivar was refined to 6 Mb region and a robust KASP assay was developed from a flanking marker. Using publicly available transcriptomics data, FHB responsive GST genes were identified in the refined 6 Mb region. Although potential candidacy of GSTs is encouraging, this information should be used cautiously. Since the transcriptomics data and gene IDs are based on the Chinese spring genome. It is possible that the underlying gene is Jamestown cultivar specific and not present in Chinese spring at all. Therefore, there is need to develop cultivar specific genomics resources and perform cultivar specific transcriptomics studies. Moving forward, more recombinants can be identified and screened to fine map the region and transcriptomics studies can be performed to narrow down the number of potential gene candidates in the target region. Furthermore, TILLING, VIGS and gene complementation, approaches can be used for gene validation to ultimately clone the underlying gene.

In order to understand the molecular mechanism of FHB resistance, *PFT* mediated resistance against FHB was functionally characterized. *PFT* when ectopically expressed in Arabidopsis, conferred resistance to multiple hemi-biotrophic and necrotrophic fungal pathogens. In agreement with our working hypothesis of PFT's mechanism of resistance, PFT's agglutinin domains exhibited binding affinity towards fungus specific monosaccharide, N-acetylglucosamine. While further studies are required to fully characterize pore-forming domain of PFT, its heterologous expression partly suggests its toxicity. Preliminary in vitro antifungal activity of purified PFT protein did not exhibit drastic effects on spore germination or hyphal morphology. Further optimization of in vitro antifungal assays is required by using different concentrations of PFT protein. Furthermore, more sensitive assays to monitor the compromise of fungal membrane permeability can be performed which includes: propidium iodide uptake assay and potassium leakage assay. Ultimately, to validate the working hypothesis of PFT's mode of action, physical interaction of PFT and fungal cell should be demonstrated. In this regard, it is critical to develop PFT specific antibodies which can be conjugated with fluorophores. Thus, live cell imaging can be performed to visualize *in planta* interaction of PFT with fungal cells.

Towards the goal of improving fungicide-based control of FHB, a novel fungicide Miravis Ace (a proprietary mix of Pydiflumetofen and Propiconazole active ingredients produced by Syngenta Inc.) was tested for its efficacy in Maryland environment. Miravis Ace effectively controlled FHB compared to standard triazole fungicides. Widening the spray application window for FHB can be very helpful for Maryland growers. Therefore, application timing for Miravis Ace was evaluated and compared to widely used fungicide Prosaro. In

general, Miravis Ace performed better than Prosaro during early application timing. Each fungicide study was performed using a susceptible cultivar over two years in Maryland locations. Therefore, further studies are needed using multiple cultivars over multiples years and location for making widely applicable recommendations.

Overall, this doctoral research studied both basic and applied aspects of controlling FHB in wheat. It emphasized the importance of investing into long-term solutions in parallel to improving short-term control measures. The fundamental knowledge obtained on the molecular mechanism of FHB resistance would contribute towards the long-term approach of engineering disease resistance. Whereas KASP assays developed can be readily used in wheat breeding programs to enhance FHB resistance in wheat cultivars. The data on fungicide efficacy and application timing is timely for improving the chemical control of FHB. In conclusion, knowledge and resources generated from this work contributes towards effective integrated management of FHB in wheat.

# Appendices

## Appendix I

### Supplementary Information for Chapter 3

**Supplementary Table 1** Genotyping results of the markers used to screen wheat lines from breeding programs of University of Minnesota and the Pacific Northwest for *Fhb1*.

| Parental lines ID | PFT_KASP | UMN10 | SGNH_GSP | PFT_GSP |
|---|---|---|---|---|
| MN16396 | S | S | S | S |
| MN11087 | R | R | R | R |
| MN09028 | R | R | R | R |
| MN11064 | S | S | S | S |
| MN11469 | S | S | S | S |
| MN13288-1-1 | R | R | R | R |
| MN13288-1-32 | R | R | R | R |
| MN15005 | S | S | S | S |
| Shelly | R | H | R | R |
| SY-Valda | R | H | R | R |
| Bolles | S | S | S | S |
| MN10201-4-A | R | H | R | R |
| MN10261-1 | R | R | R | R |
| MN14105-7 | R | R | R | R |
| MN14223-5 | R | R | R | R |
| MN15119-2 | R | R | R | R |
| MN15320-1 | R | R | R | R |
| MN16274 | R | R | R | R |
| MN16311 | S | S | S | S |
| MN16360 | R | R | R | R |

| | | | | |
|---|---|---|---|---|
| CIMMYT GID:3613474 | S | S | S | S |
| CIMMYT GID:3855011 | S | S | S | S |
| CIMMYT GID:4314513 | S | S | S | S |
| CIMMYT GID:4577963 | S | S | S | S |
| CIMMYT GID:4878569 | S | S | S | S |
| 12X118 (2015 F5#475) | S | S | S | S |
| MN15287 | S | S | S | S |
| MN15411 | R | R | R | R |
| 07x135 (180-14) | S | S | S | S |
| Wheaton | S | S | S | S |
| 14X124-136-WT | R | R | R | R |
| 14X124-136-T1 | R | R | R | R |
| 14X124-156-WT | R | H | R | R |
| 14X124-156-T1 | R | R | R | R |
| 14X124-156-T2 | R | R | R | R |
| 14X124-156-T3 | R | R | R | R |
| 14X124-203-WT | S | S | S | S |
| 14X124-203-T1 | S | S | S | S |
| H0800080 | S | S | S | S |
| H0800103L | S | S | S | S |
| H0800310 | S | S | S | S |
| H0800314 | S | S | S | S |
| H0900009 | S | S | S | S |
| H0900081 | S3 | R | S | S |
| Hollis | S | S | S | S |
| HR07005-3 | S | S | S | S |
| HR07024-5 | S | S | S | S |
| HW080169 | R | R | R | R |
| HW090006M | S | S | S | S |
| HWO90071M | S | S | S | S |
| Kelse | S | S | S | S |
| Macon | S | S | S | S |
| Otis | S | S | S | S |
| Scarlet | S | S | S | S |

| | | | | |
|---|---|---|---|---|
| Tara2002 | S | S | S | S |
| WA8016 | S | S | S | S |
| WA8034 | S | S | S | S |
| WA8074 | S | S | S | S |
| WA8099 | S | S | S | S |
| WA8100 | S | S | S | S |
| WA8123 | S | S | S | S |
| WA8133 | S | S | S | S |
| LOUISE | S | S | S | S |
| PENAWAWA | S | S | S | S |
| W14 | R | R | R | R |
| UI Pettit | R | R | R | R |
| Treasure | S | S | S | S |
| Jubilee | S | S | S | S |
| IDO629 | S | S | S | S |
| IDO851 | S | S | S | S |
| IDO852 | S | S | S | S |
| UI Winchester | S | S | S | S |
| Jerome | S | S | S | S |
| IDO702 | S | S | S | S |
| Jefferson | S | S | S | S |
| Lolo | S | S | S | S |
| UI Lochsa | S | S | S | S |
| IDO694 | S | S | S | S |
| IDO686 | S | S | S | S |
| IDO671 | S | S | S | S |
| UI Stone | S | S | S | S |
| IDO644 | S | S | S | S |
| IDO377s | S | S | S | S |
| Pomerelle | S | S | S | S |
| ID0696 | S | S | S | S |
| IDO854 | S | S | S | S |
| IDO858 | S | S | S | S |
| IDO868 | S | S | S | S |

| | | | | |
|---|---|---|---|---|
| IDO687 | S | S | S | S |
| IDO440 | S | S | S | S |
| IDO488 | S | S | S | S |
| IDO582 | S | S | S | S |
| IDO560 | S | S | S | S |
| WHITEBIRD | S | S | S | S |
| CENTENNIAL | S | S | S | S |
| Hahan-1RS | S | S | S | S |
| Hahan-1RSMA | S | S | S | S |
| Attila-1RS | S | S | S | S |
| Attila-1RSMA | S | S | S | S |
| UC1110 | S | S | S | S |
| PI610750 | S | S | S | S |
| Lassik | S3 | R | S | S |
| UC1682 | S | S | S | S |
| Summit 515 | S | S | S | S |
| Expresso | S | S | S | S |
| RSI5 Yr5 Yr15 Gpc HMW 1 | S | S | S | S |
| UC1679 | S | S | S | S |
| Blanca Grande 515 | S | S | S | S |
| UC896 5+10 Lr34/Yr18 Yr5 Gpc | S | S | S | S |
| UC1603 | S3 | R | S | S |
| Blanca Fuerte | S | S | S | S |
| UC1395 Lr34/Yr18 | S | S | S | S |
| UC1396 | S | S | S | S |
| UC1551 | S | S | S | S |
| UC1552 | S | S | S | S |
| UC1554 | S | S | S | S |
| UC1599 | S | S | S | S |
| UC1601 | S | S | S | S |
| UC1602 | S | S | S | S |
| UC1616 | S | S | S | S |
| UC1618 | S3 | R | S | S |
| UC1642 | S | S | S | S |

| | | | | |
|---|---|---|---|---|
| UC1643 | S | S | S | S |
| 11010-9, 10013-1 | S | S | S | S |
| UC1683 | S | S | S | S |
| 10014/7 | S | S | S | S |
| RIL203 UC1110xCIMMYT2 | S | S | S | S |
| RIL29 UC1110xCIMMYT2 | S | S | S | S |
| Jagger | S | S | S | S |
| Thatcher | S | S | S | S |
| Fortuna | S | S | S | S |
| Choteau | S | S | S | S |
| Vida | S | S | S | S |
| MT0802 | S | S | S | S |
| Duclair | S | S | S | S |
| MT1002 | S | S | S | S |
| MT1016 | S | S | S | S |
| MT1020 | S | S | S | S |
| MT1027 | S | S | S | S |
| MT1053 | S | S | S | S |
| MTHW1060 | S | S | S | S |
| MTHW1069 | S | S | S | S |
| MT0861 | S | S | S | S |
| MT0921 | S | S | S | S |
| MT0945 | S | S | S | S |
| CAP151-3 | S | S | S | S |
| CAP34-1 | S | S | S | S |
| MTHW0771 | S | S | S | S |
| MT0415 | S | S | S | S |
| MT0813 | S | S | S | S |
| MTHW0867 | S | S | S | S |
| Newana | S | S | S | S |
| Hi-Line | S | S | S | S |
| 9263 | S3 | R | S | S |
| 9223 | S | S | S | S |
| 9225 | S | S | S | S |

| | | | | |
|---|---|---|---|---|
| 9228 | S | S | S | S |
| 9229 | S | S | S | S |
| 9232 | S | S | S | S |
| 9233 | S | S | S | S |
| 9245 | S | S | S | S |
| 9242 | S | S | S | S |
| 9240 | S | S | S | S |
| 9241 | S | S | S | S |
| 9246 | S | S | S | S |
| 9254 | S | S | S | S |
| 9256 | S | S | S | S |
| 9252 | S | S | S | S |
| 9248 | S | S | S | S |
| 9247 | S | S | S | S |
| 9249 | S | S | S | S |
| 9261 | S | S | S | S |
| Berkut | S | S | S | S |
| 9258 | S | S | S | S |
| 9259 | S | S | S | S |
| 9260 | S | S | S | S |
| 9253 | S | S | S | S |
| AC BARRIE | S | S | S | S |
| Hilliard | S | S | S | S |
| Corrigin | S | S | S | S |
| Catodo Solid-1 | S | S | S | S |
| Catodo Solid-2 | S | S | S | S |
| IDO644 Solid-1 | S | S | S | S |
| IDO644 Solid-2 | S | S | S | S |
| IDO671 Solid-1 | S | S | S | S |
| IDO671 Solid-2 | S | S | S | S |
| WA8008 Solid-1 | S | S | S | S |
| WA8008 Solid-2 | S | S | S | S |
| Chewink | S | S | S | S |
| SRRN-6027 | S | S | S | S |

| | | | | |
|---|---|---|---|---|
| SRRN-6028 | S | S | S | S |
| SRRN-6029 | S | S | S | S |
| SRRN-6030 | S | S | S | S |
| SRRN-6032 | S | S | S | S |
| SRRN-6037 | S | S | S | S |
| SRRN-6038 | S | S | S | S |
| SRRN-6042 | S | S | S | S |
| SRRN-6044 | S | S | S | S |
| SRRN-6047 | S | S | S | S |
| SRRN-6049 | S | S | S | S |
| SRRN-6050 | S | S | S | S |
| SRRN-6097 | S | S | S | S |
| SRRN-6098 | S | S | S | S |
| SRRN-6099 | S | S | S | S |
| SRRN-6109 | S | S | S | S |
| 21HRWSN-2106 | S | S | S | S |
| 21HRWSN-2111 | S | S | S | S |
| 21HRWSN-2126 | S | S | S | S |
| 28SAWSN-3045 | S | S | S | S |
| 28SAWSN-3047 | S | S | S | S |
| 28SAWSN-3096 | S | S | S | S |
| 28SAWSN-3102 | S | S | S | S |
| 28SAWSN-3106 | S | S | S | S |
| 43IBWSN-1014 | S | S | S | S |
| 43IBWSN-1015 | S | S | S | S |
| 43IBWSN-1085 | S | S | S | S |
| 43IBWSN-1089 | S | S | S | S |
| 43IBWSN-1101 | S | S | S | S |
| 43IBWSN-1118 | S | S | S | S |
| 43IBWSN-1227 | S | S | S | S |
| UI Platinum | S | S | S | S |
| LCS Altomo | S | S | S | S |
| LCS-Star | S | S | S | S |

*Disagreements between PFT_KASP and UMN10 are highlighted in red font.

**R- presence of resistant allele; S- presence of susceptible allele in case of UMN10 and absence of allele for PFT_KASP, PFT_GSP and SGNH_GSP; H-presence of both resistant and susceptible alleles; S3- presence of non-functional *PFT* allele (S3 haplotype)

**Supplementary Table 2.** Genotyping results of various markers used in the study to screen breeding lines developed by University of Idaho for Fhb1 and validation of accuracy of PFT_KASP marker

| Breeding line ID | Pedigree | PFT_KASP | UMN10 | SGNH_GSP | PFT_GSP |
|---|---|---|---|---|---|
| A12023S-1 | IDO850/W14//IDO852 | S | S | S | S |
| A12023S-4 | IDO850/W14//IDO852 | S | S | S | S |
| A12023S-5 | IDO850/W14//IDO852 | S | S | S | S |
| A12025S-1 | IDO850/W14//IDO854 | S | S | S | S |
| A12025S-2 | IDO850/W14//IDO854 | R | R | R | R |
| A12025S-4 | IDO850/W14//IDO854 | S | S | S | S |
| A12035S-1 | IDO851/W14//IDO851 | S | S | S | S |
| A12037S-3 | IDO851/W14//IDO854 | S | S | S | S |
| A12037S-5 | IDO851/W14//IDO854 | S | S | S | S |
| A12037S-7 | IDO851/W14//IDO854 | S | S | S | S |
| A12056S-10 | IDO852//IDO852/W14 | S | S | S | S |
| A12056S-11 | IDO852//IDO852/W14 | S | S | S | S |
| A12056S-12 | IDO852//IDO852/W14 | S | S | S | S |
| A12056S-13 | IDO852//IDO852/W14 | S | S | S | S |
| A12062S-6 | IDO854/W14//IDO851 | R | R | R | R |
| A12062S-8 | IDO854/W14//IDO851 | R | H | R | R |
| A12062S-9 | IDO854/W14//IDO851 | R | H | R | R |

| | | | | | |
|---|---|---|---|---|---|
| IDO1405S | 2016 F311 E border | S | S | S | S |
| A12063S-9 | IDO854/W14//IDO854 | S | S | S | S |
| A12063S-10 | IDO854/W14//IDO854 | S | S | S | S |
| A12063S-12 | IDO854/W14//IDO854 | S | S | S | S |
| A12064S-1 | IDO854/W14//IDO854 | S | S | S | S |
| A12064S-2 | IDO854/W14//IDO854 | S | S | S | S |
| A12064S-8 | IDO854/W14//IDO854 | S | S | S | S |
| A12064S-9 | IDO854/W14//IDO854 | S | S | S | S |
| A12064S-11 | IDO854/W14//IDO854 | S | S | S | S |
| A12077S-2 | IDO696//IDO696/W14 | S | S | S | S |
| A12084S-3 | IDO687//IDO687/W14 | R | H | R | R |
| A12084S-5 | IDO687//IDO687/W14 | R | H | R | R |
| A12084S-6 | IDO687//IDO687/W14 | R | H | R | R |
| A12084S-7 | IDO687//IDO687/W14 | S | S | S | S |
| A12086S-3 | IDO687/W14//IDO687 | R | R | R | R |
| A12086S-10 | IDO687/W14//IDO687 | R | R | R | R |
| A12086S-12 | IDO687/W14//IDO687 | R | R | R | R |
| A12086S-13 | IDO687/W14//IDO687 | S | S | S | S |
| A12004S-1 | IDO694/N9016/3/JFSN*4/IDO584 (70-5)//Lassik | S | S | S | S |
| A12004S-3 | IDO694/N9016/3/JFSN*4/IDO584 (70-5)//Lassik | S | S | S | S |
| A12004S-10 | IDO694/N9016/3/JFSN*4/IDO584 (70-5)//Lassik | S | S | S | S |
| A12004S-14 | IDO694/N9016/3/JFSN*4/IDO584 (70-5)//Lassik | S | S | S | S |
| **IDO1603S** | 2016 Gp 100 | **S3** | **R** | **S** | **S** |

| UI Stone | 2016 Gp 100 | S | S | S | S |
|---|---|---|---|---|---|
| A12004S-15 | IDO694/N9016/3/JFSN*4/IDO584 (70-5)//Lassik | S | S | S | S |
| A12004S-16 | IDO694/N9016/3/JFSN*4/IDO584 (70-5)//Lassik | S | S | S | S |
| A12004S-17 | IDO694/N9016/3/JFSN*4/IDO584 (70-5)//Lassik | S | S | S | S |
| A12004S-18 | IDO694/N9016/3/JFSN*4/IDO584 (70-5)//Lassik | S | S | S | S |
| **A12004S-19** | IDO694/N9016/3/JFSN*4/IDO584 (70-5)//Lassik | **S3** | **R** | **S** | **S** |
| A12004S-20 | IDO694/N9016/3/JFSN*4/IDO584 (70-5)//Lassik | S | S | S | S |
| A12004S-21 | IDO694/N9016/3/JFSN*4/IDO584 (70-5)//Lassik | S | S | S | S |
| **A12004S-24** | IDO694/N9016/3/JFSN*4/IDO584 (70-5)//Lassik | **S3** | **R** | **S** | **S** |
| A12004S-27 | IDO694/N9016/3/JFSN*4/IDO584 (70-5)//Lassik | S | S | S | S |
| A12004S-28 | IDO694/N9016/3/JFSN*4/IDO584 (70-5)//Lassik | S | S | S | S |
| A12004S-29 | IDO694/N9016/3/JFSN*4/IDO584 (70-5)//Lassik | S | S | S | S |
| A12004S-30 | IDO694/N9016/3/JFSN*4/IDO584 (70-5)//Lassik | S | S | S | S |
| A12041S-1 | IDO851/N9016//IDO851 | S | S | S | S |
| A12041S-3 | IDO851/N9016//IDO851 | S | S | S | S |
| A12041S-4 | IDO851/N9016//IDO851 | S | S | S | S |
| A12041S-5 | IDO851/N9016//IDO851 | S | S | S | S |
| A12079S-1 | IDO686/N9016//IDO686 | S | S | S | S |
| A12089S-3 | IDO687/N9016//IDO687 | S | S | S | S |
| A12089S-6 | IDO687/N9016//IDO687 | R | H | R | R |
| A12089S-7 | IDO687/N9016//IDO687 | S | S | S | S |
| A12089S-8 | IDO687/N9016//IDO687 | S | S | S | S |
| A12089S-9 | IDO687/N9016//IDO687 | S | S | S | S |

| | | | | | |
|---|---|---|---|---|---|
| A12089S-10 | IDO687/N9016//IDO687 | S | S | S | S |
| A12089S-11 | IDO687/N9016//IDO687 | S | S | S | S |
| A12089S-12 | IDO687/N9016//IDO687 | R | R | R | R |
| A12089S-13 | IDO687/N9016//IDO687 | S | S | S | S |
| A12089S-14 | IDO687/N9016//IDO687 | S | S | S | S |
| A12089S-16 | IDO687/N9016//IDO687 | S | S | S | S |
| A12089S-18 | IDO687/N9016//IDO687 | S | S | S | S |
| A12089S-19 | IDO687/N9016//IDO687 | S | S | S | S |
| A12089S-20 | IDO687/N9016//IDO687 | S | S | S | S |
| A12089S-21 | IDO687/N9016//IDO687 | S | S | S | S |
| A12039S-2 | IDO851/Futai 8944//IDO854 | R | H | R | R |
| A12039S-3 | IDO851/Futai 8944//IDO854 | S | S | S | S |

*Disagreements between PFT_KASP and UMN10 are highlighted in red font.

**R- presence of resistant allele; S- presence of susceptible allele in case of UMN10 and absence of allele for PFT_KASP, PFT_GSP and SGNH_GSP; H-presence of both resistant and susceptible alleles; S3- presence of non-functional *PFT* allele (S3 haplotype)

**Appendix II**

**Supplementary information for Chapter 5**

**Supplementary Table 1.** Average relative fluorescent unit values (RFUs) of His-PFT and His-ETX for all the 300 glycans screened in the study.

| No. | Glycan ID | Average RFU | | Glycan Structure |
|---|---|---|---|---|
| | | **His-PFT** | **His-ETX** | |
| 1 | POS1 | 110406.9 | 110406.9 | |
| 2 | NEG | 1.0 | 57.0 | |
| 3 | G0001 | 3218.1 | 2036.9 | ß-Glc-Sp |
| 4 | G0002 | 1787.5 | 1769.5 | ß-Gal-Sp |
| 5 | G0003 | 1597.2 | 881.3 | a-Man-Sp |
| 6 | G0004 | 1797.2 | 1181.0 | a-Fuc-Sp |
| 7 | G0005 | 831.6 | 473.3 | a-Rha-Sp |
| ***8*** | ***G0006*** | ***2033.0*** | ***1616.2*** | ***ß-GlcNAc-Sp*** |
| 9 | G0007 | 2131.0 | 1875.9 | ß-GalNAc-Sp |
| 10 | G0008 | 9650.2 | 17466.1 | Tobramycin |
| 11 | G0009 | 1172.0 | 834.1 | Gal-ß-1,3-GlcNAc-ß-Sp |
| 12 | G0010 | 956.9 | 656.4 | Gal-a-1,3-Gal-ß-1,3-GlcNAc-ß-Sp |
| 13 | G0011 | 2439.7 | 2357.8 | Neu5Ac-a-2,3-Gal-ß-1,3-GlcNAc-ß-Sp |
| 14 | G0012 | 1392.2 | 799.1 | Neu5Ac-a-2,6-Gal-ß-1,3-GlcNAc-ß-Sp |

| | | | | |
|---|---|---|---|---|
| 15 | G0013 | 3165.0 | 2228.2 | Neu5Gc-a-2,3-Gal-ß-1,3-GlcNAc-ß-Sp |
| 16 | G0014 | 3887.2 | 3115.2 | Neu5Gc-a-2,6-Gal-ß-1,3-GlcNAc-ß-Sp |
| 17 | G0015 | 1359.0 | 1174.1 | Gal-ß-1,3-(Fuc-a-1,4)-GlcNAc-ß- [Lewis A] –Sp |
| 18 | G0016 | 2361.7 | 1552.9 | Gal-ß-1,4-Glc-ß-Sp |
| 19 | G0017 | 1374.5 | 555.1 | Gal-a-1,3-Gal-ß-1,4-Glc-ß-Sp |
| 20 | G0018 | 1648.6 | 1318.6 | Gal-a-1,4-Gal-ß-1,4-Glc-ß-Sp |
| 21 | G0019 | 2127.0 | 1804.7 | GlcNAc-ß-1,3-Gal-ß-1,4-Glc-ß-Sp |
| 22 | G0020 | 1288.0 | 474.3 | GalNAc-ß-1,3-Gal-ß-1,4-Glc-ß-Sp |
| 23 | G0021 | 1084.9 | 458.9 | Neu5Ac-a-2,3-Gal-ß-1,4-Glc-ß-Sp |
| 24 | G0022 | 1592.4 | 1207.4 | Neu5Ac-a-2,6-Gal-ß-1,4-Glc-ß-Sp |
| 25 | G0023 | 1219.3 | 936.6 | Neu5Gc-a-2,3-Gal-ß-1,4-Glc-ß-Sp |
| 26 | G0024 | 1150.0 | 513.5 | Neu5Gc-a-2,6-Gal-ß-1,4-Glc-ß-Sp |
| 27 | G0025 | 1553.9 | 690.1 | Gal-ß-1,4-(Fuc-a-1,3)-Glc-ß-Sp |
| 28 | G0026 | 130.3 | 22.9 | GalNAc-ß-1,3-Gal-a-1,4-Gal-ß-1,4-Glc-ß-Sp |
| ***29*** | ***G0027*** | ***2164.2*** | ***1744.7*** | ***GlcNAc-ß-1,6-GlcNAc-ß-Sp*** |
| 30 | G0028 | 1417.4 | 1697.6 | 4-P-GlcNAc-b-1,4-Man-b-Sp |
| 31 | G0029 | 1864.5 | 1714.0 | Glc-a-1,2-Gal-a-1,3-Glc-a-Sp |
| 32 | G0030 | 1065.8 | 807.9 | Gal-ß-1,3-GalNAc-a-Sp |
| 33 | G0031 | 1715.9 | 1776.0 | Gal-ß-1,4-GlcNAc-ß-Sp |
| 34 | G0032 | 1565.9 | 1362.8 | Gal-ß-1,4 -(Fuc-a-1,3)-GlcNAc-ß- [Lewis X] –Sp |
| 35 | G0033 | 582.2 | 123.4 | Neu5Ac-a-2,3-Gal-ß-1,4-(Fuc-a-1,3)-GlcNAc-ß- [Sialyl Lewis X]-Sp |
| 36 | G0034 | 209.9 | 151.4 | Neu5Ac-a-2,3-Gal-ß-1,3 -(Fuc-a-1,4)-GlcNAc-ß- [Sialyl Lewis A]-Sp |
| 37 | G0035 | 224877.3 | 223279.6 | Neu5Gc-a-2,3-Gal-ß-1,3-(Fuc-a-1,4)-GlcNAc-ß- [Sialyl LewisA]-Sp |
| 38 | G0036 | 983.6 | 505.3 | Gal-a-1,4-Gal-ß-1,3-GlcNAc-ß-Sp |
| 39 | G0037 | 1178.6 | 725.8 | Gal-ß-1,4-GlcNAc-ß-1,3-Gal-ß-1,4-Glc-ß- [LNnT]-Sp |
| 40 | G0038 | 1626.8 | 1257.6 | GlcA-ß-1,4-GlcNAc-a-1,4-GlcA-ß-Sp |

| | | | | |
|---|---|---|---|---|
| 41 | G0039 | 415.9 | 85.6 | GlcNAc-ß-1,6-(Gal-ß-1,3)-GalNAc-a-O-Ser-Sp4 |
| 42 | G0040 | 977.9 | 322.3 | Neu5Ac-a-2,3Gal-ß-1,4-(6S)GlcNAc-ß-Sp |
| 43 | G0041 | 730.1 | 246.1 | GalNAc-ß-1,4-GlcNAc-ß-Sp2 |
| 44 | G0042 | 203.8 | 97.7 | Neu5Ac-a-2,8-Neu5Ac-a-2,3-Galß-1,4-Glc-ß-Sp |
| 45 | G0043 | 467.7 | 218.6 | Neu5Gc-a-2,8-Neu5Ac-a-2,3-Gal-ß-1,4-Glc-ß-Sp |
| 46 | G0044 | 51.8 | 55.4 | GalNAc-a-1,3-(Fuc-a-1,2)-Gal-ß-1,4-Glc-ß- [Blood A antigen tetrose]-Sp1 |
| 47 | G0045 | 715.3 | 347.2 | GlcNAc-ß-1,2-Man-a-Sp |
| 48 | G0046 | 931.5 | 533.9 | Neu5Ac-a-2,3-Gal-ß-Sp1 |
| 49 | G0047 | 1062.4 | 478.0 | Gal-ß-1,3 -GalNAc-ß-1,3-Gal-ß-Sp1 |
| 50 | G0048 | 2525.4 | 1938.8 | Gal-a-1,2-Gal-a-Sp |
| 51 | G0049 | 1215.1 | 176.5 | Gal-ß-1,4-(Fuc-a-1,3)-GlcNAc-ß-1,3-Gal-ß-Sp1 |
| 52 | G0050 | 588.2 | 135.4 | Neu5Ac-a-2,3-Gal-ß-1,4-(Fuc-a-1,3)-Glc-ß- [3-Sialyl-3-fucosyllactose/ F-SL]-Sp1 |
| 53 | G0051 | 978.4 | 235.7 | GlcNAc-ß-1,4-GlcNAc-ß-Sp1 |
| 54 | G0052 | 2495.7 | 2203.2 | ß-D-GlcA-Sp |
| 55 | G0053 | 1911.3 | 2164.6 | Gal-ß-1,4-(6S)GlNAc-ß-Sp |
| 56 | G0054 | 1252.4 | 601.9 | GlcNAc-a-1,3-(Glc-a-1,2-Glc-a-1,2)-Gal-a-1,3-Glc-a-Sp |
| 57 | G0055 | 1166.2 | 427.4 | Gal-ß-1,3-GalNAc-ß-1,4-(Neu5Gc-a-2,3)-Gal-ß-1,4-Glc-ß-Sp1 |
| 58 | G0056 | 6071.5 | 6193.4 | Sisomicin Sulfate |
| 59 | G0057 | 1471.8 | 633.9 | GalNAc-a-1,3-(Fuc-a-1,2)-Gal-ß- [Blood A antigen trisaccharide]-Sp1 |
| 60 | G0058 | 778.7 | 384.9 | Fuc-a-1,2-Gal-ß-1,4-GlcNAc-ß- [Blood H antigen trisaccharide]-Sp1 |
| 61 | G0059 | 1316.8 | 812.4 | Gal-a-1,3-(Fuc-a-1,2)-Gal-ß- [Blood B antigen trisaccharide]-Sp1 |
| 62 | G0060 | 843.4 | 260.7 | Fuc-a-1,2-Gal-ß-1,3-GlcNAc-ß-1,3-Gal-ß-1,4-Glc-ß- [LNFP I]-Sp1 |
| 63 | G0061 | 1407.8 | 1087.7 | Fuc-a-1,2-Gal-ß-1,4-Glc-ß- [Blood H antigen trisaccharide]-Sp1 |

| | | | | |
|---|---|---|---|---|
| 64 | G0062 | 1360.7 | 1177.0 | Gal-a-1,3-(Fuc-a-1,2)-Gal-ß-1,4-Glc-ß- [Blood B antigen tetrasaccharide]-Sp1 |
| 65 | G0063 | 1148.8 | 728.5 | (Fuc-a-1,2)-Gal-ß-1,4-(Fuc-a-1,3)-GlcNAc-ß- [ Lewis Y]-Sp1 |
| 66 | G0064 | 951.2 | 539.6 | (Fuc-a-1,2)-Gal-ß-1,3-(Fuc-a-1,4)-GlcNAc-ß- [ Lewis B]-Sp1 |
| 67 | G0065 | 790.6 | 423.4 | Gal-ß-1,3-(Fuc-a-1,4)-GlcNAc-ß-1,3-Gal-ß-1,4-(Fuc-a-1,4)-Glc-ß- [Lewis A]-Sp1 |
| 68 | G0066 | 1060.5 | 702.5 | Gal-ß-1,3-GalNAc-ß-Sp1 |
| 69 | G0067 | 656.5 | 488.7 | Gal-ß-1,3-(Neu5Ac-a-2,6)-GalNAc-ß-Sp |
| 70 | G0068 | 1094.5 | 457.0 | Neu5Ac-a-2,6-Gal-ß-1,3-GalNAc-ß-Sp |
| 71 | G0069 | 780.5 | 272.2 | Neu5Ac-a-2,6-Gal-ß-1,3-(Neu5Ac-a-2,6)-GalNAc-ß-Sp |
| 72 | G0070 | 954.0 | 570.4 | Neu5Ac-a-2,3-Gal-ß-1,3-(Neu5Ac-a-2,6)-GalNAc-ß-Sp |
| 73 | G0071 | 1270.2 | 953.6 | Neu5Ac-a-2,6-(Neu5Ac-a-2,3)-Gal-ß-1,3-GalNAc-ß-Sp |
| 74 | G0072 | 1270.4 | 597.9 | GalNAc-ß-1,4-(Neu5Ac-a-2,3)-Gal-ß-1,4-Glc-ß- [GM2]-Sp |
| 75 | G0073 | 306.7 | 1.3 | GalNAc-ß-1,4-(Neu5Ac-a-2,8-Neu5Ac-a-2,3)-Gal-ß-1,4-Glc-ß- [GD2]-Sp |
| 76 | G0074 | 1451.5 | 1578.7 | Gal-a-1,4-Gal-ß-1,4-GlcNAc-ß-Sp1 |
| 77 | G0075 | 2807.3 | 2628.0 | ß-D-Rha-Sp |
| 78 | G0076 | 2390.0 | 1618.7 | Glc-a-1,4-Glc-ß-Sp1 |
| 79 | G0077 | 1808.5 | 1052.2 | Glc-a-1,6-Glc-a-1,4-Glc-ß-Sp1 |
| 80 | G0078 | 1482.6 | 911.1 | Maltotriose-ß-Sp1 |
| 81 | G0079 | 1339.2 | 967.9 | Glc-a-1,6-Glc-a-1,6-Glc-ß-Sp1 |
| 82 | G0080 | 1361.3 | 1008.8 | Maltotetraose-ß-Sp1 |
| 83 | G0081 | 1569.7 | 550.4 | GlcNAc-a-1,4-GlcA-ß-1,4-GlcNAc-a1,4-GlcA-ß-Sp |
| 84 | G0082 | 921.2 | 633.5 | Maltohexaose-ß-Sp1 |
| 85 | G0083 | 715.3 | 281.9 | Maltoheptaose-ß-Sp1 |
| 86 | G0084 | 1677.7 | 1438.1 | Acarbose-ß-Sp1 |
| 87 | G0085 | 3527.4 | 3778.2 | D-pentamannuronic acid-ß-Sp1 |

| | | | | |
|---|---|---|---|---|
| 88 | G0086 | 2326.9 | 1690.7 | L-pentaguluronic acid-ß-Sp1 |
| 89 | G0087 | 1635.5 | 1578.5 | D-cellose-ß-Sp1 |
| 90 | G0088 | 2529.5 | 1692.6 | Gal-a-1,3-Gal-ß-Sp1 |
| 91 | G0089 | 1275.4 | 885.8 | ß-1,4-Xylotetrose-Sp1 |
| ***92*** | ***G0090*** | ***962.2*** | ***520.0*** | ***Chitin-trisaccharide-Sp1*** |
| 93 | G0091 | 1006.2 | 374.3 | KDN-a-2,8-Neu5Ac-a-2,3-Gal-ß-1,4-Glc-ß-Sp |
| 94 | G0092 | 780.5 | 558.0 | Neu5Ac-a-2,8-Neu5Gc-a-2,3-Gal-ß-1,4-Glc-ß-Sp |
| 95 | G0093 | 136.9 | 108.0 | Neu5Ac-a-2,8-Neu5Ac-a-2,8-Neu5Ac-a-2,3-Gal-ß-1,4-Glc-ß-Sp3 |
| 96 | G0094 | 616.4 | 492.4 | Neu5Ac-a-2,8-Neu5Ac-a-2,6-Gal-b-1,4-Glc-Sp5 |
| 97 | G0095 | 721.7 | 422.1 | Gal-ß-1,3-GalNAc-ß-1,4-(Neu5Ac-a-2,3)-Gal-ß-1,4-Glc-ß-Sp1 |
| 98 | G0096 | 3964.2 | 4154.2 | Gentamicin Sulfate |
| 99 | G0097 | 5016.0 | 5841.2 | Kanamycin sulfate |
| 100 | G0098 | 1448.8 | 1362.7 | Geneticin Disulfate Salt (G418) |
| 101 | G0099 | 18553.7 | 11364.3 | Neomycin trisulfate |
| 102 | G0100 | 2881.1 | 2727.6 | SGP |
| 103 | N010 | 338.5 | 1.2 | Man-a-1,6-(Man-a-1,3-)Man-a-1,6-(GlcNAc-ß-1,2-Man-a-1,3-)Man-ß-1,4-GlcNAc-ß-1,4-GlcNAc-Sp5 |
| 104 | N011 | 210.7 | 53.8 | Man-a-1,6-(Man-a-1,3-)Man-a-1,6-(Gal-ß-1,4-GlcNAc-ß-1,2-Man-a-1,3-)Man-ß-1,4-GlcNAc-ß-1,4-GlcNAc-Sp5 |
| 105 | N012 | 262.1 | 1.2 | Man-a-1,6-(Man-a-1,3-)Man-a-1,6-(Neu5Ac-a-2,3-Gal-ß-1,4-GlcNAc-ß-1,2-Man-a-1,3-) Man-ß-1,4-GlcNAc-ß-1,4-GlcNAc-Sp5 |
| 106 | N013 | 291.5 | 1.2 | Man-a-1,6-(Man-a-1,3-)Man-a-1,6-(Neu5Ac-a-2,6-Gal-ß-1,4-GlcNAc-ß-1,2-Man-a-1,3-) Man-ß-1,4-GlcNAc-ß-1,4-GlcNAc-Sp5 |
| 107 | N014 | 223.4 | 280.3 | Man-a-1,6-(Man-a-1,3-)Man-a-1,6-[Gal-ß-1,4-(Fuc-a-1,3-)GlcNAc-ß-1,2-Man-a-1,3-]Man-ß-1,4-GlcNAc-ß-1,4-GlcNAc-Sp5 |

| | | | | |
|---|---|---|---|---|
| 108 | N015 | 429.4 | 101.0 | Man-a-1,6-(Man-a-1,3-)Man-a-1,6-[Neu5Ac-a-2,3-Gal-ß-1,4-(Fuc-a-1,3-)GlcNAc-ß-1,2- Man-a-1,3-]Man-ß-1,4-GlcNAc-ß-1,4-GlcNAc-Sp5 |
| 109 | N020 | 495.5 | 392.1 | GlcNAc-ß-1,2-Man-a-1,3-Man-ß-1,4-GlcNAc-ß-1,4-GlcNAc-Sp5 |
| 110 | N021 | 506.3 | 300.2 | Gal-ß-1,4-GlcNAc-ß-1,2-Man-a-1,3-Man-ß-1,4-GlcNAc-ß-1,4-GlcNAc-Sp5 |
| 111 | N022 | 334.9 | 90.6 | Neu5Ac-a-2,3-Gal-ß-1,4-GlcNAc-ß-1,2-Man-a-1,3-Man-ß-1,4-GlcNAc-ß-1,4-GlcNAc-Sp5 |
| 112 | N023 | 539.3 | 172.1 | Neu5Ac-a-2,6-Gal-ß-1,4-GlcNAc-ß-1,2-Man-a-1,3-Man-ß-1,4-GlcNAc-ß-1,4-GlcNAc-Sp5 |
| 113 | N024 | 398.3 | 105.7 | Gal-ß-1,4-(Fuc-a-1,3-)GlcNAc-ß-1,2-Man-a-1,3-Man-ß-1,4-GlcNAc-ß-1,4-GlcNAc-Sp5 |
| 114 | N025 | 409.4 | 4.4 | Neu5Ac-a-2,3-Gal-ß-1,4-(Fuc-a-1,3-)GlcNAc-ß-1,2-Man-a-1,3-Man-ß-1,4-GlcNAc-ß-1,4-GlcNAc-Sp5 |
| 115 | N026 | 324.6 | 1.2 | Gal-a-1,3-Gal-ß-1,4-GlcNAc-ß-1,2-Man-a-1,3-Man-ß-1,4-GlcNAc-ß-1,4-GlcNAc-Sp5 |
| 116 | N022G | 766.6 | 121.2 | Neu5Gc-a-2,3-Gal-ß-1,4-GlcNAc-ß-1,2-Man-a-1,3-Man-ß-1,4-GlcNAc-ß-1,4-GlcNAc-Sp5 |
| 117 | N023G | 467.9 | 286.8 | Neu5Gc-a-2,6-Gal-ß-1,4-GlcNAc-ß-1,2-Man-a-1,3-Man-ß-1,4-GlcNAc-ß-1,4-GlcNAc-Sp5 |
| 118 | N025G | 410.3 | 138.3 | Neu5Gc-a-2,3-Gal-ß-1,4-(Fuc-a-1,3-)GlcNAc-ß-1,2-Man-a-1,3-Man-ß-1,4-GlcNAc-ß-1,4-GlcNAc-Sp5 |
| 119 | N030 | 437.2 | 182.5 | Man-a-1,6-(GlcNAc-ß-1,2-Man-a-1,3-)Man-ß-1,4-GlcNAc-ß-1,4-GlcNAc-Sp5 |
| 120 | N210 | 403.3 | 45.1 | GlcNAc-ß-1,2-Man-a-1,6-[GlcNAc(3Ac)-ß-1,2-Man-a-1,3-Man-ß-1,4-GlcNAc-ß-1,4-GlcNAc-Sp5 |
| 121 | N040 | 399.7 | 139.3 | GlcNAc-ß-1,2-Man-a-1,6-Man-ß-1,4-GlcNAc-ß-1,4-GlcNAc-Sp5 |

| | | | | |
|---|---|---|---|---|
| 122 | N041 | 679.6 | 200.9 | Gal-ß-1,4-GlcNAc-ß-1,2-Man-a-1,6-Man-ß-1,4-GlcNAc-ß-1,4-GlcNAc-Sp5 |
| 123 | N042 | 299.8 | 1.2 | Neu5Ac-a-2,3-Gal-ß-1,4-GlcNAc-ß-1,2-Man-a-1,6-Man-ß-1,4-GlcNAc-ß-1,4-GlcNAc-Sp5 |
| 124 | N043 | 591.8 | 172.2 | Neu5Ac-a-2,6-Gal-ß-1,4-GlcNAc-ß-1,2-Man-a-1,6-Man-ß-1,4-GlcNAc-ß-1,4-GlcNAc-Sp5 |
| 125 | N044 | 390.2 | 161.6 | Gal-ß-1,4-(Fuc-a-1,3-)GlcNAc-ß-1,2-Man-a-1,6-Man-ß-1,4-GlcNAc-ß-1,4-GlcNAc-Sp5 |
| 126 | N045 | 257.4 | 225.0 | Neu5Ac-a-2,3-Gal-ß-1,4-(Fuc-a-1,3-)GlcNAc-ß-1,2-Man-a-1,6-Man-ß-1,4-GlcNAc-ß-1,4-GlcNAc-Sp5 |
| 127 | N050 | 475.4 | 262.7 | GlcNAc-ß-1,2-Man-a-1,6-(Man-a-1,3-)Man-ß-1,4-GlcNAc-ß-1,4-GlcNAc-Sp5 |
| 128 | N051 | 514.1 | 169.1 | Gal-ß-1,4-GlcNAc-ß-1,2-Man-a-1,6-(Man-a-1,3-)Man-ß-1,4-GlcNAc-ß-1,4-GlcNAc-Sp5 |
| 129 | N052 | 223.4 | 72.2 | Neu5Ac-a-2,3-Gal-ß-1,4-GlcNAc-ß-1,2-Man-a-1,6-(Man-a-1,3-)Man-ß-1,4-GlcNAc-ß-1,4-GlcNAc-Sp5 |
| 130 | N053 | 324.2 | 99.9 | Neu5Ac-a-2,6-Gal-ß-1,4-GlcNAc-ß-1,2-Man-a-1,6-(Man-a-1,3-)Man-ß-1,4-GlcNAc-ß-1,4-GlcNAc-Sp |
| 131 | N054 | 233.5 | 60.0 | Gal-ß-1,4-(Fuc-a-1,3-)GlcNAc-ß-1,2-Man-a-1,6-(Man-a-1,3-)Man-ß-1,4-GlcNAc-ß-1,4-GlcNAc-Sp5 |
| 132 | N055 | 481.2 | 116.3 | Neu5Ac-a-2,3-Gal-ß-1,4-(Fuc-a-1,3-)GlcNAc-ß-1,2-Man-a-1,6-(Man-a-1,3-)Man-ß-1,4-GlcNAc-ß-1,4-GlcNAc-Sp5 |
| 133 | TE001 | 180.0 | 1.2 | Neu5Ac-a-2,6-Gal-ß-1,4-GlcNAc-Man-a-1,3-( Neu5Ac-a-2,6-Gal-ß-1,4-GlcNAc-Man-a-1,6-)Man-ß-1,4-GlcNAc-ß-1,4-GlcNAc-ß-Asn |
| 134 | TE002 | 168.7 | 3.2 | Gal-ß-1,4-GlcNAc-ß-1,2-Man-a-1,3-(Gal-ß-1,4-GlcNAc-ß-1,2-Man-a-1,6-)Man-ß-1,4-GlcNAc-ß-1,4-GlcNAc-ß-Asn |

| | | | | |
|---|---|---|---|---|
| 135 | TE003 | 62.0 | 1.2 | Neu5Gc-a-2,6-Gal-ß-1,4-GlcNAc-ß-1,2-Man-a-1,3-( Neu5Gc-a-2,6-Gal-ß-1,4-GlcNAc-ß-1,2-Man-a-1,6-)Man-ß-1,4-GlcNAc-ß-1,4-GlcNAc-ß-Asn |
| 136 | TE004 | 1.0 | 1.2 | Neu5Ac-a-2,3-Gal-ß-1,4-GlcNAc-ß-1,2-Man-a-1,3-( Neu5Ac-a-2,3-Gal-ß-1,4-GlcNAc-ß-1,2-Man-a-1,6-)Man-ß-1,4-GlcNAc-ß-1,4-GlcNAc-ß-Asn |
| 137 | TE005 | 240.5 | 1.2 | Neu5Gc-a-2,3-Gal-ß-1,4-GlcNAc-ß-1,2-Man-a-1,3-( Neu5Gc-a-2,3-Gal-ß-1,4-GlcNAc-ß-1,2-Man-a-1,6-)Man-ß-1,4-GlcNAc-ß-1,4-GlcNAc-ß-Asn |
| 138 | TE006 | 210.3 | 62.8 | Gal-ß-1,4-(Fuca-1,3-)GlcNAc-ß-1,2-Man-a-1,3-[Gal-ß-1,4-(Fuca-1,3-)GlcNAc-ß-1,2-Man-a-1,6-]Man-ß-1,4-GlcNAc-ß-1,4-GlcNAc-ß-Asn |
| 139 | TE007 | 92.3 | 1.2 | Gal-a-1,3-Gal-ß-1,4-GlcNAc-ß-1,2-Man-a-1,3-(Gal-a-1,3-Gal-ß-1,4-GlcNAc-ß-1,2-Man-a-1,6-)Man-ß-1,4-GlcNAc-ß-1,4-GlcNAc-ß-Asn |
| 140 | TE008 | 116.3 | 1.2 | Gal-ß-1,4-(Fuca-1,3-)GlcNAc-ß-1,2-Man-a-1,3-[Gal-ß-1,4-(Fuca-1,3-)GlcNAc-ß-1,2-Man-a-1,6-]Man-ß-1,4-GlcNAc-ß-1,4-GlcNAc-ß-Asn |
| 141 | TE009 | 153.4 | 1.2 | Neu5Ac-a-2,8-Neu5Ac-a-2,6-Gal-ß-1,4-GlcNAc-ß-1,2-Man-a-1,3-(Neu5Ac-a-2,8-Neu5Ac-a-2,6-Gal-ß-1,4-GlcNAc-ß-1,2-Man-a-1,6-)Man-ß-1,4-GlcNAc-ß-1,4-GlcNAc-ß-Asn |
| 142 | TE010 | 1.0 | 1.2 | Neu5Gc-a-2,8-Neu5Ac-a-2,6-Gal-ß-1,4-GlcNAc-ß-1,2-Man-a-1,3-( Neu5Gc-a-2,8-Neu5Ac-a-2,6-Gal-ß-1,4-GlcNAc-ß-1,2-Man-a-1,6-)Man-ß-1,4-GlcNAc-ß- 1,4-GlcNAc-ß-Asn |
| 143 | TE011 | 200.6 | 1.2 | Neu5Ac-a-2,8-Neu5Gc-a-2,6-Gal-ß-1,4-GlcNAc-ß-1,2-Man-a-1,3-( Neu5Ac-a-2,8-Neu5Gc-a-2,6-Gal-ß-1,4-GlcNAc-ß-1,2-Man-a-1,6-)Man-ß-1,4-GlcNAc-ß- 1,4-GlcNAc-ß-Asn |
| 144 | TE012 | 195.0 | 1.2 | Neu5Gc-a-2,8-Neu5Gc-a-2,6-Gal-ß-1,4-GlcNAc-ß-1,2-Man-a-1,3-( Neu5Gc-a-2,8-Neu5Gc-a-2,6-Gal-ß-1,4-GlcNAc-ß-1,2-Man-a-1,6-)Man-ß-1,4-GlcNAc-ß- 1,4-GlcNAc-ß-Asn |

| | | | | |
|---|---|---|---|---|
| 145 | TE013 | 1.0 | 1.2 | Neu5Ac-a-2,8-Neu5Ac-a-2,3-Gal-ß-1,4-GlcNAc-ß-1,2-Man-a-1,3-(Neu5Ac-a-2,8-Neu5Ac-a-2,3-Gal-ß-1,4-GlcNAc-ß-1,2-Man-a-1,6-)Man-ß-1,4-GlcNAc-ß-1,4-GlcNAc-ß-Asn |
| 146 | TE014 | 80.6 | 1.2 | Neu5Gc-a-2,8-Neu5Ac-a-2,3-Gal-ß-1,4-GlcNAc-ß-1,2-Man-a-1,3-(Neu5Gc-a-2,8-Neu5Ac-a-2,3-Gal-ß-1,4-GlcNAc-ß-1,2-Man-a-1,6-)Man-ß-1,4-GlcNAc-ß- 1,4-GlcNAc-ß-Asn |
| 147 | TE015 | 21.3 | 1.2 | Neu5Ac-a-2,8-Neu5Gc-a-2,3-Gal-ß-1,4-GlcNAc-ß-1,2-Man-a-1,3-(Neu5Ac-a-2,8-Neu5Gc-a-2,3-Gal-ß-1,4-GlcNAc-ß-1,2-Man-a-1,6-)Man-ß-1,4-GlcNAc-ß- 1,4-GlcNAc-ß-Asn |
| 148 | TE016 | 17.3 | 1.2 | Neu5Gc-a-2,8-Neu5Gc-a-2,3-Gal-ß-1,4-GlcNAc-ß-1,2-Man-a-1,3-(Neu5Gc-a-2,8-Neu5Gc-a-2,3-Gal-ß-1,4-GlcNAc-ß-1,2-Man-a-1,6-)Man-ß-1,4-GlcNAc-ß- 1,4-GlcNAc-ß-Asn |
| 149 | TE017 | 42.1 | 1.2 | Neu5Ac-a-2,3-Gal-ß-1,4-(Fuca-1,3-)GlcNAc-ß-1,2-Man-a-1,3-[Neu5Ac-a-2,3-Gal-ß-1,4-(Fuca-1,3-)GlcNAc-ß-1,2-Man-a-1,6-]Man-ß-1,4-GlcNAc-ß-1,4- GlcNAc-ß-Asn |
| 150 | TE018 | 112.6 | 1.2 | Neu5Gc-a-2,3-Gal-ß-1,4-(Fuca-1,3-)GlcNAc-ß-1,2-Man-a-1,3-[Neu5Gc-a-2,3-Gal-ß-1,4-(Fuca-1,3-)GlcNAc-ß-1,2-Man-a-1,6-]Man-ß-1,4-GlcNAc-ß-1,4-GlcNAc-ß-Asn |
| 151 | TE019 | 30.4 | 1.2 | Neu5Ac-a-2,3-Gal-ß-1,4-GlcNAc-ß-1,3-Gal-ß-1,4-GlcNAc-ß-1,2-Man-a-1,3-(Neu5Ac-a-2,3-Gal-ß-1,4-GlcNAc-ß-1,3-Gal-ß-1,4-GlcNAc-ß-1,2-Man-a-1,6-)Man- ß-1,4-GlcNAc-ß-1,4-GlcNAc-ß-Asn |
| 152 | TE020 | 12.1 | 1.2 | Neu5Gc-a-2,3-Gal-ß-1,4-GlcNAc-ß-1,3-Gal-ß-1,4-GlcNAc-ß-1,2-Man-a-1,3-(Neu5Gc-a-2,3-Gal-ß-1,4-GlcNAc-ß-1,3-Gal-ß-1,4-GlcNAc-ß-1,2-Man-a-1,6-)Man-ß-1,4-GlcNAc-ß-1,4-GlcNAc-ß-Asn |
| 153 | TE021 | 1.0 | 1.2 | Neu5Ac-a-2,6-Gal-ß-1,4-GlcNAc-ß-1,3-(Neu5AC-a-2,6-)Gal-ß-1,4-GlcNAc-ß-1,2-Man-a-1,3-[Neu5Ac-a-2,6-Gal-ß-1,4-GlcNAc-ß-1,3- |

| | | | | |
|---|---|---|---|---|
| | | | | (Neu5AC-a-2,6-)Gal-ß-1,4-GlcNAc-ß-1,2-Man-a-1,6-]Man-ß-1,4-GlcNAc-ß-1,4-GlcNAc-ß-Asn |
| 154 | TE022 | 1.0 | 1.2 | Neu5Gc-a-2,6-Gal-ß-1,4-GlcNAc-ß-1,3-(Neu5GC-a-2,6-)Gal-ß-1,4-GlcNAc-ß-1,2-Man-a-1,3-[Neu5Gc-a-2,6-Gal-ß-1,4-GlcNAc-ß-1,3-(Neu5GC-a-2,6-)Gal-ß-1,4-GlcNAc-ß-1,2-Man-a-1,6-]Man-ß-1,4-GlcNAc-ß-1,4-GlcNAc-ß-Asn |
| 155 | TE023 | 55.3 | 1.2 | Neu5Ac-a-2,3-Gal-ß-1,4-GlcNAc-ß-1,3-(Neu5AC-a-2,6-)Gal-ß-1,4-GlcNAc-ß-1,2-Man-a-1,3-[Neu5Ac-a-2,3-Gal-ß-1,4-GlcNAc-ß-1,3-(Neu5AC-a-2,6-)Gal-ß-1,4-GlcNAc-ß-1,2-Man-a-1,6-]Man-ß-1,4-GlcNAc-ß-1,4-GlcNAc-ß-Asn |
| 156 | TE024 | 90.3 | 1.2 | GlcNAc-ß-1,3-Gal-ß-1,4-GlcNAc-ß-1,2-Man-a-1,3-(GlcNAc-ß-1,3-Gal-ß-1,4-GlcNAc-ß-1,2-Man-a-1,6-)Man-ß-1,4-GlcNAc-ß-1,4-GlcNAc-ß-Asn |
| 157 | TE025 | 91.1 | 1.2 | Gal-ß-1,4-GlcNAc-ß-1,3-Gal-ß-1,4-GlcNAc-ß-1,2-Man-a-1,3-(Gal-ß-1,4-GlcNAc-ß-1,3-Gal-ß-1,4-GlcNAc-ß-1,2-Man-a-1,6-)Man-ß-1,4-GlcNAc-ß-1,4-GlcNAc-ß- Asn |
| 158 | TE026 | 108.9 | 1.2 | GlcNAc-ß-1,3-Gal-ß-1,4-GlcNAc-ß-1,3-Gal-ß-1,4-GlcNAc-ß-1,2-Man-a-1,3-(GlcNAc-ß-1,3-Gal-ß-1,4-GlcNAc-ß-1,3-Gal-ß-1,4-GlcNAc-ß-1,2-Man-a-1,6-)Man-ß- 1,4-GlcNAc-ß-1,4-GlcNAc-ß-Asn |
| 159 | TE027 | 87.5 | 1.2 | Gal-ß-1,4-GlcNAc-ß-1,3-Gal-ß-1,4-GlcNAc-ß-1,3-Gal-ß-1,4-GlcNAc-ß-1,2-Man-a-1,3-(Gal-ß-1,4-GlcNAc-ß-1,3-Gal-ß-1,4-GlcNAc-ß-1,3-Gal-ß-1,4-GlcNAc-ß-1,2- Man-a-1,6-)Man-ß-1,4-GlcNAc-ß-1,4-GlcNAc-ß-Asn |
| 160 | TE028 | 5.5 | 8.6 | GlcNAc-ß-1,3-Gal-ß-1,4-GlcNAc-ß-1,3-Gal-ß-1,4-GlcNAc-ß-1,3-Gal-ß-1,4-GlcNAc-ß-1,2-Man-a-1,3-(GlcNAc-ß-1,3-Gal-ß-1,4-GlcNAc-ß-1,3-Gal-ß-1,4-GlcNAc-ß- 1,3-Gal-ß-1,4-GlcNAc-ß-1,2-Man-a-1,6-)Man-ß-1,4-GlcNAc-ß-1,4-GlcNAc-ß-Asn |

| | | | | |
|---|---|---|---|---|
| 161 | TE029 | 1.0 | 1.2 | Gal-ß-1,4-GlcNAc-ß-1,3-Gal-ß-1,4-GlcNAc-ß-1,3-Gal-ß-1,4-GlcNAc-ß-1,3-Gal-ß-1,4-GlcNAc-ß-1,2-Man-a-1,3-(Gal-ß-1,4-GlcNAc-ß-1,3-Gal-ß-1,4-GlcNAc-ß-1,3-Gal-ß-1,4-GlcNAc-ß-1,3-Gal-ß-1,4-GlcNAc-ß-1,2-Man-a-1,6-)Man-ß-1,4-GlcNAc-ß-1,4-GlcNAc-ß-Asn |
| 162 | TE030 | 1.0 | 38.6 | GlcNAc-ß-1,3-Gal-ß-1,4-GlcNAc-ß-1,3-Gal-ß-1,4-GlcNAc-ß-1,3-Gal-ß-1,4-GlcNAc-ß-1,3-Gal-ß-1,4-GlcNAc-ß-1,2-Man-a-1,3-(GlcNAc-ß-1,3-Gal-ß-1,4-GlcNAc-ß-1,3-Gal-ß-1,4-GlcNAc-ß-1,3-Gal-ß-1,4-GlcNAc-ß-1,3-Gal-ß-1,4-GlcNAc-ß-1,2-Man-a-1,6-)Man-ß-1,4-GlcNAc-ß-1,4-GlcNAc-ß-Asn |
| 163 | TE031 | 1.0 | 1.2 | Gal-ß-1,4-GlcNAc-ß-1,3-Gal-ß-1,4-GlcNAc-ß-1,3-Gal-ß-1,4-GlcNAc-ß-1,3-Gal-ß-1,4-GlcNAc-ß-1,3-Gal-ß-1,4-GlcNAc-ß-1,2-Man-a-1,3-(Gal-ß-1,4-GlcNAc-ß-1,3- Gal-ß-1,4-GlcNAc-ß-1,3-Gal-ß-1,4-GlcNAc-ß-1,3-Gal-ß-1,4-GlcNAc-ß-1,3-Gal-ß-1,4-GlcNAc-ß-1,2-Man-a-1,6-)Man-ß-1,4-GlcNAc-ß-1,4-GlcNAc-ß-Asn |
| 164 | TE032 | 92.2 | 99.8 | GlcNAc-ß-1,3-Gal-ß-1,4-(Fuca-1,3-)GlcNAc-ß-1,2-Man-a-1,3-[GlcNAc-ß-1,3-Gal-ß-1,4-(Fuca-1,3-)GlcNAc-ß-1,2-Man-a-1,6-]Man-ß-1,4-GlcNAc-ß-1,4-GlcNAc- ß-Asn |
| 165 | TE033 | 187.9 | 1.2 | Gal-ß-1,4-GlcNAc-ß-1,3-Gal-ß-1,4-(Fuca-1,3-)GlcNAc-ß-1,2-Man-a-1,3-[Gal-ß-1,4-GlcNAc-ß-1,3-Gal-ß-1,4-(Fuca-1,3-)GlcNAc-ß-1,2-Man-a-1,6-]Man-ß-1,4- GlcNAc-ß-1,4-GlcNAc-ß-Asn |
| 166 | TE034 | 23.7 | 1.2 | Neu5Ac-a-2,3-Gal-ß-1,4-GlcNAc-ß-1,3-Gal-ß-1,4-(Fuca-1,3-)GlcNAc-ß-1,2-Man-a-1,3-[Neu5Ac-a-2,3-Gal-ß-1,4-GlcNAc-ß-1,3-Gal-ß-1,4-(Fuca-1,3-)GlcNAc-ß- 1,2-Man-a-1,6-]Man-ß-1,4-GlcNAc-ß-1,4-GlcNAc-ß-Asn |
| 167 | TE035 | 201.4 | 1.2 | GlcNAc-ß-1,3-Gal-ß-1,4-GlcNAc-ß-1,3-Gal-ß-1,4-(Fuca-1,3-)GlcNAc-ß-1,2-Man-a-1,3-[GlcNAc-ß-1,3-Gal-ß-1,4-GlcNAc-ß-1,3-Gal-ß-1,4-(Fuca-1,3-)GlcNAc-ß- 1,2-Man-a-1,6-]Man-ß-1,4-GlcNAc-ß-1,4-GlcNAc-ß-Asn |

| | | | | |
|---|---|---|---|---|
| 168 | TE036 | 185.3 | 1.2 | Gal-ß-1,4-GlcNAc-ß-1,3-Gal-ß-1,4-GlcNAc-ß-1,3-Gal-ß-1,4-(Fuca-1,3-)GlcNAc-ß-1,2-Man-a-1,3-[Gal-ß-1,4-GlcNAc-ß-1,3-Gal-ß-1,4-GlcNAc-ß-1,3-Gal-ß-1,4- (Fuca-1,3-)GlcNAc-ß-1,2-Man-a-1,6-]Man-ß-1,4-GlcNAc-ß-1,4-GlcNAc-ß-Asn |
| 169 | TE037 | 86.2 | 1.2 | GlcNAc-ß-1,3-Gal-ß-1,4-GlcNAc-ß-1,3-Gal-ß-1,4-GlcNAc-ß-1,3-Gal-ß-1,4-(Fuca-1,3-)GlcNAc-ß-1,2-Man-a-1,3-[GlcNAc-ß-1,3-Gal-ß-1,4-GlcNAc-ß-1,3-Gal-ß- 1,4-GlcNAc-ß-1,3-Gal-ß-1,4-(Fuca-1,3-)GlcNAc-ß-1,2-Man-a-1,6-]Man-ß-1,4-GlcNAc-ß-1,4-GlcNAc-ß-Asn |
| 170 | TE038 | 1.0 | 1.2 | Gal-ß-1,4-GlcNAc-ß-1,3-Gal-ß-1,4-GlcNAc-ß-1,3-Gal-ß-1,4-GlcNAc-ß-1,3-Gal-ß-1,4-(Fuca-1,3-)GlcNAc-ß-1,2-Man-a-1,3-[Gal-ß-1,4-GlcNAc-ß-1,3-Gal-ß-1,4-GlcNAc-ß-1,3-Gal-ß-1,4-GlcNAc-ß-1,3-Gal-ß-1,4-(Fuca-1,3-)GlcNAc-ß-1,2-Man-a-1,6-]Man-ß-1,4-GlcNAc-ß-1,4-GlcNAc-ß-Asn |
| 171 | TE039 | 3569.9 | 1.2 | Gal-ß-1,4-(Fuca-1,3-)GlcNAc-ß-1,3-Gal-ß-1,4-(Fuca-1,3-)GlcNAc-ß-1,2-Man-a-1,3-[Gal-ß-1,4-(Fuca-1,3-)GlcNAc-ß-1,3-Gal-ß-1,4-(Fuca-1,3-)GlcNAc-ß-1,2-Man-a-1,6-]Man-ß-1,4-GlcNAc-ß-1,4-GlcNAc-ß-Asn |
| 172 | TE040 | 487.6 | 1.2 | GlcNAc-ß-1,3-Gal-ß-1,4-(Fuca-1,3-)GlcNAc-ß-1,3-Gal-ß-1,4-(Fuca-1,3-)GlcNAc-ß-1,2-Man-a-1,3-[GlcNAc-ß-1,3-Gal-ß-1,4-(Fuca-1,3-)GlcNAc-ß-1,3-Gal-ß-1,4- (Fuca-1,3-)GlcNAc-ß-1,2-Man-a-1,6-]Man-ß-1,4-GlcNAc-ß-1,4-GlcNAc-ß-Asn |
| 173 | TE041 | 5005.4 | 1.2 | Gal-ß-1,4-GlcNAc-ß-1,3-Gal-ß-1,4-(Fuca-1,3-)GlcNAc-ß-1,3-Gal-ß-1,4-(Fuca-1,3-)GlcNAc-ß-1,2-Man-a-1,3-[Gal-ß-1,4-GlcNAc-ß-1,3-Gal-ß-1,4-(Fuca-1,3-)GlcNAc-ß-1,3-Gal-ß-1,4-(Fuca-1,3-)GlcNAc-ß-1,2-Man-a-1,6-]Man-ß-1,4-GlcNAc-ß-1,4-GlcNAc-ß-Asn |
| 174 | TE042 | 10196.2 | 1.2 | Gal-ß-1,4-(Fuca-1,3-)GlcNAc-ß-1,3-Gal-ß-1,4-(Fuca-1,3-)GlcNAc-ß-1,3-Gal-ß-1,4-(Fuca-1,3-)GlcNAc-ß-1,2-Man-a-1,3-[Gal-ß-1,4-(Fuca-1,3-)GlcNAc-ß-1,3-Gal- ß-1,4-(Fuca-1,3-)GlcNAc-ß-1,3-Gal-ß-1,4-(Fuca-1,3-)GlcNAc-ß-1,2-Man-a-1,6-]Man-ß-1,4-GlcNAc-ß-1,4-GlcNAc-ß-Asn |

| | | | | |
|---|---|---|---|---|
| 175 | TE043 | 121.4 | 1.2 | Gal-a-1,3-Gal-ß-1,4-GlcNAc-ß-1,3-Gal-ß-1,4-GlcNAc-ß-1,2-Man-a-1,3-(Gal-a-1,3-Gal-ß-1,4-GlcNAc-ß-1,3-Gal-ß-1,4-GlcNAc-ß-1,2-Man-a-1,6-)Man-ß-1,4-GlcNAc-ß-1,4-GlcNAc-ß-Asn |
| 176 | TE044 | 142.3 | 1.2 | Gal-a-1,3-Gal-ß-1,4-GlcNAc-ß-1,3-Gal-ß-1,4-(Fuca-1,3-)GlcNAc-ß-1,2-Man-a-1,3-[Gal-a-1,3-Gal-ß-1,4-GlcNAc-ß-1,3-Gal-ß-1,4-(Fuca-1,3-)GlcNAc-ß-1,2-Man- a-1,6-]Man-ß-1,4-GlcNAc-ß-1,4-GlcNAc-ß-Asn |
| 177 | TE045 | 191.3 | 1.2 | Gal-a-1,3-Gal-ß-1,4-(Fuca-1,3-)GlcNAc-ß-1,3-Gal-ß-1,4-(Fuca-1,3-)GlcNAc-ß-1,2-Man-a-1,3-[Gal-a-1,3-Gal-ß-1,4-(Fuca-1,3-)GlcNAc-ß-1,3-Gal-ß-1,4-(Fuca- 1,3-)GlcNAc-ß-1,2-Man-a-1,6-]Man-ß-1,4-GlcNAc-ß-1,4-GlcNAc-ß-Asn |
| 178 | TE046 | 72.2 | 1.2 | Gal-a-1,3-Gal-ß-1,4-GlcNAc-ß-1,3-Gal-ß-1,4-GlcNAc-ß-1,3-Gal-ß-1,4-GlcNAc-ß-1,2-Man-a-1,3-(Gal-a-1,3-Gal-ß-1,4-GlcNAc-ß-1,3-Gal-ß-1,4-GlcNAc-ß-1,3-Gal-ß-1,4-GlcNAc-ß-1,2-Man-a-1,6-)Man-ß-1,4-GlcNAc-ß-1,4-GlcNAc-ß-Asn |
| 179 | TE047 | 68.0 | 1.2 | Gal-a-1,3-Gal-ß-1,4-GlcNAc-ß-1,3-Gal-ß-1,4-GlcNAc-ß-1,3-Gal-ß-1,4-(Fuca-1,3-)GlcNAc-ß-1,2-Man-a-1,3-[Gal-a-1,3-Gal-ß-1,4-GlcNAc-ß-1,3-Gal-ß-1,4-GlcNAc-ß-1,3-Gal-ß-1,4-(Fuca-1,3-)GlcNAc-ß-1,2-Man-a-1,6-]Man-ß-1,4-GlcNAc-ß-1,4-GlcNAc-ß-Asn |
| 180 | TE048 | 4165.4 | 1.2 | Gal-a-1,3-Gal-ß-1,4-GlcNAc-ß-1,3-Gal-ß-1,4-(Fuca-1,3-)GlcNAc-ß-1,3-Gal-ß-1,4-(Fuca-1,3-)GlcNAc-ß-1,2-Man-a-1,3-[Gal-a-1,3-Gal-ß-1,4-GlcNAc-ß-1,3-Gal-ß- 1,4-(Fuca-1,3-)GlcNAc-ß-1,3-Gal-ß-1,4-(Fuca-1,3-)GlcNAc-ß-1,2-Man-a-1,6-]Man-ß-1,4-GlcNAc-ß-1,4-GlcNAc-ß-Asn |
| 181 | TE049 | 305.0 | 1.2 | Gal-a-1,3-Gal-ß-1,4-(Fuca-1,3-)GlcNAc-ß-1,3-Gal-ß-1,4-(Fuca-1,3-)GlcNAc-ß-1,3-Gal-ß-1,4-(Fuca-1,3-)GlcNAc-ß-1,2-Man-a-1,3-[Gal-a-1,3-Gal-ß-1,4-(Fuca-1,3-)GlcNAc-ß-1,3-Gal-ß-1,4-(Fuca-1,3-)GlcNAc-ß-1,3-Gal-ß-1,4-(Fuca-1,3-)GlcNAc-ß-1,2-Man-a-1,6-]Man-ß-1,4-GlcNAc-ß-1,4-GlcNAc-ß-Asn |

| | | | | |
|---|---|---|---|---|
| 182 | TE050 | 3.6 | 1.2 | Gal-a-1,3-Gal-ß-1,4-GlcNAc-ß-1,3-Gal-ß-1,4-GlcNAc-ß-1,3-Gal-ß-1,4-GlcNAc-ß-1,3-Gal-ß-1,4-GlcNAc-ß-1,2-Man-a-1,3-(Gal-a-1,3-Gal-ß-1,4-GlcNAc-ß-1,3-Gal- ß-1,4-GlcNAc-ß-1,3-Gal-ß-1,4-GlcNAc-ß-1,3-Gal-ß-1,4-GlcNAc-ß-1,2-Man-a-1,6-)Man-ß-1,4-GlcNAc-ß-1,4-GlcNAc-ß-Asn |
| 183 | H0100 | 598.0 | 168.1 | GlcNAc-ß-1,3-(GlcNAc-ß-1,6-)Gal-ß-1,4-Glc-Sp5 |
| 184 | H0101 | 771.0 | 711.6 | Gal-ß-1,4-GlcNAc-ß-1,3-(Gal-ß-1,4-GlcNAc-ß-1,6-)Gal-ß-1,4-Glc-Sp5 |
| 185 | H0103 | 566.3 | 240.0 | Neu5Gc-a-2,6-Gal-ß-1,4-GlcNAc-ß-1,3-(Neu5Gc-a-2,6-Gal-ß-1,4-GlcNAc-ß-1,6-)Gal-ß-1,4-Glc-Sp5 |
| 186 | H0105 | 414.5 | 96.7 | Fuc-a-1,2-Gal-ß-1,4-GlcNAc-ß-1,3-(Fuc-a-1,2-Gal-ß-1,4-GlcNAc-ß-1,6-)Gal-ß-1,4-Glc-Sp5 |
| 187 | H0106 | 227.0 | 55.9 | Fuc-a-1,2-Gal-ß-1,4-(Fuc-a-1,3-)GlcNAc-ß-1,3-[Fuc-a-1,2-Gal-ß-1,4-(Fuc-a-1,3-)GlcNAc-ß-1,6-]Gal-ß-1,4-Glc-Sp5 |
| 188 | H0200 | 458.6 | 256.2 | Gal-ß-1,4-GlcNAc-ß-1,3-(GlcNAc-ß-1,6-)Gal-ß-1,4-Glc-Sp5 |
| 189 | H0201 | 275.1 | 1.2 | Neu5Ac-a-2,6-Gal-ß-1,4-GlcNAc-ß-1,3-(GlcNAc-ß-1,6-)Gal-ß-1,4-Glc-Sp5 |
| 190 | H0202 | 801.1 | 363.5 | Neu5Gc-a-2,6-Gal-ß-1,4-GlcNAc-ß-1,3-(GlcNAc-ß-1,6-)Gal-ß-1,4-Glc-Sp5 |
| 191 | H0203 | 12643.0 | 154.8 | Gal-ß-1,4-(Fuc-a-1,3-)GlcNAc-ß-1,3-(GlcNAc-ß-1,6-)Gal-ß-1,4-Glc-Sp5 |
| 192 | H0204 | 763.6 | 344.5 | Fuc-a-1,2-Gal-ß-1,4-GlcNAc-ß-1,3-(GlcNAc-ß-1,6-)Gal-ß-1,4-Glc-Sp5 |
| 193 | H0205 | 643.5 | 308.8 | Neu5Ac-a-2,6-Gal-ß-1,4-GlcNAc-ß-1,3-(Gal-ß-1,4-GlcNAc-ß-1,6-)Gal-ß-1,4-Glc-Sp5 |
| 194 | H0207 | 9358.6 | 635.7 | Gal-ß-1,4-(Fuc-a-1,3-)GlcNAc-ß-1,3-(Gal-ß-1,4-GlcNAc-ß-1,6-)Gal-ß-1,4-Glc-Sp5 |
| 195 | H0208 | 767.6 | 741.5 | Fuc-a-1,2-Gal-ß-1,4-GlcNAc-ß-1,3-(Gal-ß-1,4-GlcNAc-ß-1,6-)Gal-ß-1,4-Glc-Sp5 |
| 196 | H0209 | 726.0 | 524.7 | Fuc-a-1,2-Gal-ß-1,4-(Fuc-a-1,3-)GlcNAc-ß-1,3-(GlcNAc-ß-1,6-)Gal-ß-1,4-Glc-Sp5 |

| | | | | |
|---|---|---|---|---|
| 197 | H0210 | 682.9 | 264.7 | Fuc-a-1,2-Gal-ß-1,4-(Fuc-a-1,3-)GlcNAc-ß-1,3-[Gal-ß-1,4-(Fuc-a-1,3-)GlcNAc-ß-1,6-]Gal-ß-1,4-Glc-Sp5 |
| 198 | H0300 | 436.4 | 497.2 | GlcNAc-ß-1,3-(Gal-ß-1,4-GlcNAc-ß-1,6-)Gal-ß-1,4-Glc-Sp5 |
| 199 | H0301 | 491.2 | 436.6 | GlcNAc-ß-1,3-(Neu5Ac-a-2,6-Gal-ß-1,4-GlcNAc-ß-1,6-)Gal-ß-1,4-Glc-Sp5 |
| 200 | H0303 | 629.6 | 188.5 | GlcNAc-ß-1,3-[Gal-ß-1,4-(Fuc-a-1,3-)GlcNAc-ß-1,6-]Gal-ß-1,4-Glc-Sp5 |
| 201 | H0304 | 690.5 | 94.5 | Fuc-a-1,2-GlcNAc-ß-1,3-(Gal-ß-1,4-GlcNAc-ß-1,6-)Gal-ß-1,4-Glc-Sp5 |
| 202 | H0305 | 511.5 | 181.1 | Gal-ß-1,4-GlcNAc-ß-1,3-(Neu5Ac-a-2,6-Gal-ß-1,4-GlcNAc-ß-1,6-)Gal-ß-1,4-Glc-Sp5 |
| 203 | H0306 | 667.0 | 337.6 | Gal-ß-1,4-GlcNAc-ß-1,3-(Neu5Gc-a-2,6-Gal-ß-1,4-GlcNAc-ß-1,6-)Gal-ß-1,4-Glc-Sp5 |
| 204 | H0307 | 686.9 | 688.3 | Gal-ß-1,4-GlcNAc-ß-1,3-[Gal-ß-1,4-(Fuc-a-1,3-)GlcNAc-ß-1,6-]Gal-ß-1,4-Glc-Sp5 |
| 205 | H0400 | 1754.5 | 1616.1 | Gal-ß-1,4-Glc-Sp |
| 206 | H0402 | 558.4 | 142.4 | GalNAc-ß-1,3-Gal-ß-1,4-Glc-Sp |
| 207 | H0403 | 1002.7 | 372.8 | Neu5Ac-a-2,3-Gal-ß-1,4-Glc-Sp |
| 208 | H0404 | 1822.3 | 846.6 | Neu5Gc-a-2,3-Gal-ß-1,4-Glc-Sp |
| 209 | H0405 | 1195.3 | 1004.4 | Neu5Ac-a-2,6-Gal-ß-1,4-Glc-Sp |
| 210 | H0406 | 1474.2 | 1124.5 | Neu5Gc-a-2,6-Gal-ß-1,4-Glc-Sp |
| 211 | H0407 | 1795.3 | 1236.9 | Gal-a-1,3-Gal-ß-1,4-Glc-Sp |
| 212 | H0408 | 706.3 | 269.0 | Neu5Ac-a-2,8-Neu5Ac-a-2,3-Gal-ß-1,4-Glc-Sp |
| 213 | H0409 | 709.3 | 723.8 | Neu5Ac-a-2,8-Neu5Ac-a-2,6-Gal-ß-1,4-Glc-Sp |
| 214 | H0410 | 751.0 | 388.9 | Neu5Ac-a-2,3-Gal-a-1,3-Gal-ß-1,4-Glc-Sp |
| 215 | H0411 | 829.1 | 297.4 | Neu5Ac-a-2,6-Gal-a-1,3-Gal-ß-1,4-Glc-Sp |
| 216 | H0500 | 1249.8 | 1287.1 | Gal-a-1,4-Gal-ß-1,4-Glc-Sp5 |
| 217 | H0503 | 648.8 | 495.2 | GalNAc-ß-1,3-Gal-a-1,4-Gal-ß-1,4-Glc-Sp5 |

| | | | | |
|---|---|---|---|---|
| 218 | H0504 | 612.3 | 348.2 | Gal-ß-1,3-GalNAc-ß-1,3-Gal-a-1,4-Gal-ß-1,4-Glc-Sp5 |
| 219 | H0505 | 566.2 | 432.4 | Fuc-a-1,2-Gal-ß-1,3-GalNAc-ß-1,3-Gal-a-1,4-Gal-ß-1,4-Glc-Sp5 |
| 220 | H0600 | 645.8 | 229.5 | Gal-ß-1,4-GlcNAc-ß-1,3-Gal-ß-1,4-Glc-Sp5 |
| 221 | H0601 | 23748.7 | 551.6 | Gal-ß-1,4-(Fuc-a-1,3-)GlcNAc-ß-1,3-Gal-ß-1,4-Glc-Sp5 |
| 222 | H0602 | 862.0 | 431.8 | Fuc-a-1,2-Gal-ß-1,4-GlcNAc-ß-1,3-Gal-ß-1,4-Glc-Sp5 |
| 223 | H0603 | 799.1 | 582.8 | GlcNAc-ß-1,3-Gal-ß-1,4-GlcNAc-ß-1,3-Gal-ß-1,4-Glc-Sp5 |
| 224 | H0604 | 519.4 | 1.2 | Neu5Ac-a-2,3-Gal-ß-1,4-GlcNAc-ß-1,3-Gal-ß-1,4-Glc-Sp5 |
| 225 | H0606 | 1564.8 | 1421.9 | Gal-ß-1,4-GlcNAc-ß-1,3-(Neu5Ac-a-2,6-)Gal-ß-1,4-Glc-Sp5 |
| 226 | H0608 | 742.2 | 595.8 | Fuc-a-1,2-Gal-ß-1,4-(Fuc-a-1,3-)GlcNAc-ß-1,3-Gal-ß-1,4-Glc-Sp5 |
| 227 | H0609 | 895.7 | 913.0 | Neu5Ac-a-2,3-Gal-ß-1,4-(Fuc-a-1,3-)GlcNAc-ß-1,3-Gal-ß-1,4-Glc-Sp5 |
| 228 | H0610 | 3710.8 | 938.4 | GlcNAc-ß-1,3-Gal-ß-1,4-(Fuc-a-1,3-)GlcNAc-ß-1,3-Gal-ß-1,4-Glc-Sp5 |
| 229 | H0700 | 1088.0 | 927.9 | Gal-ß-1,4-GlcNAc-ß-1,3-Gal-ß-1,4-GlcNAc-ß-1,3-Gal-ß-1,4-Glc-Sp5 |
| 230 | H0701 | 653.3 | 266.7 | GlcNAc-ß-1,3-Gal-ß-1,4-GlcNAc-ß-1,3-Gal-ß-1,4-GlcNAc-ß-1,3-Gal-ß-1,4-Glc-Sp5 |
| 231 | H0800 | 645.3 | 578.5 | Gal-ß-1,4-GlcNAc-ß-1,3-Gal-ß-1,4-GlcNAc-ß-1,3-Gal-ß-1,4-GlcNAc-ß-1,3-Gal-ß-1,4-Glc-Sp5 |
| 232 | H0900 | 871.6 | 984.9 | Gal-ß-1,3-GlcNAc-ß-1,3-(GlcNAc-ß-1,6-)Gal-ß-1,4-Glc-Sp5 |
| 233 | L1001 | 480.5 | 168.2 | Neu5Ac-a-2,3-Gal-ß-1,4-Glc-Sp5 |
| 234 | L1002 | 363.6 | 528.8 | Neu5Gc-a-2,3-Gal-ß-1,4-Glc-Sp5 |
| 235 | L1003 | 504.1 | 308.7 | Kdn-a-2,3-Gal-ß-1,4-Glc-Sp5 |
| 236 | L1011 | 173.8 | 256.7 | Neu5Ac-a-2,3-(GalNAc-b-1,4-)Gal-b-1,4-Glc-Sp5 |
| 237 | L1012 | 469.2 | 217.8 | Neu5Gc-a-2,3-(GalNAc-b-1,4-)Gal-b-1,4-Glc-Sp5 |
| 238 | L1013 | 400.6 | 209.8 | Kdn-a-2,3-(GalNAc-b-1,4-)Gal-b-1,4-Glc-Sp5 |
| 239 | L1021 | 313.7 | 121.1 | Neu5Ac-a-2,3-(Gal-b-1,3-GalNAc-b-1,4-)Gal-b-1,4-Glc-Sp5 |
| 240 | L1022 | 335.2 | 265.0 | Neu5Gc-a-2,3-(Gal-b-1,3-GalNAc-b-1,4-)Gal-b-1,4-Glc-Sp5 |
| 241 | L1023 | 526.2 | 565.1 | Kdn-a-2,3-(Gal-b-1,3-GalNAc-b-1,4-)Gal-b-1,4-Glc-Sp5 |

| | | | | |
|---|---|---|---|---|
| 242 | L1201 | 432.9 | 73.2 | Neu5Ac-a-2,8-Neu5Ac-a-2,3-Gal-ß-1,4-Glc-Sp5 |
| 243 | L1202 | 247.2 | 694.1 | Neu5Gc-a-2,8-Neu5Ac-a-2,3-Gal-ß-1,4-Glc-Sp5 |
| 244 | L1203 | 184.0 | 159.0 | Kdn-a-2,8-Neu5Ac-a-2,3-Gal-ß-1,4-Glc-Sp5 |
| 245 | L1204 | 254.5 | 13.7 | Neu5Ac-a-2,8-Neu5Gc-a-2,3-Gal-ß-1,4-Glc-Sp5 |
| 246 | L1205 | 728.2 | 350.6 | Neu5Gc-a-2,8-Neu5Gc-a-2,3-Gal-ß-1,4-Glc-Sp5 |
| 247 | L1206 | 719.3 | 379.2 | Kdn-a-2,8-Neu5Gc-a-2-,3-Gal-ß-1,4-Glc-Sp5 |
| 248 | L1207 | 408.1 | 275.4 | Neu5Ac-a-2,8-Kdn-a-2,3-Gal-ß-1,4-Glc-Sp5 |
| 249 | L1209 | 809.9 | 589.8 | Kdn-a-2,8-Kdn-a-2,3-Gal-ß-1,4-Glc-Sp5 |
| 250 | L1211 | 159.5 | 1.2 | Neu5Ac-a-2,8-Neu5Ac-a-2,3-(GalNAc-b-1,4-)Gal-ß-1,4-Glc-Sp5 |
| 251 | L1212 | 392.3 | 155.1 | Neu5Gc-a-2,8-Neu5Ac-a-2,3-(GalNAc-b-1,4-)Gal-ß-1,4-Glc-Sp5 |
| 252 | L1213 | 250.6 | 23.9 | Kdn-a-2,8-Neu5Ac-a-2,3-(GalNAc-b-1,4-)Gal-ß-1,4-Glc-Sp5 |
| 253 | L1214 | 224.9 | 95.8 | Neu5Ac-a-2,8-Neu5Gc-a-2,3-(GalNAc-b-1,4-)Gal-ß-1,4-Glc-Sp5 |
| 254 | L1215 | 205.9 | 21.5 | Neu5Gc-a-2,8-Neu5Gc-a-2,3-(GalNAc-b-1,4-)Gal-ß-1,4-Glc-Sp5 |
| 255 | L1216 | 643.3 | 242.5 | Kdn-a-2,8-Neu5Gc-a-2,3-(GalNAc-b-1,4-)Gal-ß-1,4-Glc-Sp5 |
| 256 | L1221 | 340.2 | 8.1 | Neu5Ac-a-2,8-Neu5Ac-a-2,3-(Gal-b-1,3-GalNAc-b-1,4-)Gal-ß-1,4-Glc-Sp5 |
| 257 | L1222 | 339.3 | 213.1 | Neu5Gc-a-2,8-Neu5Ac-a-2,3-(Gal-b-1,3-GalNAc-b-1,4-)Gal-ß-1,4-Glc-Sp5 |
| 258 | L1225 | 391.2 | 239.6 | Neu5Gc-a-2,8-Neu5Gc-a-2,3-(Gal-b-1,3-GalNAc-b-1,4-)Gal-ß-1,4-Glc-Sp5 |
| 259 | L1226 | 428.7 | 57.6 | Kdn-a-2,8-Neu5Gc-a-2,3-(Gal-b-1,3-GalNAc-b-1,4-)Gal-ß-1,4-Glc-Sp5 |
| 260 | L2000 | 619.8 | 219.7 | GlcNAc-ß-1,3-Gal-ß-1,4-Glc-Sp5 |
| 261 | L2100 | 835.6 | 856.0 | Gal-ß-1,4-GlcNAc-ß-1,3-Gal-ß-1,4-Glc-Sp5 |
| 262 | L2101 | 640.6 | 181.9 | Gal-a-1,3-Gal-ß-1,4-GlcNAc-ß-1,3-Gal-ß-1,4-Glc-Sp5 |
| 263 | L2102 | 1198.8 | 992.9 | Gal-a-1,4-Gal-ß-1,4-GlcNAc-ß-1,3-Gal-ß-1,4-Glc-Sp5 |
| 264 | L2111 | 756.2 | 276.7 | Neu5Ac-a-2,3-Gal-ß-1,4-GlcNAc-ß-1,3-Gal-ß-1,4-Glc-Sp5 |

| | | | | |
|---|---|---|---|---|
| 265 | L2112 | 788.7 | 173.2 | Neu5Gc-a-2,3-Gal-ß-1,4-GlcNAc-ß-1,3-Gal-ß-1,4-Glc-Sp5 |
| 266 | L2113 | 542.5 | 841.7 | Kdn-a-2,3-Gal-ß-1,4-GlcNAc-ß-1,3-Gal-ß-1,4-Glc-Sp5 |
| 267 | L2121 | 539.3 | 427.7 | Neu5Ac-a-2,8-Neu5Ac-a-2,3-Gal-ß-1,4-GlcNAc-ß-1,3-Gal-ß-1,4-Glc-Sp5 |
| 268 | L2122 | 470.9 | 186.8 | Neu5Gc-a-2,8-Neu5Ac-a-2,3-Gal-ß-1,4-GlcNAc-ß-1,3-Gal-ß-1,4-Glc-Sp5 |
| 269 | L2103 | 53038.5 | 1.2 | Gal-ß-1,4-(Fuc-a-1,3-)GlcNAc-ß-1,3-Gal-ß-1,4-Glc-Sp5 |
| 270 | L2104 | 435.2 | 43.6 | Gal-a-1,3-Gal-ß-1,4-(Fuc-a-1,3-)GlcNAc-ß-1,3-Gal-ß-1,4-Glc-Sp5 |
| 271 | L2131 | 138.2 | 121.2 | Neu5Ac-a-2,3-Gal-ß-1,4-(Fuc-a-1,3-)GlcNAc-ß-1,3-Gal-ß-1,4-Glc-Sp5 |
| 272 | L2132 | 316.2 | 1.2 | Neu5Gc-a-2,3-Gal-ß-1,4-(Fuc-a-1,3-)GlcNAc-ß-1,3-Gal-ß-1,4-Glc-Sp5 |
| 273 | L2133 | 193.6 | 1.2 | Kdn-a-2,3-Gal-ß-1,4-(Fuc-a-1,3-)GlcNAc-ß-1,3-Gal-ß-1,4-Glc-Sp5 |
| 274 | L2191 | 229.2 | 337.4 | |
| 275 | L2192 | 290.5 | 144.5 | |
| 276 | L2200 | 280.4 | 1.2 | GlcNAc-ß-1,3-Gal-ß-1,4-GlcNAc-ß-1,3-Gal-ß-1,4-Glc-Sp5 |
| 277 | L2300 | 327.1 | 152.5 | Gal-ß-1,4-GlcNAc-ß-1,3-Gal-ß-1,4-GlcNAc-ß-1,3-Gal-ß-1,4-Glc-Sp5 |
| 278 | L2301 | 231.2 | 1.2 | Gal-a-1,3-Gal-ß-1,4-GlcNAc-ß-1,3-Gal-ß-1,4-GlcNAc-ß-1,3-Gal-ß-1,4-Glc-Sp5 |
| 279 | L2302 | 236.3 | 21.9 | Gal-a-1,4-Gal-ß-1,4-GlcNAc-ß-1,3-Gal-ß-1,4-GlcNAc-ß-1,3-Gal-ß-1,4-Glc-Sp5 |
| 280 | L2311 | 67.2 | 74.6 | Neu5Ac-a-2,3-Gal-ß-1,4-GlcNAc-ß-1,3-Gal-ß-1,4-GlcNAc-ß-1,3-Gal-ß-1,4-Glc-Sp5 |
| 281 | L2312 | 552.1 | 192.7 | Neu5Gc-a-2,3-Gal-ß-1,4-GlcNAc-ß-1,3-Gal-ß-1,4-GlcNAc-ß-1,3-Gal-ß-1,4-Glc-Sp5 |
| 282 | L2303 | 12704.6 | 1.2 | Gal-ß-1,4-GlcNAc-ß-1,3-Gal-ß-1,4-(Fuc-a-1,3-)GlcNAc-ß-1,3-Gal-ß-1,4-Glc-Sp5 |
| 283 | L2304 | 8369.7 | 33.1 | Gal-ß-1,4-(Fuc-a-1,3-)GlcNAc-ß-1,3-Gal-ß-1,4-(Fuc-a-1,3-)GlcNAc-ß-1,3-Gal-ß-1,4-Glc-Sp5 |
| 284 | L2391 | 81.9 | 32.2 | |
| 285 | L2392 | 102.2 | 1.2 | |

| | | | | |
|---|---|---|---|---|
| 286 | L2900 | 550.3 | 69.6 | Gal-ß-1,3-GlcNAc-ß-1,3-Gal-ß-1,4-Glc-Sp5 |
| 287 | L2911 | 448.4 | 49.4 | Neu5Ac-a-2,3-Gal-ß-1,3-GlcNAc-ß-1,3-Gal-ß-1,4-Glc-Sp5 |
| 288 | L2912 | 209.7 | 508.4 | Neu5Gc-a-2,3-Gal-ß-1,3-GlcNAc-ß-1,3-Gal-ß-1,4-Glc-Sp5 |
| 289 | L2913 | 156.4 | 232.6 | Kdn-a-2,3-Gal-ß-1,3-GlcNAc-ß-1,3-Gal-ß-1,4-Glc-Sp5 |
| 290 | L3100 | 883.4 | 300.6 | Gal-a-1,4-Gal-ß-1,4-Glc-Sp5 |
| 291 | L3101 | 303.0 | 52.5 | GalNAc-ß-1,3-Gal-a-1,4-Gal-ß-1,4-Glc-Sp5 |
| 292 | L3102 | 115.4 | 1.2 | Gal-ß-1,3-GalNAc-ß-1,3-Gal-a-1,4-Gal-ß-1,4-Glc-Sp5 |
| 293 | L3111 | 11.0 | 1.2 | Neu5Ac-a-2,3-Gal-ß-1,3-GalNAc-ß-1,3-Gal-a-1,4-Gal-ß-1,4-Glc-Sp5 |
| 294 | L3112 | 135.6 | 1.2 | Neu5Gc-a-2,3-Gal-ß-1,3-GalNAc-ß-1,3-Gal-a-1,4-Gal-ß-1,4-Glc-Sp5 |
| 295 | L3113 | 150.4 | 1.2 | Kdn-a-2,3-Gal-ß-1,3-GalNAc-ß-1,3-Gal-a-1,4-Gal-ß-1,4-Glc-Sp5 |
| 296 | L3103 | 348.8 | 57.7 | |
| 297 | L3200 | 594.6 | 247.6 | Gal-a-1,3-Gal-ß-1,4-Glc-Sp5 |
| 298 | L3201 | 190.4 | 122.0 | GalNAc-ß-1,3-Gal-a-1,3-Gal-ß-1,4-Glc-Sp5 |
| 299 | L3202 | 161.5 | 122.9 | Gal-ß-1,3-GalNAc-ß-1,3-Gal-a-1,3-Gal-ß-1,4-Glc-Sp5 |
| 300 | L3211 | 69.7 | 1.2 | Neu5Ac-a-2,3-Gal-ß-1,3-GalNAc-ß-1,3-Gal-a-1,3-Gal-ß-1,4-Glc-Sp5 |
| 301 | L3212 | 133.7 | 36.3 | Neu5Gc-a-2,3-Gal-ß-1,3-GalNAc-ß-1,3-Gal-a-1,3-Gal-ß-1,4-Glc-Sp5 |
| 302 | L3213 | 148.3 | 1.2 | Kdn-a-2,3-Gal-ß-1,3-GalNAc-ß-1,3-Gal-a-1,3-Gal-ß-1,4-Glc-Sp5 |

# Bibliography

Alexander, N. J., McCormick, S. P., Waalwijk, C., van der Lee, T., and Proctor, R. H. (2011). The genetic basis for 3-ADON and 15-ADON trichothecene chemotypes in Fusarium. *Fungal Genetics and Biology* 48, 485–495. doi: 10.1016/j.fgb.2011.01.003.

Allen, A. M., Barker, G. L. A., Wilkinson, P., Burridge, A., Winfield, M., Coghill, J., et al. (2013). Discovery and development of exome-based, co-dominant single nucleotide polymorphism markers in hexaploid wheat (Triticum aestivum L.). *Plant Biotechnol J* 279–295. doi: 10.1111/pbi.12009.

Andargie, M., and Li, J. (2016). Arabidopsis thaliana: A Model Host Plant to Study Plant–Pathogen Interaction Using Rice False Smut Isolates of Ustilaginoidea virens. *Front Plant Sci* 7, 192. doi: 10.3389/fpls.2016.00192.

Anderson, J. A., Chao, S., and Liu, S. (2007). Molecular Breeding Using a Major QTL for Fusarium Head Blight Resistance in Wheat. *Crop Science* 47, S-112-S-119. doi: 10.2135/cropsci2007.04.0006IPBS.

Anderson, J. A., Stack, R. W., Liu, S., Waldron, B. L., Fjeld, A. D., Coyne, C., et al. (2001). DNA markers for Fusarium head blight resistance QTLs in two wheat populations. *Th Appl Genet* 102, 1164–1168. doi: 10.1007/s001220000509.

Aoki, T., Ward, T. J., Kistler, H. C., and O'donnell, K. (2012). Systematics, Phylogeny and Trichothecene Mycotoxin Potential of *Fusarium* Head Blight Cereal Pathogens. *JSM Mycotoxins* 62, 91–102. doi: 10.2520/myco.62.91.

Armstrong, R. N. (1997). Structure, Catalytic Mechanism, and Evolution of the Glutathione Transferases. *Chem. Res. Toxicol.* 10, 2–18. doi: 10.1021/tx960072x.

Arumuganathan, K., and Earle, E. D. (1991). Nuclear DNA content of some important plant species. *Plant Mol Biol Rep* 9, 208–218. doi: 10.1007/BF02672069.

Audenaert, K., Landschoot, S., Vanheule, A., Waegeman, W., Baets, B. D., and Haesaert, G. (2011a). *Impact of Fungicide Timing on the Composition of the Fusarium Head Blight Disease Complex and the Presence of Deoxynivalenol (DON) in Wheat*. IntechOpen do 10.5772/26322.

Audenaert, K., Landschoot, S., Vanheule, A., Waegeman, W., De Baets, B., and Haesaert, G. (2011b). "Impact of Fungicide Timing on the Composition of the Fusarium Head Blig

Disease Complex and the Presence of Deoxynivalenol (DON) in Wheat," in doi: 10.5772/26322.

Babiker, E. M., Gordon, T. C., Chao, S., Newcomb, M., Rouse, M. N., Jin, Y., et al. (2015). Mapping resistance to the Ug99 race group of the stem rust pathogen in a spring wheat landrace. *Theoretical and Applied Genetics* 128, 605–612. doi: 10.1007/s00122-015-2456-6.

Bai, G. H., Desjardins, A. E., and Plattner, R. D. (2002). Deoxynivalenol-nonproducing fusarium graminearum causes initial infection, but does not cause disease spread in wheat spikes. *Mycopathologia* 153, 91–98. doi: 10.1023/a:1014419323550.

Bai, G., and Shaner, G. (2004). Management and resistance in wheat and barley to fusarium head blight. *Annu Rev Phytopathol* 42, 135–161. doi: 10.1146/annurev.phyto.42.040803.140340.

Bailey-Serres, J., Parker, J. E., Ainsworth, E. A., Oldroyd, G. E. D., and Schroeder, J. I. (2019). Genetic strategies for improving crop yields. *Nature* 575, 109–118. doi: 10.1038/s41586-019-1679-0.

Bari, R., and Jones, J. D. G. (2009). Role of plant hormones in plant defence responses. *Plant Mol Biol* 69, 473–488. doi: 10.1007/s11103-008-9435-0.

Bennett, J. W., and Klich, M. (2003). Mycotoxins. *Clin. Microbiol. Rev.* 16, 497–516. doi: 10.1128/CMR.16.3.497-516.2003.

Bernardo, A. N., Ma, H., Zhang, D., and Bai, G. (2012). Single nucleotide polymorphism in wheat chromosome region harboring Fhb1 for Fusarium head blight resistance. *Mol Breeding* 29, 477–488. doi: 10.1007/s11032-011-9565-y.

Bhatwa, A., Wang, W., Hassan, Y. I., Abraham, N., Li, X.-Z., and Zhou, T. (2021). Challenges Associated With the Formation of Recombinant Protein Inclusion Bodies in Escherichia coli and Strategies to Address Them for Industrial Applications. *Frontiers in Bioengineering and Biotechnology* 9. Available at: https://www.frontiersin.org/article/10.3389/fbioe.2021.630551 [Accessed June 3, 2022].

Boenisch, M. J., and Schäfer, W. (2011). Fusarium graminearumforms mycotoxin producing infection structures on wheat. *BMC Plant Biology* 11, 110. doi: 10.1186/1471-2229-11-110.

Boni, R., Chauhan, H., Hensel, G., Roulin, A., Sucher, J., Kumlehn, J., et al. (2018). Pathogen-inducible Ta-Lr34res expression in heterologous barley confers disease resistance

without negative pleiotropic effects. *Plant Biotechnology Journal* 16, 245–253. doi: 10.1111/pbi.12765.

Borrill, P., Ramirez-Gonzalez, R., and Uauy, C. (2016). expVIP: a Customizable RNA-seq Data Analysis and Visualization Platform. *Plant Physiol* 170, 2172–2186. doi: 10.1104/pp.15.01667.

Bräunlich, S., Koller, T., Glauser, G., Krattinger, S. G., and Keller, B. (2021). Expression of the wheat disease resistance gene Lr34 in transgenic barley leads to accumulation of abscisic acid at the leaf tip. *Plant Physiology and Biochemistry* 166, 950–957. doi: 10.1016/j.plaphy.2021.07.001.

Brown, N. A., Antoniw, J., and Hammond-Kosack, K. E. (2012). The Predicted Secretome of the Plant Pathogenic Fungus Fusarium graminearum: A Refined Comparative Analysis. *PLOS ONE* 7, e33731. doi: 10.1371/journal.pone.0033731.

Buerstmayr, H., Ban, T., and Anderson, J. A. (2009a). QTL mapping and marker-assisted selection for Fusarium head blight resistance in wheat: a review. *Plant Breeding* 128, 1–26. doi: 10.1111/j.1439-0523.2008.01550.x.

Buerstmayr, H., Ban, T., and Anderson, J. A. (2009b). QTL mapping and marker-assisted selection for Fusarium head blight resistance in wheat: a review. *Plant Breeding* 128, 1–26. doi: 10.1111/j.1439-0523.2008.01550.x.

Buerstmayr, M., Steiner, B., and Buerstmayr, H. (2020). Breeding for Fusarium head blight resistance in wheat—Progress and challenges. *Plant Breeding* 139, 429–454. doi: 10.1111/pbr.12797.

Bushnell, W., Hazen, B., and Pritsch, C. (2003). "Histology and Physiology of Fusarium Head Blight," in *Fusarium Head Blight of Wheat and Barley*, 44–83.

Cabral, A. L., Jordan, M. C., McCartney, C. A., You, F. M., Humphreys, D. G., MacLachlan, R., et al. (2014). Identification of candidate genes, regions and markers for pre-harvest sprouting resistance in wheat (Triticum aestivum L.). *BMC Plant Biology* 14, 340. doi: 10.1186/s12870-014-0340-1.

Cainong, J. C., Bockus, W. W., Feng, Y., Chen, P., Qi, L., Sehgal, S. K., et al. (2015a). Chromosome engineering, mapping, and transferring of resistance to Fusarium head blight disease from Elymus tsukushiensis into wheat. *Theor Appl Genet* 128, 1019–1027. doi: 10.1007/s00122-015-2485-1.

Cainong, J. C., Bockus, W. W., Feng, Y., Chen, P., Qi, L., Sehgal, S. K., et al. (2015b). Chromosome engineering, mapping, and transferring of resistance to Fusarium head blight disease from Elymus tsukushiensis into wheat. *Theor Appl Genet* 128, 1019–1027. doi: 10.1007/s00122-015-2485-1.

Carpenter, N. R., Wright, E., Malla, S., Singh, L., Van Sanford, D., Clark, A., et al. (2020). Identification and validation of Fusarium head blight resistance QTL in the U.S. soft red winter wheat cultivar 'Jamestown.' *Crop Science* 60, 2919–2930. doi: 10.1002/csc2.20307.

Chain (CONTAM), E. P. on C. in the F., Knutsen, H. K., Alexander, J., Barregård, L., Bignami, M., Brüschweiler, B., et al. (2017). Risks to human and animal health related to the presence of deoxynivalenol and its acetylated and modified forms in food and feed. *EFSA Journal* 15, e04718. doi: 10.2903/j.efsa.2017.4718.

Chapman, S., Kavanagh, T., and Baulcombe, D. (1992). Potato virus X as a vector for gene expression in plants. *The Plant Journal* 2, 549–557. doi: 10.1046/j.1365-313X.1992.t01-24-00999.x.

Chen X., Steed A., Travella S., Keller B., and Nicholson P. (2009). Fusarium graminearum exploits ethylene signalling to colonize dicotyledonous and monocotyledonous plants. *New Phytologist* 182, 975–983. doi: 10.1111/j.1469-8137.2009.02821.x.

Consortium (IWGSC), T. I. W. G. S. (2014). A chromosome-based draft sequence of the hexaploid bread wheat (Triticum aestivum) genome. *Science* 345. doi: 10.1126/science.1251788.

Consortium (IWGSC), T. I. W. G. S., Appels, R., Eversole, K., Stein, N., Feuillet, C., Keller, B., et al. (2018a). Shifting the limits in wheat research and breeding using a fully annotated reference genome. *Science* 361. doi: 10.1126/science.aar7191.

Consortium (IWGSC), T. I. W. G. S., Appels, R., Eversole, K., Stein, N., Feuillet, C., Keller, B., et al. (2018b). Shifting the limits in wheat research and breeding using a fully annotated reference genome. *Science* 361. doi: 10.1126/science.aar7191.

Corwin, J. A., and Kliebenstein, D. J. (2017). Quantitative Resistance: More Than Just Perception of a Pathogen. *The Plant Cell* 29, 655–665. doi: 10.1105/tpc.16.00915.

Cowger, C., Patton-Özkurt, J., Brown-Guedira, G., and Perugini, L. (2009). Post-Anthesis Moisture Increased Fusarium Head Blight and Deoxynivalenol Levels in North Carolina Winter Wheat. *Phytopathology*® 99, 320–327. doi: 10.1094/PHYTO-99-4-0320.

Cowger, C., Weisz, R., Arellano, C., and Murphy, P. (2016). Profitability of Integrated Management of Fusarium Head Blight in North Carolina Winter Wheat. *Phytopathology*® 106, 814–823. doi: 10.1094/PHYTO-10-15-0263-R.

Cuomo, C. A., Güldener, U., Xu, J.-R., Trail, F., Turgeon, B. G., Di Pietro, A., et al. (2007). The Fusarium graminearum Genome Reveals a Link Between Localized Polymorphism and Pathogen Specialization. *Science* 317, 1400–1402. doi: 10.1126/science.1143708.

Cuthbert, P. A., Somers, D. J., and Brulé-Babel, A. (2007a). Mapping of Fhb2 on chromosome 6BS: a gene controlling Fusarium head blight field resistance in bread wheat (Triticum aestivum L.). *Theor Appl Genet* 114, 429–437. doi: 10.1007/s00122-006-0439-3.

Cuthbert, P. A., Somers, D. J., and Brulé-Babel, A. (2007b). Mapping of Fhb2 on chromosome 6BS: a gene controlling Fusarium head blight field resistance in bread wheat (Triticum aestivum L.). *Theor Appl Genet* 114, 429–437. doi: 10.1007/s00122-006-0439-3.

Cuthbert, P. A., Somers, D. J., Thomas, J., Cloutier, S., and Brulé-Babel, A. (2006a). Fine mapping Fhb1, a major gene controlling fusarium head blight resistance in bread wheat (Triticum aestivum L.). *Theor Appl Genet* 112, 1465–1472. doi: 10.1007/s00122-006-0249-7.

Cuthbert, P. A., Somers, D. J., Thomas, J., Cloutier, S., and Brulé-Babel, A. (2006b). Fine mapping Fhb1, a major gene controlling fusarium head blight resistance in bread wheat (Triticum aestivum L.). *Theor Appl Genet* 112, 1465. doi: 10.1007/s00122-006-0249-7.

Cuthbert, P. A., Somers, D. J., Thomas, J., Cloutier, S., and Brulé-Babel, A. (2006c). Fine mapping Fhb1, a major gene controlling fusarium head blight resistance in bread wheat (Triticum aestivum L.). *Theor Appl Genet* 112, 1465–1472. doi: 10.1007/s00122-006-0249-7.

Dang, L., Rougé, P., and Van Damme, E. J. M. (2017). Amaranthin-Like Proteins with Aerolysin Domains in Plants. *Front. Plant Sci.* 8. doi: 10.3389/fpls.2017.01368.

D'Angelo, D. L., Bradley, C. A., Ames, K. A., Willyerd, K. T., Madden, L. V., and Paul, P. A. (2014). Efficacy of Fungicide Applications During and After Anthesis Against Fusarium Head Blight and Deoxynivalenol in Soft Red Winter Wheat. *Plant Disease* 98, 1387–1397. doi: 10.1094/PDIS-01-14-0091-RE.

Desmond, O. J., Manners, J. M., Stephens, A. E., Maclean, D. J., Schenk, P. M., Gardiner, D. M., et al. (2008). The Fusarium mycotoxin deoxynivalenol elicits hydrogen peroxide production, programmed cell death and defence responses in wheat. *Molecular Plant Pathology* 9, 435–445. doi: 10.1111/j.1364-3703.2008.00475.x.

Dill-Macky, R., and Jones, R. K. (2000). The Effect of Previous Crop Residues and Tillage on Fusarium Head Blight of Wheat. *Plant Disease* 84, 71–76. doi: 10.1094/PDIS.2000.84.1.71.

Ding, L., Xu, H., Yi, H., Yang, L., Kong, Z., Zhang, L., et al. (2011). Resistance to Hemi-Biotrophic F. graminearum Infection Is Associated with Coordinated and Ordered Expression of Diverse Defense Signaling Pathways. *PLOS ONE* 6, e19008. doi: 10.1371/journal.pone.0019008.

Dixon, D. P., Skipsey, M., and Edwards, R. (2010). Roles for glutathione transferases in plant secondary metabolism. *Phytochemistry* 71, 338–350. doi: 10.1016/j.phytochem.2009.12.012.

Dodds, P. N., and Rathjen, J. P. (2010). Plant immunity: towards an integrated view of plant–pathogen interactions. *Nature Reviews Genetics* 11, 539–548. doi: 10.1038/nrg2812.

Eberhardt, J., Santos-Martins, D., Tillack, A. F., and Forli, S. (2021). AutoDock Vina 1.2.0: New Docking Methods, Expanded Force Field, and Python Bindings. *J. Chem. Inf. Model.* 61, 3891–3898. doi: 10.1021/acs.jcim.1c00203.

Edwards, S. g., and Godley, N. p. (2010). Reduction of Fusarium head blight and deoxynivalenol in wheat with early fungicide applications of prothioconazole. *Food Additives & Contaminants. Part A: Chemistry, Analysis, Control, Exposure & Risk Assessment* 27, 629–635. doi: 10.1080/19440040903515942.

Ellner, F. M. (2005). Results of long-term field studies into the effect of strobilurin containing fungicides on the production of mycotoxins in several winter wheat varieties. *Mycotox Res* 21, 112–115. doi: 10.1007/BF02954432.

Endo, T. R., and Gill, B. S. (1996). The Deletion Stocks of Common Wheat. *Journal of Heredity* 87, 295–307. doi: 10.1093/oxfordjournals.jhered.a023003.

Eswar, N., Webb, B., Marti-Renom, M. A., Madhusudhan, M. S., Eramian, D., Shen, M., et al. (2006). Comparative Protein Structure Modeling Using Modeller. *Curr Protoc Bioinformatics* 0 5, Unit-5.6. doi: 10.1002/0471250953.bi0506s15.

FAOSTAT. (2020). Crop Production Summary. https://www.fao.org/faostat/en/#data/QCL

FAOSTAT. (2019). Food Balance Sheet. https://www.fao.org/faostat/en/#data/FBS

Faruque, K., Begam, R., and Deyholos, M. K. (2015). The Amaranthin-Like Lectin (LuALL) Genes of Flax: a Unique Gene Family with Members Inducible by Defence Hormones. *Plant Mol Biol Rep* 33, 731–741. doi: 10.1007/s11105-014-0791-4.

Fernando, W. G. D., Oghenekaro, A. O., Tucker, J. R., and Badea, A. (2021). Building on a foundation: advances in epidemiology, resistance breeding, and forecasting research for reducing the impact of fusarium head blight in wheat and barley. *Canadian Journal of Plant Pathology* 43, 495–526. doi: 10.1080/07060661.2020.1861102.

Gerten, D., Heck, V., Jägermeyr, J., Bodirsky, B. L., Fetzer, I., Jalava, M., et al. (2020). Feeding ten billion people is possible within four terrestrial planetary boundaries. *Nat Sustain* 3, 200–208. doi: 10.1038/s41893-019-0465-1.

Gilbert, J., and Woods, S. M. (2006). Strategies and considerations for multi□location FHB screening nurseries. in *The Global Fusarium Initiative for International Collaboration: A Strategic Planning Workshop* (CIMMYT, El Batan, Mexico), 10.

Glazebrook, J. (2005). Contrasting Mechanisms of Defense Against Biotrophic and Necrotrophic Pathogens. *Annual Review of Phytopathology* 43, 205–227. doi: 10.1146/annurev.phyto.43.040204.135923.

Goswami, R. S., and Kistler, H. C. (2004). Heading for disaster: Fusarium graminearum on cereal crops. *Molecular Plant Pathology* 5, 515–525. doi: 10.1111/j.1364-3703.2004.00252.x.

Griffey, C. A., Thomason, W. E., Pitman, R. M., Beahm, B. R., Paling, J. J., Chen, J., et al. (2010). Registration of 'Jamestown' Wheat. *Journal of Plant Registrations* 4, 28–33. doi: 10.3198/jpr2009.05.0257crc.

Guenther, J. C., and Trail, F. (2005). The development and differentiation of Gibberella zeae (anamorph: Fusarium graminearum) during colonization of wheat. *Mycologia* 97, 229–237. doi: 10.1080/15572536.2006.11832856.

Guo, J., Zhang, X., Hou, Y., Cai, J., Shen, X., Zhou, T., et al. (2015a). High-density mapping of the major FHB resistance gene Fhb7 derived from Thinopyrum ponticum and its pyramiding with Fhb1 by marker-assisted selection. *Theor Appl Genet* 128, 2301–2316. doi: 10.1007/s00122-015-2586-x.

Guo, J., Zhang, X., Hou, Y., Cai, J., Shen, X., Zhou, T., et al. (2015b). High-density mapping of the major FHB resistance gene Fhb7 derived from Thinopyrum ponticum and its pyramiding with Fhb1 by marker-assisted selection. *Theor Appl Genet* 128, 2301–2316. doi: 10.1007/s00122-015-2586-x.

Gupta, A., Rico-Medina, A., and Caño-Delgado, A. I. (2020). The physiology of plant responses to drought. *Science*. doi: 10.1126/science.aaz7614.

Gupta, P. K., Roy, J. K., and Prasad, M. (2001). Single nucleotide polymorphisms: a new paradigm for molecular marker technology and DNA polymorphism detection with emphasis on their use in plants. *Curr Sci* 80, 524–535.

Hammond, R. W., Swift, S. M., Foster-Frey, J. A., Kovalskaya, N. Y., and Donovan, D. M. (2019). Optimized production of a biologically active Clostridium perfringens glycosyl hydrolase phage endolysin PlyCP41 in plants using virus-based systemic expression. *BMC Biotechnology* 19, 101. doi: 10.1186/s12896-019-0594-7.

He, F., Pasam, R., Shi, F., Kant, S., Keeble-Gagnere, G., Kay, P., et al. (2019a). Exome sequencing highlights the role of wild-relative introgression in shaping the adaptive landscape of the wheat genome. *Nat Genet* 51, 896–904. doi: 10.1038/s41588-019-0382-2.

He, Y., Wu, L., Liu, X., Zhang, X., Jiang, P., and Ma, H. (2019b). Yeast two-hybrid screening for proteins that interact with PFT in wheat. *Scientific Reports* 9, 1–10. doi: 10.1038/s41598-019-52030-x.

Hellin, P., King, R., Urban, M., Hammond-Kosack, K. E., and Legrève, A. (2018). The adaptation of Fusarium culmorum to DMI Fungicides Is Mediated by Major Transcriptome Modifications in Response to Azole Fungicide, Including the Overexpression of a PDR Transporter (FcABC1). *Frontiers in Microbiology* 9. Available at: https://www.frontiersin.org/article/10.3389/fmicb.2018.01385 [Accessed June 28, 2022].

Hernández, P., Debray, H., Jaekel, H., Garfias, Y., Jiménez, M. del C., Martínez-Cairo, S., et al. (2001). Chemical characterization of the lectin from Amaranthus leucocarpus syn. hypocondriacus by 2-D proteome analysis. *Glycoconj J* 18, 321–329. doi: 10.1023/A:1013760915738.

Homdork, S., Fehrmann, H., and Beck, R. (2000). Effects of Field Application of Tebuconazole on Yield, Yield Components and the Mycotoxin Content of Fusarium-infected Wheat Grain. *Journal of Phytopathology* 148, 1–6. doi: 10.1046/j.1439-0434.2000.00460.x.

Horevaj, P., Milus, E. a., and Bluhm, B. h. (2011). A real-time qPCR assay to quantify Fusarium graminearum biomass in wheat kernels. *Journal of Applied Microbiology* 111, 396–406. doi: 10.1111/j.1365-2672.2011.05049.x.

Houterman, P. M., Cornelissen, B. J. C., and Rep, M. (2008). Suppression of Plant Resistance Gene-Based Immunity by a Fungal Effector. *PLOS Pathogens* 4, e1000061. doi: 10.1371/journal.ppat.1000061.

Ilgen, P., Maier, F., and Schäfer, W. (2008). Trichothecenes and lipases are host-induced and secreted virulence factors of Fusarium graminearum. *Cereal Research Communications* 36, 421–428. doi: 10.1556/crc.36.2008.suppl.b.35.

Jansen, C., Wettstein, D. von, Schäfer, W., Kogel, K.-H., Felk, A., and Maier, F. J. (2005). Infection patterns in barley and wheat spikes inoculated with wild-type and trichodiene synthase gene disrupted Fusarium graminearum. *PNAS* 102, 16892–16897. doi: 10.1073/pnas.0508467102.

Jia, N., Liu, N., Cheng, W., Jiang, Y.-L., Sun, H., Chen, L.-L., et al. (2016). Structural basis for receptor recognition and pore formation of a zebrafish aerolysin-like protein. *EMBO Rep* 17, 235–248. doi: 10.15252/embr.201540851.

Jones, J. D. G., and Dangl, J. L. (2006). The plant immune system. *Nature* 444, 323–329. doi: 10.1038/nature05286.

Jones, R. K., and Mirocha, C. J. (1999). Quality Parameters in Small Grains from Minnesota Affected by Fusarium Head Blight. *Plant Disease* 83, 506–511. doi: 10.1094/PDIS.1999.83.6.506.

Jordan, K. W., Wang, S., He, F., Chao, S., Lun, Y., Paux, E., et al. (2018). The genetic architecture of genome-wide recombination rate variation in allopolyploid wheat revealed by nested association mapping. *The Plant Journal* 95, 1039–1054. doi: 10.1111/tpj.14009.

Julius, B. T., Leach, K. A., Tran, T. M., Mertz, R. A., and Braun, D. M. (2017). Sugar Transporters in Plants: New Insights and Discoveries. *Plant and Cell Physiology* 58, 1442–1460. doi: 10.1093/pcp/pcx090.

Jumper, J., Evans, R., Pritzel, A., Green, T., Figurnov, M., Ronneberger, O., et al. (2021). Highly accurate protein structure prediction with AlphaFold. *Nature* 596, 583–589. doi: 10.1038/s41586-021-03819-2.

Kamoun, S. (2007). Groovy times: filamentous pathogen effectors revealed. *Current Opinion in Plant Biology* 10, 358–365. doi: 10.1016/j.pbi.2007.04.017.

Karimi, M., Inzé, D., and Depicker, A. (2002). GATEWAY$^{TM}$ vectors for Agrobacterium-mediated plant transformation. *Trends in Plant Science* 7, 193–195. doi: 10.1016/S1360-1385(02)02251-3.

Kaur, B., Mavi, G. S., Gill, M. S., and Saini, D. K. (2020). Utilization of KASP technology for wheat improvement. *CEREAL RESEARCH COMMUNICATIONS* 48, 409–421. doi: 10.1007/s42976-020-00057-6.

Klix, M. B., Verreet, J.-A., and Beyer, M. (2007). Comparison of the declining triazole sensitivity of Gibberella zeae and increased sensitivity achieved by advances in triazole fungicide development. *Crop Protection* 26, 683–690. doi: 10.1016/j.cropro.2006.06.006.

Kou, Y., and Wang, S. (2010). Broad-spectrum and durability: understanding of quantitative disease resistance. *Current Opinion in Plant Biology* 13, 181–185. doi: 10.1016/j.pbi.2009.12.010.

Kovalskaya, N., Foster-Frey, J., Donovan, D. M., Bauchan, G., and Hammond, R. W. (2016). Antimicrobial Activity of Bacteriophage Endolysin Produced in Nicotiana benthamiana Plants. *J Microbiol Biotechnol* 26, 160–170. doi: 10.4014/jmb.1505.05060.

Kovalskaya, N., Zhao, Y., and W. Hammond, R. (2011). Antibacterial and Antifungal Activity of a Snakin-Defensin Hybrid Protein Expressed in Tobacco and Potato Plants. *The Open Plant Science Journal* 5. Available at: https://benthamopen.com/ABSTRACT/TOPSJ-5-29 [Accessed May 20, 2022].

Krattinger, S. G., Kang, J., Bräunlich, S., Boni, R., Chauhan, H., Selter, L. L., et al. (2019). Abscisic acid is a substrate of the ABC transporter encoded by the durable wheat disease resistance gene Lr34. *New Phytol* 223, 853–866. doi: 10.1111/nph.15815.

Krattinger, S. G., Lagudah, E. S., Spielmeyer, W., Singh, R. P., Huerta-Espino, J., McFadden, H., et al. (2009). A Putative ABC Transporter Confers Durable Resistance to Multiple Fungal Pathogens in Wheat. *Science* 323, 1360–1363. doi: 10.1126/science.1166453.

Krattinger, S. G., Sucher, J., Selter, L. L., Chauhan, H., Zhou, B., Tang, M., et al. (2016). The wheat durable, multipathogen resistance gene Lr34 confers partial blast resistance in rice. *Plant Biotechnology Journal* 14, 1261–1268. doi: 10.1111/pbi.12491.

Lagudah, E. S., and Krattinger, S. G. (2019). A new player contributing to durable Fusarium resistance. *Nat Genet* 51, 1070–1071. doi: 10.1038/s41588-019-0454-3.

Lang-Pauluzzi, I., and Gunning, B. E. S. (2000). A plasmolytic cycle: The fate of cytoskeletal elements. *Protoplasma* 212, 174–185. doi: 10.1007/BF01282918.

Lannoo, N., and Van Damme, E. J. M. (2014). Lectin domains at the frontiers of plant defense. *Front. Plant Sci.* 5. doi: 10.3389/fpls.2014.00397.

Laskowski, R. A., Jabłońska, J., Pravda, L., Vařeková, R. S., and Thornton, J. M. (2018). PDBsum: Structural summaries of PDB entries. *Protein Science* 27, 129–134. doi: 10.1002/pro.3289.

Lee, H. J., and Ryu, D. (2017). Worldwide Occurrence of Mycotoxins in Cereals and Cereal-Derived Food Products: Public Health Perspectives of Their Co-occurrence. *J. Agric. Food Chem.* 65, 7034–7051. doi: 10.1021/acs.jafc.6b04847.

Li, G., and Yen, Y. (2008). Jasmonate and Ethylene Signaling Pathway May Mediate Fusarium Head Blight Resistance in Wheat. *Crop Science* 48, 1888–1896. doi: 10.2135/cropsci2008.02.0097.

Li, G., Zhou, J., Jia, H., Gao, Z., Fan, M., Luo, Y., et al. (2019). Mutation of a histidine-rich calcium-binding-protein gene in wheat confers resistance to Fusarium head blight. *Nat. Genet.* 51, 1106–1112. doi: 10.1038/s41588-019-0426-7.

Li, H., Zhang, F., Zhao, J., Bai, G., Amand, P. St., Bernardo, A., et al. (2022). Identification of a novel major QTL from Chinese wheat cultivar Ji5265 for Fusarium head blight resistance in greenhouse. *Theor Appl Genet*. doi: 10.1007/s00122-022-04080-5.

Li, W., Deng, Y., Ning, Y., He, Z., and Wang, G.-L. (2020). Exploiting Broad-Spectrum Disease Resistance in Crops: From Molecular Dissection to Breeding. *Annual Review of Plant Biology* 71, 575–603. doi: 10.1146/annurev-arplant-010720-022215.

Lim, H.-S., Vaira, A. M., Domier, L. L., Lee, S. C., Kim, H. G., and Hammond, J. (2010). Efficiency of VIGS and gene expression in a novel bipartite potexvirus vector delivery system as a function of strength of TGB1 silencing suppression. *Virology* 402, 149–163. doi: 10.1016/j.virol.2010.03.022.

Liu, S., Griffey, C. A., Hall, M. D., McKendry, A. L., Chen, J., Brooks, W. S., et al. (2013). Molecular characterization of field resistance to Fusarium head blight in two US soft red winter wheat cultivars. *Theor Appl Genet* 126, 2485–2498. doi: 10.1007/s00122-013-2149-y.

Liu, S., Pumphrey, M., Gill, B., Trick, H., Zhang, J., Dolezel, J., et al. (2008). Toward positional cloning of Fhb1 , a major QTL for Fusarium head blight resistance in wheat. *Cereal Research Communications* 36, 195–201. doi: 10.1556/CRC.36.2008.Suppl.B.15.

Livak, K. J., and Schmittgen, T. D. (2001). Analysis of Relative Gene Expression Data Using Real-Time Quantitative PCR and the 2−ΔΔCT Method. *Methods* 25, 402–408. doi: 10.1006/meth.2001.1262.

Lofgren, L. A., LeBlanc, N. R., Certano, A. K., Nachtigall, J., LaBine, K. M., Riddle, J., et al. (2018). Fusarium graminearum: pathogen or endophyte of North American grasses? *New Phytologist* 217, 1203–1212. doi: 10.1111/nph.14894.

Loyall, L., Uchida, K., Braun, S., Furuya, M., and Frohnmeyer, H. (2000). Glutathione and a UV Light–Induced Glutathione S-Transferase Are Involved in Signaling to Chalcone Synthase in Cell Cultures. *The Plant Cell* 12, 1939–1950. doi: 10.1105/tpc.12.10.1939.

Lu, S., Wang, J., Chitsaz, F., Derbyshire, M. K., Geer, R. C., Gonzales, N. R., et al. (2020). CDD/SPARCLE: the conserved domain database in 2020. *Nucleic Acids Res* 48, D265–D268. doi: 10.1093/nar/gkz991.

Ma, L.-J., Geiser, D. M., Proctor, R. H., Rooney, A. P., O'Donnell, K., Trail, F., et al. (2013). Fusarium Pathogenomics. *Annual Review of Microbiology* 67, 399–416. doi: 10.1146/annurev-micro-092412-155650.

Ma, L.-J., van der Does, H. C., Borkovich, K. A., Coleman, J. J., Daboussi, M.-J., Di Pietro, A., et al. (2010). Comparative genomics reveals mobile pathogenicity chromosomes in Fusarium. *Nature* 464, 367–373. doi: 10.1038/nature08850.

Ma, Z., Xie, Q., Li, G., Jia, H., Zhou, J., Kong, Z., et al. (2020). Germplasms, genetics and genomics for better control of disastrous wheat Fusarium head blight. *Theor Appl Genet* 133, 1541–1568. doi: 10.1007/s00122-019-03525-8.

Makandar, R., Nalam, V., Chaturvedi, R., Jeannotte, R., Sparks, A. A., and Shah, J. (2010). Involvement of Salicylate and Jasmonate Signaling Pathways in Arabidopsis Interaction with Fusarium graminearum. *MPMI* 23, 861–870. doi: 10.1094/MPMI-23-7-0861.

Makhoul, M., Rambla, C., Voss-Fels, K. P., Hickey, L. T., Snowdon, R. J., and Obermeier, C. (2020). Overcoming polyploidy pitfalls: a user guide for effective SNP conversion into KASP markers in wheat. *Theor Appl Genet* 133, 2413–2430. doi: 10.1007/s00122-020-03608-x.

Manstretta, V., Gourdain, E., and Rossi, V. (2015). Deposition patterns of Fusarium graminearum ascospores and conidia within a wheat canopy. *Eur J Plant Pathol* 143, 873–880. doi: 10.1007/s10658-015-0722-8.

Manzano, S., Megías, Z., Martínez, C., García, A., Aguado, E., Chileh, T., et al. (2017). Overexpression of a flower-specific aerolysin-like protein from the dioecious plant Rumex acetosa alters flower development and induces male sterility in transgenic tobacco. *The Plant Journal* 89, 58–72. doi: 10.1111/tpj.13322.

Maria Menniti, A., Pancaldi, D., Maccaferri, M., and Casalini, L. (2003). Effect of Fungicides on Fusarium Head Blight and Deoxynivalenol Content in Durum Wheat Grain. *European Journal of Plant Pathology* 109, 109–115. doi: 10.1023/A:1022557819214.

Markell, S. G., and Francl, L. J. (2003). Fusarium Head Blight Inoculum: Species Prevalence and Gibberella zeae Spore Type. *Plant Disease* 87, 814–820. doi: 10.1094/PDIS.2003.87.7.814.

Mauch-Mani, B., and Slusarenko, A. J. (1993). Arabidopsis as a model host for studying plant-pathogen interactions. *Trends Microbiol* 1, 265–270. doi: 10.1016/0966-842x(93)90049-w.

McMullen, M., Bergstrom, G., De Wolf, E., Dill-Macky, R., Hershman, D., Shaner, G., et al. (2012). A Unified Effort to Fight an Enemy of Wheat and Barley: Fusarium Head Blight. *Plant Disease* 96, 1712–1728. doi: 10.1094/PDIS-03-12-0291-FE.

McMullen, M., Jones, R., and Gallenberg, D. (1997). Scab of Wheat and Barley: A Re-emerging Disease of Devastating Impact. *Plant Disease* 81, 1340–1348. doi: 10.1094/PDIS.1997.81.12.1340.

Mellersh, D. G., and Heath, M. C. (2001). Plasma Membrane–Cell Wall Adhesion Is Required for Expression of Plant Defense Responses during Fungal Penetration. *The Plant Cell* 13, 413–424. doi: 10.1105/tpc.13.2.413.

Mengiste, T. (2012). Plant Immunity to Necrotrophs. *Annual Review of Phytopathology* 50, 267–294. doi: 10.1146/annurev-phyto-081211-172955.

Mesterházy, A. (1995). Types and components of resistance to Fusarium head blight of wheat. *Plant Breeding* 114, 377–386. doi: 10.1111/j.1439-0523.1995.tb00816.x.

Mesterházy, Á., Tóth, B., Varga, M., Bartók, T., Szabó-Hevér, Á., Farády, L., et al. (2011). Role of Fungicides, Application of Nozzle Types, and the Resistance Level of Wheat Varieties in the Control of Fusarium Head Blight and Deoxynivalenol. *Toxins* 3, 1453–1483. doi: 10.3390/toxins3111453.

Miedaner, T., Kalih, R., Großmann, M. S., and Maurer, H. P. (2016). Correlation between Fusarium head blight severity and DON content in triticale as revealed by phenotypic and molecular data. *Plant Breeding* 135, 31–37. doi: 10.1111/pbr.12327.

Miedaner, T., Wilde, F., Steiner, B., Buerstmayr, H., Korzun, V., and Ebmeyer, E. (2006). Stacking quantitative trait loci (QTL) for <Emphasis Type="Italic">Fusarium</Emphasis> head blight resistance from non-adapted sources in

an European elite spring wheat background and assessing their effects on deoxynivalenol (DON) content and disease severity. *Theor Appl Genet* 112, 562–569. doi: 10.1007/s00122-005-0163-4.

Moore, J. W., Herrera-Foessel, S., Lan, C., Schnippenkoetter, W., Ayliffe, M., Huerta-Espino, J., et al. (2015). A recently evolved hexose transporter variant confers resistance to multiple pathogens in wheat. *Nature Genetics* 47, 1494–1498. doi: 10.1038/ng.3439.

Moran, Y., Fredman, D., Szczesny, P., Grynberg, M., and Technau, U. (2012). Recurrent Horizontal Transfer of Bacterial Toxin Genes to Eukaryotes. *Mol Biol Evol* 29, 2223–2230. doi: 10.1093/molbev/mss089.

NAKAGAWA, T., SUZUKI, T., MURATA, S., NAKAMURA, S., HINO, T., MAEO, K., et al. (2007). Improved Gateway Binary Vectors: High-Performance Vectors for Creation of Fusion Constructs in Transgenic Analysis of Plants. *Bioscience, Biotechnology, and Biochemistry* 71, 2095–2100. doi: 10.1271/bbb.70216.

Neelam, K., Brown-Guedira, G., and Huang, L. (2013). Development and validation of a breeder-friendly KASPar marker for wheat leaf rust resistance locus <Emphasis Type="Italic">Lr21</Emphasis>. *Mol Breeding* 31, 233–237. doi: 10.1007/s11032-012-9773-0.

Nemchinov, L. G., Paape, M. J., Sohn, E. J., Bannerman, D. D., Zarlenga, D. S., and Hammond, R. W. (2006). Bovine CD14 receptor produced in plants reduces severity of intramammary bacterial infection. *The FASEB Journal* 20, 1345–1351. doi: 10.1096/fj.05-5295com.

Ning, Y., and Wang, G.-L. (2018). Breeding plant broad-spectrum resistance without yield penalties. *Proc Natl Acad Sci U S A* 115, 2859–2861. doi: 10.1073/pnas.1801235115.

Nutrition, C. for F. S. and A. (2020). Guidance for Industry and FDA: Advisory Levels for Deoxynivalenol (DON) in Finished Wheat Products for Human Consumption and Grains and Grain By-Products used for Animal Feed. *U.S. Food and Drug Administration*. Available at: https://www.fda.gov/regulatory-information/search-fda-guidance-documents/guidance-industry-and-fda-advisory-levels-deoxynivalenol-don-finished-wheat-products-human [Accessed January 2, 2021].

O'Donnell, K., Ward, T. J., Geiser, D. M., Corby Kistler, H., and Aoki, T. (2004). Genealogical concordance between the mating type locus and seven other nuclear genes supports formal recognition of nine phylogenetically distinct species within the Fusarium graminearum clade. *Fungal Genetics and Biology* 41, 600–623. doi: 10.1016/j.fgb.2004.03.003.

Ono, E., Mise, K., and Takano, Y. (2020). RLP23 is required for Arabidopsis immunity against the grey mould pathogen Botrytis cinerea. *Sci Rep* 10, 13798. doi: 10.1038/s41598-020-70485-1.

Parry, D. W., Jenkinson, P., and McLEOD, L. (1995). Fusarium ear blight (scab) in small grain cereals—a review. *Plant Pathology* 44, 207–238. doi: 10.1111/j.1365-3059.1995.tb02773.x.

Paul, P. A., Bradley, C. A., Madden, L. V., Dalla Lana, F., Bergstrom, G. C., Dill-Macky, R., et al. (2018a). Effects of Pre- and Postanthesis Applications of Demethylation Inhibitor Fungicides on Fusarium Head Blight and Deoxynivalenol in Spring and Winter Wheat. *Plant Disease* 102, 2500–2510. doi: 10.1094/PDIS-03-18-0466-RE.

Paul, P. A., Bradley, C. A., Madden, L. V., Lana, F. D., Bergstrom, G. C., Dill-Macky, R., et al. (2018b). Meta-Analysis of the Effects of QoI and DMI Fungicide Combinations on Fusarium Head Blight and Deoxynivalenol in Wheat. *Plant Disease* 102, 2602–2615. doi: 10.1094/PDIS-02-18-0211-RE.

Paul, P. A., Lipps, P. E., Hershman, D. E., McMullen, M. P., Draper, M. A., and Madden, L. V. (2008). Efficacy of triazole-based fungicides for fusarium head blight and deoxynivalenol control in wheat: a multivariate meta-analysis. *Phytopathology* 98, 999–1011. doi: 10.1094/PHYTO-98-9-0999.

Peng, J. H., Sun, D., and Nevo, E. (2011). Domestication evolution, genetics and genomics in wheat. *Mol Breeding* 28, 281. doi: 10.1007/s11032-011-9608-4.

Peraro, M. D., and van der Goot, F. G. (2016). Pore-forming toxins: ancient, but never really out of fashion. *Nat Rev Microbiol* 14, 77–92. doi: 10.1038/nrmicro.2015.3.

Pestka, J. (2010). Toxicological mechanisms and potential health effects of deoxynivalenol and nivalenol. *World Mycotoxin Journal*. doi: 10.3920/WMJ2010.1247.

Pettersen, E. F., Goddard, T. D., Huang, C. C., Meng, E. C., Couch, G. S., Croll, T. I., et al. (2021). UCSF ChimeraX: Structure visualization for researchers, educators, and developers. *Protein Science* 30, 70–82. doi: 10.1002/pro.3943.

Poland, J. A., Balint-Kurti, P. J., Wisser, R. J., Pratt, R. C., and Nelson, R. J. (2009). Shades of gray: the world of quantitative disease resistance. *Trends in Plant Science* 14, 21–29. doi: 10.1016/j.tplants.2008.10.006.

Puthoff, D. P., Sardesai, N., Subramanyam, S., Nemacheck, J. A., and Williams, C. E. (2005). Hfr-2, a wheat cytolytic toxin-like gene, is up-regulated by virulent Hessian fly larval

feeding‡. *Molecular Plant Pathology* 6, 411–423. doi: 10.1111/j.1364-3703.2005.00289.x.

Qi, H., Guo, F., Lv, L., Zhu, X., Zhang, L., Yu, J., et al. (2021). The Wheat Wall-Associated Receptor-Like Kinase TaWAK-6D Mediates Broad Resistance to Two Fungal Pathogens Fusarium pseudograminearum and Rhizoctonia cerealis. *Frontiers in Plant Science* 12. Available at: https://www.frontiersin.org/article/10.3389/fpls.2021.758196 [Accessed January 16, 2022].

Qi, L. L., Pumphrey, M. O., Friebe, B., Chen, P. D., and Gill, B. S. (2008a). Molecular cytogenetic characterization of alien introgressions with gene Fhb3 for resistance to Fusarium head blight disease of wheat. *Theor Appl Genet* 117, 1155–1166. doi: 10.1007/s00122-008-0853-9.

Qi, L. L., Pumphrey, M. O., Friebe, B., Chen, P. D., and Gill, B. S. (2008b). Molecular cytogenetic characterization of alien introgressions with gene Fhb3 for resistance to Fusarium head blight disease of wheat. *Theor Appl Genet* 117, 1155–1166. doi: 10.1007/s00122-008-0853-9.

Ramírez-González, R. H., Borrill, P., Lang, D., Harrington, S. A., Brinton, J., Venturini, L., et al. (2018). The transcriptional landscape of polyploid wheat. *Science*. doi: 10.1126/science.aar6089.

Rasheed, A., Wen, W., Gao, F., Zhai, S., Jin, H., Liu, J., et al. (2016). Development and validation of KASP assays for genes underpinning key economic traits in bread wheat. *Theor Appl Genet* 129, 1843–1860. doi: 10.1007/s00122-016-2743-x.

Rawat, N., Pumphrey, M. O., Liu, S., Zhang, X., Tiwari, V. K., Ando, K., et al. (2016). Wheat Fhb1 encodes a chimeric lectin with agglutinin domains and a pore-forming toxin-like domain conferring resistance to Fusarium head blight. *Nature Genetics* 48, 1576–1580. doi: 10.1038/ng.3706.

Ribichich, K. F., Lopez, S. E., and Vegetti, A. C. (2000). Histopathological Spikelet Changes Produced by Fusarium graminearum in Susceptible and Resistant Wheat Cultivars. *Plant Disease* 84, 794–802. doi: 10.1094/PDIS.2000.84.7.794.

Roxas, V. P., Lodhi, S. A., Garrett, D. K., Mahan, J. R., and Allen, R. D. (2000). Stress Tolerance in Transgenic Tobacco Seedlings that Overexpress Glutathione S-Transferase/Glutathione Peroxidase. *Plant and Cell Physiology* 41, 1229–1234. doi: 10.1093/pcp/pcd051.

Rudd, J. c., Horsley, R. d., McKendry, A. l., and Elias, E. m. (2001). Host Plant Resistance Genes for Fusarium Head Blight: Sources, Mechanisms, and Utility in Conventional Breeding Systems. *Crop Science* 41, 620–627. doi: 10.2135/cropsci2001.413620x.

Saintenac, C., Falque, M., Martin, O. C., Paux, E., Feuillet, C., and Sourdille, P. (2009). Detailed Recombination Studies Along Chromosome 3B Provide New Insights on Crossover Distribution in Wheat (Triticum aestivum L.). *Genetics* 181, 393–403. doi: 10.1534/genetics.108.097469.

Salgado, J. D., Wallhead, M., Madden, L. V., and Paul, P. A. (2011). Grain Harvesting Strategies to Minimize Grain Quality Losses Due to Fusarium Head Blight in Wheat. *Plant Disease* 95, 1448–1457. doi: 10.1094/PDIS-04-11-0309.

Salomon, S., Gácser, A., Frerichmann, S., Kröger, C., Schäfer, W., and Voigt, C. A. (2012). The secreted lipase FGL1 is sufficient to restore the initial infection step to the apathogenic Fusarium graminearum MAP kinase disruption mutant Δgpmk1. *Eur J Plant Pathol* 134, 23–37. doi: 10.1007/s10658-012-0017-2.

Salvador-Guirao, R., Baldrich, P., Weigel, D., Rubio-Somoza, I., and San Segundo, B. (2018). The MicroRNA miR773 Is Involved in the Arabidopsis Immune Response to Fungal Pathogens. *Mol Plant Microbe Interact* 31, 249–259. doi: 10.1094/MPMI-05-17-0108-R.

Sarver, B. A. J., Ward, T. J., Gale, L. R., Broz, K., Kistler, H. C., Aoki, T., et al. (2011). Novel Fusarium head blight pathogens from Nepal and Louisiana revealed by multilocus genealogical concordance. *Fungal Genet Biol* 48, 1096–1107. doi: 10.1016/j.fgb.2011.09.002.

Savary, S., Willocquet, L., Pethybridge, S. J., Esker, P., McRoberts, N., and Nelson, A. (2019). The global burden of pathogens and pests on major food crops. *Nature Ecology & Evolution* 3, 430–439. doi: 10.1038/s41559-018-0793-y.

Schmittgen, T. D., and Livak, K. J. (2008). Analyzing real-time PCR data by the comparative $C_T$ method. *Nature Protocols* 3, 1101–1108. doi: 10.1038/nprot.2008.73.

Schnippenkoetter, W., Lo, C., Liu, G., Dibley, K., Chan, W. L., White, J., et al. (2017). The wheat Lr34 multipathogen resistance gene confers resistance to anthracnose and rust in sorghum. *Plant Biotechnol J* 15, 1387–1396. doi: 10.1111/pbi.12723.

Schroeder, H., and Christensen, J. (1963). Factors affecting resistance of wheat to scab caused by Gibberella zeae. *Phytopathology* 53, 831–838.

Schweiger, W., Steiner, B., Vautrin, S., Nussbaumer, T., Siegwart, G., Zamini, M., et al. (2016). Suppressed recombination and unique candidate genes in the divergent haplotype encoding Fhb1, a major Fusarium head blight resistance locus in wheat. *Theor Appl Genet* 129, 1607–1623. doi: 10.1007/s00122-016-2727-x.

Sears, E. R. (1953). Nullisomic Analysis in Common Wheat. *The American Naturalist* 87, 245–252.

Semagn, K., Babu, R., Hearne, S., and Olsen, M. (2014). Single nucleotide polymorphism genotyping using Kompetitive Allele Specific PCR (KASP): overview of the technology and its application in crop improvement. *Mol Breeding* 33, 1–14. doi: 10.1007/s11032-013-9917-x.

Shaw, S. L. Imaging the live plant cell. *The Plant Journal* 45, 573–598. doi: 10.1111/j.1365-313X.2006.02653.x.

Singh, B. D., and Singh, A. K. (2015). *Marker-assisted plant breeding: principles and practices*. Springer.

Singh, L., Anderson, J. A., Chen, J., Gill, B. S., Tiwari, V. K., and Rawat, N. (2019). Development and Validation of a Perfect KASP Marker for Fusarium Head Blight Resistance Gene Fhb1 in Wheat. *Plant Pathol J* 35, 200–207. doi: 10.5423/PPJ.OA.01.2019.0018.

Singh, L., Schulden, T., Wight, J. P., Crank, J., Thorne, L., Erwin, J. E., et al. (2021). Evaluation of Application Timing of Miravis Ace for Control of Fusarium Head Blight in Wheat. *Plant Health Progress* 22, 94–100. doi: 10.1094/PHP-01-21-0007-RS.

Singh, L., Wight, J. P., Crank, J., Thorne, L., Dong, Y., and Rawat, N. (2020). Efficacy Assessment of a New Fungicide, Miravis Ace, for Control of Fusarium Head Blight in Wheat. *Plant Health Progress* 21, 365–368. doi: 10.1094/PHP-06-20-0050-RS.

Snijders, C. H. A., and Van Eeuwijk, F. A. (1991). Genotype x strain interactions for resistance to Fusarium head blight caused by Fusarium culmorum in winter wheat. *Theoret. Appl. Genetics* 81, 239–244. doi: 10.1007/BF00215729.

Spolti, P., Del Ponte, E. M., Dong, Y., Cummings, J. A., and Bergstrom, G. C. (2014). Triazole Sensitivity in a Contemporary Population of Fusarium graminearum from New York Wheat and Competitiveness of a Tebuconazole-Resistant Isolate. *Plant Disease* 98, 607–613. doi: 10.1094/PDIS-10-13-1051-RE.

Spolti, P., Jorge, B. C. de, and Del Ponte, E. M. (2012). Sensitivity of Fusarium graminearum causing head blight of wheat in Brazil to tebuconazole and metconazole fungicides. *Trop. plant pathol.* 37, 419–423. doi: 10.1590/S1982-56762012000600007.

Stam, R., and McDonald, B. A. (2018). When resistance gene pyramids are not durable—the role of pathogen diversity. *Mol Plant Pathol* 19, 521–524. doi: 10.1111/mpp.12636.

Su, Z., Bernardo, A., Tian, B., Chen, H., Wang, S., Ma, H., et al. (2019). A deletion mutation in TaHRC confers Fhb1 resistance to Fusarium head blight in wheat. *Nat Genet* 51, 1099–1105. doi: 10.1038/s41588-019-0425-8.

Su, Z., Jin, S., Zhang, D., and Bai, G. (2018). Development and validation of diagnostic markers for Fhb1 region, a major QTL for Fusarium head blight resistance in wheat. *Theor Appl Genet*. doi: 10.1007/s00122-018-3159-6.

Sucher, J., Boni, R., Yang, P., Rogowsky, P., Büchner, H., Kastner, C., et al. (2017). The durable wheat disease resistance gene Lr34 confers common rust and northern corn leaf blight resistance in maize. *Plant Biotechnology Journal* 15, 489–496. doi: 10.1111/pbi.12647.

Suga, H., Karugia, G. W., Ward, T., Gale, L. R., Tomimura, K., Nakajima, T., et al. (2008). Molecular Characterization of the Fusarium graminearum Species Complex in Japan. *Phytopathology*® 98, 159–166. doi: 10.1094/PHYTO-98-2-0159.

Sutton, J. C. (1982). Epidemiology of wheat head blight and maize ear rot caused by Fusarium graminearum. *Canadian Journal of Plant Pathology* 4, 195–209. doi: 10.1080/07060668209501326.

Szczesny, P., Iacovache, I., Muszewska, A., Ginalski, K., van der Goot, F. G., and Grynberg, M. (2011). Extending the Aerolysin Family: From Bacteria to Vertebrates. *PLoS One* 6. doi: 10.1371/journal.pone.0020349.

Tan, C.-T., Assanga, S., Zhang, G., Rudd, J. C., Haley, S. D., Xue, Q., et al. (2017). Development and Validation of KASP Markers for Wheat Streak Mosaic Virus Resistance Gene Wsm2. *Crop Science* 57, 340–349. doi: 10.2135/cropsci2016.04.0234.

Tanz, S. K., Castleden, I., Small, I. D., and Millar, A. H. (2013). Fluorescent protein tagging as a tool to define the subcellular distribution of proteins in plants. *Front. Plant Sci.* 4. doi: 10.3389/fpls.2013.00214.

Tian, J., Xu, G., and Yuan, M. (2020). Towards Engineering Broad-Spectrum Disease-Resistant Crops. *Trends in Plant Science* 25, 424–427. doi: 10.1016/j.tplants.2020.02.012.

Trail, F. (2009). For Blighted Waves of Grain: Fusarium graminearum in the Postgenomics Era. *Plant Physiology* 149, 103–110. doi: 10.1104/pp.108.129684.

Trail, F., Xu, H., Loranger, R., and Gadoury, D. (2002). Physiological and environmental aspects of ascospore discharge in Gibberella zeae (anamorph Fusarium graminearum). *Mycologia* 94, 181–189. doi: 10.1080/15572536.2003.11833223.

Transue, T. R., Smith, A. K., Mo, H., Goldstein, I. J., and Saper, M. A. (1997). Structure of benzyl T-antigen disaccharide bound to Amaranthus caudatus agglutinin. *Nature Structural Biology* 4, 779–783. doi: 10.1038/nsb1097-779.

Van Damme, E. J. M., Barre, A., Rougé, P., and Peumans, W. J. (2004). Cytoplasmic/nuclear plant lectins: a new story. *Trends in Plant Science* 9, 484–489. doi: 10.1016/j.tplants.2004.08.003.

van Eeuwijk, F. A., Mesterhazy, A., Kling, Ch. I., Ruckenbauer, P., Saur, L., Bürstmayr, H., et al. (1995). Assessing non-specificity of resistance in wheat to head blight caused by inoculation with European strains of Fusarium culmorum, F. graminearum and F. nivale using a multiplicative model for interaction. *Theoret. Appl. Genetics* 90, 221–228. doi: 10.1007/BF00222205.

Varga, E., Wiesenberger, G., Hametner, C., Ward, T. J., Dong, Y., Schöfbeck, D., et al. (2015). New tricks of an old enemy: isolates of Fusarium graminearum produce a type A trichothecene mycotoxin. *Environmental Microbiology* 17, 2588–2600. doi: 10.1111/1462-2920.12718.

Vaughan, M., Backhouse, D., and Ponte, E. M. D. (2016). Climate change impacts on the ecology of Fusarium graminearum species complex and susceptibility of wheat to Fusarium head blight: a review. *World Mycotoxin Journal* 9, 685–700. doi: 10.3920/WMJ2016.2053.

Velásquez, A. C., Castroverde, C. D. M., and He, S. Y. (2018). Plant–Pathogen Warfare under Changing Climate Conditions. *Current Biology* 28, R619–R634. doi: 10.1016/j.cub.2018.03.054.

Walkowiak, S., Gao, L., Monat, C., Haberer, G., Kassa, M. T., Brinton, J., et al. (2020). Multiple wheat genomes reveal global variation in modern breeding. *Nature* 588, 277–283. doi: 10.1038/s41586-020-2961-x.

Wang, H., Sun, S., Ge, W., Zhao, L., Hou, B., Wang, K., et al. (2020). Horizontal gene transfer of Fhb7 from fungus underlies Fusarium head blight resistance in wheat. *Science*. doi: 10.1126/science.aba5435.

Wang, L., Li, Q., Liu, Z., Surendra, A., Pan, Y., Li, Y., et al. (2018). Integrated transcriptome and hormone profiling highlight the role of multiple phytohormone pathways in wheat resistance against fusarium head blight. *PLOS ONE* 13, e0207036. doi: 10.1371/journal.pone.0207036.

Wang, W., Wen, Y., Berkey, R., and Xiao, S. (2009). Specific Targeting of the Arabidopsis Resistance Protein RPW8.2 to the Interfacial Membrane Encasing the Fungal Haustorium Renders Broad-Spectrum Resistance to Powdery Mildew. *The Plant Cell* 21, 2898–2913. doi: 10.1105/tpc.109.067587.

Wang, Y., Tiwari, V. K., Rawat, N., Gill, B. S., Huo, N., You, F. M., et al. (2016). GSP: a web-based platform for designing genome-specific primers in polyploids. *Bioinformatics* 32, 2382–2383. doi: 10.1093/bioinformatics/btw134.

Ward, T. J., Clear, R. M., Rooney, A. P., O'Donnell, K., Gaba, D., Patrick, S., et al. (2008). An adaptive evolutionary shift in Fusarium head blight pathogen populations is driving the rapid spread of more toxigenic Fusarium graminearum in North America. *Fungal Genetics and Biology* 45, 473–484. doi: 10.1016/j.fgb.2007.10.003.

Wei, W., Xu, L., Peng, H., Zhu, W., Tanaka, K., Cheng, J., et al. (2022). A fungal extracellular effector inactivates plant polygalacturonase-inhibiting protein. *Nat Commun* 13, 2213. doi: 10.1038/s41467-022-29788-2.

Wilde, F., Korzun, V., Ebmeyer, E., Geiger, H. H., and Miedaner, T. (2007). Comparison of phenotypic and marker-based selection for <Emphasis Type="Italic">Fusarium</Emphasis> head blight resistance and DON content in spring wheat. *Mol Breeding* 19, 357–370. doi: 10.1007/s11032-006-9067-5.

Willyerd, K. T., Li, C., Madden, L. V., Bradley, C. A., Bergstrom, G. C., Sweets, L. E., et al. (2012). Efficacy and Stability of Integrating Fungicide and Cultivar Resistance to Manage Fusarium Head Blight and Deoxynivalenol in Wheat. *Plant Disease* 96, 957–967. doi: 10.1094/PDIS-09-11-0763.

Wilson, W., Dahl, B., and Nganje, W. (2018). Economic costs of Fusarium Head Blight, scab and deoxynivalenol. *World Mycotoxin Journal* 11, 291–302. doi: 10.3920/WMJ2017.2204.

Windels, C. E. (2000). Economic and Social Impacts of Fusarium Head Blight: Changing Farms and Rural Communities in the Northern Great Plains. *Phytopathology* 90, 17–21. doi: 10.1094/PHYTO.2000.90.1.17.

Wu, L., and Wang, B. (2015). Evaluation on levels and conversion profiles of DON, 3-ADON, and 15-ADON during bread making process. *Food Chemistry* 185, 509–516. doi: 10.1016/j.foodchem.2015.03.082.

Xiao, J., Jia, X., Wang, H., Zhao, R., Fang, Y., Gao, R., et al. (2011). A fast-neutron induced chromosome fragment deletion of 3BS in wheat landrace Wangshuibai increased its susceptibility to <Emphasis Type="Italic">Fusarium</Emphasis> head blight. *Chromosome Res* 19, 225–234. doi: 10.1007/s10577-011-9192-9.

Xiao, J., Jin, X., Jia, X., Wang, H., Cao, A., Zhao, W., et al. (2013). Transcriptome-based discovery of pathways and genes related to resistance against Fusarium head blight in wheat landrace Wangshuibai. *BMC Genomics* 14, 197. doi: 10.1186/1471-2164-14-197.

Xie, G. Q., Zhang, M. C., Chakraborty, S., and Liu, C. J. (2007). The effect of 3BS locus of Sumai 3 on Fusarium head blight resistance in Australian wheats. *Aust. J. Exp. Agric.* 47, 603–607. doi: 10.1071/EA05250.

Xu, G., Yuan, M., Ai, C., Liu, L., Zhuang, E., Karapetyan, S., et al. (2017). uORF-mediated translation allows engineered plant disease resistance without fitness costs. *Nature* 545, 491–494. doi: 10.1038/nature22372.

Xue, S., Li, G., Jia, H., Xu, F., Lin, F., Tang, M., et al. (2010a). Fine mapping Fhb4, a major QTL conditioning resistance to Fusarium infection in bread wheat (Triticum aestivum L.). *Theor Appl Genet* 121, 147–156. doi: 10.1007/s00122-010-1298-5.

Xue, S., Li, G., Jia, H., Xu, F., Lin, F., Tang, M., et al. (2010b). Fine mapping Fhb4, a major QTL conditioning resistance to Fusarium infection in bread wheat (Triticum aestivum L.). *Theor Appl Genet* 121, 147–156. doi: 10.1007/s00122-010-1298-5.

Xue, S., Xu, F., Tang, M., Zhou, Y., Li, G., An, X., et al. (2011a). Precise mapping Fhb5, a major QTL conditioning resistance to Fusarium infection in bread wheat (Triticum aestivum L.). *Theor Appl Genet* 123, 1055–1063. doi: 10.1007/s00122-011-1647-z.

Xue, S., Xu, F., Tang, M., Zhou, Y., Li, G., An, X., et al. (2011b). Precise mapping Fhb5, a major QTL conditioning resistance to Fusarium infection in bread wheat (Triticum aestivum L.). *Theor Appl Genet* 123, 1055–1063. doi: 10.1007/s00122-011-1647-z.

Yang, L., van der Lee, T., Yang, X., Yu, D., and Waalwijk, C. (2008). Fusarium Populations on Chinese Barley Show a Dramatic Gradient in Mycotoxin Profiles. *Phytopathology*® 98, 719–727. doi: 10.1094/PHYTO-98-6-0719.

Yin, Y., Liu, X., Li, B., and Ma, Z. (2009). Characterization of Sterol Demethylation Inhibitor-Resistant Isolates of Fusarium asiaticum and F. graminearum Collected from Wheat in China. *Phytopathology*® 99, 487–497. doi: 10.1094/PHYTO-99-5-0487.

Yoshida, M., Nakajima, T., Tomimura, K., Suzuki, F., Arai, M., and Miyasaka, A. (2012). Effect of the Timing of Fungicide Application on Fusarium Head Blight and Mycotoxin Contamination in Wheat. *Plant Disease* 96, 845–851. doi: 10.1094/PDIS-10-11-0819.

Zhang, H., Zhang, Z., van der Lee, T., Chen, W. Q., Xu, J., Xu, J. S., et al. (2010). Population Genetic Analyses of Fusarium asiaticum Populations from Barley Suggest a Recent Shift Favoring 3ADON Producers in Southern China. *Phytopathology*® 100, 328–336. doi: 10.1094/PHYTO-100-4-0328.

Zhou, W.-C., Kolb, F. L., Bai, G.-H., Domier, L. L., Boze, L. K., and Smith, N. J. (2003). Validation of a major QTL for scab resistance with SSR markers and use of marker-assisted selection in wheat. *Plant Breeding* 122, 40–46. doi: 10.1046/j.1439-0523.2003.00802.x.

Zhuge, X.-L., Xu, H., Xiu, Z.-J., and Yang, H.-L. (2020). Biochemical Functions of Glutathione S-Transferase Family of Salix babylonica. *Frontiers in Plant Science* 11. Available at: https://www.frontiersin.org/article/10.3389/fpls.2020.00364 [Accessed June 8, 2022].

Ziogas, B. N., and Malandrakis, A. A. (2015). "Sterol Biosynthesis Inhibitors: C14 Demethylation (DMIs)," in *Fungicide Resistance in Plant Pathogens: Principles and a Guide to Practical Management*, eds. H. Ishii and D. W. Hollomon (Tokyo: Springer Japan), 199–216. doi: 10.1007/978-4-431-55642-8_13.